Preparation And Characterization Of Monodisperse Porous Polymer Particles.

Order Number 9513156

Preparation and characterization of monodisperse porous polymer particles

Cheng, Chieh-Min, Ph.D.

Lehigh University, 1991

U·M·I
300 N. Zeeb Rd.
Ann Arbor, MI 48106

PREPARATION AND CHARACTERIZATION

OF MONODISPERSE

POROUS POLYMER PARTICLES

by

Chieh-Min Cheng

A Dissertation

Presented to the Graduate Committee

of Lehigh University

in Candidacy for the Degree of

Doctor of Philosophy

in

Polymer Science and Engineering

Lehigh University

1991

Certificate of Approval

Approved and recommended for acceptance as a dissertation in partial fulfillment of the requirements for the degree of Doctor of Philosophy.

MAY 17, 1991
(date)

M. S. El-Aasser, Professor in Charge

Accepted June 27, 1991
(date)

Special committee directing
the doctoral work of
Chieh-Min Cheng

M. S. El-Aasser, Chairman & Co-advisor

J. W. Vanderhoff, Co-advisor

F. J. Micale

E. D. Sudol

C. M. Tseng

Acknowledgements

I would like to express my sincere gratitude and appreciation to the following people and institutions for their contributions during my years of graduate studies:

Drs. M. S. El-Aasser and J. W. Vanderhoff for their advice, guidance, and support throughout this work.

Dr. F. J. Micale for his advice on pore structural studies.

Drs. E. D. Sudol and C. M. Tseng for their many helpful discussions.

Mr. J. R. Martain of Supelco, Inc. and Dr. J. A. Lavelle of Rohm and Haas Company for their assistance with mercury porosimetry measurements.

Mrs. J. S. Lavelle for her friendship in these Lehigh years.

The staff and colleagues of the Emulsion Polymers Institute for the many good times together.

The Emulsion Polymers Institute, Lehigh University, and the National Aeronautics and Space Administration for financial support.

My parents for their tremendous support and encouragement.

Most of all, my wife, Nienwen, for her heartfelt love, understanding, and emotional support throughout my graduate studies.

Table of Contents

Abstract 1

1. General Introduction 3

1.1 POROUS POLYMER PARTICLES 3
1.2 MONODISPERSE POLYMER PARTICLES 4
1.2.1 Methods for Preparing Monodisperse Polymer Particles 5
1.2.2 Successive Seeded Emulsion Polymerization 7
1.3 MONODISPERSE POROUS POLYMER PARTICLES 9
1.4 OBJECTIVES AND SCOPE OF THE RESEARCH 13
1.5 REFERENCES 15

2. Synthesis and Characterization of Monodisperse Porous Polymer Particles 19

2.1 INTRODUCTION 19
2.2 EXPERIMENTAL 20
2.2.1 Materials 20
2.2.2 Monodisperse Seed Particle Preparation 21
2.2.3 Preparation of Monodisperse Porous Styrene-Divinylbenzene Copolymer Particles 23
2.2.4 Characterization 27
2.3 RESULTS AND DISCUSSION 31
2.3.1 Monodisperse Polystyrene Latex Particles 31
2.3.2 Monodisperse Crosslinked Latex Particles 35
2.3.3 Monodisperse Porous Polymer Particles 39
2.3.3.1 Effect of divinylbenzene content 54
2.3.3.2 Effect of molecular weight of linear polystyrene seed 56
2.3.3.3 Effect of crosslinking level of seed particles 61
2.4 SUMMARY AND CONCLUSIONS 65
2.5 REFERENCES 68

3. Pore Structural Studies of Monodisperse Porous Polymer Particles 71

3.1 INTRODUCTION 71
3.2 EXPERIMENTAL 72
3.2.1 Materials and Preparation 72
3.2.2 Characterization of Porous Particles 73
3.3 RESULTS AND DISCUSSION 75
3.3.1 Mercury Porosimetry 79
3.3.1.1 Analysis of intrusion porogram 79
3.3.1.2 Pore size distribution 88
3.3.2 Nitrogen Adsorption Isotherms 92
3.3.2.1 Classification of adsorption isotherms and hysteresis 94
3.3.2.2 Nitrogen adsorption 97
3.3.2.3 Analysis of isotherms: a_s-plot 107
3.4 SUMMARY AND CONCLUSIONS 114
3.5 REFERENCES 116

4. Monodisperse Porous Polymer Particles: Formation of the Porous Structure 118
4.1 INTRODUCTION 118
4.2 EXPERIMENTAL 119
4.2.1 Materials 119
4.2.2 Seeded Emulsion Polymerization 121
4.2.3 Polymer Analysis 122
4.3 RESULTS AND DISCUSSION 125
4.3.1 Copolymerization 131
4.3.2 Mechanism of Pore Formation in the Copolymerization Process 144
4.3.3 Solvent Extraction 148
4.4 SUMMARY AND CONCLUSIONS 153
5. Monodisperse Porous Polymer Particles: Influence of Synthesis Parameters on Pore Structure 160
5.1 INTRODUCTION 160
5.2 EXPERIMENTAL 163
5.2.1 Materials 163
5.2.2 Preparation of Monodisperse Porous Styrene-Divinylbenzene Copolymer Particles 163
5.2.3 Characterization 165
5.3 RESULTS AND DISCUSSION 165
5.3.1 Effect of Type of Solvent or Nonsolvent 173
5.3.2 Effect of Diluent Amount 180
5.3.3 Effect of Initiator Concentration 188
5.3.4 Effect of Polymerization Temperature 188
5.4 SUMMARY AND CONCLUSIONS 192
5.5 REFERENCES 195
6. Conclusions and Recommendations 197
6.1 CONCLUSIONS 197
6.2 RECOMMENDATIONS 200
6.3 REFERENCES 204
Appendix A. Development and Evaluation of a 2L Rotating-Cylinder Reactor for Use in Preparing Large-Particle-Size Latexes 206
A.1 Introduction 206
A.2 Rotating-Cylinder and Piston-Cylinder (RC/PC) Reactor 208
A.3 Reactor Evaluation 210
A.4 Summary 216
A.5 References 216
Appendix B. Determination of Styrene, Divinylbenzene, and Ethylvinylbenzene Concentration by Gas Chromatography 218
B.1 Gas Chromatogram 218
B.2 Calibration Curves 218
B.3 References 219

List of Figures

Figure 2-1: *Scanning electron micrograph of monodisperse polystyrene latex particles prepared by emulsion polymerization.* 32

Figure 2-2: *Scanning electron micrographs of monodisperse polystyrene latex particles prepared by successive seeded emulsion polymerization: (A) 0.3 μm; (B) 1.1 μm; (C) 10 μm; and (D) 56 μm.* 34

Figure 2-3: *Scanning electron micrographs of the larger polystyrene latexes prepared from the improved seeding sequence: (A) 104 μm; and (B) 205 μm.* 36

Figure 2-4: *Scanning electron micrographs of the 10 μm crosslinked styrene-divinylbenzene latex particles with (A) 0.015%, and (B) 33% divinylbenzene contents.* 38

Figure 2-5: *Scanning electron micrographs of the 11 μm monodisperse porous styrene-divinylbenzene copolymer particles: (A) 400 x; and (B) 10,000 x. [diluent: linear polystyrene/n-hexane, 15% DVB, $M_{W,LP}$= 1.49 x 10^6]* 41

Figure 2-6: *Particle-size histogram of the monodisperse porous styrene-divinylbenzene copolymer particles prepared with linear polystyrene and n-hexane as diluents. D_n is number-average diameter, D_w is weight-average diameter, S_d is standard deviation, SD_n is coefficient of variation based on number-average diameter (= S_d/D_n), PDI is polydispersity index, and N is the number of particles counted. [15% DVB, $M_{W,LP}$= 1.49 x 10^6]* 42

Figure 2-7: *Pore size distributions of monodisperse porous polymer particles prepared with different diluents: (A) LP-H: linear polystyrene/n-hexane; (B) LP-T: linear polystyrene/toluene; and (C) LP: linear polystyrene. The dotted line indicates the position of 250 Å pore radius. [15% DVB, $M_{W,LP}$= 1.49 x 10^6]* 43

Figure 2-8: *Nitrogen adsorption and desorption isotherms at 77 °K on 11 μm monodisperse porous polymer particles. [diluent: linear polystyrene/n-hexane, 15% DVB, $M_{W,LP}$= 1.49 x 10^6]* 44

Figure 2-9: *Scanning electron micrograph of the interior structure of a monodisperse porous polymer particle. [Diluent: linear polystyrene/n-hexane, 15% DVB, $M_{W,LP}$= 1.49 x 10^6]* 46

Figure 2-10: *Scanning electron micrographs of the monodisperse porous styrene-divinylbenzene copolymer particles prepared using a mixture of linear polystyrene with (A) n-heptane; or (B) 1-hexanol as inert diluents. [15% DVB, $M_{W,LP}$= 1.49 x 10^6]* 48

Figure 2-11: *Scanning electron micrographs of the monodisperse* 50

porous styrene-divinylbenzene copolymer particles prepared using: (A) linear polystyrene; and (B) linear polystyrene/toluene as inert diluent. [15% DVB, $M_{W,LP}$= 1.49 x 10^6]

Figure 2-12: *Scanning electron micrograph of the monodisperse porous methyl methacrylate/diethylene glycol methacrylate copolymer particles. [diluent: linear poly(methyl methacrylate)/n-heptane; 15% DEGMA, $M_{W,LP}$= 1.49 x 10^6]* 53

Figure 2-13: *Specific surface area as a function of the divinylbenzene content for monodisperse porous polymer particles prepared with various diluents: (A) LP-H: linear polystyrene/n-hexane; (B) LP-nH: linear polystyrene/n-heptane; (C) LP-T: linear polystyrene/toluene; and (D) LP: linear polystyrene. [$M_{W,LP}$= 1.49 x 10^6]* 57

Figure 2-14: *Effect of divinylbenzene content on pore volume. [diluent: linear polystyrene/n-heptane, $M_{W,LP}$= 1.49 x 10^6]* 58

Figure 2-15: *Pore size distributions of monodisperse porous polymer particles prepared with varying divinylbenzene content: (A) 5%; (B) 15%; and (C) 25%. The dotted line indicates the position of 250 Å pore radius. [diluent: linear polystyrene/n-heptane, $M_{W,LP}$= 1.49 x 10^6]* 59

Figure 2-16: *Gel permeation chromatograms of monodisperse polystyrene seed particles dissolved in tetrahydrofuran: (A) LP1: $M_{W,LP}$= 14.9 x 10^5, PDI= 4.98; (B) LP2: $M_{W,LP}$= 10.8 x 10^5, PDI= 7.32; (C) LP3: $M_{W,LP}$= 5.68 x 10^5, PDI= 16.9; and (D) LP4: $M_{W,LP}$= 4.46 x 10^5, PDI= 16.0.* 62

Figure 2-17: *Pore size distributions of monodisperse porous polymer particles prepared with linear polystyrene seed of different molecular weight $M_{W,LP}$ and molecular weight distribution PDI: (A) LP1-H: $M_{W,LP}$= 14.9 x 10^5, PDI= 4.98; (B) LP2-H: $M_{W,LP}$= 10.8 x 10^5, PDI= 7.32; (C) LP3-H: $M_{W,LP}$= 5.68 x 10^5, PDI= 16.9; and (D) LP4-H: $M_{W,LP}$= 4.46 x 10^5, PDI= 16.0. The dotted line indicates the position of 250 Å pore radius. [diluent: linear polystyrene/n-hexane, 15% DVB]* 64

Figure 2-18: *Pore size distributions of monodisperse porous polymer particles prepared with polystyrene seed of different crosslinking levels: (A) 0% DVB; (B) 0.015% DVB; and (C) 0.025% DVB. The dotted line indicates the position of 250 Å pore radius. [diluent: polystyrene seed/n-hexane, 15% DVB]* 66

Figure 3-1: *Scanning electron micrographs of the 11 μm* 77

monodisperse porous styrene-divinylbenzene copolymer particles: (A) 400 x; and (B) 10,000 x. [diluent: linear polystyrene / n-hexane, 15% DVB, $M_{W,LP}$= 1.49 x 10^6]

Figure 3-2: *Scanning electron micrograph of the interior structure of monodisperse porous polymer particles. [Diluent: linear polystyrene / n-hexane, 15% DVB, $M_{W,LP}$= 1.49 x 10^6]* 78

Figure 3-3: *Pore size distribution of the Excil silica porous particles. The dotted line indicates the position of the 250 Å pore radius.* 81

Figure 3-4: *Mercury intrusion porograms for Excil silica porous particles: (A) intruded volume versus pressure; and (B) intruded volume versus pore radius.* 82

Figure 3-5: *Mercury intrusion porograms for: (I) intruded volume versus pressure; and (II) intruded volume versus pore radius. Curve A: 11 μm-diameter monodisperse porous styrene-divinylbenzene copolymer particles [diluent: linear polystyrene / n-hexane; 15% DVB; $M_{W,LP}$= 1.49 x 10^6]; Curve B: 10 μm-diameter nonporous, monodisperse polystyrene latex particles; and Curve C: 0.25 μm-diameter nonporous, monodisperse crosslinked polystyrene particles [15% DVB].* 84

Figure 3-6: *Pore size distributions of: (A) 11 μm-diameter monodisperse porous polymer particles [diluent: linear polystyrene / n-hexane; 15% DVB; $M_{W,LP}$=1.49 x 10^6]; and (B) interparticle pores of 0.25 μm-diameter nonporous, monodisperse crosslinked polystyrene particles. The dotted line indicates the position of the 250 Å pore radius.* 87

Figure 3-7: *Pore size distributions of monodisperse porous polymer particles prepared with different diluents: (A) LP1-H: linear polystyrene / n-hexane; (B) LP1-T: linear polystyrene / toluene; and (C) LP1: linear polystyrene. The dotted line indicates the position of the 250 Å pore radius. [15% DVB, $M_{W,LP}$= 1.49 x 10^6]* 90

Figure 3-8: *Pore size distributions of monodisperse porous polymer particles prepared with varying divinylbenzene content: (A) 5%; (B) 15%; and (C) 25%. The dotted line indicates the position of the 250 Å pore radius. [diluent: linear polystyrene / n-hexane, $M_{W,LP}$= 1.49 x 10^6]* 91

Figure 3-9: *Pore size distributions of monodisperse porous polymer particles prepared with linear polystyrene seed of different molecular weight $M_{W,LP}$ and molecular weight distribution PDI: (A) LP1-H: $M_{W,LP}$= 14.9 x 10^5, PDI= 4.98; (B) LP2-H: $M_{W,LP}$= 10.8 x 10^5, PDI= 7.32; (C) LP3-H: $M_{W,LP}$= 5.68 x 10^5, PDI= 16.9; and (D) LP4-H: $M_{W,LP}$= 4.46 x 10^5, PDI= 16.0. The dotted line indicates* 93

the position of the 250 Å pore radius. [diluent: linear polystyrene/n-hexane, 15% DVB]

Figure 3-10: *The six physisorption isotherm classifications according to BDDT. P: adsorbate equilibrium pressure; P_o: adsorbate saturated equilibrium vapor pressure; and P/P_o: relative pressure* . 95

Figure 3-11: *Types of hysteresis loop. P: adsorbate equilibrium pressure; P_o: adsorbate saturated equilibrium vapor pressure; and P/P_o: relative pressure* . 98

Figure 3-12: *Nitrogen adsorption and desorption isotherms at 77 °K on 11 μm-diameter monodisperse porous polymer particles prepared with linear polystyrene seed of different molecular weight $M_{W,LP}$: (A) LP1-H: $M_{W,LP}$= 14.9 x 10^5; (B) LP2-H: $M_{W,LP}$= 10.8 x 10^5; (C) LP3-H: $M_{W,LP}$= 5.68 x 10^5; and (D) LP4-H: $M_{W,LP}$= 4.46 x 10^5. [diluent: linear polystyrene/n-hexane, 15% DVB]* 100

Figure 3-13: *Nitrogen adsorption and desorption isotherms at 77 °K on: (A) nonporous 0.25 μm-diameter monodisperse crosslinked polystyrene latex particles (with 15 % DVB); (B) nonporous 10 μm-diameter monodisperse uncrosslinked polystyrene latex particles.* 102

Figure 3-14: *Nitrogen adsorption and desorption isotherms at 77 °K on 0.078 μm monodisperse uncrosslinked polystyrene latex particles* . 103

Figure 3-15: *BET plots for 11 μm-diameter monodisperse porous polymer particles prepared with linear polystyrene seed of different molecular weight $M_{W,LP}$: (A) LP1-H: $M_{W,LP}$= 14.9 x 10^5; (B) LP2-H: $M_{W,LP}$= 10.8 x 10^5; (C) LP3-H: $M_{W,LP}$= 5.68 x 10^5; and (D) LP4-H: $M_{W,LP}$= 4.46 x 10^5. [diluent: linear polystyrene/n-hexane, 15% DVB]* 106

Figure 3-16: *Derived mesopore size distributions based on nitrogen desorption isotherms of 11 μm-diameter monodisperse porous polymer particles prepared with linear polystyrene seed of different molecular weights $M_{W,LP}$: (A) LP1-H: $M_{W,LP}$= 14.9 x 10^5; (B) LP2-H: $M_{W,LP}$= 10.8 x 10^5; (C) LP3-H: $M_{W,LP}$= 5.68 x 10^5; and (D) LP4-H: $M_{W,LP}$= 4.46 x 10^5. The dotted line indicates the position of the 250 Å pore radius. [diluent: linear polystyrene/n-hexane, 15% DVB]* 108

Figure 3-17: *a_s-plots for 11 μm-diameter monodisperse porous polymer particles prepared with linear polystyrene seed of different molecular weight $M_{W,LP}$: (A) LP1-H: $M_{W,LP}$= 14.9 x 10^5; (B) LP2-H: $M_{W,LP}$= 10.8 x 10^5; (C) LP3-H: $M_{W,LP}$= 5.68 x 10^5; and (D) LP4-H: $M_{W,LP}$= 4.46* 112

x 10^5. The dotted lines correspond to the linear portion of the a_s-plots which pass through origin. [diluent: linear polystyrene / n-hexane, 15% DVB]

Figure 4-1: *A schematic model for the preparation of the monodisperse porous polymer particles using linear polymer seed and solvent or nonsolvent as inert diluents.* 120

Figure 4-2: *Overall comonomer (styrene-divinylbenzene) conversion for the preparation of monodisperse porous polymer particles with different diluents: (A) LP: linear polystyrene; (B) LP-nH: linear polystyrene / n-heptane; and (C) LP-T: linear polystyrene / toluene. [15% DVB]* 127

Figure 4-3: *Overall comonomer (styrene-divinylbenzene) conversion for the preparation of monodisperse porous polymer particles with different divinylbenzene contents: (A) 5%; (B) 15%; and (C) 25%. [diluent: linear polystyrene / n-heptane]* 128

Figure 4-4: *Individual monomer conversions (as determined by GC analysis) of para- and meta-divinylbenzene (p-DVB & m-DVB), para- and meta-ethylvinylbenzene (p-EVB & m-EVB), and styrene (St). The dotted lines represents the overall comonomer conversion. [diluent: linear polystyrene / n-heptane; 15% DVB; $M_{W,LP}$= 1.49 x 10^6]* 133

Figure 4-5: *Residual sol fraction (soluble fraction in methylene chloride) and calculated gel fraction versus polymerization time. [diluent: linear polystyrene / n-heptane; 15% DVB; $M_{W,LP}$= 1.49 x 10^6]* 134

Figure 4-6: *Relative concentration of residual double bonds in the copolymer versus reaction time. [diluent: linear polystyrene / n-heptane; 15% DVB; $M_{W,LP}$= 1.49 x 10^6]* 136

Figure 4-7: *Scanning electron micrographs of methylene chloride-extracted copolymer at different conversions (reaction times): (A) 5% (2 hr); (B) 20% (6 hr); (C) 65% (14 hr); and (D) 93% (22 hr). [diluent: linear polystyrene / n-heptane; 15% DVB; $M_{W,LP}$= 1.49 x 10^6]* 138

Figure 4-8: *Weight fraction of linear polymer (LP), used as diluent, included in the copolymer network during the copolymerization process. [diluent: linear polystyrene / n-heptane; 15% DVB; $M_{W,LP}$= 1.49 x 10^6]* 140

Figure 4-9: *Specific surface area (S) and pore volume (V_p) changes during copolymer synthesis. [diluent: linear polystyrene / n-heptane; 15% DVB; $M_{W,LP}$= 1.49 x 10^6]* 143

Figure 4-10: *Crosslinking density of copolymer versus polymerization time. [diluent: linear polystyrene / n-heptane; 15% DVB; $M_{W,LP}$= 1.49 x 10^6]* 145

Figure 4-11: *A schematic model for the process of pore formation in the copolymerization stage using linear polymer and nonsolvent as inert diluents.* 147

Figure 4-12: *Scanning electron micrographs of copolymer particles: (A) after polymerization; (B) extracted with methanol only; (C) extracted with methylene chloride only; and (D) extracted with methylene chloride, then methanol. [diluent: linear polystyrene/n-heptane; 15% DVB; $M_{W,LP}$= 1.49 x 10^6]* 150

Figure 4-13: *Effect of solvent extraction using benzene and methylene chloride as solvents on pore size distribution of porous polymer particles with different divinylbenzene contents: (A) 5% DVB; (B) 15% DVB; and (C) 25% DVB. The dotted lines indicate the position of 250 Å pore radius. [diluent: linear polystyrene/n-heptane; $M_{W,LP}$= 1.49 x 10^6]* 154

Figure 5-1: *Schematic representation of the morphology of monodisperse porous polymer particles.* 162

Figure 5-2: *Crosslinking density of the monodisperse porous styrene-divinylbenzene copolymer particles as a function of divinylbenzene content. [diluent: linear polystyrene/n-heptane, $M_{W,LP}$= 1.49 x 10^6]* 169

Figure 5-3: *Scanning electron micrographs of the monodisperse porous styrene-divinylbenzene copolymer particles: (A) 3 μm; and (B) 30 μm. [Diluent: linear polystyrene/n-hexane; 15% DVB, $M_{W,LP}$= 1.49 x 10^6]* 172

Figure 5-4: *Scanning electron micrographs of the monodisperse porous styrene-divinylbenzene copolymer particles prepared using a mixture of linear polystyrene with different solvents as inert diluents: (A) xylene; and (B) methylene chloride. [15% DVB, $M_{W,LP}$= 1.49 x 10^6]* 176

Figure 5-5: *Scanning electron micrographs of the monodisperse porous styrene-divinylbenzene copolymer particles prepared using a mixture of linear polystyrene with different aliphatic hydrocarbons (alkanes) as inert diluents: (A) 1-octane; and (B) nonane. [15% DVB, $M_{W,LP}$= 1.49 x 10^6]* 177

Figure 5-6: *Scanning electron micrographs of the monodisperse porous styrene-divinylbenzene copolymer particles prepared using a mixture of linear polystyrene with different alcohols as inert diluents: (A) 1-heptanol; (B) 1-octanol. [15% DVB, $M_{W,LP}$= 1.49 x 10^6]* 178

Figure 5-7: *Specific surface area as a function of the molecular size of aliphatic hydrocarbons (alkanes) and alcohols used with linear polystyrene as inert diluents in the preparation of monodisperse macroporous polymer particles. [Diluent: linear polystryrene seed (8.7 μm)/alkane or alcohol; 15% DVB; $M_{W,LP}$= 1.49 x 10^6]* 181

Figure 5-8: *Specific surface area as a function of the amount of linear polymer in the preparation of monodisperse porous* 182

polymer particles with diluent. [diluent: linear polystyrene seed; 15% DVB; $M_{W,LP}$= 1.49 x 10^6]

Figure 5-9: *Pore volume as a function of nonsolvent to monomer molar ratio for the preparation of monodisperse porous polymer particles. [diluent: linear polystyrene/n-heptane; 15% DVB; $M_{W,LP}$=1.49 x 10^6]* 184

Figure 5-10: *Specific surface area as a function of solvent or nonsolvent to monomer molar ratio for monodisperse macroporous polymer particles prepared with diluent: (A) LP-T: linear polystyrene/toluene; (B) LP-H: linear polystyrene/n-hexane; and (C) LP-nH: linear polystyrene/n-heptane. [15% DVB; $M_{W,LP}$=1.49 x 10^6]* 185

Figure 5-11: *Pore size distributions of monodisperse porous polymer particles prepared with different molar ratio of nonsolvent to monomers: (A) 0.5; (B) 1.0; and (C) 2.0. The dotted line indicates the position of 250 Å pore radius. [diluent: linear polystyrene/n-heptane; 15% DVB; $M_{W,LP}$= 1.49 x 10^6]* 186

Figure 5-12: *Specific surface area of porous polymer particles prepared with different divinylbenzene content as a function of polymerization temperatures. [diluent: linear polystyrene/n-heptane, $M_{W,LP}$= 1.49 x 10^6]* 190

Figure 5-13: *Effect of polymerization temperature on pore volume of monodisperse porous polymer particles. [diluent: linear polystyrene/n-heptane, $M_{W,LP}$= 1.49 x 10^6, DVB= 15%]* 191

Figure 5-14: *Pore size distributions of monodisperse porous polymer particles prepared at different temperatures: (A) 60 °C; (B) 70 °C; and (C) 90 °C. The dotted line indicates the position of 250 Å pore radius. [diluent: linear polystyrene/n-hexane; 15% DVB; $M_{W,LP}$=1.49 x 10^6]* 193

Figure A-1: *Schematic diagram of the RC/PC reactor.* 209

Figure A-2: *LVDT and fluid temperature (T_f) histories for seeded emulsion polymerizations in the static mode (SM).* 213

Figure A-3: *LVDT and fluid temperature (T_f) histories for seeded emulsion polymerizations in the rotating mode (RM).* 214

Figure A-4: *LVDT and fluid temperature (T_f) vs. time profiles for water test: in both static (SM) and rotating (RM) modes.* 215

Figure B-1: *Representative gas chromatograph result for seeded emulsion samples using toluene as an external standard and tetrahydrofuran as diluent. 1: n-heptane; 2: tetrahydrofuran; 3: toluene; 4: styrene; 5: meta-ethylvinylbenzene; 6: para-ethylvinylbenzene; 7: meta-divinylbenzene; and 8: para-divinylbenzene.* 220

Figure B-2: *Gas chromatography calibration curves for meta-divinylbenzene and para-divinylbenzene using toluene as an external standard.* 221

Figure B-3: *Gas chromatography calibration curves for meta-* 222

ethylvinylbenzene, para-ethylvinylbenzene and styrene using toluene as an external standard.

List of Tables

Table 1-1:	Polymerization Recipes for Monodisperse Polystyrene Latex Particles (0.1 - 100 μm)	10
Table 2-1:	Recipe for Emulsion Polymerization of Styrene with Aerosol MA Emulsifier	22
Table 2-2:	Polymerization Recipes for Monodisperse Polystyrene Latexes (0.2 - 56 μm)	24
Table 2-3:	Seeded Emulsion Polymerization Recipes for Monodisperse Polystyrene Latexes	25
Table 2-4:	Polymerization Recipes for 8.7 -Diameter Monodisperse Polystyrene Latex Particles	26
Table 2-5:	Typical Polymerization Recipes for Monodisperse Porous Polymer Particles	28
Table 2-6:	Improved Polymerization Recipes for Large-Particle-Size Monodisperse Polystyrene Latexes	37
Table 2-7:	Physical Features of Monodisperse Polystyrene Latex Particles	39
Table 2-8:	Physical Characteristics of Monodisperse Porous Polymer Particles	51
Table 2-9:	Polymerization Recipes for 8 μm-Diameter Monodisperse MMA-DEGMA Copolymer Particles	54
Table 2-10:	Recipe for Preparation of Monodisperse Poly(methyl methacrylate) Latex by Dispersion Polymerization	55
Table 2-11:	Recipe for Seeded Emulsion Polymerization of Methyl Methacrylate	55
Table 2-12:	Molecular Weight of Linear Polystyrene Seed Particles	61
Table 2-13:	Physical Characteristics of Monodisperse Porous Polymer Particles	63
Table 2-14:	Influence of the Crosslinking Level of Seed Particles on Some Physical Features of Porous Polymer Particles	65
Table 3-1:	Physical Characteristics of Monodisperse Porous Polymer Particles	79
Table 3-2:	Surface Areas, C, and Pore Volumes Derived from Nitrogen Adsorption-Desorption Isotherms	107
Table 4-1:	Composition of Divinylbenzene 55	121
Table 4-2:	Typical Polymerization Recipes for 11 μm-Diameter Monodisperse Porous Polymer Particles	123
Table 4-3:	Experimental Results of Methylene Chloride Extraction	129
Table 4-4:	Experimental Results of Methylene Chloride Extractions	130
Table 4-5:	Extracted Molecular Weight of Linear Polystyrene	141
Table 4-6:	Inclusion and Extracted Molecular Weight of Linear Polystyrene	142
Table 4-7:	Experimental Results of Different Solvent Extraction	151
Table 5-1:	Particle Size Distribution of Interior Microspheres within the Monodisperse Porous Polymer Particles	168
Table 5-2:	Polymerization Recipes and Specific Surface Areas of Monodisperse Porous Polymer Particles	170

Table 5-3: Polymerization Recipes and Specific Surface Areas of Monodisperse Porous Polymer Particles 171
Table 5-4: Characteristics of the Diluents 174
Table 5-5: Typical Polymerization Recipes for 11 μm-Diameter Monodisperse Porous Polymer Particles 175
Table 5-6: Solvents used with Linear Polystyrene as Diluents for Preparing Monodisperse Porous Polymer Particles 179
Table 5-7: Effect of Initiator Concentration on the Physical Features of Monodisperse Porous Copolymer Particles 189
Table A-1: Recipe for Seeded Emulsion Polymerization 211
Table A-2: Conversions and Particle Size Distribution 212

Abstract

Monodisperse porous styrene-divinylbenzene copolymer particles in the size range of 3 to 30 μm in diameter were prepared via seeded emulsion polymerization. Linear polymer (polystyrene seed) with molecular weight on the order of 10^6, or a mixture of linear polymer and solvent or nonsolvent were used as inert diluents. Porous structure was formed by the removal of diluents by solvent extraction after polymerization. The pore diameters of these porous polymer particles were on the order of 1,000 $\mathring{A}$ with pore volumes up to 0.9 ml/g and specific surface areas up to 200 m^2/g. A polymer seed with a low degree of crosslinking could also be used instead of linear polymer to prepare monodisperse porous polymer particles with smaller pore volume and pore size.

Mercury porosimetry and nitrogen adsorption-desorption were used in a complementary fashion to assess pore structure and pore size distribution. The pore size distribution was very sensitive to the molecular weight of the polystyrene latex particles used as inert diluent. Qualitative evidence from the techniques used indicated that the monodisperse porous polymer particles were macroporous (average pore diameter > 500 $\mathring{A}$) in nature. As the molecular weight of linear polymer decreased, the porous structure of the polymer particles ranged in complexity across the spectrum of macro-mesopore structures. Scanning electron microscopy showed the existence of voids between microspheres and their agglomerates within the porous polymer particle, and nitrogen adsorption isotherms confirmed that the pores were due to interstices between these crosslinked microspheres and agglomerates.

Experimental evidence was presented to describe the mechanism of formation of porous polymer particles during the copolymerization and solvent

extraction stages, in which porosity was a consequence of phase separation in the presence of diluents. Pore structure formation was investigated by changes in copolymerization kinetics, gel content, crosslinking density, particle morphology, surface area, pore volume, and pore size distribution. The process of copolymerization was identified, based on the concepts of production, agglomeration, and fixation of the interior gel microspheres of the polymer particles. A portion of linear polymer used as diluent was found to participate in the network structure while the porous matrix was built-up. The influence of the removal of the linear polymer from the matrix pores during the solvent extraction process on the porous structure was also discussed.

A systematic study of the effects of the synthesis parameters on the specific surface area, pore volume, and pore size distribution of the monodisperse porous polymer particles was conducted. The physical characteristics of the monodisperse porous polymer particles depended on various synthesis parameters including: (1) diluent type; (2) overall crosslink density; (3) molecular wight of the polystyrene seed particles; (4) type of nonsolvent; (5) amount of diluent; (6) initiator concentration; and (7) polymerization temperature. By the variation of these parameters, porous polymer particles with different physical features could be prepared.

Chapter 1
General Introduction

1.1 POROUS POLYMER PARTICLES

There has been an increasing interest in porous polymer particles in recent years. Especially, styrene-divinylbenzene copolymers have been used as precursors for ion exchangers, adsorbents, and gel permeation chromatography column materials[1, 2, 3, 4, 5, 6, 7, 8, 9, 10, 11, 12, 13, 14, 15]. Crosslinked polymer particles with a permanent macroporous structure (pore size > 500 $\mathring{A}$ in diameter) are the most efficient materials for many separation processes; the macropores of the particles allow biomolecules in the general sizes of 500,000 dalton to be separated[16, 17, 18]. These macroporous copolymer particles are used more and more in the synthesis of ion exchangers with high mechanical and chemical stability[6, 19]. Hydrodynamic or liquid exclusion chromatography columns containing porous polymer particles have also become increasingly popular because these columns have chemical stability that cannot be achieved with silica columns[20, 21, 22]. Though silica gel columns are still by far the most widely used due to their desirable characteristics[23], such as uniform pore structure, their lack of stability in basic media and the presence of residual acidic silanol groups on their surface restricts their use in many applications.

Porous polymer particles are normally produced by suspension polymerization by adding an inert diluent to the polymerizing mixture [4, 6, 9, 19, 21, 24, 25, 26, 27, 28, 29]. After polymerization, the inert diluent is removed either by solvent extraction or steam distillation, leaving a porous structure within the polymer particles. The diluents used are solvating or nonsolvating diluents (solvent or nonsolvent) for polymer chains, or inert linear polymer[17, 18, 30, 31, 32, 33, 34, 35, 36, 37]. The suspension process gives relatively

large particles with a broad particle size distribution. Although gradual improvements in reactor design and suspension polymerization methodology have allowed the production of smaller (3 - 15 μm in diameter) porous polymer particles for use in the most recent trend of fast protein liquid and high pressure liquid chromatography columns[22, 38], particles with broad size distribution still suffer some disadvantages such as low packing and separation efficiency and may induce backpressure in the columns. It is expected that porous polymer particles with a monodisperse particle size distribution shall overcome these problems.

1.2 MONODISPERSE POLYMER PARTICLES

Polymer latexes are colloidal dispersions of submicroscopic polymer particles in a continuous medium. They are widely used in industry to produce polymeric materials such as synthetic elastomers, coatings, and adhesives. Polymer particles prepared by emulsion, suspension, or dispersion polymerization, in general, have a relatively broad particle size distribution. Monodisperse polymer latexes are those in which the particle size distribution is extremely narrow, typically with a coefficient of variation less than 2%. The first monodisperse latex was the famous Dow Chemical 580G Lot 3584 monodisperse polystyrene latex of 0.259 μm in diameter, which was prepared, apparently by accident, by an emulsion polymerization process in a pilot plant in 1947. The uniformity of this latex was first noted by Backus and Williams[39, 40]. At first a curiosity, the particles quickly found applications as calibration standards. In 1952, Vanderhoff reproduced the preparation process of the 580G Lot 3584 latex and prepared a series of monodisperse polystyrene latexes in the size range of 0.088 to 2.02 μm in diameter by seeded emulsion polymerization[41, 42, 43], i.e., by polymerizing monomer in a previously prepared monodisperse latex.

Monodisperse polymer particles are characterized by a variety of unique properties such as perfect spherical shape, extremely narrow size distribution (coefficient of variation < 2%), accurately determined diameter, and well-characterized surfaces. Because of these special properties the particles have found wide applications[44, 45], such as calibration standards for scientific measuring instruments (e.g., optical and electron microscopes, light scattering instruments, ultracentrifuges, and electronic particle counters); as column packing materials for chromatographic separation (e.g., gel permeation chromatography, hydrodynamic chromatography, liquid exclusion chromatography, and fast protein liquid chromatography); as a means of measuring membrane pore sizes (e.g., pore size of the stomach, internal membranes, exit channels of the human eye); as substrates in medical serological tests (e.g., rheumatoid arthritis, human pregnancy, trichinosis, histoplasmosis); and as a model to test theories (e.g., mechanism of emulsion polymerization, Brownian motion, colloidal stability, and rheology).

1.2.1 Methods for Preparing Monodisperse Polymer Particles

Many applications demand monodisperse polymer particles of large sizes. However, monodisperse polymer microspheres with diameters greater than 2 μm are not easy to prepare by the conventional emulsion polymerization process due to the sensitivity of the latexes to emulsifier concentration and mechanical shear. If the added emulsifier is insufficient to stabilize the latex particles, they will flocculate to form coagulum. If too much emulsifier is added, a new crop of particles will be generated, and the latex particle size will be biomodal rather than monodisperse. Several methods have been developed for the preparation of monodisperse polymer particles in the micron size range, as briefly reviewed in the following.

1. Successive Seeded Emulsion Polymerization[41, 42, 43, 46, 47, 48, 49, 50]:

Seeded emulsion polymerization was first developed by Vanderhoff to grow small monodisperse particles, which were prepared by emulsion polymerization. Polymerization is generally carried out by first swelling a smaller seed latex in the presence of monomer, initiator, inhibitor, and emulsifiers. The swollen seed particles are then polymerized to produce larger polymer particles. The final particle size of the latex depends on the monomer/polymer swelling ratio as well as the number of seeding steps. Monodisperse polymer particles of 0.1 - 100 μm have been prepared by this process.

2. Emulsifier-Free Polymerization[51, 52, 53]:

This method produces latexes of particle size 0.1 to 1 μm-diameter with low solids contents (< 10%). Polymerizations are carried out in the absence of emulsifier. Particle size is controlled by the monomer concentration, initiator concentration, and the ionic strength of the aqueous phase. It has been claimed that polymer particles up to ca. 5 μm in diameter can be prepared by seeded emulsifier-free polymerization.

3. Dispersion Polymerization[54, 55, 56, 57, 58]:

Monodisperse polymer particles in the size range of 1 to 10 μm can be prepared by this method in a single polymerization step. The process involves the polymerization of a monomer dissolved in a solvent in the presence of initiator and a polymeric steric stabilizer. Particle size depends upon the solvancy of the dispersion medium and the concentrations of monomer and initiator.

4. Two-Step Swelling Method[59, 60, 61, 62, 63, 64]:

The Ugelstad two-step swelling method is also a seeding technique. In the

first step, a relatively low molecular weight water-soluble compound is incorporated into the seed particles to increase the swellability of the particles. The second step involves swelling and polymerization. The methods allows high monomer/polymer swelling ratios and hence large particle size buildups. It has been claimed that the monomer/polymer swelling ratio (based on volume) can be as large as 1,000, and monodisperse polymer particles of 2 to 100 μm in diameter can be prepared. Although the method of increasing the swellability has been frequently mentioned in publications, no details on the polymerization process itself have been given. It is been found that many small particles are generated along with the large particles during polymerization, and these small particles must be separated out later.

Among the four preparation methods, emulsifier-free and dispersion polymerizations cannot be used to prepare polymer particles of large size (> 10 μm); the two-step swelling method is tedious and difficult to carry out and additionally gives small particles; the successive seeding method requires a significant number of steps to achieve large size monodisperse latexes. Nevertheless, successive seeded emulsion polymerization is a promising technique for producing large size monodisperse polymer particles with narrow particle size distribution. Therefore, its further development has been continued in this laboratory.

1.2.2 Successive Seeded Emulsion Polymerization

The preparation of monodisperse polystyrene latexes larger than 2 μm in diameter by seeded emulsion polymerization is difficult owing to the sensitivity of the particles to the emulsifier concentration and mechanical shear. The concentration of emulsifier in the seeded polymerization is critical: too little results in flocculation of the latex and too much results in nucleation of a new

crop of particles. Particles larger than 2 μm in diameter show little or no Brownian motion, and polystyrene seed latex particles swollen with styrene monomer (0.905 g/cm^3) cream and the polymerized particles (1.050 g/cm^3) settle. Of course, the creaming or settling of the particles can be offset by stirring, which is always used in emulsion polymerizations; however, the soft and sticky monomer-swollen particles are sensitive to mechanical shear and thus are easily coagulated by too vigorous stirring. The result is that the larger the particle size, the more vigorous must be the stirring to prevent creaming and settling, but too-vigorous stirring causes mechanical coagulation, so that it is difficult to prepare large size monodisperse latexes without excessive coagulum[46, 47]. In addition, the preparation of larger particles usually requires more stabilization than small particles polymerized under the same mechanical shear conditions because larger particles have a greater tendency to coalesce and form coagulum.

The development of recipes for the preparation of large-particle-size latexes by successive seeded polymerization was first undertaken in this laboratory by Tseng[46], and later modified by Sheu[47]. These recipes were developed in an empirical fashion through the testing of many combinations of stabilizers, initiators, and inhibitors. The proven stabilization system consisted of a combination of three types of surfactants: anionic Aerosol MA (sodium dihexyl sulfosuccinate; American Cyanamid); oligomeric Polywet KX-3 (n-octyl-S-[acrylontrile]$_8$-[acrylic acid]$_8$-H, M_w= 1,500; Uniroyal Chemical); and polymeric PVP [poly(N-vinyl pyrrolidone) K-30 or K-90; GAF Corp.]. The use of polymeric surfactant in seeded polymerizations provided steric stabilization as well as a thickening contribution, which reduced the tendency of particles to flocculate and coalesce, and hence gave large-particle-size polystyrene latexes having good uniformity and little coagulum. The initiator, 2,2'-azobis-(2-methylbutyronitrile) (AMBN) was chosen because of its low water solubility (<

0.04%) and a favorable decomposition rate at 70 °C (half life = 6.5 hours). Hydroquinone, a nonionic and water soluble inhibitor was used to suppress aqueous phase free radical polymerization without inducing any destabilization. Polymerizations carried out in microgravity have given latexes of good uniformity up to 30 μm with essentially no coagulum. The development of ground-based polymerization recipes allowed the preparation of monodisperse latexes as large as 100 μm in diameter by bottle polymerization. This successive seeded polymerization sequence began with a 0.13 μm-diameter monodisperse polystyrene latex particles prepared with a 0.015% divinylbenzene content, which was sebquently grown in successive seeding steps to sizes of 0.20, 0.35, 0.62, 1.1, 1.9, 3.5, 6.3, 11.5, 20.0, 33.3, 56.6, and 100.7 μm, as summarized in Table 1-1. An optimum concentration of divinylbenzene (0.015% based on monomers) in the seed particles was used to reduce the tendency of the particles to coalesce during swelling and polymerization.

1.3 MONODISPERSE POROUS POLYMER PARTICLES

Porous polymer particles are normally produced by suspension polymerization. The suspension process gives relatively large particles (100 - 10,000 μm in diameter) with a broad particle size distribution, which is disadvantageous with regards to separation and packing efficiency. Monodisperse porous styrene-divinylbenzene copolymer particles have been applied in size exclusion chromatography in both aqueous and nonaqueous media[65, 66, 67]. The monodispersity of the particles gives superior efficiency in packing, speed, and resolution as compared with systems with polydisperse particles. Experimental results in fast protein liquid chromatography show that the separation efficiency of monodisperse porous polymer particles increases 10-fold compared with the polydisperse separation media[64, 68, 69, 70]. With

Table 1-1: Polymerization Recipes for Monodisperse Polystyrene Latex Particles (0.1 - 100 μm)[47]

Step #	1	2	3	4	5	6	7	8	9	10	11	12
Seed Diameter (μm)	0.13	0.20	0.35	0.6	1.1	1.9	3.5	6.3	11.5	20.0	33.3	56.6
Monomer/Polymer Swelling Ratio	3	4	4	4	4	5	5	5	4	4	4	5
Final Particle Diameter (μm)	0.20	0.35	0.6	1.1	1.9	3.5	6.3	11.5	20.0	33.3	56.6	100.7
Seed												
PS Particles	5	5	6	6	6	5	5	5	6	6	6	5
Monomers												
Styrene	15	20	24	24	24	25	25	25	24	24	24	25
DVB (%M)	0.015	0.015	0.015	0.015	0.015	0.015	0.015	0.015	0.015	0.015	0.015	0.015
Initiator												
AMBN (%M)	0.12	0.12	0.12	0.12	0.12	0.12	0.12	0.12	0.12	0.12	0.12	0.12
Surfactants												
AMA (%aq)	0.11	0.11	0.14	0.07	0.007	0.007	0.007	0.007	0.007	0.007	0.007	0.007
KX-3 (%aq)	---	---	---	---	0.01	0.015	0.02	0.02	0.02	0.02	0.02	0.02
PVP K-30 (%aq)	---	---	---	---	0.10	0.15	0.15	---	---	---	---	---
PVP K-90 (%aq)	---	---	---	---	---	---	---	0.28	0.28	0.28	0.28	0.28
Buffer												
NaHCO3 (%aq)	---	---	---	---	0.04	0.04	0.04	0.04	0.04	0.04	0.04	0.04
Inhibitor												
HQ (%aq)	0.03	0.03	0.03	0.03	0.03	0.03	0.03	0.03	0.03	0.03	0.03	0.03
Water	79.87	74.87	69.85	69.95	69.84	69.80	69.80	69.71	69.71	69.71	69.71	69.71

Seed, Monomer and Water: % based on total.
%M: wt.% based on monomer.
%aq: wt.% based on aqueous phase.
Cleaned seed latex particles were used in steps 10, 11, and 12.

monodisperse porous particles relatively low and acceptable backpressures are achieved as compared to polydisperse separation media.

The two-step swelling method developed by Ugelstad et al[60, 62, 63, 67] has been used for the production of these monodisperse porous polymer particles in the size range of 2 - 20 μm. Very high swelling ratios, the monomer to seed particle volume ratio, up to 300 were employed in the preparation process. Porosity is obtained by introducing inert solvents together with monomer into swellable monodisperse polymer particles. Toluene, hexane, or cyclohexane were used as inert diluents. Monodisperse macroporous polymer particles with pore volumes up to 2.0 ml/g and specific surface areas up to 500 m^2/g have been reported. Although this method can increase the swellability up to 1,000/1 monomer to polymer by volume, no details on the polymerization process itself have been given. The initiation and stabilization system used in the polymerization, the particle size distribution of the product immediately after polymerization, and the separation methods involved have never been disclosed. It is been found that many small particles are generated along with the large particles during polymerization, and these small particles must be separated out later[71].

The use of the higher swelling ratio caused the monomer-swollen particles which were soft and sticky to cream in the early stages of polymerization and coalesce into a big mass[46, 47, 72]. The use of a low swelling ratio prevented coagulation of the soft monomer-swollen latex particles, which also eliminated the free monomer phase after swelling the seed particles, so that the chances of nucleating a new crop of particles were reduced. An attempt was made to prepare monodisperse porous styrene-divinylbenzene copolymer particles via seeded emulsion polymerization through the use of low swelling ratios (3 - 8)[73, 74]. Solvent or nonsolvent or a mixture of solvent and nonsolvent were

added together with a mixture of styrene and divinylbenzene into swellable monodisperse polystyrene seed latex particles. Following the polymerization, the solvent or nonsolvent was removed from the polymer particles. However, no visual pore structure was observed by scanning electron microscopy. The surface areas of those monodisperse polymer particles prepared with low swelling ratios were too low to indicate the presence of pores in the particles.

Monodisperse polystyrene latexes prepared by seeded emulsion polymerization generally have average molecular weights of 10^6 g/mole or greater and therefore have a maximum monomer/polymer volume swelling ratio of about 8/1[47, 72, 75]. This high molecular weight polymer also reduces the solvent-uptake efficiency of the polystyrene seed particles. An approach to increase the swellability of latex particles was to form low-molecular-weight polymers *in situ*, i.e., to swell the latex particles with monomer and a high concentration of chain transfer agent and carry out telomerization in the particles[46, 76]. Polymerizations in the presence of a chain transfer agent (telogen, e.g., mercaptan) to yield a series of low-molecular-weight polymers (usually < 5,000) were termed telomerizations. The seeded telomerization swelling method developed by Tseng[46] had been applied in the preparation of large-particle-size monodisperse polystyrene latexes. An overall volume increase > 5,000 could be obtained after two cycles of seeded-telomerization swelling. However, as the particles grew larger, it became more and more difficult to prevent coagulation of the latex and generation of small particles at the same time. One major drawback of using this swelling method in the large-particle-size range was the limited shelf-life of the telomerized latex. Telomerized particles were soft and sticky; once they settled, they would coalesce into a big rubbery ball[46].

1.4 OBJECTIVES AND SCOPE OF THE RESEARCH

The objectives of this research are:

1. To develop methods to prepare monodisperse porous polymer particles.

2. To characterize the pore structure of the monodisperse porous polymer particles.

3. To investigate the mechanism of pore formation by the use of the linear polymer seed as inert diluent.

4. To study the synthesis parameters which affect the physical properties of the monodisperse porous polymer particles.

A new synthesis approach is presented in Chapter 2 for the preparation of monodisperse porous polymer particles 10 μm in diameter. The approach involves seeded emulsion polymerization, using linear polystyrene seed or a mixture of linear polystyrene seed and solvent or nonsolvent as inert diluents. The influence of synthesis parameters such as the diluent type, the crosslinker content, and the nature of the polymer seed particles on the physical features of the porous polymer particles is also investigated.

In the synthesis of monodisperse porous polymer particles, monodisperse polymer latex particles with molecular weights on the order of 10^6 are used as inert diluent. Chapter 3 assesses the pore structure of these monodisperse porous polymer particles by mercury porosimetry, nitrogen adsorption-desorption isotherms, and scanning electron microscopy. Of particular interest is the internal structure, as well the magnitude and distribution of the pore size distribution.

In the use of linear polymer seed as inert diluent, Chapter 4 provides an experimental basis for the mechanism of pore formation of the porous structure during copolymerization and solvent extraction processes. Pore structure formation was investigated by changes in copolymerization kinetics, gel content,

crosslinking density, particle morphology, surface area, pore volume, and pore size distribution.

Chapter 5 studies the effect of synthesis parameters on the specific surface area, pore volume, and pore size distribution of the monodisperse porous polymer particles. Emphasis was placed on the kind of solvent and nonsolvent used as inert diluent, the amount of diluent, the initiator concentration, and the reaction temperature of the seeded emulsion polymerization process.

1.5 REFERENCES

1. J. R. Millar, D. G. Smith, W. E. Marr, and T. R. E. Kressman, *J. Chem. Soc.*, 218 (1963).
2. J. R. Millar, D. G. Smith, W. E. Marr, and T. R. E. Kressman, *J. Chem. Soc.*, 2779 (1963).
3. J. R. Millar, D. G. Smith, W. E. Marr, and T. R. E. Kressman, *J. Chem. Soc.*, 2740 (1964).
4. J. R. Millar, D. G. Smith, and T. R. E. Kressman, *J. Chem. Soc.*, 304 (1965).
5. J. R. Millar, *J. Polym. Sci., Polym. Symp.*, **68**, 167 (1980).
6. J. Seidl, J. Malinsky, K. Dusek, and W. Heitz, *Adv. Polym. Sci.*, **5**, 113 (1967).
7. W. Heitz, *Adv. Polym. Sci*, **23**, 1 (1977).
8. H. Beranova and K. Dusek, *Coll. Czech. Chem. Commun.*, **34**, 2932 (1969).
9. K. A. Kun and R. Kunin, *J. Polym. Sci.*, **C16**, 1457 (1967).
10. H. Hilgen, G. J. de Jong, and W. L. Sederel, *J. Appl. Polym. Sci.*, **19**, 2647 (1975).
11. S. Maxim, I. C. Poinescu, S. Dragan, and M. Dima, *Rev. Roumaine Chim.*, **7**, 1447 (1972).
12. C. Beldie, I. C. Poinescu, and V. Cotan, *J. Appl. Polym. Sci.*, **29**, 13 (1984).
13. R. L. Albright, *React. Polym.*, **4**, 155 (1986).
14. J. Lieto, D. Milstein, R. L. Albright, J. V. Minkiewicz, B. C. Gates, *Chemtech*, 46 (1983).
15. P. P. Wieczorek, M. Ilavsky, B. N. Kolarz, and K. Dusek, *J. Appl. Polym. Sci.*, **27**, 277 (1982).
16. J. Haradil, M. Wojaczynska, F. Svec, and B. N. Kolarz, *React. Polym.*, **4**, 277 (1986).
17. I. C. Poinescu, C. Vald, and A. Carpov, *React. Polym.*, **2**, 261 (1984).
18. I. C. Poinescu and A. Carpov, *Rev. Roumaine Chim.*, **34**, 1061 (1989).
19. W. L. Sederel and G. J. de Jong, *J. Appl. Polym. Sci.*, **17**, 2835 (1973).
20. A. Guyot, *Pure & Appl. Chem.*, **60**, 365 (1988).

21. A. Guyot, A. Revillon, and Q. Yuan, *Polym. Bull.*, **21**, 577 (1989).

22. W. Rolls, F. Svec, and J. M. Frechet, *Polymer*, **31**, 165 (1990).

23. J. R. Benson and D. J. Woo, *J. Chromatogr. Sci.*, **22**, 386 (1984).

24. K. A. Kun and R. Kunin, *J. Polym. Sci.*, **A6**, 2689 (1968).

25. H. Galina, *Macromolecules*, **19**, 1222 (1986).

26. G. Hild, R. Okasha, M. Macret, and Y. Gnanou, *Makromol. Chem.*, **187**, 2271 (1986).

27. H. Jacobelli, M. Bartholin, and A. Guyot, *J. Appl. Polym. Sci.*, **23**, 927 (179).

28. H. Jacobelli, M. Bartholin, and A. Guyot, *Angew. Makromol. Chem.*, **80**, 31 (1979).

29. G. J. Howard and C. A. Midgley, *J. Appl. Polym. Sci.*, **26**, 3845 (1981).

30. C. Luca, I C. Poinescu, E. Avram, A. Ioanid, I. Petrariu, and A. Carpov, *J. Appl. Polym. Sci.*, **28**, 3701 (1983).

31. I. C. Poinescu, C. Beldie, and C. Vald, *J. Appl. Polym. Sci.*, **29**, 23 (1984).

32. I. C. Poinescu, V. Popescu, and A. Carpov, *Angew. Makromol. Chem.*, **135**, 21 (1985).

33. I. C. Poinescu and C. Beldie, *Angew. Makromol. Chem.*, **164**, 45 (1988).

34. O. Okay, E. Soner, A. Gungor, and T. I. Balkas, *J. Appl. Polym. Sci.*, **30**, 2065 (1985).

35. O. Okay, *J. Appl. Polym. Sci.*, **32**, 5533 (1986).

36. O. Okay, *J. Appl. Polym. Sci.*, **34**, 307 (1987).

37. O. Okay and W. Funke, *Macromolecules*, **23**, 2623 (1990).

38. A. Guyot and M. Bartholin, *Prog. Polym. Sci.*, **8**, 277 (1982).

39. R. C. Backus and R. C. Williams, *J. Appl. Phys.*, **19**, 1186 (1948).

40. R. C. Backus and R. C. Williams, *J. Appl. Phys.*, **20**, 224 (1949).

41. T. Alfrey, Jr., E. B. Bradford, J. W. Vanderhoff, and G. Oster, *J. Opt. Soc. Am.*, **44**, 603 (1954).

42. E. B. Bradford and J. W. Vanderhoff, *J. Appl. Phys.*, **26**, 684 (1955).

43. E. B. Bradford, J. W. Vanderhoff and T. Alfrey, Jr., *J. Colloid Sci.*, **11**, 684 (1956).

44. L. B. Bangs, *"Uniform Latex Particles"*, Seradyn Inc. Technical Bulletin (1987).

45. L. B. Bangs, *"Uniform Latex Particles"*, Bangs Laboratories, Inc. Technical Bulletin (1988).

46. C. M. Tseng, *Ph.D. Dissertation*, Lehigh University (1983).

47. H. R. Sheu, *Ph.D. Dissertation*, Lehigh University (1988).

48. J. W. Vanderhoff, M. S. El-Aasser, F. J. Micale, E. D. Sudol, C. M. Tseng, A. Silwanowwicz, D. M. Kornfeld, and F. A. Vicente, *J. Disp. Sci. Tech.*, 5, 231 (1984).

49. J. W. Vanderhoff, M. S. El-Aasser, F. J. Micale, E. D. Sudol, C. M. Tseng, A. Silwanowicz, H. R. Sheu, and D. M. Kornfeld, *Polym. Mater. Sci. Eng.*, **54**, 587 (1986).

50. J. W. Vanderhoff, M. S. El-Aasser, D. M. Kornfeld, F. J. Micale, E. D. Sudol, C. M. Tseng, and H. R. Sheu, *Mat. Res. Soc. Symp. Proc.*, **87**, 213 (1987).

51. A. Kotera, K. Furusawa, and Y. Takeda, *Kolloid Z. u. Z. Polym.*, **239**, 677 (1970).

52. A. Kotera, K. Furusawa, and Y. Takeda, *Kolloid Z. u. Z. Polym.*, **240**, 837 (1970).

53. R. H. Ottewill and J. N. Shaw, *Kolloid Z. u. Z. Polym.*, **218**, 34 (1967).

54. C. M. Tseng, Y. Y. Lu, M. S. El-Aasser, and J. W. Vanderhoff, *J. Polym. Sci. Polym. Chem. Ed.*, **24**, 2995 (1986).

55. Y. Y. Lu, *Ph.D. Dissertation*, Lehigh University (1988).

56. Y. Almog, S. Reich, and M. Levy, *Br. Polym. J.*, **14**, 131 (1982).

57. C. K. Ober, K. P. Lok, and M. L. Hair, *J. Polym. Sci. Polym. Lett. Ed.*, **23**, (1985).

58. K. P. Lok and C. K. Ober, *Can. J. Chem.*, **63**, 209 (1985).

59. J. Ugelstad, P. C. Mork, H. R. Mfutakamba, E. Soleimany, I. Nordhuus, K. Nustad, R. Schmid, A. Berge, T. Ellingsen, and O. Aune, in *"Science and Technology of Polymer Colloids"*, Vol. 1, G. W. Poehlein, R. H. Ottewill, and J. W. Goodwin, eds., NATO Series, 1983, p. 51.

60. J. Ugelstad, P. C. Mork, K. Herder Kaggerud, T. Ellingsen and A. Berge, *Adv. Colloid Interface Sci.*, **13**, 101 (1980).

61. J. Ugelstad, P. C. Mork, A. Berge, T. Ellingsen, and A. A. Khan, in *"Emulsion Polymerization"*, I. Piirma, ed., Academic Press, New York, 383 (1982).

62. J. Ugelstad, *U. S. Patent 4,459,378* (1984).

63. J. Ugelstad, T. Ellingsen, A. Berge, and B. Helgee, *PCT Int. Appl.* WO 83 03,920 (1983).

64. J. Ugelstad, H. R. Mfutakamba, P. C. Mork, T. Ellingsen, A. Berge, R. Schmid, L. Holm, A. Jorgedal, F. K. Hansen, and K. Nustad, *J. Polym. Sci. Polym. Symp.*, **72**, 225 (1985).

65. J. Ugelstad, L. Soderberg, A. Berge, and J Bergstrom, *Nature*, **303**, 95 (1983).

66. J. Ugelstad, A Berge, T. Ellingsen, O. Aune, L. Kilaas, T. N. Nilsen, R. Schmid, P. Stenstad, S. Funderud, G. Kvalheim, K. Nustad, T. Lea, F. Vartdal, and H. Danielsen, *Makromol. Chem., Makromol. Symp.*, **17**, 177 (1988).

67. J. Ugelstad and T. Ellingsen, presented at *"64th Colloid and Surface Science Symposium"*, Lehigh University, Bethlehem, PA, June 18-20, 1990.

68. A. Berge, T. Ellingsen, A. T. Skjeltorp, and J. Ugelstad, in *"Scientific Methods for the Study of Polymer Colloids and Their Applications"*, F. Candau and R. H. Ottewill, Eds., Kluwer Academic, Netherlands, 435 (1990).

69. J. Bergstrom, L. Soderberg, L. Wahlstrom, R. M. Muller, A. Domicelj, G. Hagstrom, R. Stalberg, and K. A. Hansson, *Protides Biol. Fluids*, **30**, 641 (1983).

70. G. Lindgren, B. Lundstrom, I. Kallman, and K. A. Hansson, *J. Chromatogr.*, **296**, 83 (1984).

71. M. Abouelezz, *Bio-Rad Chemical Division*, Private Communication (1989).

72. C. M. Tseng, M. S. El-Aasser, and J. W. Vanderhoff, in *"Computer Applications in Applied Polymer Science"*, T. Provder, ed., ACS Symp. Series No. 197, American Chemical Society, Washington, D.C., 1982, p. 197.

73. C. M. Cheng, M. S. El-Aasser, and J. W. Vanderhoff, *Graduate Research Progress Reports*, Emulsion Polymers Institute, Lehigh University, **31**, 6 (1989).

74. C. M. Cheng, M. S. El-Aasser, and J. W. Vanderhoff, *Graduate Research Progress Reports*, Emulsion Polymers Institute, Lehigh University, **32**, 5 (1989).

75. L. H. Jansson, M. C. Wellon, and G. W. Poehlein, *J. Polym. Sci., Polym. Lett. Ed.*, **21**, 937 (1983).

76. C. M. Starks, *"Free Radical Telomerization"*, Academic Press, New York (1974).

Chapter 2
Synthesis and Characterization of Monodisperse Porous Polymer Particles

2.1 INTRODUCTION

There has been an increasing interest in porous polymer particles in recent years. Especially, styrene-divinylbenzene copolymers have been used as precursors for ion exchangers, adsorbents and GPC column materials[1, 2, 3]. Crosslinked polymer particles with a permanent macroporous structure (pore size > 500 $\mathring{A}$ in diameter) are the most efficient materials for many separation processes; the macropores of the particles allow biomolecules in the general size of 500,000 dalton to be separated[4]. Such polymer particles are normally produced by suspension polymerization by adding an inert diluent to the polymerizing mixture[1, 5]. After polymerization, the inert diluent is removed, leaving a porous structure within the polymer particles. The diluents used are solvating or nonsolvating diluents (solvent or nonsolvent) for polymer chains, or inert linear polymer. The suspension process gives relatively large particles with a broad particle size distribution, which is disadvantageous with regards to flow conditions, separation, and packing efficiency. It is expected that the improved separation efficiency, optimal packing, and lower backpressure can be achieved with monodisperse macroporous polymer particles as compared to polydisperse separation media[6, 7, 8].

Seeded emulsion polymerization, which has been developed for the production of monodisperse polymer particles, may be applied to the production of monodisperse, porous polymer particles[9, 10]. By introducing an inert diluent, which is a solvent or nonsolvent or an inert linear polymer, together with monomers into swellable monodisperse polymer particles, porous structures

within the particles may be obtained by removal of the diluent after polymerization.

This chapter describes the new approach of the use of monodisperse polystyrene seed particles as inert diluents for the preparation of monodisperse porous styrene-divinylbenzene copolymer particles in the size range of 10 μm in diameter via seeded emulsion polymerization. The influence of parameters such as the diluent type, the crosslinker content, and the nature of the polymer seed particles on the physical characteristics of the porous polymer particles is also investigated.

2.2 EXPERIMENTAL

2.2.1 Materials

Styrene (Polysciences) and divinylbenzene 55 crosslinking monomer (DVB 55) [55.9% divinylbenzene (DVB) and 42.9% ethylvinylbenzene (EVB), by GC; Dow Chemical] were washed with 10% aqueous sodium hydroxide solution and water, dried over sodium sulfate, and passed through an activated aluminum oxide column to remove the inhibitors. The other materials were used as received: 2,2'-azobis-(2-methylbutyronitrile) initiator (VAZO 67; E. I. duPont de Nemours), potassium persulfate initiator ($K_2S_2O_8$; Fisher Scientific), hydroquinone inhibitor (Fisher Scientific), sodium bicarbonate buffer (Fisher Scientific), Aerosol MA emulsifier (sodium dihexyl sulfosuccinate; American Cyanamid), Polywet KX-3 oligomeric surfactant (n-octyl-S-[acrylonitrile]$_8$-[acrylic acid]$_8$-H, M_w= 1,500; Uniroyal Chemical), poly(N-vinyl pyrrolidone) K-30 and K-90 surfactants (GAF Corp.), and solvents such as n-hexane, n-heptane, 1-hexanol, toluene, methylene chloride, and methanol (Fisher Scientific). Distilled deionized water was used in the preparation of aqueous solutions.

2.2.2 Monodisperse Seed Particle Preparation

The 0.17 μm monodisperse polystyrene seed latexes were prepared by direct emulsion polymerization of styrene and divinylbenzene using potassium persulfate initiator and Aerosol MA emulsifier, following the procedure reported by Dezelic et al[11]. The polymerization recipe given in Table 2-1 is a modified version of the one used by Dezelic et al with the addition of divinylbenzene to reduce the tendency of the particles to coalesce during the subsequent polymerization. The styrene and divinylbenzene monomers were charged into a 12 oz. capped bottle which contained an aqueous solution of the Aerosol MA emulsifier, potassium persulfate initiator, and sodium bicarbonate buffer. Emulsification was conducted by shaking the mixture for 3 minutes followed by tumbling the capped bottle end-over-end for 40 minutes at room temperature. The polymerization was then carried out by tumbling the bottle end-over-end at 32 rpm in a thermostated water bath at 70 °C for 24 hours. Monodisperse polystyrene latexes with 0.17 μm in diameter were obtained after polymerization.

Successive seeded emulsion polymerization is the method of choice to prepare large-size monodisperse latex particles in which the small particle size latexes are swollen with monomer and polymerized in a series of growth cycles. Monodisperse polystyrene latex particles prepared by direct emulsion polymerization were used as the original seed particles. The ingredients used in successive seeded emulsion polymerizations comprised seed particles, styrene and divinylbenzene monomers, 2,2'-azobis-(2-methylbutyronitrile) initiator (AMBN), hydroquinone inhibitor (HQ), sodium bicarbonate buffer ($NaHCO_3$), and Aerosol MA (AMA), Polywet KX-3 and poly(N-vinyl pyrrolidone) K-30 (PVP K-30) or K-90 (PVP K-90) emulsifiers[12, 13]. For seeded polymerizations using *uncleaned* seed latexes, all the ingredients were added into 12 oz. capped

Table 2-1: Recipe for Emulsion Polymerization of Styrene with Aerosol MA Emulsifier

Ingredient	wt%
Monomers	
styrene	19.994
divinylbenzene 55	0.006
Aerosol MA	0.75
Potassium persulfate	0.10
Sodium bicarbonate buffer	0.125
Water	79.025

• *Total charge amount = 300 grams; solids content = 20%; and polymerization temperature = 70 °C.*

bottles, which were tumbled end-over-end for 12 hours at room temperature to allow the seed particles to swell. For seeded polymerizations using *cleaned* seed latexes (by repeated sedimentation and decantation), a two-step swelling process was used. The cleaned seed latexes were diluted with the water and charged into 12 oz. capped bottles. The surfactants, Aerosol MA, Polywet KX-3, and poly(N-vinyl pyrrolidone) K-90 and sodium bicarbonate buffer were added, and the mixture was tumbled end-over-end at room temperature for 12 hours to allow the surfactants to adsorb onto the latex particle surfaces. Monomers (styrene and divinylbenzene), AMBN initiator and hydroquinone inhibitor were added to the seed latex mixture, which was then tumbled end-over-end for 16 hours at room temperature. Polymerizations were carried out by tumbling the bottles end-over-end for 24 hours at 70 °C. For the seed particles having size larger than 20 μm in diameter, polymerizations were carried out at 70 °C for 24 hours, followed by 12 hours at 90 °C. Monodisperse polystyrene latexes as large

as 56 μm in diameter were prepared by modifying previous polymerization recipes[12, 13] by adjusting the surfactant concentration. The polymerization process began with the 0.17 μm diameter polystyrene latexes prepared using 0.015% divinylbenzene (DVB), which was grown in successive seeding steps to sizes from 0.3 μm up to 56 μm. Table 2-2 summarizes the polymerization recipes which were used to prepare monodisperse polystyrene latexes as large as 56 μm in diameter. Following this preparation scheme, monodisperse polystyrene latex particles with desired particle size could be prepared, as demonstrated in Table 2-3, by using different sizes of seed latexes and varying the monomer to polymer weight swelling ratio.

A series of monodisperse polystyrene latexes having a size of 8.7 μm in diameter were prepared according to the recipes listed in Table 2-4 via the method of seeded emulsion polymerization with different concentrations of initiator and chain transfer agent. These monodisperse polystyrene latex particles with different molecular weights and molecular weight distributions were used as inert diluent for the preparation of monodisperse porous polymer particles.

2.2.3 Preparation of Monodisperse Porous Styrene-Divinylbenzene Copolymer Particles

A series of 11 μm monodisperse porous styrene-divinylbenzene copolymer particles were prepared by seeded emulsion polymerization using different types of diluent and concentrations of divinylbenzene starting with the 8.7 μm-diameter monodisperse polystyrene latexes which were prepared according to Table 2-4. The seeded emulsion polymerizations were carried out at 30% organic phase and comprised cleaned monodisperse polystyrene seed latex, styrene and divinylbenzene (DVB) monomers, diluent, initiator, inhibitor,

Table 2-2: Polymerization Recipes for Monodisperse Polystyrene Latexes (0.2 - 56 μm)

Step#	1	2	3	4	5	6	7	8	9	10	11
d_{seed} (μm)	0.16	0.25	0.40	0.67	1.1	1.9	3.6	6.6	11.8	20	34
M/P	3	4	4	4	4	5	5	5	4	4	4
d (μm)	0.25	0.40	0.67	1.1	1.9	3.6	6.6	11.8	20	34	56
Seed											
PS particles	5.0	5.0	6.0	6.0	6.0	5.0	5.0	5.0	6.0	6.0	6.0
Monomers											
Styrene	15.0	20.0	24.0	24.0	24.0	25.0	25.0	25.0	24.0	24.0	24.0
DVB (%M)	0.015	0.015	0.015	0.015	0.015	0.015	0.015	0.015	0.015	0.015	0.015
Initiator											
AMBN (%M)	0.12	0.12	0.12	0.12	0.12	0.12	0.12	0.12	0.12	0.12	0.12
Surfactants											
AMA (%aq)	0.11	0.11	0.14	0.07	0.007	0.007	0.007	0.007	0.007	0.007	0.007
KX-3 (%aq)	-	-	-	-	0.01	0.015	0.02	0.02	0.02	0.02	0.02
K-30 (%aq)	-	-	-	-	0.10	0.45	0.45	-	-	-	-
K-90 (%aq)	-	-	-	-	-	-	-	0.28	0.28	0.56	0.28
Buffer											
$NaHCO_3$ (%aq)	-	-	-	-	0.04	0.04	0.04	0.04	0.04	0.04	0.04
Inhibitor											
HQ (%aq)	0.03	0.03	0.03	0.03	0.03	0.03	0.03	0.03	0.03	0.03	0.03
Water	79.86	74.86	69.83	69.90	69.82	69.46	69.46	69.62	69.62	69.34	69.62

* *d_{seed}: diameter of monodisperse polystyrene seed latex; M/P: monomer/polymer weight swelling ratio; and d: diameter of final polystyrene latex.*

- *Total charge amount: 300 grams in 12 oz. bottles; seed, monomer and water: % based on total; %M: wt. % based on monomer; and %aq: wt.% based on aqueous phase.*
- *Cleaned seed latex particles were used in steps 8, 9, 10, and 11.*

Table 2-3: Seeded Emulsion Polymerization Recipes for Monodisperse Polystyrene Latexes

d_{seed} (μm)	1.9	3.0	3.6	6.6[a]	10[a]	16[a]
M/P	4	4	3	3	3	3
d (μm)	3.0	5.0	5.5	10	16	23
Seed						
PS particles	6.0	6.0	7.5	7.5	7.5	7.5
Monomers						
Styrene	24.0	24.0	22.5	22.5	22.5	22.5
DVB (%M)	0.015	0.015	-	0.015	-	-
Initiator						
AMBN (%M)	0.12	0.12	0.12	0.12	0.12	0.12
Surfactants						
AMA (%aq)	0.007	0.007	0.007	0.007	0.007	0.007
KX-3 (%aq)	0.015	0.02	0.02	0.02	0.02	0.02
K-30 (%aq)	0.45	0.45	0.45	-	-	-
K-90 (%aq)	-	-	-	0.28	0.28	0.28
Buffer						
$NaHCO_3$ (%aq)	0.04	0.04	0.04	0.04	0.04	0.04
Inhibitor						
HQ (%aq)	0.03	0.03	0.03	0.03	0.03	0.03
Water	69.62	69.61	69.61	69.73	69.73	69.73

[a] *Cleaned seed latex particles were used in polymerization.*
* d_{seed}*: diameter of monodisperse polystyrene seed latex; M/P: monomer/polymer weight swelling ratio; and d: diameter of final polystyrene latex.*
• *Total charged amount of 80 grams in 4 oz. bottles; seed, monomer and water: % based on total; %M: wt. % based on monomer; and %aq: wt.% based on aqueous phase.*

Table 2-4: Polymerization Recipes for 8.7 μm-Diameter Monodisperse Polystyrene Latex Particles

Sample	LP1	LP2	LP3	LP4
Ingredient		wt%		
PS seed[a]	5.0	5.0	5.0	5.0
Styrene	25.0	25.0	25.0	25.0
AMBN	0.014	0.28	0.56	0.56
n-BM	-	0.25	0.25	0.50
AMA	0.005	0.005	0.005	0.005
KX-3	0.014	0.014	0.014	0.014
PVP K-90	0.40	0.40	0.50	0.50
$NaHCO_3$	0.027	0.027	0.027	0.027
HQ	0.021	0.021	0.028	0.028
Water	69.57	69.57	69.40	69.40

[a] *Monodisperse polystyrene seed latex particles (5 μm in diameter prepared according to the recipe given in Table 2-3).*
* *n-BM: n-butyl mercaptan.*
• *Total charge amount of 300 grams in 12 oz. capped bottles; solids content = 30%; and polymerization temperature = 70 °C.*

buffer, and emulsifiers. The molar ratio of solvent-type diluent (if used) to monomers was 1 with the swelling ratio (the weight ratio of the mixture of solvent-type diluent plus monomers to polystyrene seed) set to 3. The use of a low swelling ratios prevented coagulation of the soft monomer-swollen latex particles. The use of higher swelling ratios caused the monomer-swollen particles which were soft and sticky to cream in the early stages of polymerization and coalesce into a big mass. The use of low swelling ratios also eliminated the free monomer phase after swelling the seed particles, so that the

chances of nucleating a new crop of particles was reduced. Table 2-5 gives a typical polymerization recipes using a mixture of linear polystyrene seed and n-hexane as inert diluents. The ingredients were added to 4 oz. capped bottles, which were tumbled end-over-end for 12 hours at room temperature (23 °C) to allow the seed particles to swell with the n-hexane-monomer mixture. The polymerizations were carried out by tumbling the bottles end-over-end at 16 rpm in a thermostated water bath at 70 °C for 24 hours. The concentration of emulsifiers was selected to prevent formation of coagulum or small secondary particles during polymerization. The use of polymeric surfactant poly(N-vinyl pyrrolidone) K-90 with molecular weight of 3.6×10^5 to stabilize the latex particles by steric stabilization mechanism also increased the viscosity of the medium, which reduced the tendency of the swollen particles to cream and coalesce. After polymerization, the latex particles were extracted with methylene chloride (a good solvent for polystyrene) in a Soxhlet apparatus for 36 hours to remove the linear polymer portion, followed by washing with methanol to remove residual methylene chloride and low molecular weight solvent-type diluents (solvent or nonsolvent). During the solvent extraction processes, the aqueous polymer latex particles were added to methylene chloride or methanol at low concentration (latex/solvent weight ratio less than 1%). After solvent extraction, the polymer particles were dried in air at room temperature and then vacuum-dried in an oven at 45 °C.

2.2.4 Characterization

The surface morphology and particle size of porous polymer particles were characterized by an ETEC Autoscan scanning electron microscope. A particle-size histogram was constructed from measurements of 250 - 300 individual particles from the electron micrographs. A Zeiss MOP-3 digital image analyzer

Table 2-5: Typical Polymerization Recipes for Monodisperse Porous Polymer Particles

Diluent	LP/n-Hexane	LP/Toluene	LP
Ingredient		wt%	
PS seed[a]	7.5	7.5	7.5
Monomers			
styrene	13.0 - variable	12.0 - variable	22.5 - variable
DVB 55	variable[c]	variable[c]	variable[c]
Diluent[b]	9.5	10.5	-
AMBN	0.018	0.017	0.034
AMA	0.005	0.005	0.010
KX-3	0.014	0.014	0.028
PVP K-90	0.80	0.60	0.80
HQ	0.021	0.021	0.042
$NaHCO_3$	0.027	0.027	0.027
Water	69.14	69.34	69.09

* *LP: linear polystyrene seed.*
[a] *Linear, monodisperse polystyrene latex particles (8.7 μm in diameter).*
[b] *Solvent-type diluent (solvent or nonsolvent).*
[c] *Different levels: 5, 8, 15, 25, and 33% divinylbenzene content (based on total polymer and monomers).*
• *Total charged amount = 80 grams; polymerization temperature = 70 °C.*

was used for the measurements of the particle diameter.

The surface area *(S)* of the particles was measured by nitrogen adsorption isotherms. Nitrogen adsorption at 77 °K was determined volumetrically in a Quantasorb Sorption System (Quantachrome Corp., Model OS-9). Typically, 0.1 - 0.2 gram of sample was used for the measurement and the sample was outgassed at 45 °C prior to nitrogen adsorption. The BET equation was used to

analyze the low relative pressure region of the isotherm in order to find the surface areas of the particles[14, 15, 16, 17]:

$$\frac{1}{V_{ads}[(P/P_o)-1]} = \frac{1}{V_{ads,m}C} + \frac{C-1}{V_{ads,m}C}\left(\frac{P}{P_o}\right) \tag{2.1}$$

where V_{ads} is the volume of adsorbate adsorbed at relative pressure P/P_o, P is adsorbate equilibrium pressure, P_o is adsorbate saturated equilibrium pressure, C is the BET constant, and $V_{ads,m}$ is the volume of adsorbate adsorbed in a monolayer. The specific surface area is given by[14, 15]

$$S = \frac{V_{ads,m}\overline{N}a_m}{\overline{V}} \tag{2.2}$$

where a_m is the cross sectional area of adsorbate, $\overline{V}$ is the molar volume of adsorbate, and $\overline{N}$ is Avogadro's number.

Pore volume and pore size distribution were determined by mercury intrusion porosimetry on a Micromeritics AutoPore 9200 porosimeter. Typically, 0.1 - 0.2 gram of sample was used for the measurement and the sample was outgassed at room temperature prior to mercury intrusion measurement. The pore radii (r) quoted were those of equivalent hollow cylinders obtained from the intruded pressure (P), using the Washburn equation[15, 18]:

$$r = -\frac{2\gamma\cos\theta}{P} \tag{2.3}$$

where the terms γ and θ are the surface tension and wetting angle of mercury, respectively. In these measurements, γ of 485 dyne/cm and θ of 130° were assumed[1, 19]. The cumulative pore volumes (V_p) were estimated from the intruded mercury volumes of the pores larger than 50 $\mathring{A}$-equivalent radius.

The volume *ln* pore radius distribution function $D_v(ln\ r)$ was used to express the pore size distribution to reduce the wide range of values which the volume pore-size distribution function $D_v(r)$ could exhibit[20]:

$$D_v(\ln r)=\frac{dV}{d\ln r}=r\frac{dV}{dr}=rD_v(r) \tag{2.4}$$

where dV is the corresponding pore volume change when the radius of a cylindrical pore changes from r to $r - dr$. The volume distribution function $D_v(r)$ is defined as the volume of mercury intruded per unit change in pore radius and was determined by

$$D_v(r)=\frac{P\,dV}{r\,dP} \tag{2.5}$$

where dP is the pressure change. For plots of $D_v(r)$ and $D_v(ln\ r)$ versus pore radius (r) the height of the curve at any point along the pore radius axis will reflect not only the intruded volume at that point but also the fact that the numerical value of the function is determined by the pressure at which a given volume is intruded.

The porosity Φ was calculated according to the equation[21, 22]:

$$\Phi=1-\frac{\rho_a}{\rho} \tag{2.6}$$

where ρ_a is the apparent density of the porous polymer particles estimated using the equation:

$$\frac{1}{\rho_a}=V_p+\frac{1}{\rho} \tag{2.7}$$

where V_p is the cumulative pore volume determined from mercury porosimetry and ρ is the skeletal density determined by the picnometric technique in n-

heptane. The value of ρ was taken as 1.068 g/cm^3, which is the density of homogeneous styrene-divinylbenzene copolymer particles. The porosity represents pore fraction contained by the porous particles.

2.3 RESULTS AND DISCUSSION

2.3.1 Monodisperse Polystyrene Latex Particles

Monodisperse polystyrene latexes with a particle diameter of 0.17 μm were prepared by direct emulsion polymerization of styrene and divinylbenzene using Aerosol MA emulsifier according to the recipe given in Table 2-1 (as shown in Figure 2-1). To obtain monodisperse, uniform polymer latexes, two conditions are necessary: (1) the nucleation stage in emulsion polymerization process must be as short as possible; and (2) the colloidal stability of the growing particles must suffice to avoid any aggregation. Polystyrene latexes prepared by emulsion polymerization generally have weight-average molecular weights of 10^6 g/mole, and therefore have a maximum monomer/polymer swelling ratio of about 8 to 1[13, 23, 24].

Successive seeded emulsion polymerization is the method of choice to prepare large-size monodisperse latex particles. Monodisperse polystyrene latexes as large as 56 μm in diameter were prepared by modifying previous polymerization recipes[12, 13] by adjusting the surfactant concentrations. The polymerization process began with the 0.17 μm diameter polystyrene latexes prepared using 0.015% divinylbenzene (DVB), which were grown in successive seeding steps to sizes from 0.3 μm up to 56 μm, as represented in Figure 2-2. Table 2-2 summarizes the polymerization recipes which were used to prepare monodisperse polystyrene latexes as large as 56 μm in diameter. Following this scheme, the size was extended to 200 μm and larger. However, the uniformity of

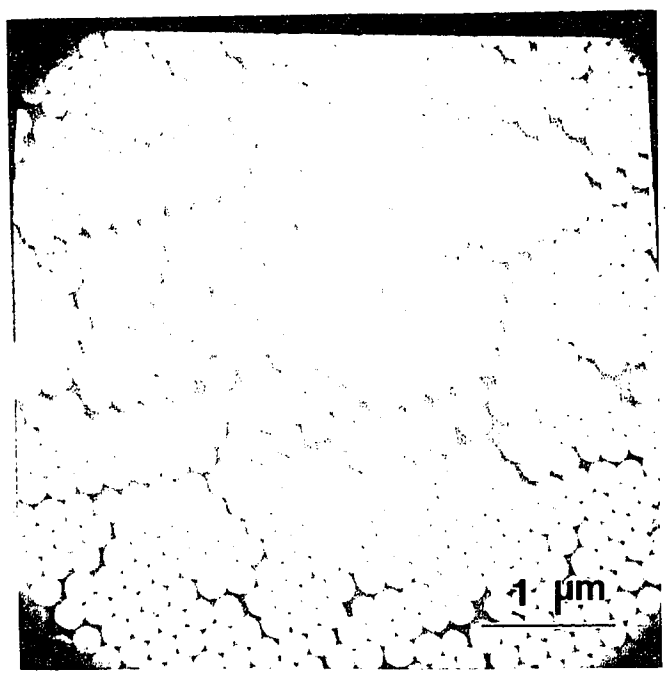

Figure 2-1: *Scanning electron micrograph of monodisperse polystyrene latex particles prepared by emulsion polymerization.*

the larger size latexes was poor; significant numbers of odd-shaped and off-sized particles were found. These were apparently formed by the coalescence of two or more particles of the main distribution during swelling or during the initial stages of polymerization.

Several approaches were used to extend the preparation of monodisperse latexes larger than 100 μm without forming an excessive number of off-sized and odd-shaped particles:

1. Shorten the swelling time: to limit number of collisions between swollen particles in order to reduce the number of oversized particles;

2. Reduction of the monomer/polymer swelling ratio: to decrease the amount of coagulum which is attributed to unabsorbed monomer after swelling;

3. Stabilization of the seed latex with higher concentrations of poly(n-vinyl pyrrolidone) (PVP) K-90 stabilizer: to impart steric stabilization to the particles and to increase the viscosity of the medium;

4. Lower the solids content: to reduce the frequency of colloision and coalescence of particles during swelling and polymerization.

A combination of these approaches has produced latexes of fair uniformity without the formation of excessive off-sized and odd-shaped particles up to 200 μm (Figure 2-3). Table 2-6 summarizes the improved polymerization recipes which were used to prepare these large-particle-size monodisperse polystyrene latexes as large as 200 μm in diameter. However, the sphericity of the particles decreased with increasing size. Some off-sized particles still existed which might have been grown from those particles formed in the earlier steps, which were very difficult to remove by the repeating sedimentation and decantation of the latex particles. Preparation in microgravity will obviate the creaming and settling of the large-particle-size latex particles. The use of the NASA rotating reactor to eliminate the gravity effect may provide a promising means of

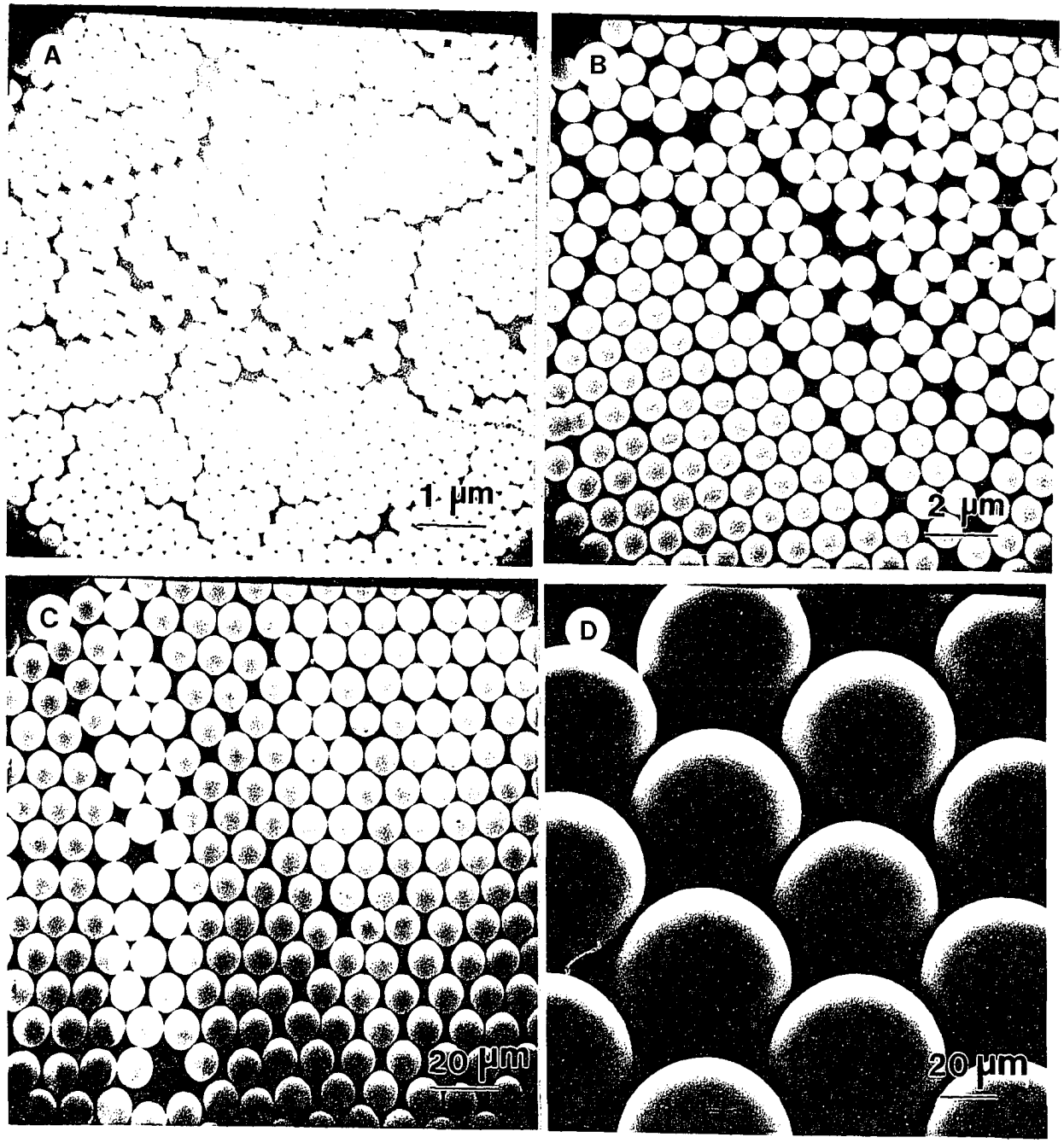

Figure 2-2: *Scanning electron micrographs of monodisperse polystyrene latex particles prepared by successive seeded emulsion polymerization: (A) 0.3 μm; (B) 1.1 μm; (C) 10 μm; and (D) 56 μm.*

preparing large-particle-size monodisperse polystyrene latexes with good uniformity and sphericity (see Appendix A). In addition, it is also suggested that another stabilizer system, such as colloidal stabilizers be sought, or an improved sedimentation/decantation method be developed in order to prepare monodisperse polystyrene latex particles having sizes larger than 200 μm in diameter.

2.3.2 Monodisperse Crosslinked Latex Particles

Highly crosslinked latex particles were prepared by seeded emulsion polymerization using a mixture of styrene and divinylbenzene (DVB) monomers according to the recipe given in Table 2-5 for the preparation of porous polymer particles using linear polystyrene seed particles alone as inert diluents. Figure 2-4 shows scanning electron micrographs of the crosslinked latex particles prepared with 0.015% and 33% divinylbenzene contents. The specific surface area of the smooth particles with 0.015% divinylbenzene content was 0.75 m^2/g. As the divinylbenzene content increased, the particle surfaces became reticulated, which revealed the formation of microgels. However, the surface roughness only contributed around a 1.5 fold increase in the specific surface area value, as presented in Table 2-7. This indicated that crosslinked latex particles with reticulated surface morphology only had relatively low specific surface areas. The particle density increased with the increase in the divinylbenzene content owing to the more compact packing of the polymer network. However, the density increase was minimal with further increases in the divinylbenzene content in the particles.

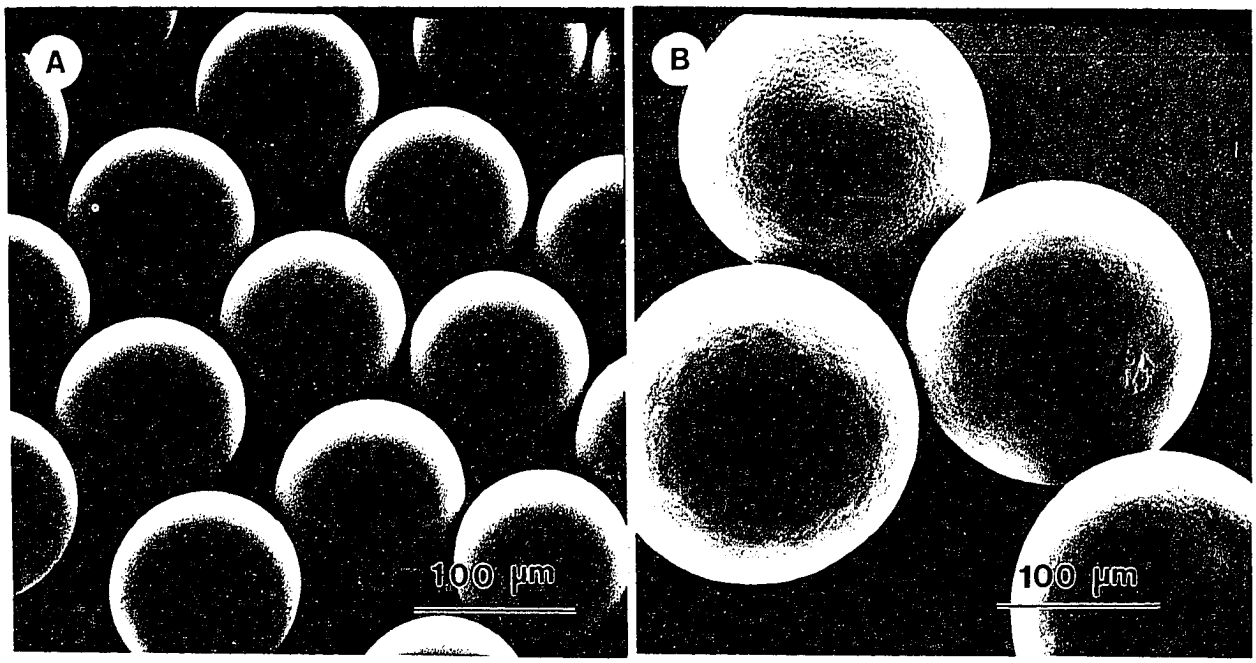

Figure 2-3: *Scanning electron micrographs of the larger polystyrene latexes prepared from the improved seeding sequence: (A) 104 µm; and (B) 205 µm.*

Table 2-6: Improved Polymerization Recipes for Large-Particle-Size Monodisperse Polystyrene Latexes

Step#	1	2	3	4
d_{seed} (μm)	56	75	103	147
M/P	2	2	2	2
d (μm)	75	103	147	205
Seed				
PS particles	5.3	5.3	3.3	3.3
Monomers				
Styrene	14.7	14.7	6.7	6.7
DVB (%M)	0.015	0.015	0.030	0.030
Initiator				
AMBN (%M)	0.12	0.12	0.12	0.12
Surfactants				
AMA (%aq)	0.007	0.007	0.007	0.007
KX-3 (%aq)	0.020	0.020	0.020	0.020
K-90 (%aq)	0.40	1.20	1.20	1.60
Buffer				
$NaHCO_3$ (%aq)	0.04	0.04	0.04	0.04
Inhibitor				
HQ (%aq)	0.03	0.03	0.03	0.03
Water	79.50	78.70	88.70	88.30

** d_{seed}: diameter of monodisperse polystyrene seed latex; M/P: monomer/polymer weight swelling ratio; and d: diameter of final polystyrene latex.*

- *Total charged amount of 80 grams in 4 oz. bottles; seed, monomer and water: % based on total; %M: wt. % based on monomer; and %aq: wt.% based on aqueous phase.*
- *Cleaned seed latex particles were used in all steps.*

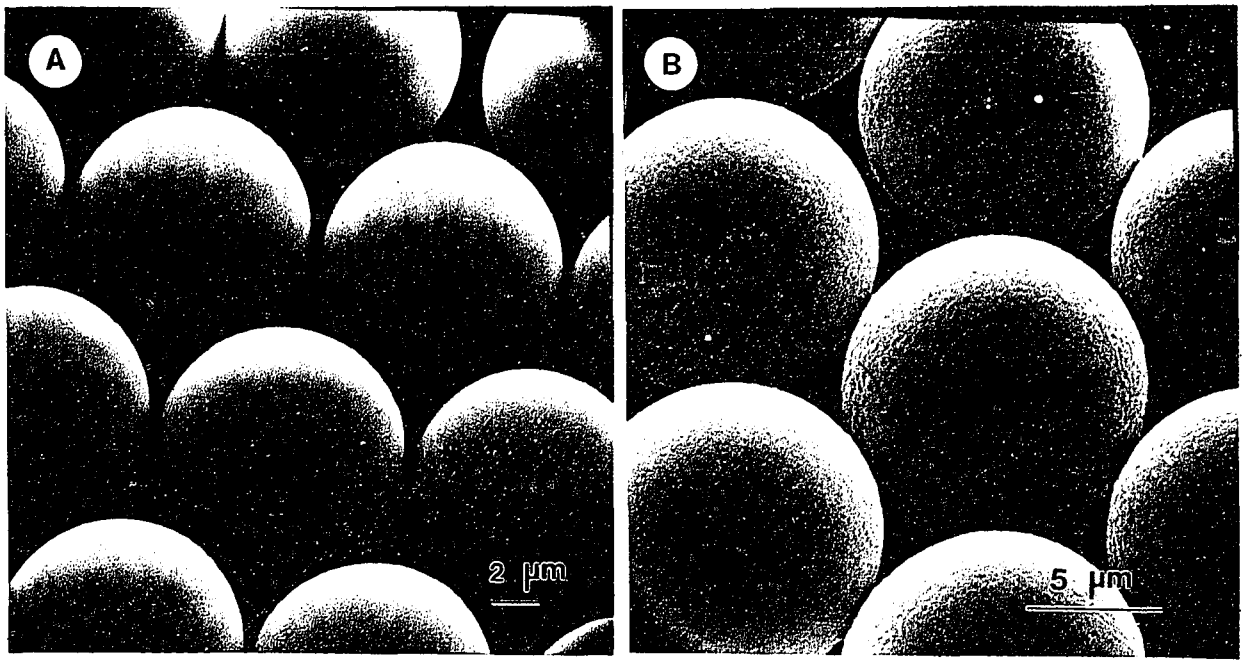

Figure 2-4: *Scanning electron micrographs of the 10 μm crosslinked styrene-divinylbenzene latex particles with (A) 0.015%, and (B) 33% divinylbenzene contents.*

Table 2-7: Physical Features of Monodisperse Polystyrene Latex Particles

d μm	DVB %	S m^2/g	ρ g/cm^3
0.25	15	30	1.068
0.30	0.0	23	1.053
10	0.015	0.75	1.051
11	15	1.05	1.067
11	33	1.30	1.071

* *d: diameter of polystyrene latex particles; DVB%: weight percentages of divinylbenzene in the polymer particles; S: specific surface area; and ρ: density of polystyrene latex particles determined by the picnometric technique in n-heptane.*

2.3.3 Monodisperse Porous Polymer Particles

Monodisperse porous styrene-divinylbenzene copolymer particles in the size range of about 10 μm in diameter were prepared via seeded emulsion polymerization techniques. Mixtures of linear polymer (polystyrene seed) and nonsolvent (e.g., aliphatic hydrocarbon or alcohol) were used as inert diluents. As far as we know, this represents the first preparation of monodisperse macroporous polymer particles formed via seeded emulsion polymerization using these types of diluents[25, 26]. Figure 2-5 shows scanning electron micrographs of the 11 μm porous styrene-divinylbenzene copolymer particles prepared by the use of linear polystyrene (weight-average molecular weight $M_{W,LP} = 1.49 \times 10^6$) and n-hexane as inert diluents with 15% divinylbenzene content according to the recipe listed in Table 2-5. The porous polymer particles possess pores with diameters on the order of 1,000 $\mathring{A}$, which are evenly distributed at the particle surface. The pore shape, similar to common porous

polymer particles, is somewhat irregular as compared to silica packing materials[27]. A particle-size histogram for these polymer particles is given in Figure 2-6. The coefficient of variation of 3% indicates good particle uniformity. The monodispersity is maintained during the synthesis process.

Figure 2-7 illustrates the pore size distribution by mercury porosimetry in the differential mode. Only 5 - 10% of the total pores are smaller than 250 $\mathring{A}$ equivalent radius; this is represented by the area of Curve A left of the dotted line in Figure 2-7. The main portion of the pores are distributed within 400 - 1,000 $\mathring{A}$ with the average pore radius being around 600 $\mathring{A}$, which implies that the polymer particles have a macroporous structure. The nitrogen adsorption-desorption isotherm determined at 77 °K for the 11 μm monodisperse porous polymer particles is shown in Figure 2-8. The typical type II isotherm shows indications of leveling-off at high relative pressures with a very low BET constant ($C = 20$), which is encountered when adsorption occurs on porous particles with pore diameters larger than micropores (a microporous structure is considered to have pore radius less than 10 $\mathring{A}$)[28]. The lack of hysteresis also implies only a small fraction of pores lying in the transitional region (mesopores, pore radii between 10 and 250 $\mathring{A}$). A large portion of the pores are in the macroporous region. This indicates that the macroporous structure observed by scanning electron microscopy and mercury porosimetry is also confirmed by nitrogen adsorption measurements.

Direct observation of the interior structure by scanning electron microscopy was made on samples prepared by a liquid nitrogen freeze-fracture technique. Figure 2-9 shows that the macroporous polymer particles are composed of many interior microspheres and their agglomerates. The pores of the macroporous polymer particles are indeed due to interstices formed between microspheres and agglomerates. The specific surface area of these porous

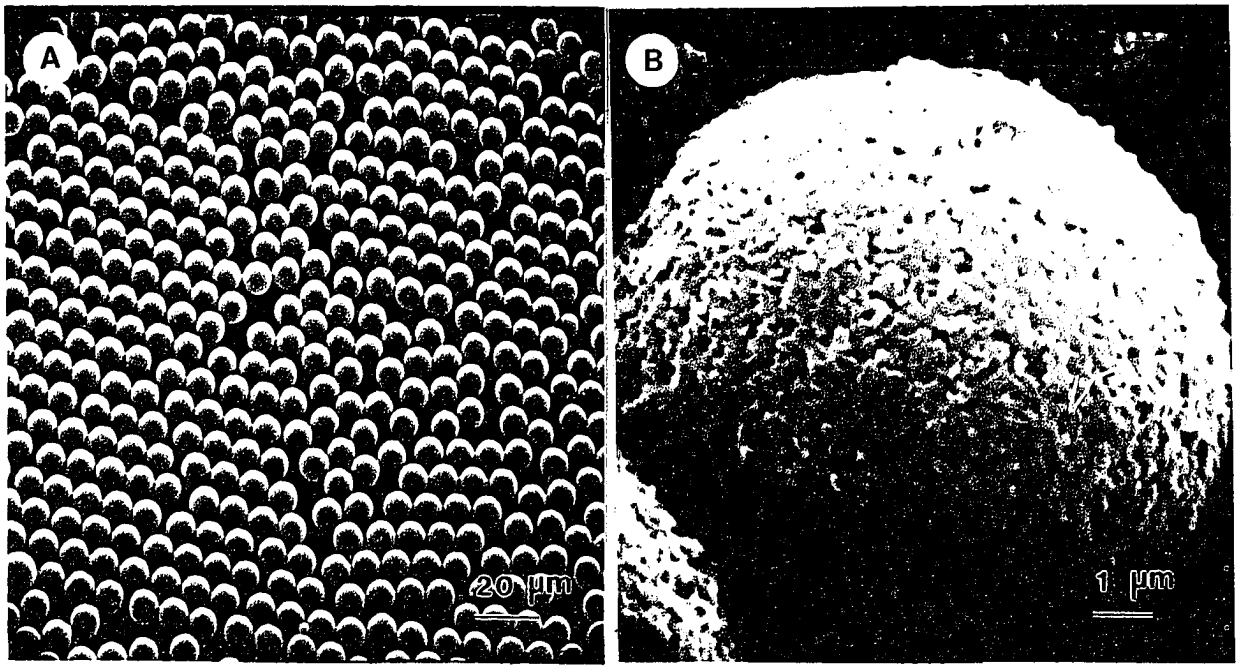

Figure 2-5: *Scanning electron micrographs of the 11 µm monodisperse porous styrene-divinylbenzene copolymer particles: (A) 400 x; and (B) 10,000 x. [diluent: linear polystyrene/n-hexane, 15% DVB, $M_{W,LP}$= 1.49 x 10^6]*

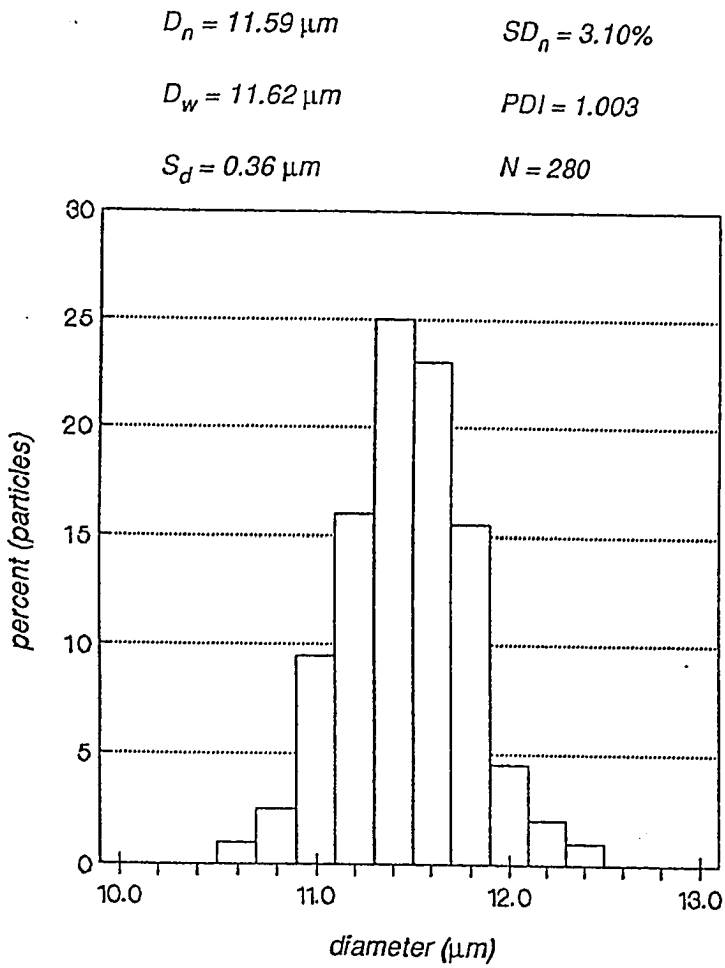

Figure 2-6: *Particle-size histogram of the monodisperse porous styrene-divinylbenzene copolymer particles prepared with linear polystyrene and n-hexane as diluents. D_n is number-average diameter, D_w is weight-average diameter, S_d is standard deviation, SD_n is coefficient of variation based on number-average diameter (= S_d/D_n), PDI is polydispersity index, and N is the number of particles counted. [15% DVB, $M_{W,LP}$= 1.49 x 10^6]*

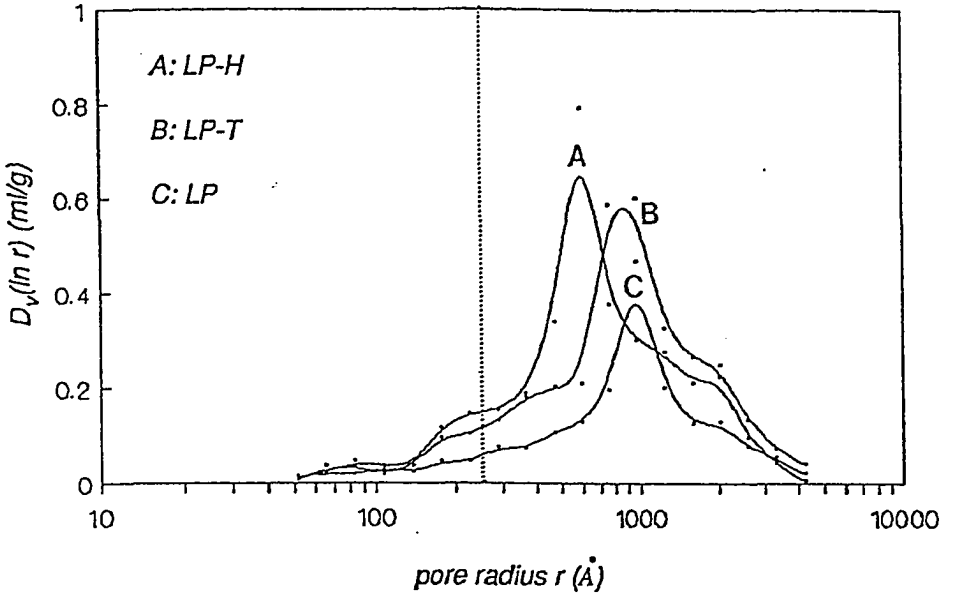

Figure 2-7: *Pore size distributions of monodisperse porous polymer particles prepared with different diluents: (A) LP-H: linear polystyrene/n-hexane; (B) LP-T: linear polystyrene/toluene; and (C) LP: linear polystyrene. The dotted line indicates the position of 250 Å pore radius. [15% DVB, $M_{W,LP}$= 1.49 x 10^6]*

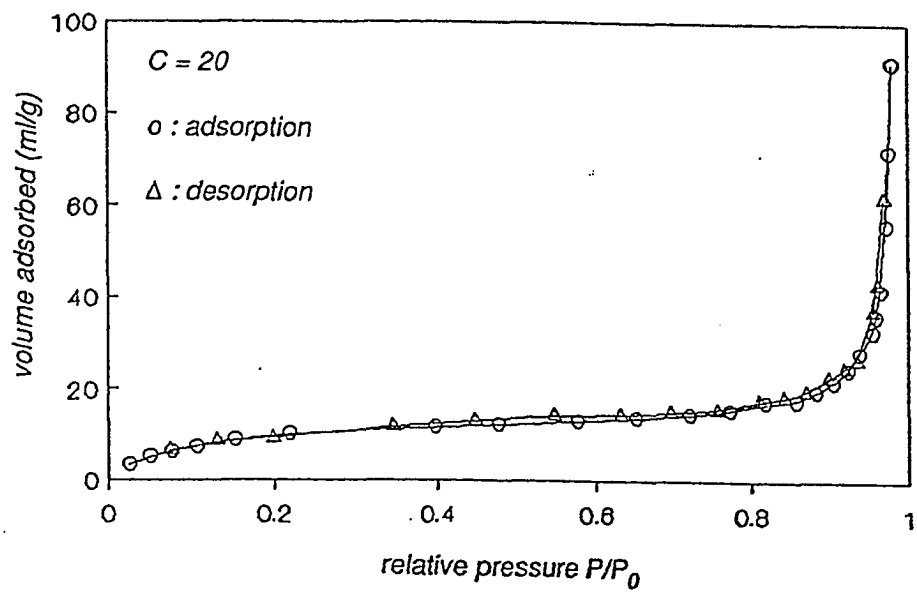

Figure 2-8: *Nitrogen adsorption and desorption isotherms at 77 °K on 11 μm monodisperse porous polymer particles. [diluent: linear polystyrene / n-hexane, 15% DVB, $M_{W,LP}$= 1.49 x 10^6]*

polymer particles is 44 m^2/g, which is much higher than the corresponding 10 μm monodisperse nonporous polystyrene latex particles (0.7 m^2/g); this corresponds to an average compact (nonporous) particle diameter of 0.15 μm. This value is in the same range as those microgels within the macroporous polymer particles. This implies that the working surface area of the porous polymer particles is actually the surface area of those interior microspheres.

Comparing the exterior and interior structures of the porous polymer particles, it is found that at the exterior the individual particle exhibits a flat surface shell consisting of more compactly arranged globules. The formation of such a flat surface shell is attributed to radial forces, arising due to interfacial tension, which affect the surface of the polymerizing particle and compress the surface layer of the globules. The high interfacial tension between the continuous and disperse phases is ascribed to the presence of high-molecular-weight poly(N-vinyl pyrrolidone) K-90 used as stabilizer. This polymeric surfactant increases the viscosity of the medium and the interfacial tension at the boundary of the two phases, thus leading to a flat and more compact structure of the particle surface[29, 30].

The process of formation of pore structure using a mixture of linear polymer and nonsolvent as inert diluent is complex because the copolymerization reaction takes place in the presence of a mixture of the precipitating diluents (both diluents are nonsolvents for the polystyrene and polydivinylbenzene chains). In the early stages of the polymerization, the polymer chains will be in a swollen state because the monomers themselves are good solvents. As the reaction proceeds the monomers are transformed into crosslinked copolymer chains, and phase separation occurs between the styrene-divinylbenzene copolymer and the linear polystyrene and the nonsolvent (e.g.,

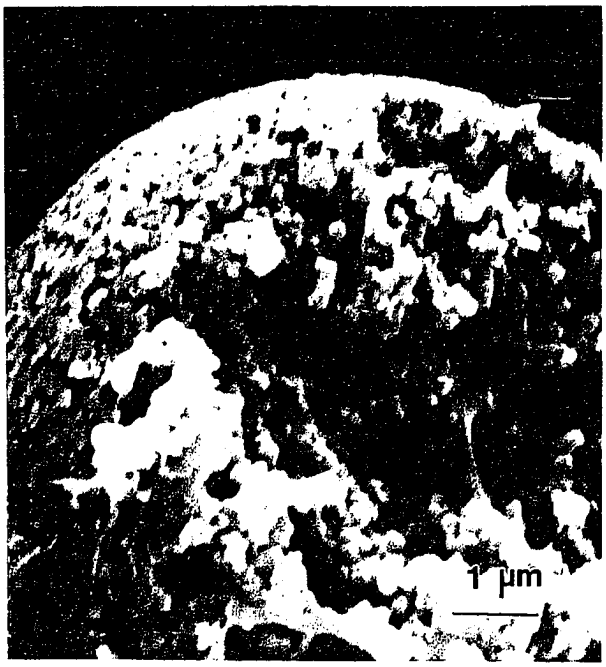

Figure 2-9: *Scanning electron micrograph of the interior structure of a monodisperse porous polymer particle. [Diluent: linear polystyrene/n-hexane, 15% DVB, $M_{W,LP}$= 1.49 x 10^6]*

n-hexane). The consumption of the monomers leads to copolymers whose macromolecular chains become less swollen and also entangle by the continuing copolymerization. As a result, similar to the onset of copolymerization of styrene and divinylbenzene[1, 5, 31, 32, 33, 34, 35], divinylbenzene-rich nuclei are formed and agglomerate. These nuclei are nonprours particles of about 100 $\mathring{A}$ diameter. The agglomeration of the nuclei yields microspheres of about 1,000 $\mathring{A}$ diameter, which in the case of such a mixture of diluents are expected to be spongy. The pores of the porous polymer particles are due to the interspaces formed between the microspheres and their agglomerates.

Nonsolvents such as aliphatic hydrocarbons other than n-hexane or alcohols can also be used in combination with linear polystyrene as inert diluents to prepare monodisperse porous polymer particles. Figure 2-10 shows scanning electron micrographs of the 11 μm porous styrene-divinylbenzene copolymer particles prepared using linear polystyrene and n-heptane (an aliphatic hydrocarbon) or 1-hexanol (an alcohol) as inert diluents. The porous polymer particles also possess pores with average diameters on the order of 1,000 $\mathring{A}$.

Monodisperse macroporous polymer particles can also be prepared using linear polymer alone or a mixture of linear polymer and solvent (e.g., toluene) as inert diluent. The porous polymer particles prepared in this way possess pores with size on the order of 1,000 $\mathring{A}$, which implies that the monodisperse polymer particles also have a macroporous structure (Figure 2-11). Curves B and C in Figure 2-7 show that the average pore radius is around 800 $\mathring{A}$, which is greater than the porous particles prepared with a mixture of linear polymer and nonsolvent as inert diluent as shown in Curve A. This shift in the pore size distribution towards the larger pores is accounted for by the decrease in entanglement of the linear polymer. In the diluent domains, entanglement of

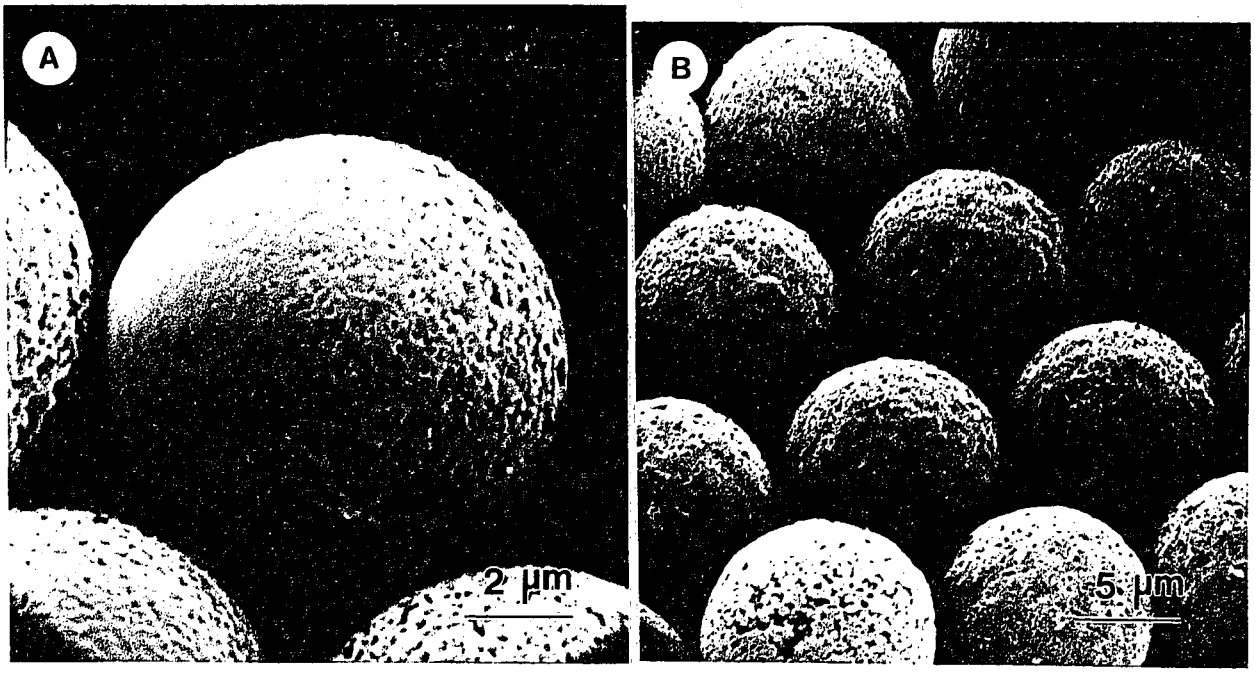

Figure 2-10: *Scanning electron micrographs of the monodisperse porous styrene-divinylbenzene copolymer particles prepared using a mixture of linear polystyrene with (A) n-heptane; or (B) 1-hexanol as inert diluents. [15% DVB, $M_{W,LP}$= 1.49 x 10^6]*

the linear polymer takes place which depends on the interaction of the linear polymer with the copolymer matrix, and with the solvent or nonsolvent. In the absence of the nonsolvent, the linear polymer used as diluent is in a more expanded state during the onset of polymerization, thus it can create large pores within the polymer particles.

Table 2-8 lists the physical characteristics of the monodisperse porous polymer particles prepared using various diluents according to the recipe given in Table 2-5. Depending on the type of diluent used, monodisperse porous polymer particles with different surface areas, pore volumes, porosities, and apparent densities can be synthesized. For the series with 15% divinylbenzene content, the surface area, pore volume, and porosity of the polymer particles prepared using only linear polymer as diluent are much lower than those obtained with the mixture of linear polymer and solvent or nonsolvent as diluents.

The development of pore structure using only the linear polymer as inert diluent may be considered as follows. Early in the reaction, the polymer chains will be in a swollen state because the styrene and divinylbenzene monomers act as solvent. As the monomers are converted into polymer, phase separation occurs between the styrene-divinylbenzene copolymer and the linear polymer, which collapses by loss of solvating monomer. The surface area and pore volume are low because of the low extent of phase separation and collapse during the synthesis process. The linear seed polymer thus prevents the resulting network from having a complete gel structure.

The presence of a solvent during the copolymerization of styrene and divinylbenzene holds the network together after being swollen with the monomer in a more expanded state. Compared to the particles prepared only with linear polymer as inert diluent, less collapse will occur, resulting in a

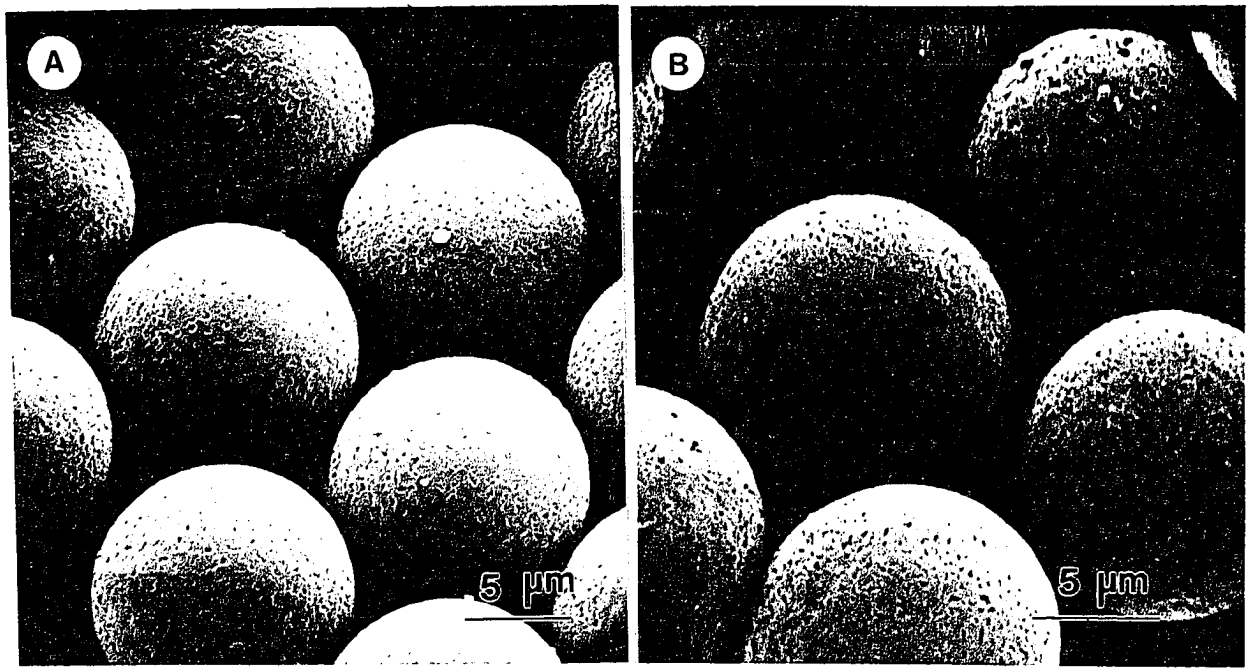

Figure 2-11: *Scanning electron micrographs of the monodisperse porous styrene-divinylbenzene copolymer particles prepared using: (A) linear polystyrene; and (B) linear polystyrene/toluene as inert diluent. [15% DVB, $M_{W,LP}$= 1.49 x 10^6]*

Table 2-8: Physical Characteristics of Monodisperse Porous Polymer Particles

[$M_{W,LP}$= 1.49 x 10^6; 15% DVB[a]]

Diluent	d μm	S m^2/g	V_p ml/g	Φ %	ρ_a g/ml
LP/n-Hexane	11	44	0.75	45	0.593
LP/n-Heptane	11	54	0.73	44	0.600
LP/1-Hexanol	11	35	0.72	43	0.604
LP	13	16	0.40	30	0.748
LP/Toluene	12	32	0.72	43	0.604

[a] *%DVB: weight percentage of divinylbenzene in the polymer particles.*
* *LP: linear polystyrene seed; d: diameter of porous polymer particles; S: specific surface area; V_p: pore volume; Φ: porosity; and ρ_a: apparent density of porous polymer particles.*

higher surface area and pore volume. However, the removal of the solvent after the isolation of the polymer particles results in the shrinkage of the pore structure and some of the small pores collapse as a consequence of cohesion when agglomeration of the crosslinked microdomains cause the polymer chains to approach each other[5, 36]. The specific surface area determined by nitrogen adsorption isotherms for the particles prepared with a mixture of linear polymer and solvent as inert diluent is lower than the particles prepared using a mixture of linear polymer and nonsolvent as inert diluent.

The above observation indicates that the role of linear polymer as inert diluent is to create macropores in the polymer particles. The presence of the solvent-type diluent, especially nonsolvent, enhances the phase separation and structure heterogeneity, which leads to higher specific surface area and pore volume of the polymer particles.

Following this research scheme, different monodisperse porous copolymer particles can be prepared. Figure 2-12 shows a scanning electron micrograph of the 8 μm monodisperse porous methyl methacrylate/diethylene glycol methacrylate copolymer particles prepared according to the recipe given in Table 2-9 using 6 μm-in diameter linear poly(methyl methacrylate) and n-heptane as inert diluents. Acetone was used to remove the linear poly(methyl methacrylate) portion[37, 38]. A dispersion-emulsion two stage polymerization process was used to prepare 6 μm-in diameter monodisperse, linear poly (methyl methacrylate) latex particles[37, 39, 40]. The recipes and polymerization conditions are shown in Tables 2-10 and 2-11. First, monodisperse, linear poly(methyl methacrylate) particles of 3.3 μm in diameter were prepared by dispersion polymerization of methyl methacrylate in methanol according to the recipe given in Table 2-10 using 2,2'-azobis-(isobutyronitrile) initiator, and poly(N-vinyl pyrrolidone) K-30 stabilizer[41]. These particles were used as seed in a seeded emulsion polymerization with methyl methacrylate, according to the recipe given in Table 2-11. The porous methyl methacrylate/diethylene glycol methacrylate copolymer particles possess pores with diameters on the order of 1,000 $\mathring{A}$ with a specific surface area of 52 m^2/g. Therefore, it demonstrates the potential that monodisperse macroporous polymer particles carrying different functional groups may be prepared using this approach, and the particles can be readily used as ion-exchangers or in separation columns. The secondary monomers should be compatible with the seed particles to avoid serious phase separation in order to prepare monodisperse, spherical porous polymer particles which can increase the packing and separation efficiency in the separation column.

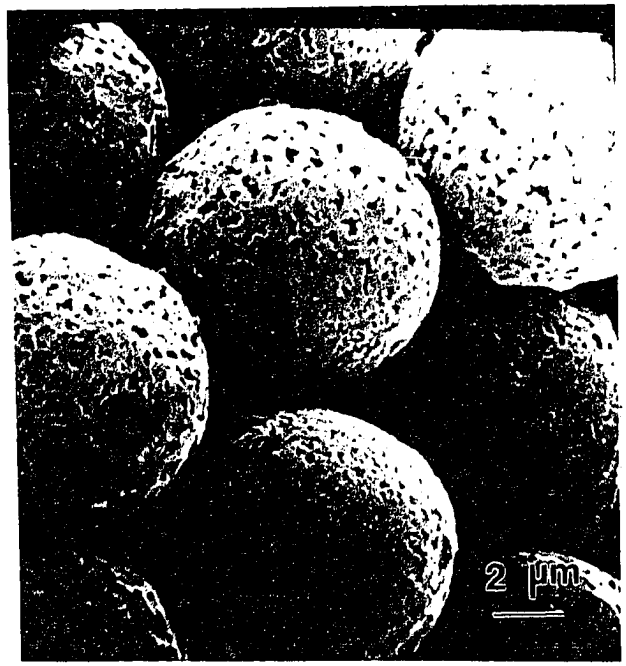

Figure 2-12: *Scanning electron micrograph of the monodisperse porous methyl methacrylate/diethylene glycol methacrylate copolymer particles. [diluent: linear poly(methyl methacrylate)/n-heptane; 15% DEGMA, $M_{W,LP}$= 1.49 x 10^6]*

Table 2-9: Polymerization Recipes for 8 μm-Diameter Monodisperse MMA-DEGMA Copolymer Particles

Ingredient	wt%
Monodisperse PMMA seed[a]	7.5
Monomers	
MMA	10.0
DEGMA	3.0
n-Heptane	9.5
2,2'-Azobis-(2-methylbutyronitrile)	0.018
Aerosol MA	0.005
Polywet KX-3	0.014
Poly(N-vinyl pyrrolidone) K-90	0.800
Hydroquinone	0.021
Sodium bicarbonate	0.027
Water	69.14

[a] Monodisperse poly(methyl methacrylate) seed latex particles (6 μm in diameter).
** MMA: methyl methacrylate; and DEGMA: diethylene glycol methacrylate.*
• Total charged amount of 20 grams in à 1 oz. capped bottle; polymerization temperature at 70 °C for 24 hours.

2.3.3.1 Effect of divinylbenzene content

Figure 2-13 shows the specific surface area measured by nitrogen adsorption as a function of the overall divinylbenzene content for different diluent systems. A high content of divinylbenzene is necessary to obtain a high surface area. An increasing amount of divinylbenzene will increase the specific surface area, due to the decrease in the size of the interior microspheres. The higher the divinylbenzene content, the higher the crosslinking density, and the more dense and smaller the interior microspheres. This can be observed from the interior structure of the particles. Figure 2-13 shows that for a given divinylbenzene concentration, the surface areas of porous polymer particles

Table 2-10: Recipe for Preparation of Monodisperse Poly(methyl methacrylate) Latex by Dispersion Polymerization

Ingredient	wt%
Methyl methacrylate	10.0
2,2'-Azobis(isobutyronitrile)	0.1
Poly(N-vinyl pyrrolidone) K-30	4.0
Methanol	85.9

• *Total charged amount of 40 grams in a 2 oz. capped bottle; polymerization temperature at 55 °C for 48 hours.*

Table 2-11: Recipe for Seeded Emulsion Polymerization of Methyl Methacrylate

Ingredient	wt%
Monodisperse PMMA seed[a]	5.0
Methyl methacrylate	25.0
2,2'-Azobis-(2-methylbutyronitrile)	0.014
Aerosol MA	0.005
Polywet KX-3	0.014
Poly(N-vinyl pyrrolidone) K-90	0.500
Hydroquinone	0.021
Sodium bicarbonate	0.027
Water	69.47

[a] *Monodisperse poly(methyl methacrylate) seed latex particles (3.3 μm in diameter).*
• *Total charged amount of 40 grams in a 2 oz. capped bottle; polymerization temperature at 70 °C for 36 hours.*

prepared using a mixture of linear polymer and nonsolvent (i.e., n-hexane or n-heptane) as inert diluents are larger than those prepared using linear polymer or a mixture of linear polymer and solvent (toluene). Again, the presence of

nonsolvent enhances the phase separation and structure inhomogeneity, which leads to higher surface areas of the porous polymer particles.

Using linear polymer/n-heptane as diluent, the pore volume increased with divinylbenzene content (Figure 2-14). A relatively higher divinylbenzene concentration results in a greater increase in the elastic-retractile force, which would cause the formation of a more crosslinked microsphere and give a higher degree of phase separation[42]. As a result, porous polymer particles with a higher pore volume were synthesized. With 33% divinylbenzene content, monodisperse macroporous polymer particles having pore volume of 0.9 ml/g (porosity of 50%, apparent density of 0.55 g/ml) and surface areas up to 200 m^2/g were prepared.

Figure 2-15 compares the pore size distribution of porous polymer particles made with various divinylbenzene contents. Using the same diluent system of linear polystyrene/n-heptane, the absolute distributions are rather similar, but at higher divinylbenzene content, the pore size distribution shifts to smaller pores. Conversely, at low crosslinker contents, the pores are noticeably larger. The interstices between the microspheres and agglomerates tend to decrease in sizes as the size of the microspheres decreases owing to the higher crosslinker contents.

2.3.3.2 Effect of molecular weight of linear polystyrene seed

To determine the effect of the molecular weight of the linear polystyrene on the pore size distribution of monodisperse porous styrene-divinylbenzene copolymer particles, a series of 8.7 μm-diameter monodisperse polystyrene seed latexes with different molecular weights and molecular weight distributions were used in combination with n-hexane as inert diluents. The seed latexes were prepared according to the recipes listed in Table 2-4 via seeded emulsion polymerization with different concentrations of initiator and chain transfer

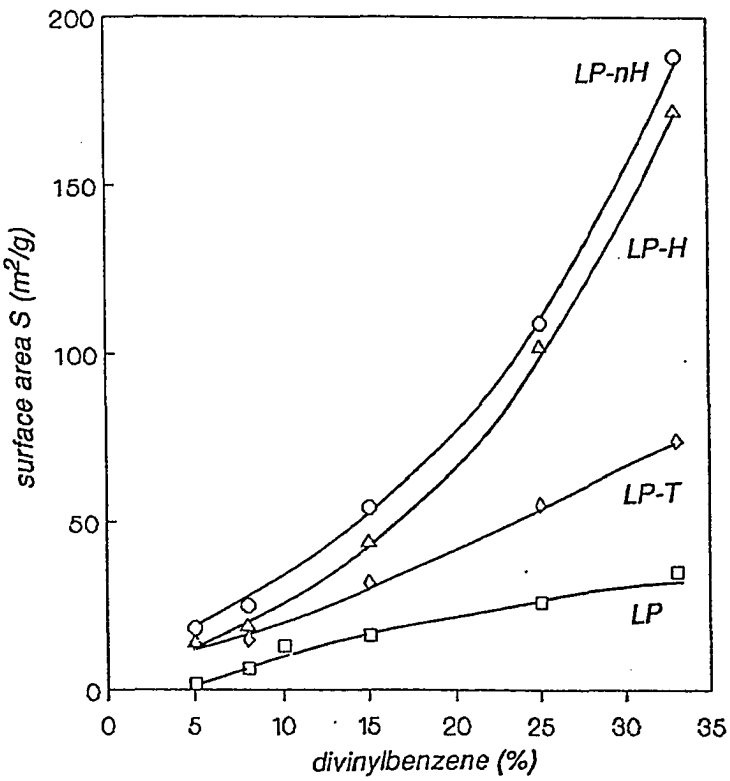

Figure 2-13: *Specific surface area as a function of the divinylbenzene content for monodisperse porous polymer particles prepared with various diluents: (A) LP-H: linear polystyrene/n-hexane; (B) LP-nH: linear polystyrene/n-heptane; (C) LP-T: linear polystyrene/toluene; and (D) LP: linear polystyrene.* $[M_{W,LP} = 1.49 \times 10^6]$

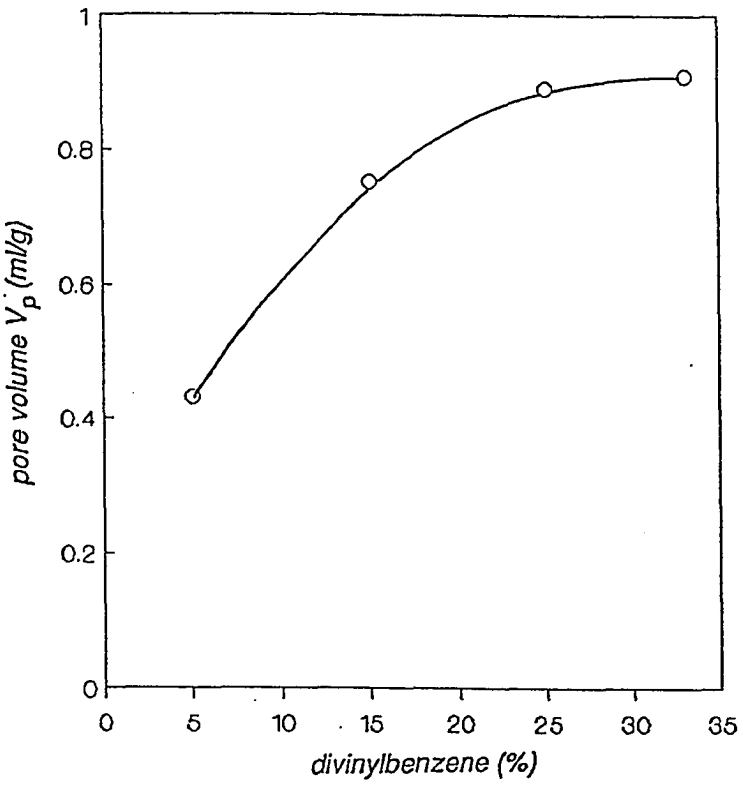

Figure 2-14: *Effect of divinylbenzene content on pore volume. [diluent: linear polystyrene / n-heptane, $M_{W,LP}$= 1.49 x 10^6]*

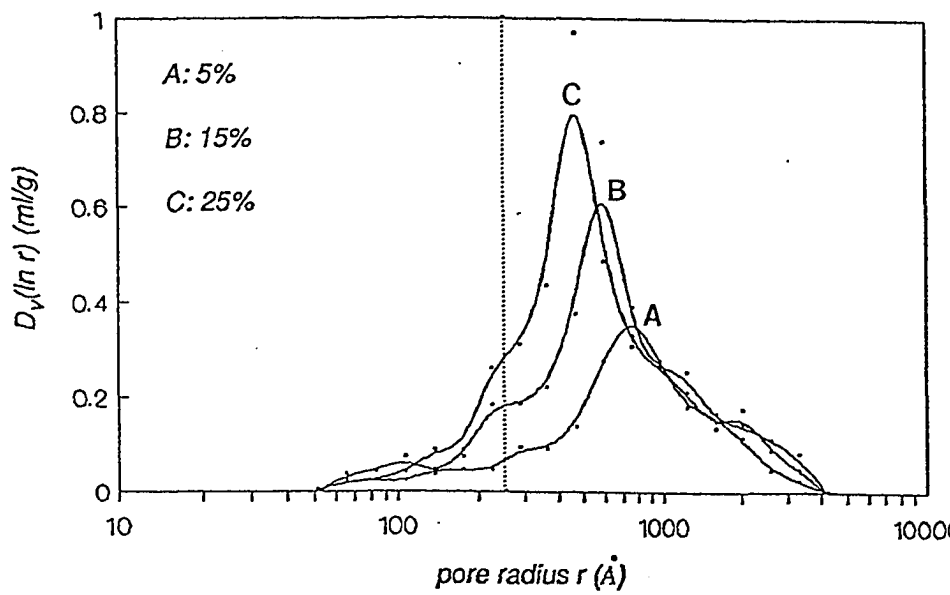

Figure 2-15: *Pore size distributions of monodisperse porous polymer particles prepared with varying divinylbenzene content: (A) 5%; (B) 15%; and (C) 25%. The dotted line indicates the position of 250 Å pore radius. [diluent: linear polystyrene / n-heptane, $M_{W,LP}$= 1.49 x 10^6]*

agent. Thus, the weight-average molecular weight varied from 1.5 x 10^6 to 0.5 x 10^6 and the molecular weight polydispersity indexes ranged from 5 up to 17 as indicated in Table 2-12. Figure 2-16 shows gel permeation chromatograms of these monodisperse polystyrene latexes dissolved in tetrahydrofuran. The characterization results in Table 2-13 show that for the series with constant divinylbenzene content at 15%, the surface area is approximately constant, and so are the pore volume and porosity. However, the pore size distributions are sensitive to the molecular weight of the linear polymer, as shown in Figure 2-17. As the molecular weight of the linear polystyrene is increased, the average pore size becomes larger and the pore size distribution shifts towards the larger pores as demonstrated by Curves D, C, B and A, respectively. Figure 2-17 also shows that there is an increase in the proportion of pores with pore size below the macroporous region of 250 $\mathring{A}$-radius while the molecular weight is decreased as demonstrated by the areas under the curves to the left of the dotted line. The large radius of gyration or hydrodynamic diameter of high molecular polystyrene is responsible for creating large pores during the phase separation and solvent extraction processes. Although the radius of gyration of the linear polystyrene listed in Table 2-12 was estimated in toluene solutions, this should follow the same trend even in a different solvent with the radius of gyration increasing with molecular weight. The shape of the curves obtained for the pore size distributions strongly depend on the molecular weight distribution of the linear polymer. The pore size distribution is narrowest for the linear polymer with the narrowest molecular weight distribution as represented by Curve A in Figure 2-17. The rather broad pore size distribution containing both large and small pores corresponds to the broader molecular weight distribution of the linear polystyrene as represented by Curves C and D. In the diluent phase,

entanglement of the linear polymer takes place, depending on the molecular weight of the polymer, thus explaining the extreme sensitivity of the pore size distribution to the molecular weight of the polymer. This demonstrates the advantage of using linear polymer as diluent: the pore size distribution can be controlled by the molecular weight of the linear polymer seed used as inert diluent.

Table 2-12: Molecular Weight of Linear Polystyrene Seed Particles

Seed	M_N x 10^{-5}	M_W x 10^{-5}	PDI	M_V x 10^{-5}	R_g Å
LP1	2.99	14.9	4.98	11.0	753
LP2	1.48	10.8	7.32	7.28	602
LP3	0.34	5.68	16.9	3.02	366
LP4	0.28	4.46	16.0	2.32	316

* *M_N and M_W: number-average and weight-average molecular weights estimated from gel permeation chromatography; PDI: molecular weight distribution polydispersity index; M_V: viscosity-average molecular weight determined by dilution viscometry in toluene; R_g: radius of gyration estimated from the viscosity-average molecular weight*[43, 44, 45].

2.3.3.3 Effect of crosslinking level of seed particles

Slightly crosslinked monodisperse polymer latex particles can be used instead of linear polystyrene latexes to prepare monodisperse porous polymer particles. Porous polymer particles prepared using slightly crosslinked polystyrene seed latex particles (0.015 - 0.025% divinylbenzene content) were found to possess low surface areas and pore volumes (Table 2-14). As shown in Figure 2-18, the pore size distributions of these particles shift towards smaller pores with a larger portion of the pores lying below the macroporous region (left

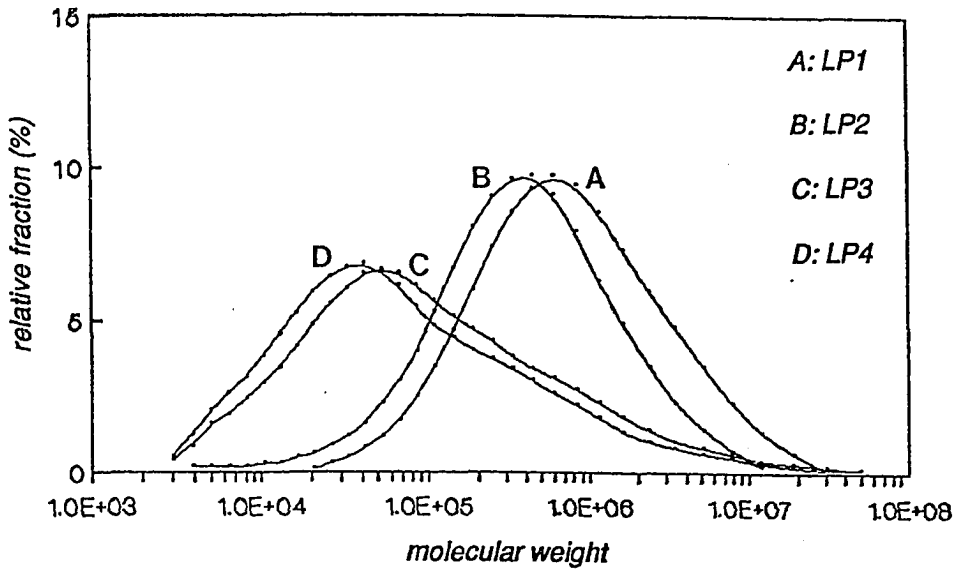

Figure 2-16: *Gel permeation chromatograms of monodisperse polystyrene seed particles dissolved in tetrahydrofuran: (A) LP1: $M_{W,LP}$= 14.9 x 10^5, PDI= 4.98; (B) LP2: $M_{W,LP}$= 10.8 x 10^5, PDI= 7.32; (C) LP3: $M_{W,LP}$= 5.68 x 10^5, PDI= 16.9; and (D) LP4: $M_{W,LP}$= 4.46 x 10^5, PDI= 16.0.*

Table 2-13: Physical Characteristics of Monodisperse Porous Polymer Particles

[Diluent: linear polystyrene/n-hexane; 15% DVB]

Sample	$M_{W,LP}$ x 10^{-5}	PDI	d μm	S m^2/g	V_p ml/g	Φ %	ρ_a g/ml
LP1-H	14.9	4.98	11	44	0.75	45	0.593
LP2-H	10.8	7.32	11	50	0.74	44	0.597
LP3-H	5.68	16.9	11	46	0.72	43	0.604
LP4-H	4.46	16.0	11	42	0.72	43	0.604

* *$M_{W,LP}$: weight average molecular weight of linear polystyrene seed; and PDI: molecular weight distribution polydispersity index.*

of the dotted line). The higher the crosslinking level of the seed particles, the smaller the pore size of the porous polymer particles. This slightly IPN (interpenetrating polymer network) modification restricts the extraction of seed polymer and hence leads to the production of porous polymer particles with small pores and low surface area and pore volume. This IPN modification is an alternative way to control the physical features of porous polymer particles. However, by using a higher level of crosslinking agent in the seed particles (> 0.03% divinylbenzene concentration), the polymerization resulted in a mass of coagulum, which was attributed to serious phase separation and incompatibility between the seed particle and the second-stage highly crosslinked copolymer.

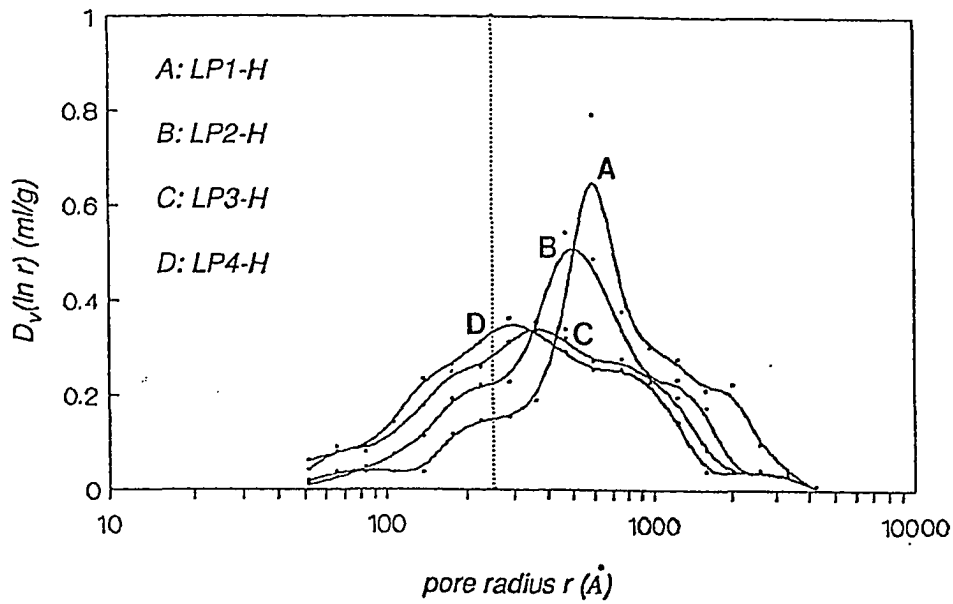

Figure 2-17: *Pore size distributions of monodisperse porous polymer particles prepared with linear polystyrene seed of different molecular weight $M_{W,LP}$ and molecular weight distribution PDI: (A) LP1-H: $M_{W,LP}$= 14.9 x 10^5, PDI= 4.98; (B) LP2-H: $M_{W,LP}$= 10.8 x 10^5, PDI= 7.32; (C) LP3-H: $M_{W,LP}$= 5.68 x 10^5, PDI= 16.9; and (D) LP4-H: $M_{W,LP}$= 4.46 x 10^5, PDI= 16.0. The dotted line indicates the position of 250 Å pore radius. [diluent: linear polystyrene/n-hexane, 15% DVB]*

Table 2-14: Influence of the Crosslinking Level of Seed Particles on Some Physical Features of Porous Polymer Particles

[Diluent: polystyrene seed/n-hexane; 15% DVB]

Sample	CL %	d μm	S m^2/g	V_p ml/g	Φ %	ρ_a g/ml
LP1-H	0.000	11	44	0.75	45	0.593
$LP1^+$-H	0.015	11	22	0.53	36	0.682
$LP2^+$-H	0.025	11	18	0.47	33	0.711

** CL%: weight percentages of divinylbenzene in the seed particles.*

2.4 SUMMARY AND CONCLUSIONS

A new synthesis approach was presented for the preparation of monodisperse porous polymer particles in the size range of 10 μm in diameter. The approach involves seeded emulsion polymerization, using linear polystyrene seed or a mixture of linear polystyrene seed and solvent or nonsolvent as inert diluents. The role of the linear polymer was to create the macroporous structure; the presence of low molecular weight solvent-type diluent enhanced the phase separation and structure heterogeneity. Porous structures were formed by the removal of diluents by solvent extraction after polymerization. The monodispersity of the particles was maintained during this synthesis process. The pore diameters of the resulting macroporous polymer particles were on the order of 1,000 $\mathring{A}$ with pore volumes up to 0.9 ml/g and specific surface areas up to 200 m^2/g.

The physical properties of monodisperse porous polymer particles depended on the diluent type and the crosslinker content, as well as the

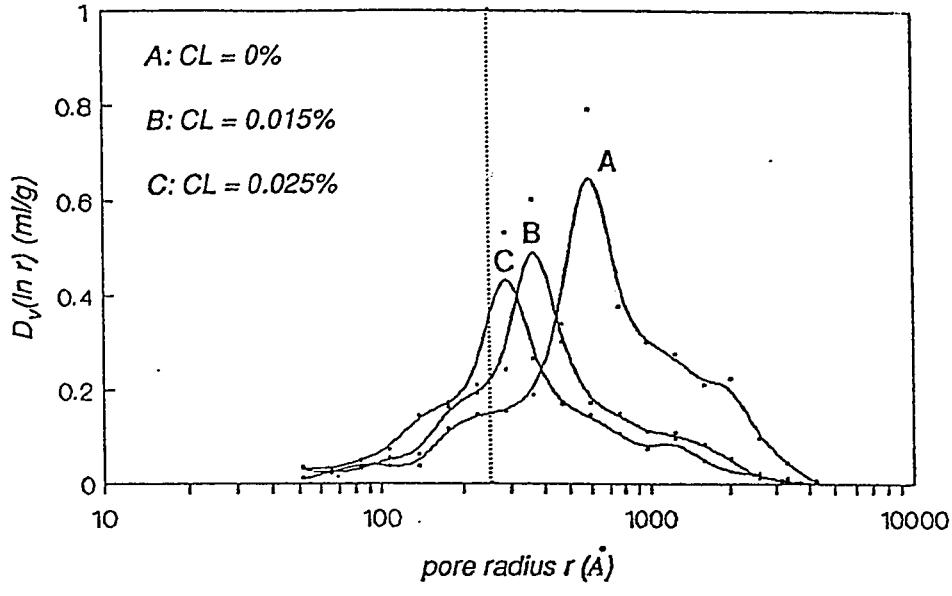

Figure 2-18: *Pore size distributions of monodisperse porous polymer particles prepared with polystyrene seed of different crosslinking levels: (A) 0% DVB; (B) 0.015% DVB; and (C) 0.025% DVB. The dotted line indicates the position of 250 Å pore radius. [diluent: polystyrene seed / n-hexane, 15% DVB]*

molecular weight of the polymer seed particles. Particles prepared using a mixture of linear polymer and nonsolvent as inert diluent resulted in the largest pore volumes and specific surface areas, while particles prepared using linear polymer alone or a mixture of linear polymer and solvent resulted in larger pore sizes compared to the linear polymer-nonsolvent system. Particles prepared using linear polymer alone yielded the smallest pore volume and surface area. Specific surface area and pore volume increased as the divinylbenzene content increased. Pore size distribution was very sensitive to the molecular weight of polymer seed particles. Furthermore, polymer seed with a low degree of crosslinking could also be used to prepare porous polymer particles with smaller pores and pore volumes.

2.5 REFERENCES

1. J. Seidl, J. Malinsky, K. Dusek, and W. Heitz, *Adv. Polym. Sci.*, **5**, 113 (1967).
2. J. R. Millar, *J. Polym. Sci., Polym. Symp.*, **68**, 167 (1980).
3. W. Rolls, F. Svec, and J. M. Frechet, *Polymer*, **31**, 165 (1990).
4. J. Haradil, M. Wojaczynska, F. Svec, and B. N. Kolarz, *React. Polym.*, **4**, 277 (1986).
5. W. L. Sederel and G. J. de Jong, *J. Appl. Polym. Sci.*, **17**, 2835 (1973).
6. J. Ugelstad, L. Soderberg, A. Berge, and J Bergstrom, *Nature*, **303**, 95 (1983).
7. J. Ugelstad and T. Ellingsen, presented at *"64th Colloid and Surface Science Symposium"*, Lehigh University, Bethlehem, PA, June 18-20, 1990.
8. Y. Kato, T. Kitamura, A. Mitsui, and T. Hashimoto, *J. Chromatogr.*, **398**, 327 (1987).
9. E. B. Bradford and J. W. Vanderhoff, *J. Appl. Phys.*, **26**, 684 (1955).
10. J. Ugelstad, P. C. Mork, K. Herder Kaggerud, T. Ellingsen and A. Berge, *Adv. Colloid Interface Sci.*, **13**, 101 (1980).
11. N. Dezelic, J. J. Petres, and G. J. Dezelic, *Kolloid-Z. u. Z. Polym.*, **242**, 1142 (1970).
12. C. M. Tseng, *Ph.D. Dissertation*, Lehigh University (1983).
13. H. R. Sheu, *Ph.D. Dissertation*, Lehigh University (1988).
14. S. Brunauer, P. H. Emmett, and E. Teller, *J. Amer. Chem. Soc.*, **60**, 309 (1938).
15. S. J. Gregg and K. S. W. Sing, *"Adsorption, Surface Area and Porosity"*, 2nd ed., Academic Press, London (1982).
16. F. J. Micale, J. W. Vanderhoff, M. S. El-Aasser, A. C. Ying, N. A. Marshall, and J. M. Hanna, *Preprints Org. Coat. Plast. Div. March 1980*, **42**, 38 (1980).
17. A. A. M. Kamel, *Ph.D. Dissertation*, Lehigh University (1981).
18. E. W. Washburn, *Proc. Nat. Acad. Sci.*, **7**, 115 (1921).
19. I. Dobrevsky and A. Zvezdov, *Powder Technol.*, **29**, 205 (1981).
20. S. Lowell and J. E. Shields, *"Powder Surface Area and Porosity"*, 2nd ed.,

Chapman & Hall, London (1984).

21. C. Luca, I C. Poinescu, E. Avram, A. Ioanid, I. Petrariu, and A. Carpov, *J. Appl. Polym. Sci.*, **28**, 3701 (1983).

22. I. C. Poinescu, C. Beldie, and C. Vald, *J. Appl. Polym. Sci.*, **29**, 23 (1984).

23. C. M. Tseng, M. S. El-Aasser, and J. W. Vanderhoff, in *"Computer Applications in Applied Polymer Science"*, T. Provder, ed., ACS Symp. Series No. 197, American Chemical Society, Washington, D.C., 1982, p. 197.

24. L. H. Jansson, M. C. Wellon, and G. W. Poehlein, *J. Polym. Sci., Polym. Lett. Ed.*, **21**, 937 (1983).

25. C. M. Cheng, M. S. El-Aasser, and J. W. Vanderhoff, presented at *"64th Colloid and Surface Science Symposium"*, Lehigh University, Bethlehem, PA, June 18-20, 1990.

26. C. M. Cheng, M. S. El-Aasser, and J. W. Vanderhoff, Presented at *"AIChE 1990 Annual Meeting"*, Chicago, November 11-16, 1990.

27. J. R. Benson and D. J. Woo, *J. Chromatogr. Sci.*, **22**, 386 (1984).

28. K. S. W. Sing, D. H. Everett, R. A. W. Haul, L. Moscou, R. A. Pierotti, J. Rouquerol, and T. Siemieniewska, *Pure & Appl. Chem.*, **57**, 603 (1985).

29. D. Horak, Z. Pelzbauer, F. Svec, and J. Kalal, *J. Appl. Polym. Sci.*, **26**, 3205 (1981).

30. Z. Pelzbauer, J. Lukas, F. Svec, and J. Kalal, *J. Chromatogr.*, **171**, 101 (1979).

31. K. A. Kun and R. Kunin, *J. Polym. Sci.*, **A6**, 2689 (1968).

32. H. Jacobelli, M. Bartholin, and A. Guyot, *J. Appl. Polym. Sci.*, **23**, 927 (179).

33. H. Jacobelli, M. Bartholin, and A. Guyot, *Angew. Makromol. Chem.*, **80**, 31 (1979).

34. D. Y. D. Chung, M. Bartholin, and A. Guyot, *Angew. Makromol. Chem.*, **103**, 109 (1982).

35. O. Okay, *J. Appl. Polym. Sci.*, **32**, 5533 (1986).

36. O. Okay, *Angew. Makromol. Chem.*, **153**, 125 (1987).

37. S. Shen, V. L. Domonie, E. D. Sudol, M. S. El-Aasser, and J. W. Vanderhoff, *Polym. Mat. Sci. Eng.*, **63**, 967 (1990).

38. S. Shen, V. L. Dimonie, M. S. El-Aasser, and J. W. Vanderhoff, *Graduate Research Progress Reports*, Emulsion Polymers Institute, Lehigh University, **30**, 20 (1988).

39. M. A. Winnik, R. Lukas, W. F. Chen, P. Furlong, and M. D. Croucher, *Makromol. Chem., Macromol. Symp.*, **10/11**, 483 (1987).

40. K. E. J. Barreet, *Br. Polym. J.*, **5**, 259 (1973).

41. S. Shen, M. S. El-Aasser, and J. W. Vanderhoff, *Graduate Research Progress Reports*, Emulsion Polymers Institute, Lehigh University, **32**, 21 (1989).

42. H. R. Sheu, M. S. El-Aasser, and J. W. Vanderhoff, *J. Polym. Sci. Polym. Chem. Ed.*, **28**, 653 (1990).

43. J. P. Cotton, *J. Physique - Letters*, **41**, 231 (1980).

44. Y. C. Chen, *M.S. Research Report*, Lehigh University (1989).

45. R. D. Jenkins, *Ph.D. Dissertation*, Lehigh University (1990).

Chapter 3
Pore Structural Studies of Monodisperse Porous Polymer Particles

3.1 INTRODUCTION

Monodisperse porous styrene-divinylbenzene copolymer particles in the size range of 10 μm in diameter were prepared via seeded emulsion polymerization[1, 2, 3, 4]. Linear polymer (polystyrene seed) or a mixture of linear polymer and solvent or nonsolvent were used as inert diluents. Porous structure was formed by the removal of diluents via solvent extraction after polymerization. Monodisperse porous polymer particles can be adopted for use as polymeric adsorbents, particularly in extractions from water by exploiting molecular sieve properties and as packings for chromatography columns[5]. Porous polymer particles with large pore structures are useful for the separation of biomolecules[6]. It is expected that the improved separation efficiency and optimal packing can be achieved with monodisperse porous polymer particles as compared to polydisperse separation media[7].

In the analysis of pore structure of porous materials, a convenient classification based on the pore width has been adopted by the IUPAC[8, 9, 10]: (a) *micropores* have widths of up to 20 $\mathring{A}$; (b) *mesopores* have widths in the range 20 - 500 $\mathring{A}$; and (c) *macropores* have widths greater than 500 $\mathring{A}$. A porous domain was defined, where the structure can be described as an agglomeration of quasi-spherical particles with different levels of agglomeration[5, 11, 12, 13, 14, 15, 16]: the smaller particles, nuclei, are nonporous particles of about 100 $\mathring{A}$ diameter. Nuclei are agglomerated in microspheres of about 1,000 $\mathring{A}$ diameter and microspheres are agglomerated again in larger irregular moieties inside the polymer bead. It has been asserted[12, 17] that porous polymer particles may

have different levels of particle substructure with the particle consisting of randomly packed microspheres and the microspheres in turn packed with crosslinked nuclei. Macropores and mesopores may exist between microspheres and their agglomerates, and micropores may be generated within the microspheres.

Monodisperse polystyrene latex particles prepared via seeded emulsion polymerization usually have high molecular weight on the order of 10^6. In the synthesis of monodisperse porous styrene-divinylbenzene copolymer particles, monodisperse polystyrene latex particles were used as inert diluent. These high molecular weight polystyrene, which have large average radius of gyration or hydrodynamic diameter, should create large pores during the phase separation and solvent extraction processes. Thus, this chapter is intended to analyze the pore structure of these monodisperse porous polymer particles prepared by the use of high molecular weight linear polymer as inert diluent. Of particular interest is the internal structure, as well as the magnitude and distribution of pore size.

3.2 EXPERIMENTAL

3.2.1 Materials and Preparation

Monodisperse porous styrene-divinylbenzene copolymer particles in the size range of 10 μm in diameter were prepared by seeded emulsion polymerization using different types of diluents and varying the concentration of divinylbenzene. The general procedure for the preparation was previously described in Chapter 2. A series of 8.7 μm-diameter monodisperse polystyrene seed latexes with different molecular weights and molecular weight distributions were used as inert diluents (Table 2-12). The seeded emulsion polymerizations were carried out at 30% organic phase according to the basic

recipe given in Table 2-5 in Chapter 2. The ingredients used comprised monodisperse polystyrene seed latex, styrene and divinylbenzene (DVB) monomers, diluent (solvent or nonsolvent), 2,2'-azobis-(2-methylbutyronitrile) initiator (E. I. duPont de Nemours), hydroquinone inhibitor, sodium bicarbonate buffer, Aerosol MA emulsifier (dihexylester of sodium sulfosuccinic acid; American Cyanamid), Polywet KX-3 oligomeric surfactant (n-octyl-S-[acrylonitrile]$_8$-[acrylic acid]$_8$-H, M_w= 1,500; Uniroyal Chemical), poly(N-vinyl pyrrolidone) K-90 surfactant (GAF Corp.). Distilled deionized water was used to prepare aqueous solutions. The ingredients, with a total weight of 80 grams, were added to 4 oz. capped bottles, which were tumbled end-over-end for 12 hours at room temperature (23 °C) to allow the seed particles to swell with the monomer-diluent mixture. The polymerizations were carried out by tumbling the bottles end-over-end at 16 rpm in a thermostated water bath at 70 °C for 24 hours. The concentration of emulsifiers was selected to prevent formation of coagulum or small secondary particles during polymerization. After polymerization, the latex particles were extracted with methylene chloride (a good solvent for polystyrene) in a Soxhlet apparatus for 36 hours to remove the linear polymer portion, followed by washing with methanol to remove residual methylene chloride and low molecular weight solvent-type diluent (solvent or nonsolvent). After solvent extraction, the polymer particles were dried in air at room temperature and then vacuum-dried in an oven at 45 °C.

3.2.2 Characterization of Porous Particles

The surface morphology and particle size of the porous polymer particles were characterized using an ETEC Autoscan scanning electron microscope.

The surface area *(S)* of the particles was measured by nitrogen adsorption isotherms. Nitrogen adsorption at 77 °K was determined volumetrically in a

Quantasorb Sorption System as described in Chapter 2. The BET equation was used to analyze the nitrogen adsorption isotherms in order to calculate the surface areas of the particles[18, 19]:

$$\frac{1}{V_{ads}[(P/P_o)-1]} = \frac{1}{V_{ads,m}C} + \frac{C-1}{V_{ads,m}C}\left(\frac{P}{P_o}\right) \tag{3.1}$$

where V_{ads} is the volume of adsorbate adsorbed at relative pressure P/P_o, P is adsorbate equilibrium pressure, P_o is adsorbate saturated equilibrium pressure, C is the BET constant, and $V_{ads,m}$ is the volume of adsorbate adsorbed in a monolayer. The specific surface area is given by[18, 19]

$$S = \frac{V_{ads,m}\overline{N}a_m}{\overline{V}} \tag{3.2}$$

where a_m is the cross sectional area of adsorbate (a_m = *16.2* $\mathring{A}^2$ for nitrogen), $\overline{V}$ is the molar volume of adsorbate, and $\overline{N}$ is Avogadro's number. The complete nitrogen adsorption-desorption isotherms were measured and analyzed for the pore size distribution based on the Kelvin equation which relates condensation pressure to radius of curvature[19]:

$$ln\frac{P}{P_o} = -\frac{2\gamma\overline{V}}{rRT}cos\theta \tag{3.3}$$

where P is the equilibrium vapor pressure of the liquid contained in a narrow pore of radius r and P_o is the equilibrium pressure exhibiting a plane surface. The terms γ and $\overline{V}$ are the surface tension and molar volume of the liquid, respectively, and θ is the contact angle with which the liquid meets the pore wall. The gas constant and absolute temperature were indicated by R and T.

Pore volume and pore size distribution were determined by mercury intrusion porosimetry on a Micromeritics AutoPore 9200 porosimeter as described in Chapter 2. The pore radii (r) quoted were those of equivalent hollow cylinders obtained from the intruded pressure (P), using the Washburn equation[19, 20]:

$$r = -\frac{2\gamma \cos\theta}{P} \tag{3.4}$$

where the terms γ and θ were the surface tension and wetting angle of mercury, respectively. In these measurements, γ of 485 dyne/cm and θ of 130° were assumed. The cumulative pore volumes (V_p) were estimated from the intruded mercury volumes of the pores larger than 50 $\mathring{A}$-equivalent radius.

The volume *ln* pore radius distribution function $D_v(ln\ r)$ as described in Chapter 2 was used to express pore size distribution to reduce the wide range of values which the volume pore-size distribution function $D_v(r)$ could exhibit[21].

3.3 RESULTS AND DISCUSSION

Monodisperse porous styrene-divinylbenzene copolymer particles in the size of 10 μm in diameter were prepared via seeded emulsion polymerization techniques. Linear polymer (polystyrene seed) or a mixture of linear polymer and solvent or nonsolvent were used as inert diluents. Porous structure was obtained by the removal of diluents via solvent extraction after polymerization. Of relevance to this discussion are the representative examples cited in Figures 3-1 and 3-2, and Table 3-1.

Figure 3-1 shows scanning electron micrographs of typical 11 μm monodisperse porous styrene-divinylbenzene copolymer particles. Very good particle uniformity indicates that monodispersity was maintained during the

synthesis process. Figure 3-1B shows that the porous polymer particles possess pores with diameters on the order of 1,000 $\mathring{A}$, which are evenly distributed at the particle surface. The pore shape, which is similar to common porous polymer particles, is somewhat irregular as compared to silica packing materials[22]. A scanning electron micrograph of the interior of a porous polymer particle is shown in Figure 3-2, where the sample was prepared by a liquid nitrogen freeze-fracture technique. The indication is that the porous polymer particles are composed of many voids created between interior microspheres and their agglomerates. Thus, the pores of the porous polymer particles are considered to be the interstices between these crosslinked microspheres and agglomerates[4].

The physical characteristics of monodisperse porous polymer particles, as listed in Table 3-1, depend on the diluent type and the crosslinker concentration. At constant divinylbenzene concentration, the specific surface area and pore volume of porous polymer particles prepared using only linear polymer as diluent are much lower than the porous particles prepared with a mixture of linear polymer and solvent (toluene) or nonsolvent (n-hexane) as diluents. The role of high molecular weight linear polymer used as inert diluent was in the creation of macropores[3]. The presence of low molecular weight solvent-type diluent (solvent or nonsolvent) enhances the phase separation and structure heterogeneity, which leads to higher specific surface areas and pore volumes of the porous polymer particles. The specific surface areas and pore volumes of the porous polymer particles were found to increase with increasing divinylbenzene concentration. The data in Table 3-1 also show that the surface area and pore volume were approximately constant when using linear polystyrene with different molecular weights (LP1, 2, 3 & 4) in combination with n-hexane as inert diluent. These results indicate that the high molecular weight linear polymers, having weight-average molecular weight $M_{W,LP}$ on the

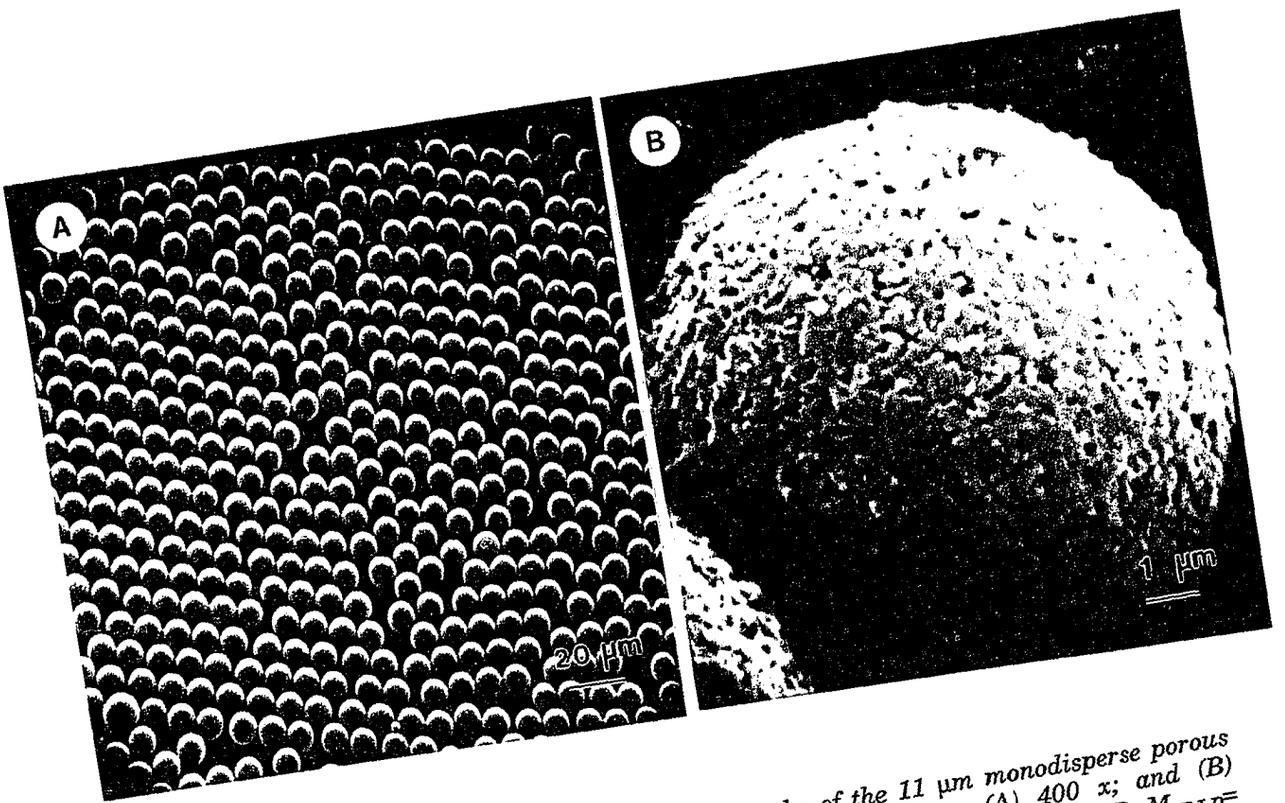

Figure 3-1: *Scanning electron micrographs of the 11 μm monodisperse porous styrene-divinylbenzene copolymer particles: (A) 400 x; and (B) 10,000 x. [diluent: linear polystyrene/n-hexane, 15% DVB, $M_{W,LP}$= 1.49 x 10^6]*

Figure 3-2: *Scanning electron micrograph of the interior structure of monodisperse porous polymer particles. [Diluent: linear polystyrene/n-hexane, 15% DVB, $M_{W,LP}$= 1.49 x 10^6]*

order of 10^6, show the same precipitating ability to create porous polymer particles with the same specific surface area. The almost identical pore volume is owed to the same diluent content.

Table 3-1: Physical Characteristics of Monodisperse Porous Polymer Particles

Diluent	DVB %	d μm	S m^2/g	V_p ml/g
LP1	15	13	16	0.40
LP1/Toluene	15	12	32	0.72
LP1/n-Hexane	15	11	44	0.75
LP1/n-Hexane	5	11	14	0.43
LP1/n-Hexane	25	11	102	0.89
LP1/n-Hexane	33	11	172	0.91
LP2/n-Hexane	15	11	50	0.74
LP3/n-Hexane	15	11	46	0.72
LP4/n-Hexane	15	11	42	0.72

** LP1, 2, 3 and 4 are linear polystyrene seeds with different average molecular weights and molecular weight distributions (see Table 2-12);*
*** DVB%: weight percentage of divinylbenzene in the polymer particles; d: diameter of porous polymer particles; S: apparent BET specific surface area; and V_p: cumulative pore volume estimated from mercury porosimetry.*

3.3.1 Mercury Porosimetry

3.3.1.1 Analysis of intrusion porogram

In the analysis of mercury porosimetry data, the Excil silica porous particles (Supleco Inc.) for ion-exchangers were used as calibration standards. These 5 μm-diameter uniform silica porous particles have very narrow pore size distribution with an average pore size of 300 $\mathring{A}$ in pore radius. Figure 3-3 shows the pore size distribution of the Excil porous particles by mercury porosimetry

in the differential mode. A plot of the intruded volume of mercury versus pressure or pore radius is called a porogram[21, 23, 24, 25, 26]. Figure 3-4 shows the porograms of cumulative volume plotted versus pressure and pore radius for the Excil silica porous particles. As shown in Figure 3-4A, the initial intrusion (between points 1 and 2) at very low pressure is due to filling of the dilatometer. The positive slope between points 2 and 3 on the intrusion curve results from the penetration into the interparticle voids when the sample is a powder and continued filling of the torroidal volume between the contacting particles. As the pressure is further increased mercury will penetrate deeper into the narrowing cavities between the particles. Between points 4 and 5 on the intrusion curve in Figure 3-4A intrusion commences into a new range of cavities which, if cylindrical in shape, would posses circular openings of about 300 $\mathring{A}$ radius. Little further intrusion taking places up to the maximum pressure corresponding to point 5 indicated that the majority of the pores were larger than 100 $\mathring{A}$ radius. This can also be observed in Figure 3-4B. This range of intrusion occurs at a pressure substantially greater than was required to fill the interparticle voids. Therefore, mercury is intruding into small pores within the particles.

Mercury porosimetry results on Excil silica porous particles show a rapid penetration over a small pressure range, with little further penetration as the intrusion pressure is increased. This result is indicative of a uniform pore structure with a narrow pore size distribution.

Figure 3-5 illustrates the porograms of cumulative volume plotted versus pressure and pore radius for the 11 μm monodisperse porous polymer particles, 10 μm nonporous polystyrene latexes, and 0.25 μm nonporous crosslinked polystyrene latexes. Compared with the porogram of the Excil porous particles, these porograms indicated that the initial intrusion at very low pressure is due to filling of the porosimetric dilatometer and penetration into the interparticle

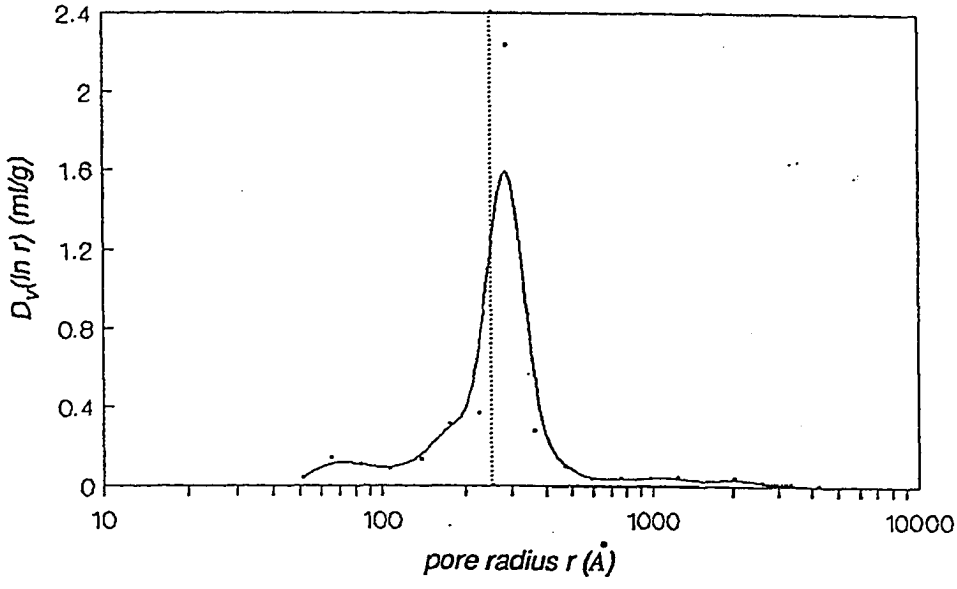

Figure 3-3: *Pore size distribution of the Excil silica porous particles. The dotted line indicates the position of the 250 Å pore radius.*

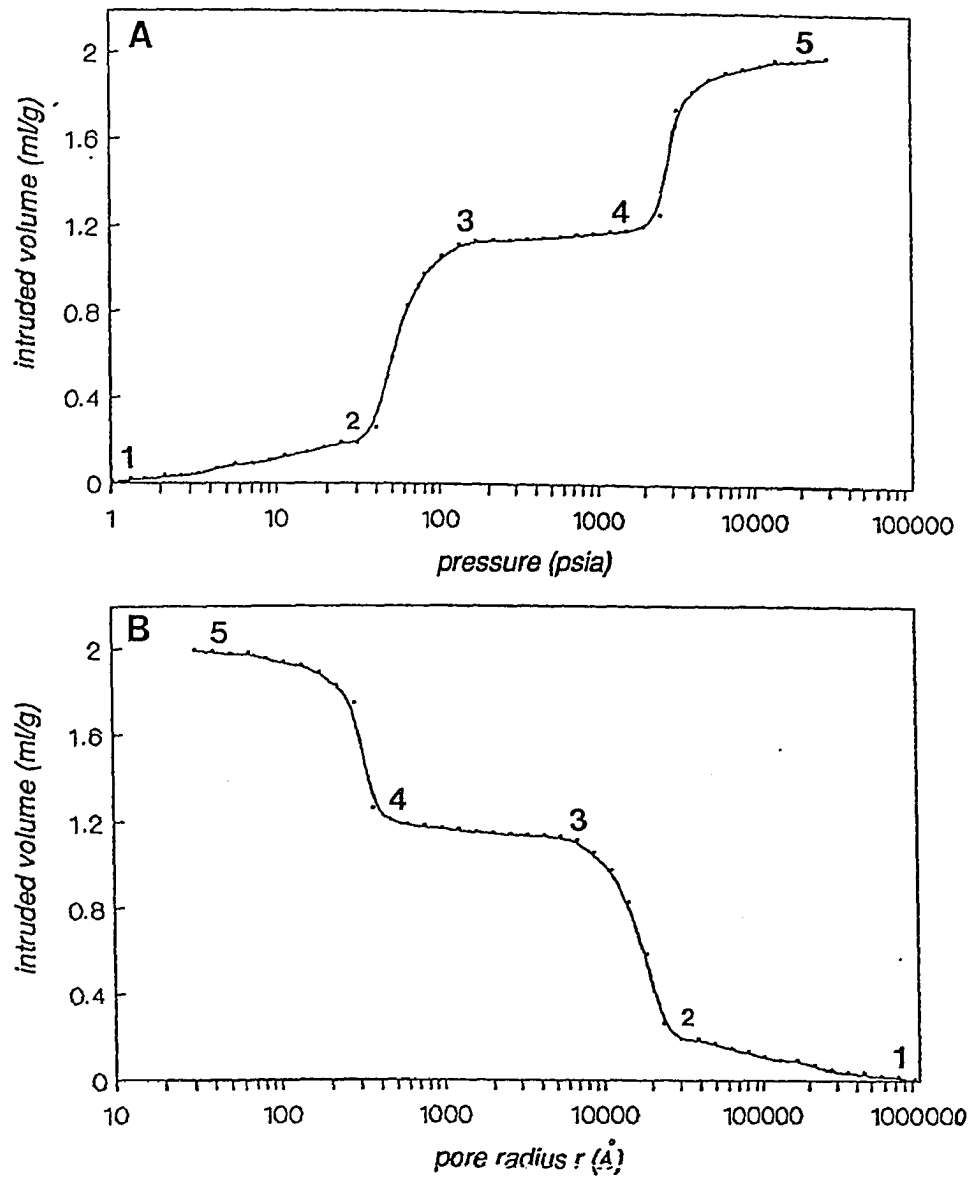

Figure 3-4: *Mercury intrusion porograms for Excil silica porous particles: (A) intruded volume versus pressure; and (B) intruded volume versus pore radius.*

voids in the dried powder sample. The curves between points 1 and 2 on the intrusion curve results from the continued filling of the torroidal volume between the contacting particles. Between points 2 and 3 on the intrusion curve A in Figure 3-5 intrusion commences into a new range of cavities which, if cylindrical in shape, would possess circular openings of about 1,000 $\mathring{A}$ radius. This range of intrusion occurs at a pressure substantially greater than was required to fill the interparticle voids. Therefore, mercury is intruding into small pores within the particles. The sharp increase in intruded volume in the low pressure region (below 100 psia) of the porosimeter results was indicative of the narrow particle size distribution of the 10 μm-diameter nonporous monodisperse polymer particle samples (which were prepared via seeded emulsion polymerization according to the recipe given in Table 2-3), as demonstrated by Curves A and B in Figure 3-5. Slightly more than one-third of the total intruded pore volume is due to the pores in between the particles.

By using a random packing model of uniform spherical particles to simulate the process of fine powder compaction during mercury porosimetry, Smith[27] demonstrated the relative magnitudes of the pore volume distribution curve corresponding to interparticle void filling and pore filling. A dimensionless pressure P^* and a dimensionless radius β were used to describe the interparticle void filling and pore filling process, respectively:

$$P^* = \frac{PR_o}{\gamma} \tag{3.5}$$

$$\beta = \frac{r}{R_o} = \frac{2\cos\theta}{P^*} \tag{3.6}$$

where P is the intruded pressure, R_o the radius of the particle, r the pore radius,

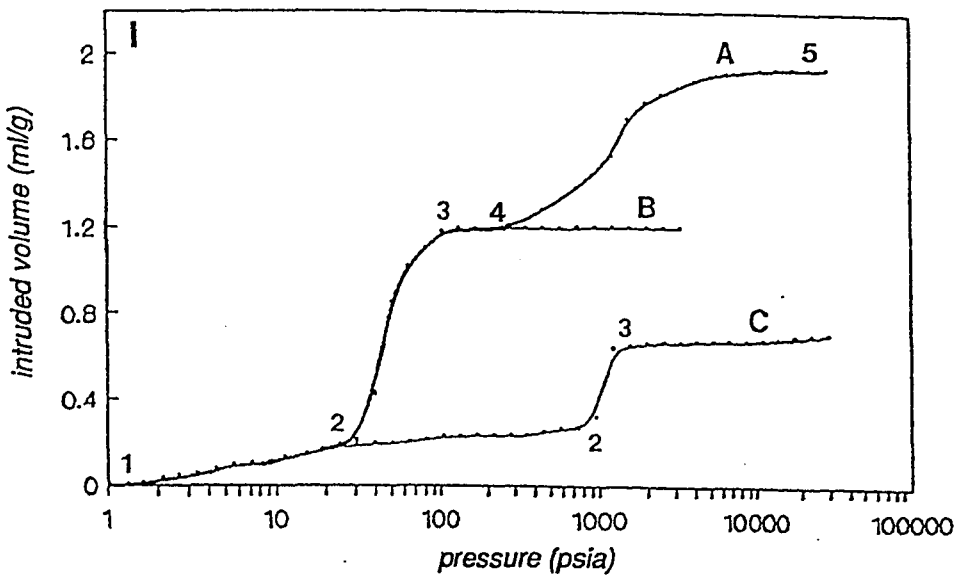

Figure 3-5: *Mercury intrusion porograms for: (I) intruded volume versus pressure; and (II) intruded volume versus pore radius. Curve A: 11 μm-diameter monodisperse porous styrene-divinylbenzene copolymer particles [diluent: linear polystyrene/n-hexane; 15% DVB; $M_{W,LP}$= 1.49 x 10^6]; Curve B: 10 μm-diameter nonporous, monodisperse polystyrene latex particles; and Curve C: 0.25 μm-diameter nonporous, monodisperse crosslinked polystyrene particles [15% DVB].*

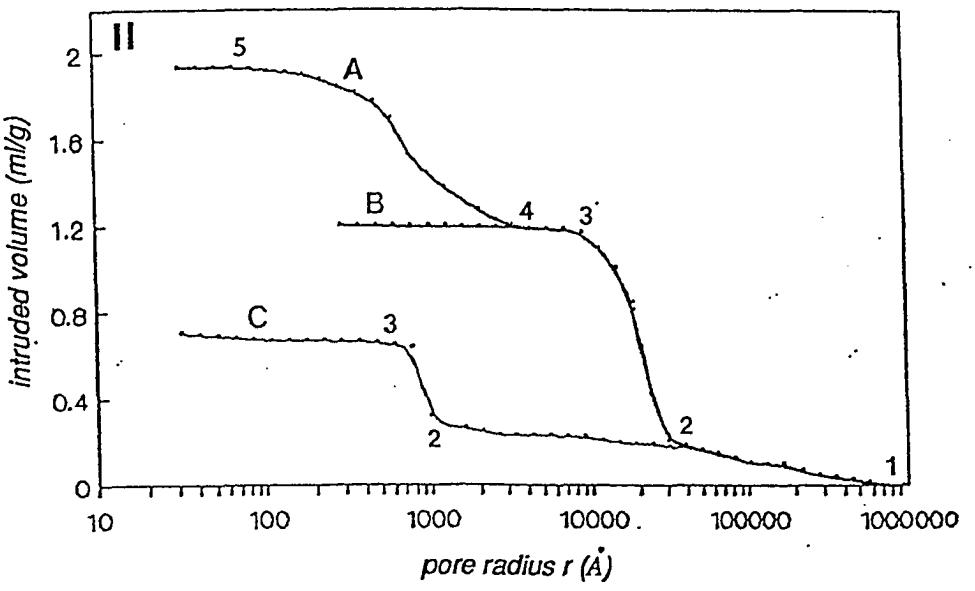

Figure 3-5: continued.

and γ and θ the surface tension and wetting angle of mercury, respectively. Interparticle void filling is not complete until a dimensionless pressures, P^*, of around 50 are obtained. Besides, the largest pore size which can be accurately measured is approximately 4% of the particle size (β = 0.04). Since the monodisperse porous polymer particles had an average particle radius of 5 μm, a minimum pressure of 400 psia is required for interparticle void filling, and the upper limit for mercury porosimetry pore size analysis would be 2,000 $\mathring{A}$.

Curve C in Figure 3-5 represents the porogram of the 0.25 μm-diameter nonporous, monodisperse crosslinked polystyrene latexes (with 15% divinylbenzene content). The rapid intrusion, with only a small increase in pressure, followed by little further intrusion as the pressure was increased to the maximum, is characteristic of a nonporous solid with a narrow particle size distribution. Based on the observation by scanning electron microscopy, the large (11 μm in diameter) monodisperse porous polymer particles are composed of many interior microspheres (with an average particle diameter of 0.15 μm) and their agglomerates. The pores of these porous polymer particles are considered to be due to interstices formed between theses microspheres and agglomerates. Figure 3-6 compares the pore size distribution of the monodisperse 11 μm-diameter porous polymer particles and the interparticle pores of the monodisperse 0.25 μm-diameter nonporous polystyrene latexes. Curve A in Figure 3-6 reveals the broad size distribution of the interior microspheres within the porous polymer particles in comparison to the monodisperse 0.25 μm-diameter particles (Curve B). The complex phase separation process during the formation of pore structure induces the broad pore size distribution of the porous polymer particles.

To summarize the porogram analyses, the mercury porosimetry curve for the monodisperse porous polymer particles showed penetration over the whole

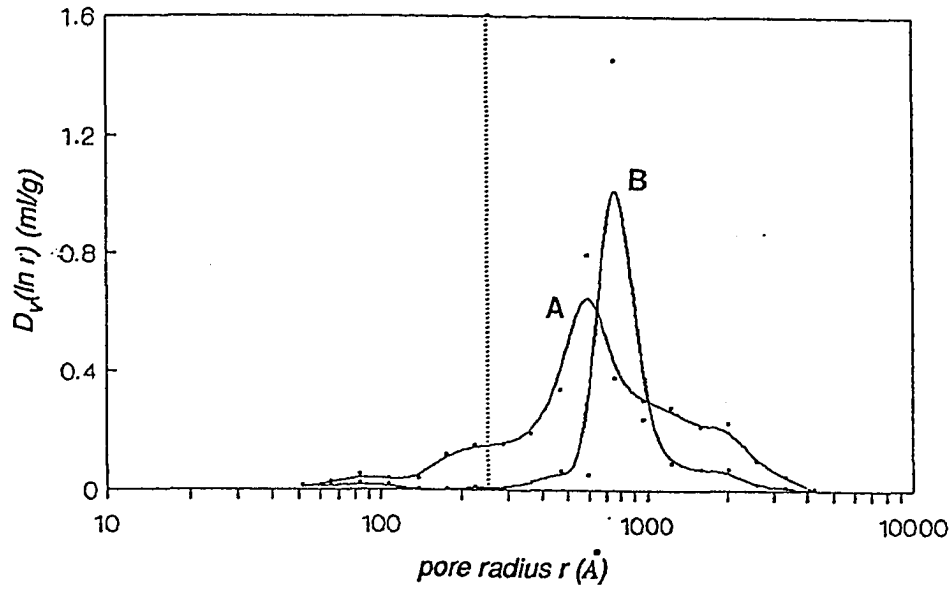

Figure 3-6: *Pore size distributions of: (A) 11 μm-diameter monodisperse porous polymer particles [diluent: linear polystyrene/n-hexane; 15% DVB; $M_{W,LP}$=1.49 x 10^6]; and (B) interparticle pores of 0.25 μm-diameter nonporous, monodisperse crosslinked polystyrene particles. The dotted line indicates the position of the 250 Å pore radius.*

pressure range - a rapid penetration over a small pressure range at low pressures with further penetration at pressures in excess of 400 psia. The initial penetration would be into interparticle voids and intraparticle penetration would occur at higher pressures. This type of curve implies that the porous polymer particles are monodisperse in particle size and the pore matrix is formed by the aggregation of small primary polymer particles. The mercury porosimetry curve for the monodisperse porous polymer particles shows penetration over the wide pressure range, indicating a wide pore size distribution.

3.3.1.2 Pore size distribution

Figures 3-7, 3-8, and 3-9 illustrate the pore size distributions obtained by mercury porosimetry in the differential mode. The results show that the majority of the pores for all samples are larger than 250 $\mathring{A}$ equivalent radius. This shows that the monodisperse porous polymer particles have macroporous structure, and indicates that the high molecular weight linear polystyrene used as inert diluent can create macropores. The average pore size, furthermore, is of the same order of magnitude as observed by scanning electron microscopy.

Similar to the surface area and pore volume, the pore size distribution was also dependent on the diluent type and the crosslinker content. Figure 3-7 shows that the monodisperse porous polymer particles prepared using linear polymer alone (Curve C), or a mixture of linear polymer and solvent (Curve B) as inert diluents, have average pore size larger than the porous particles prepared with a mixture of linear polymer and nonsolvent (Curve A) as inert diluents. This shift in the pore size distribution towards the larger pores is accounted for by the decrease in entanglement of the linear polymer. Entanglement of the linear polymer takes place in the diluent domain and depends on the interaction of the linear polymer with the copolymer matrix, and

with the solvent or nonsolvent. In the absence of the nonsolvent, the linear polymer used as diluent is in a more expanded state during the onset of polymerization, and thus it can create large pores in the polymer particles. Figure 3-8 compares the pore size distribution of porous polymer particles made with varying divinylbenzene content. The pores tend to be noticeably larger as the crosslinker concentration decreases as demonstrated by Curves C, B & A, respectively. At the higher divinylbenzene concentration (Curve C), the pore size distribution shifts to smaller pores. This increase in the number of smaller pores was caused by the disintegration of aggregates into smaller microspheres owing to the higher crosslinker content. Although the pore size distribution was dependent on the diluent type and divinylbenzene content, the pore size distribution patterns are rather similar when the same linear polymer ($M_{W,LP}$= 1.49×10^6) is used as diluent.

Figure 3-9 compares the pore size distributions of monodisperse porous polymer particles made with linear polystyrene having different molecular weights in the presence of n-hexane (an inert nonsolvent) and 15% divinylbenzene content. The pore size distributions are very sensitive to the molecular weight of the linear polymer. As the molecular weight of the linear polystyrene is increased, the average pore size becomes larger and the pore size distribution shifts towards the larger pores as demonstrated by Curves D, C, B and A, respectively. Figure 3-9 also shows that there is an increase in the proportion of pores with pore size below the macroporous region of 250 Å-radius while the molecular weight is decreased as demonstrated by the areas under the curves to the left of the dotted line. The large radius of gyration or hydrodynamic diameter of high molecular polystyrene is responsible for creating large pores during the phase separation and solvent extraction processes (see Tables 2-12 and 2-13). The shapes of pore size distributions strongly depend on

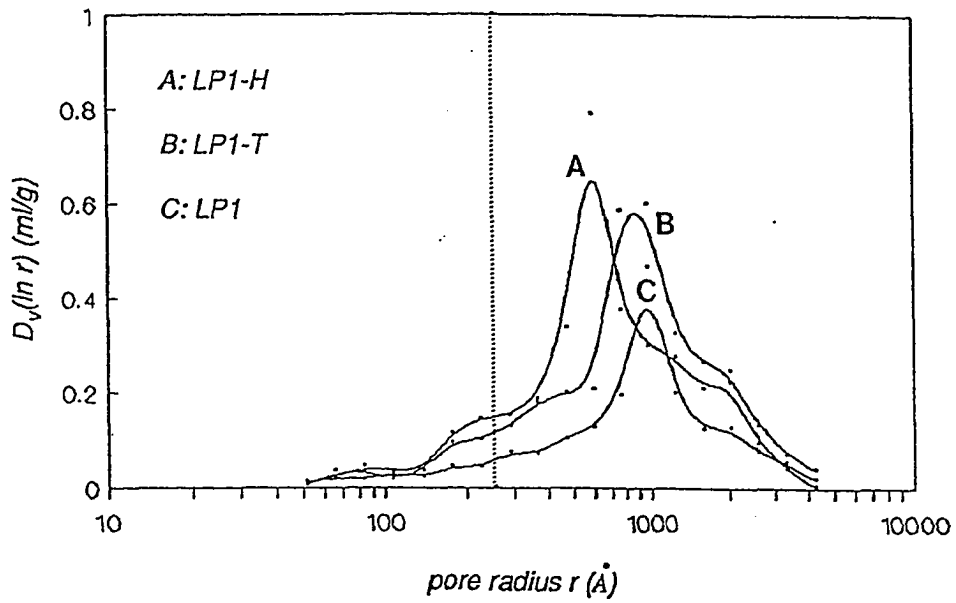

Figure 3-7: *Pore size distributions of monodisperse porous polymer particles prepared with different diluents: (A) LP1-H: linear polystyrene/n-hexane; (B) LP1-T: linear polystyrene/toluene; and (C) LP1: linear polystyrene. The dotted line indicates the position of the 250 Å pore radius. [15% DVB, $M_{W,LP}$= 1.49 x 10^6]*

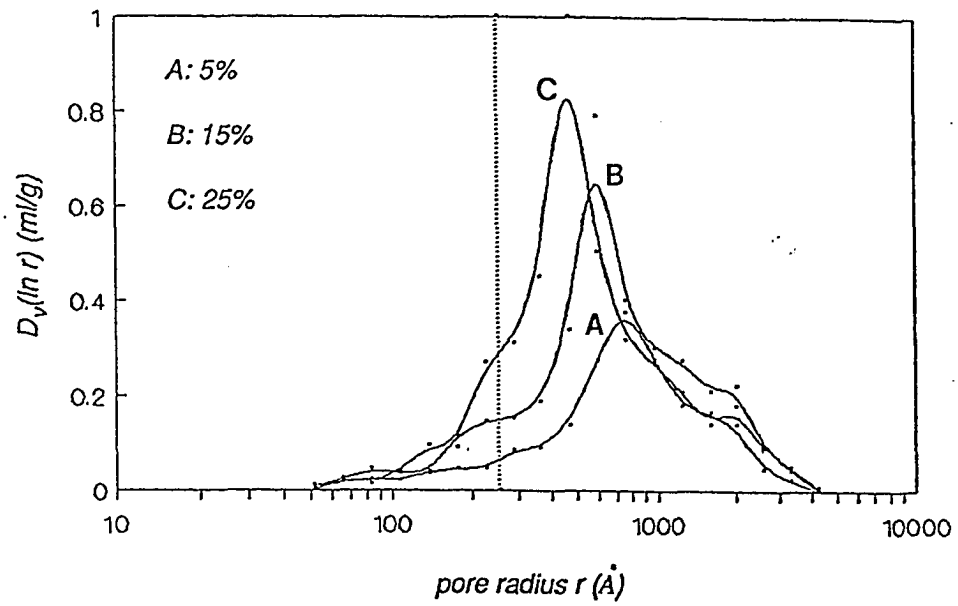

Figure 3-8: *Pore size distributions of monodisperse porous polymer particles prepared with varying divinylbenzene content: (A) 5%; (B) 15%; and (C) 25%. The dotted line indicates the position of the 250 Å pore radius. [diluent: linear polystyrene/n-hexane,* $M_{W,LP}$= *1.49 x* 10^6*]*

the molecular weight distribution of the linear polymer. The pore size distribution is narrowest for the linear polymer with narrowest molecular weight distribution, as represented by Curve A in Figure 3-9. The rather broad pore size distribution containing both large and small pores corresponds to the broader molecular weight distribution of linear polystyrene, as represented by Curves C and D. In the diluent phase, entanglement of the linear polymer takes place, depending on the molecular weight of the polymer, thus explaining the extreme sensitivity of the pore size distribution to the molecular weight of the polymer. This demonstrates the advantage of using linear polymer as diluent: the pore size distribution can be controlled by the molecular weight of the linear polymer seed used as inert diluent.

3.3.2 Nitrogen Adsorption Isotherms

Based on the above observation, monodisperse porous polymer particles prepared using high molecular weight linear polymer as inert diluent was found to have a large fraction of the porosity due to macropores, as indicated by mercury porosimeter measurements. However, mercury porosimetry is generally regarded as the best method available for the determination of pore size in the macropore and upper mesopore range[21]. The very high pressure involved in the detection of small pores may raise the potential problem of collapse of the polymer samples; and thus when small pores are present the analyses are considered less reliable. Nitrogen adsorption is suitable for the measurement of micropores and mesopores[19], with a practical upper limit of 250 $\mathring{A}$-radius. It appears that these two methods are best regarded as complementary, for each becomes increasingly uncertain as the pore size range approaches a limit: nitrogen adsorption at the upper end of the mesopore range and mercury porosimetry at the lower end. Progressively smaller pores are filled

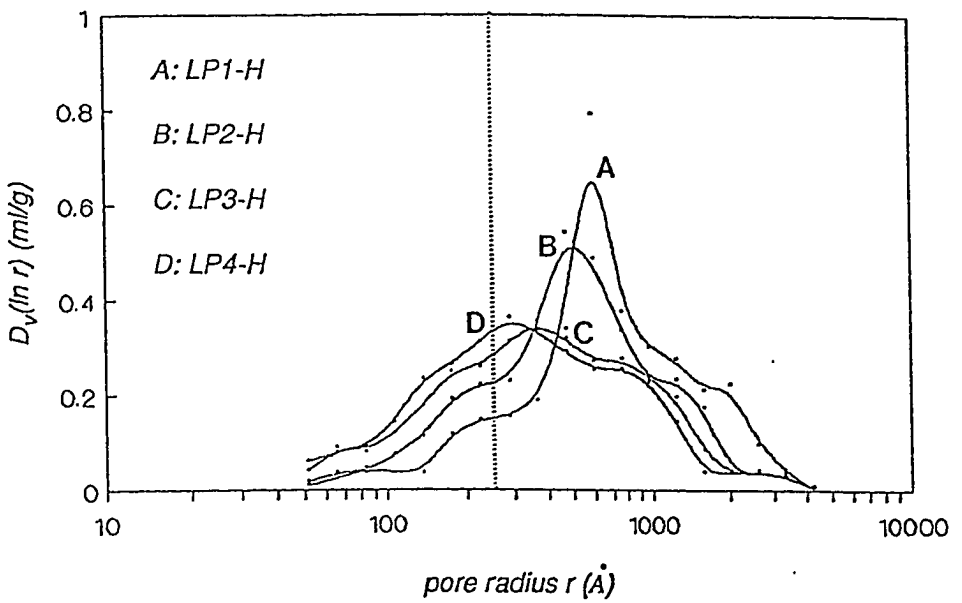

Figure 3-9: *Pore size distributions of monodisperse porous polymer particles prepared with linear polystyrene seed of different molecular weight $M_{W,LP}$ and molecular weight distribution PDI: (A) LP1-H: $M_{W,LP}$= 14.9 x 10^5, PDI= 4.98; (B) LP2-H: $M_{W,LP}$= 10.8 x 10^5, PDI= 7.32; (C) LP3-H: $M_{W,LP}$= 5.68 x 10^5, PDI= 16.9; and (D) LP4-H: $M_{W,LP}$= 4.46 x 10^5, PDI= 16.0. The dotted line indicates the position of the 250 Å pore radius. [diluent: linear polystyrene/n-hexane, 15% DVB]*

as the hydraulic pressure is increased in mercury porosimetry; progressively larger pores are filled as the adsorbate pressure is increased in nitrogen vapor adsorption[28, 29, 30]. The two processes occur in reverse since nitrogen and mercury on most surfaces are wetting and nonwetting liquids, respectively. Therefore, the combination of mercury porosimetry and nitrogen adsorption should provide quantitative analysis of pore structure in the entire pore size range.

3.3.2.1 Classification of adsorption isotherms and hysteresis

The majority of physisorption isotherms may be grouped into six types shown in Figure 3-10 according to Brunauer et al[8, 31]. In most cases at sufficiently low surface coverage the isotherm reduces to a linear form, which is often referred to as the Henry's Law region.

The reversible Type I isotherm is concave to the P/P_o axis and n approaches a limiting value as P/P_o approaches 1. Type I isotherms are given by microporous solids having relatively small external surfaces, the limiting uptake being governed by the accessible micropore volume rather than by the internal surface area.

The reversible Type II isotherm is the normal form of an isotherm obtained for a nonporous or macroporous adsorbent. The Type II isotherm represents unrestricted monolayer-multilayer adsorption. Point B, the beginning of the almost linear middle section of the isotherm, is often taken to indicate the stage at which monolayer coverage is complete and multilayer adsorption about to begin.

The reversible Type III isotherm is convex to the P/P_o axis over its entire range and therefore does not exhibit a Point B. Isotherms of this type are characterized principally by heats of adsorption which are less than the adsorbate heat of liquefaction. Thus, as adsorption proceeds, additional

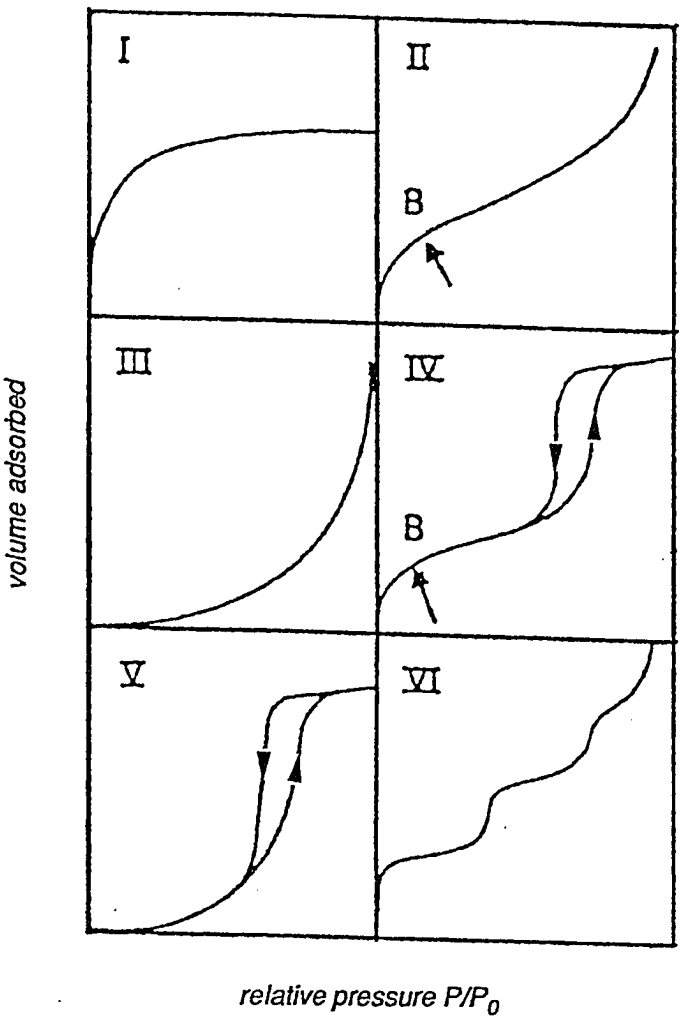

Figure 3-10: *The six physisorption isotherm classifications according to BDDT. P: adsorbate equilibrium pressure; P_o: adsorbate saturated equilibrium vapor pressure; and P/P_o: relative pressure*[8].

adsorption is facilitated because the adsorbate interaction with an adsorbed layer is greater than the interaction with the adsorbent surface.

Characteristic features of the Type IV isotherm are its hysteresis loop, which is associated with capillary condensation in mesopores, and the limiting uptake over a range of high P/P_o. The initial part of the Type IV isotherm is attributed to monolayer-multilayer adsorption since it follows the same path as the corresponding part of a Type II isotherm obtained with the given adsorbate on the same surface area of the adsorbent in a nonporous form. Type IV isotherms are typical of by many mesoporous industrial adsorbents.

The Type V isotherm is uncommon; it is related to the Type III isotherm in that the adsorbent-adsorbate interaction is weak, but is obtained with certain porous adsorbents.

The Type VI isotherm represents stepwise multilayer adsorption on a uniform nonporous surface. The step-height represents the monolayer capacity for each adsorbed layer and remains nearly constant for two or three adsorbed layers.

The hysteresis appearing in the multilayer range of physisorption isotherms is usually associated with capillary condensation in mesopore structures. Such hysteresis loops may exhibit a wide variety of shapes[8]. Two extreme types are shown as H1 and H4 in Figure 3-11. In the former the two branches are almost vertical and nearly parallel over an appreciable range of gas uptake, whereas in the latter they remain nearly horizontal and parallel over a wide range of P/P_o. In certain respects, Types H2 and H3 may be regarded as intermediate between these two extremes. A feature common to many hysteresis loops is that the steep region of the desorption branch leading to the lower closure point occurs at a relative pressure which is almost independent of the nature of the porous adsorbent but depends mainly on the

nature of the adsorbate (e.g. for nitrogen at its boiling point at $P/P_o = 0.42$).

The shapes of hysteresis loops have often been identified with specific pore structures[8, 19]. Type H1 is often associated with porous materials which consist of agglomerates or compacts of approximately uniform spheres in fairly regular arrays, and hence having narrow distributions of pore size. Type H2 loops have been attributed to a difference in mechanism between condensation and evaporation processes occurring in pores with narrow necks and wide bodies (often referred to as "ink bottle" pores) or due to network effects of the pore matrix.

The Type H3 loop, which does not exhibit any limiting adsorption at high P/P_o, is observed with aggregates of plate-like particles given rise to slit-shaped pores. Similarly, the Type H4 loop is often associated with narrow slit-like pores, but in this case the Type I isotherm character is indicative of microporosity.

With many systems, especially those containing micropores, low pressure hysteresis (indicated by the dashed lines in Figure 3-11), may be observed extending to the lowest attainable pressures. Removal of the residual adsorbed material is then possible only if the adsorbent is outgassed at higher temperatures. This phenomenon may be associated with the swelling of a nonrigid porous structure or with the irreversible uptake of molecules in pores of about the same width as that of the adsorbate molecule.

3.3.2.2 Nitrogen adsorption

Nitrogen adsorption-desorption isotherms were measured on monodisperse porous polymer particles in order to analyze the pore structure prepared with linear polymers having different molecular weights, since the pore size distributions were shown to be very sensitive to the molecular weight of the linear polymer. The nitrogen adsorption-desorption isotherm results for

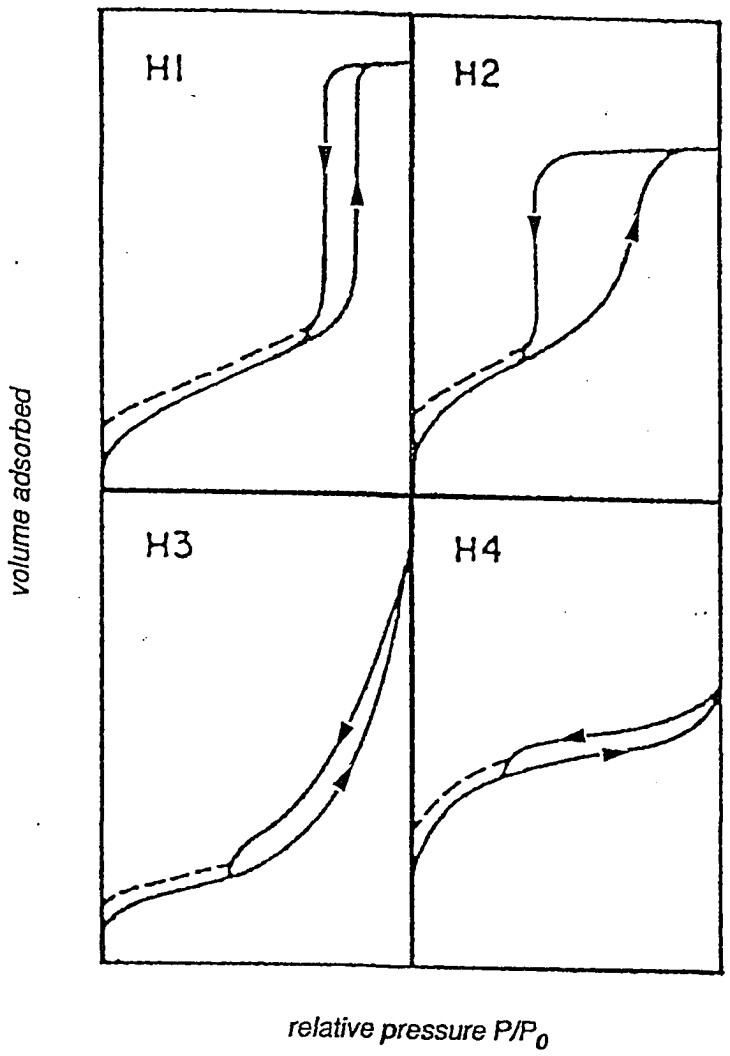

Figure 3-11: *Types of hysteresis loop. P: adsorbate equilibrium pressure; P_o: adsorbate saturated equilibrium vapor pressure; and P/P_o: relative pressure*[8].

the monodisperse porous polymer particles prepared with linear polystyrene of different molecular weight are shown in Figure 3-12. All the isotherms were Type II according to the IUPAC classification[8]. These results are very similar to the adsorption-desorption isotherms of the monodisperse nonporous 10 μm polystyrene latex particles and the 0.25 μm crosslinked (with 15% divinylbenzene content) polystyrene latex particles as shown in Figure 3-13, and the isotherm of 0.078 μm monodisperse polystyrene latex particles reported by Vanderhoff and van den Hul[32] as depicted in Figure 3-14. The adsorption isotherm has no limiting uptake of nitrogen at high relative pressures. The relative reversibility of the isotherms are characteristic of nonporous or macroporous materials: in the latter case the pores are too large to have any significant effect on the course of the isotherm. As the molecular weight of the linear polystyrene decreased, the isotherms became less reversible as indicated in Figure 3-12 by an increase in the hysteresis loop in Curves D, C, B & A, respectively. The hysteresis loop is often associated with capillary condensation in mesopores. In general, physisorption in mesopores takes place in two stages: first, monolayer-multilayer adsorption on the pore walls; second, capillary condensation with the formation of a curved liquid-like meniscus and the filling of cavities located within groups of particles. Owing to the pore blocking effects[19], the condensation and evaporation processes would follow different paths, which invariably give rise to hysteresis. However, the isotherms have no limiting uptake of nitrogen and an upturn as the relative pressure P/P_o approaches one, indicates the vast majority of pores present are macropores and the pore structure is complex owing to the combination of macropores and mesopores[33].

Examining the shape of the isotherms, the type of hysteresis loop presented is often associated with porous polymer particles known, from other

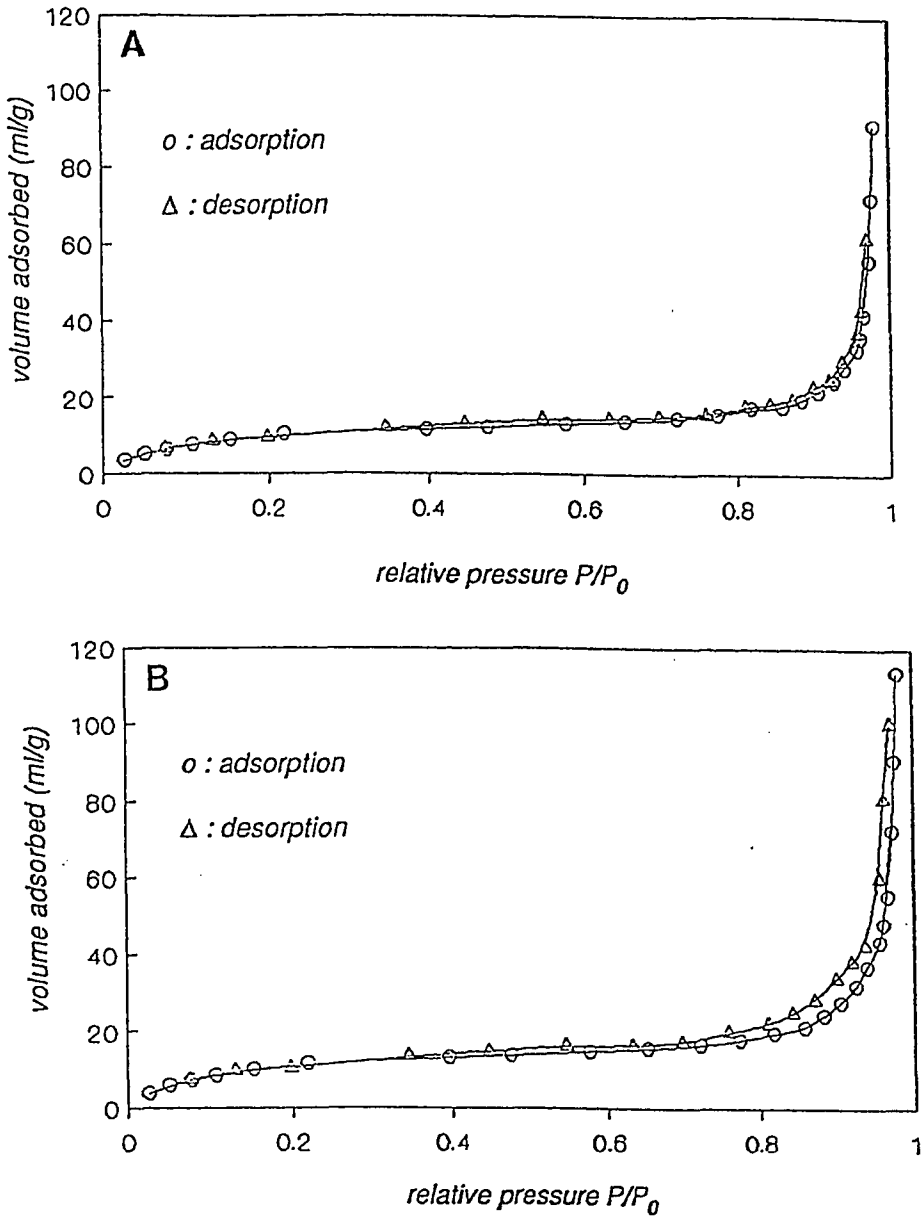

Figure 3-12: *Nitrogen adsorption and desorption isotherms at 77 °K on 11 μm-diameter monodisperse porous polymer particles prepared with linear polystyrene seed of different molecular weight $M_{W,LP}$: (A) LP1-H: $M_{W,LP}$= 14.9 x 10^5; (B) LP2-H: $M_{W,LP}$= 10.8 x 10^5; (C) LP3-H: $M_{W,LP}$= 5.68 x 10^5; and (D) LP4-H: $M_{W,LP}$= 4.46 x 10^5. [diluent: linear polystyrene/n-hexane, 15% DVB]*

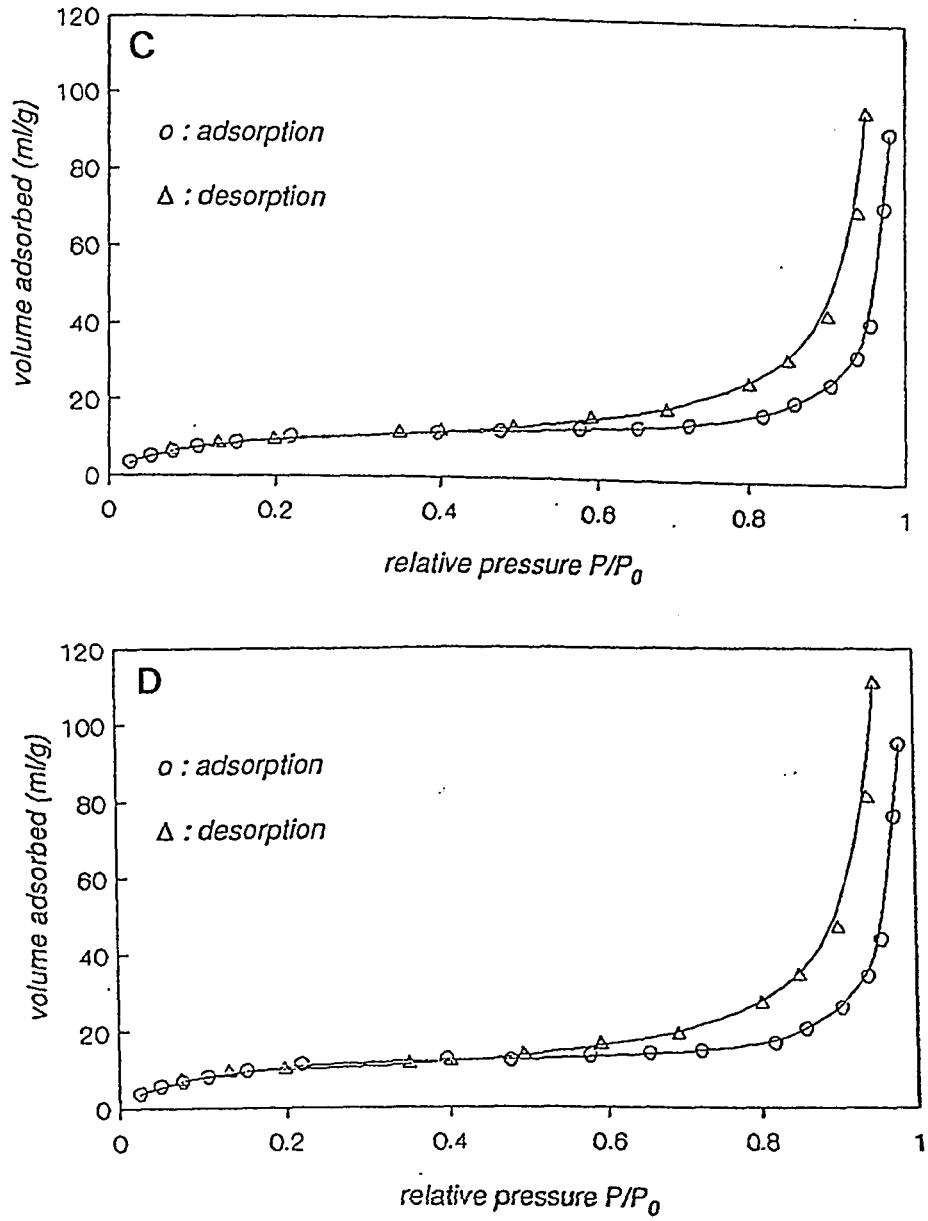

Figure 3-12: continued.

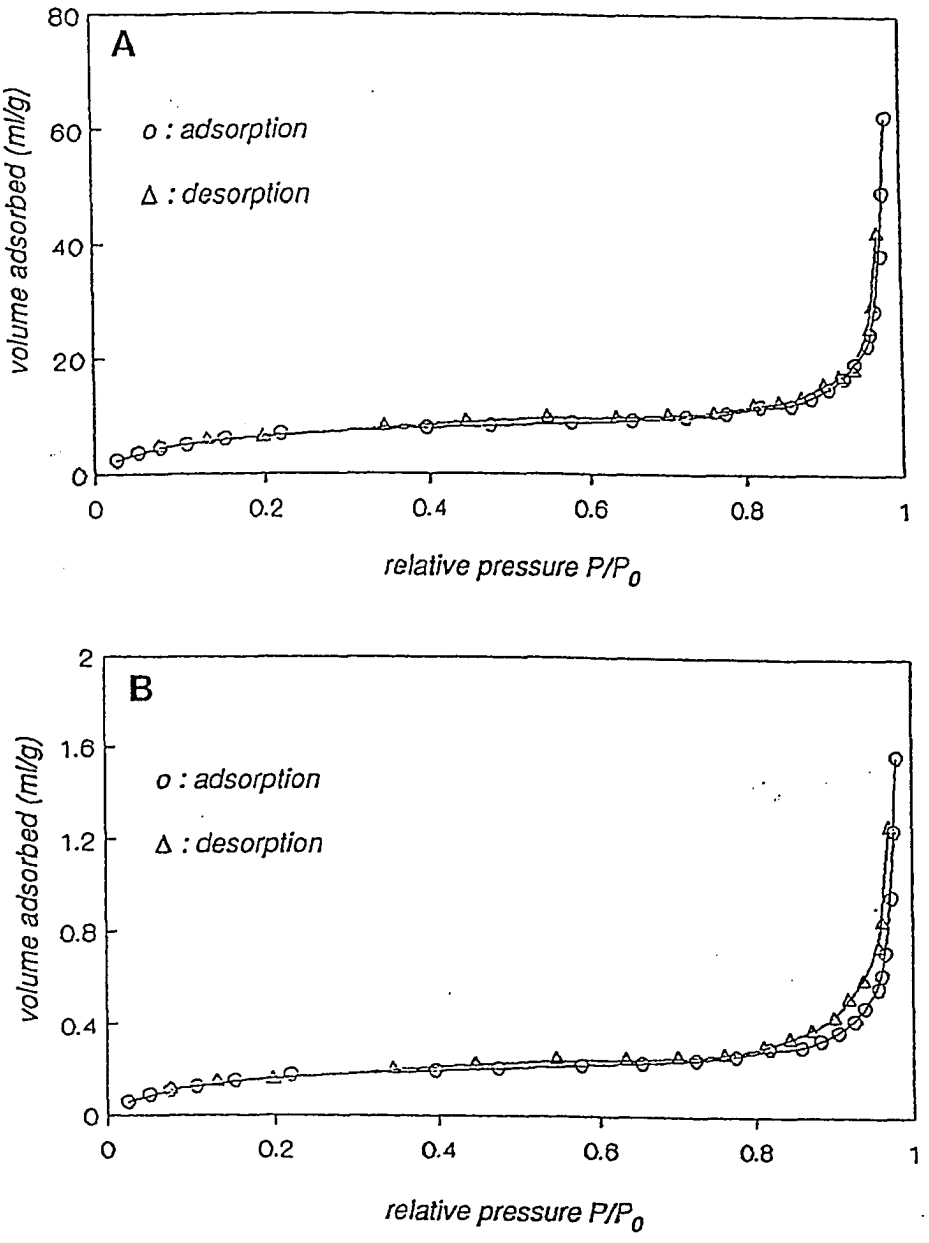

Figure 3-13: *Nitrogen adsorption and desorption isotherms at 77 °K on: (A) nonporous 0.25 μm-diameter monodisperse crosslinked polystyrene latex particles (with 15 % DVB); (B) nonporous 10 μm-diameter monodisperse uncrosslinked polystyrene latex particles.*

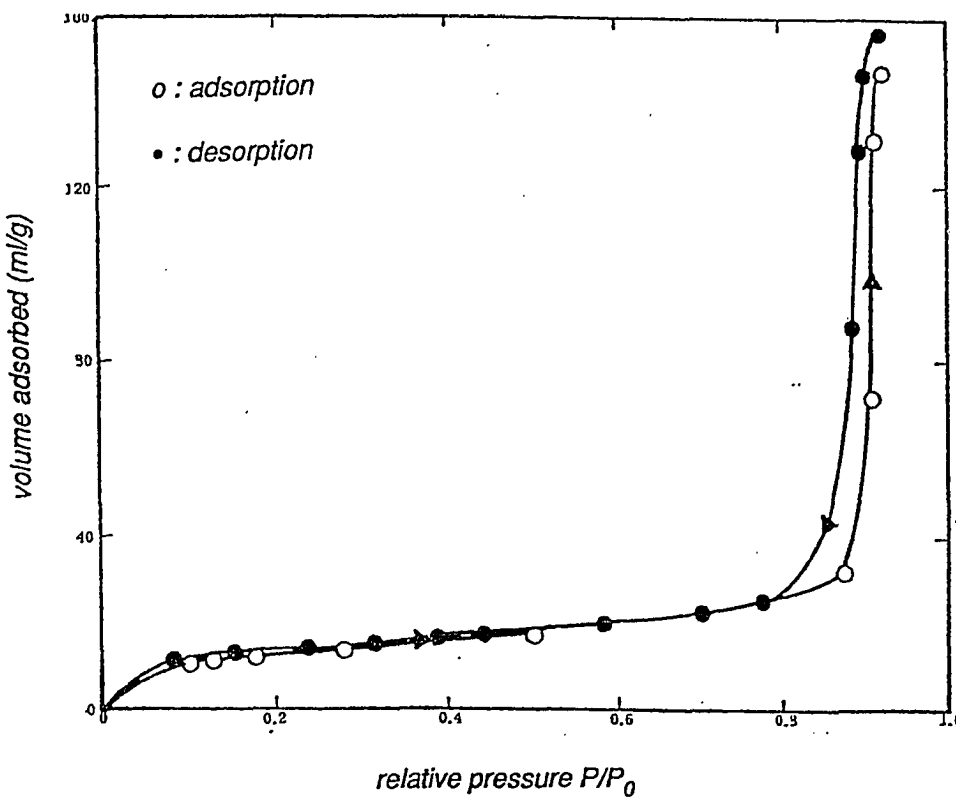

Figure 3-14: *Nitrogen adsorption and desorption isotherms at 77 °K on 0.078 μm monodisperse uncrosslinked polystyrene latex particles*[32].

evidence such as scanning electron microscopy, to consist of agglomerates or compacts of spheres[8, 10, 19, 21]. These agglomerates are represented as an assemblage of microspheres rigidly joined together. The adsorption on such a surface was considered to be in three forms: multilayers; pendular rings or a tours-shaped condensate held at the points of contact between microspheres; and condensate between groups of spheres. The pores of the porous polymer particles are indeed due to interstices formed between the crosslinked microspheres and their agglomerates.

All the isotherms depicted in Figure 3-12 have been analyzed by conventional BET means[19] based on Equation (3.1). The BET plots were all linear over the relative pressure range 0.03 - 0.30, thus enabling the BET constant C and surface area S for each material to be obtained from the respective intercept and slope of a given plot (as shown in Figure 3-15). The slope s and the intercept i of a BET plot are

$$s=\frac{C-1}{V_{ads,m}C} \tag{3.7}$$

$$i=\frac{1}{V_{ads,m}C} \tag{3.8}$$

Solving the proceeding equations for $V_{ads,m}$, the volume adsorbed in a monolayer, gives

$$V_{ads,m}=\frac{1}{s+i} \tag{3.9}$$

and the solution for C, the BET constant, gives

$$C=\frac{s}{i}+1 \tag{3.10}$$

Then, the specific surface area S can be calculated form Equation (3.2). Irrespective of the molecular weight of the linear polymer used as inert diluent, the calculated values of C were low as indicated in Table 3-2, reflecting the absence of micropores which tend to give high C values[34, 35]. The specific surface areas of these porous polymer particles are around 45 m^2/g, which is much higher than the 0.7 m^2/g obtained for the 10 μm monodisperse nonporous polystyrene latex particles, and corresponds to an average compact particle diameter of 0.15 μm. This value is in the same range as the microspheres observed within the macroporous polymer particles (see Figure 3-2), and implies that the working surface area of the porous polymer particles is actually the surface area of those interior microspheres within the porous polymer particles.

The mesopore size distribution could also be estimated from the multilayer descending part of the desorption isotherms based on the Kelvin equation which relates condensation pressure to radius of curvature[19, 21, 36, 37]. The pore size was related to the equilibrium pressure, the isotherms were then plotted as the cumulative pore volume from which nitrogen was desorbed versus pore radius. The derivative of the cumulative pore volume with respect to pore radius yields the pore size distribution. The pore size distribution in differential mode is depicted in Figure 3-16, where the dominant maxima in the upper mesopore range clearly correspond to the macroporous nature of the porous polymer particles. Again, the pore size distributions are sensitive to the molecular weight of the linear polymer. As the molecular weight of the linear polystyrene is decreased, the pore size distribution shifts towards the mesopores; there is an increase in the proportion of mesopores as indicated by the mesopore volumes (V_{meso}) estimated from the Kelvin equation and listed in Table 3-2. Compared with the cumulative pore volume determined from mercury porosimetry (listed in Table 3-1), only 7 - 30 % of the total pores are

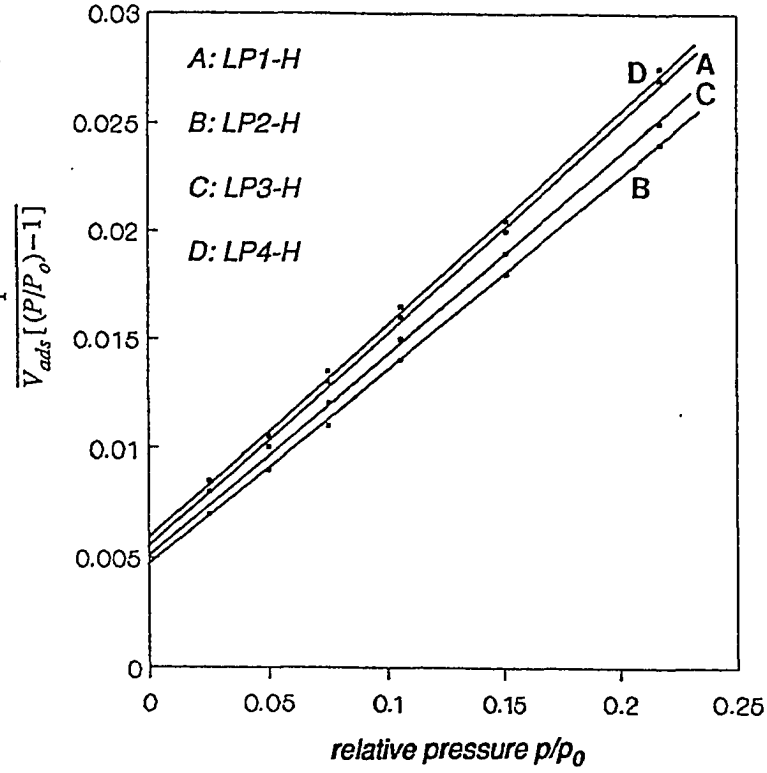

Figure 3-15: *BET plots for 11 μm-diameter monodisperse porous polymer particles prepared with linear polystyrene seed of different molecular weight $M_{W,LP}$: (A) LP1-H: $M_{W,LP}$= 14.9 x 10^5; (B) LP2-H: $M_{W,LP}$= 10.8 x 10^5; (C) LP3-H: $M_{W,LP}$= 5.68 x 10^5; and (D) LP4-H: $M_{W,LP}$= 4.46 x 10^5. [diluent: linear polystyrene/n-hexane, 15% DVB]*

Table 3-2: Surface Areas, C, and Pore Volumes Derived from Nitrogen Adsorption-Desorption Isotherms

Sample	S m^2/g	C	S_α m^2/g	V_{meso} ml/g
• Monodisperse porous polymer particles (11 μm)				
LP1/n-Hexane	44	20.4	43	0.07
LP2/n-Hexane	50	23.2	48	0.12
LP3/n-Hexane	46	21.9	43	0.20
LP4/n-Hexane	42	19.3	47	0.22
• Monodisperse nonporous polystyrene latexes				
0.25 μm	30	23.0	-	-
10 μm	0.7	18.2	-	-

** LP: linear polystyrene seed (see Table 2-9 for molecular weights); S: apparent BET specific surface area; C: BET constant; S_α: surface area estimated from α_s-plot; and V_{meso}: pore volume estimated from mesopore region.*

within the mesopore region. Thus by using linear polymer with molecular weights on the order of 10^6 as inert diluent to prepare monodisperse porous polymer particles, the vast majority of pores present in the polymer particles are macropores.

3.3.2.3 Analysis of isotherms: a_s-plot

The task of detecting deviation from the standard isotherm is essentially one of comparing the shape of the sample isotherm with that of the standard, by finding whether the two can be brought into coincidence by mere adjustment of the ordinate scale. A convenient means of testing for such superimposability is provided by the α_m-plot of Lippens and de Boer[19, 38, 39, 40, 41]. This is based on the α_m-curve, which is a plot of the standard isotherm with α_m, the statistical thickness of the film, rather than $V_{ads}/V_{ads,m}$, as the dependent variable. The

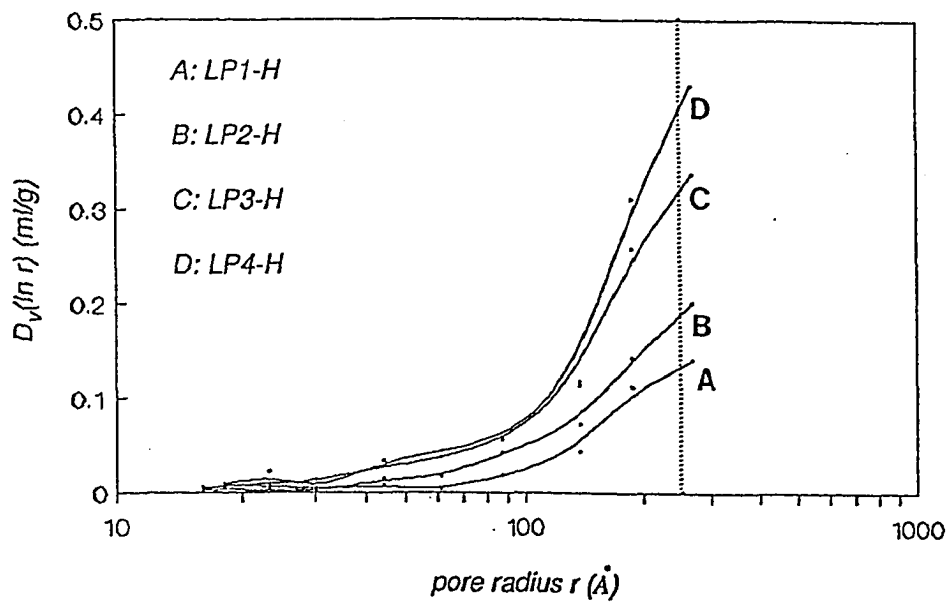

Figure 3-16: *Derived mesopore size distributions based on nitrogen desorption isotherms of 11 μm-diameter monodisperse porous polymer particles prepared with linear polystyrene seed of different molecular weights $M_{W,LP}$: (A) LP1-H: $M_{W,LP}$= 14.9 x 10^5; (B) LP2-H: $M_{W,LP}$= 10.8 x 10^5; (C) LP3-H: $M_{W,LP}$= 5.68 x 10^5; and (D) LP4-H: $M_{W,LP}$= 4.46 x 10^5. The dotted line indicates the position of the 250 Å pore radius. [diluent: linear polystyrene/n-hexane, 15% DVB]*

conversion is accomplished by taking $V_{ads}/V_{ads,m}$ to be equal to the number of statistical molecular layers in the film and multiplying by the thickness of a single molecular layer (σ), so that $\alpha_m = (V_{ads}/V_{ads,m}\sigma)$ (α_m of course represents the average thickness; the actual thickness must vary from place to place). For nitrogen at 77 °K, Lippens, Lisen and de Boer[42] put $\sigma = 3.54$ Å, on the assumption that the arrangement of molecules in the film is hexagonal close packing[19].

The α_m-curve and its associated α_m-plot were originally devised as a means of allowing for the thickness of the adsorbed layer on the walls of the pores when calculating pore size distribution from the isotherm. For the purpose of testing for conformity to the isotherm, however, a knowledge of the numerical thickness is irrelevant; since the objective is to compare the shape of the isotherm under test with that of the standard isotherm, it is not necessary to involve the number of molecular layers $V_{ads}/V_{ads,m}$ or the monolayer capacity itself.

It is sufficient to replace $V_{ads,m}$ as normalizing factor by $V_{ads,s}$, the number adsorbed at some fixed relative pressure $(P/P_o)_s$. In practice, $(P/P_o)_s = 0.4$ was taken, i.e., at relative pressure values roughly similar to that expected from a consideration of the tensile strength of liquid nitrogen. The α_s-method offers a simple but effective means of testing for the identity in shape of the isotherms on a given set of materials of the same substance. A nonporous material can be taken as a reference for the construction of the α_s-curve. The normalized adsorption $V_{ads}/V_{ads,m}$ ($= \alpha_s$), obtained from the isotherm on a reference material, is then plotted against P/P_o, to obtain a standard α_s-curve rather than a α_m-curve. The α_s-curve can then be used to construct an α_s-plot from the isotherm of a porous material. If a straight line through the origin results, one may infer that the isotherm under test is identical in shape with the

standard.

The isotherm under test is then re-drawn as a α_s-plot, i.e., a curve of the amount adsorbed plotted against α_s rather than against P/P_o; the change of independent variable from P/P_o to α_s is effected by reference to the standard α_s-curve. If the isotherm under test is identical in shape with the reference and differs only in the surface area and not in porosity, the α_s-plot must be a straight line passing through the origin.

If the adsorbent contains mesopores, capillary condensation will occur in each pore when the relative pressure reaches a value which is related to the radius of the pore by the Kelvin equation, and a Type IV isotherm will result. It is noted that when capillary condensation takes place the uptake at a given relative pressure is enhanced by the amount of adsorbate condensing in the pores. The α_s-plot therefore shows an upward deviation from linearity commencing at the relative pressure at which the finest pores are just being filled.

If micropores are introduced into a porous material which originally gave a standard Type II isotherm, the uptake is enhanced in the low-pressure region and the isotherm is correspondingly distorted. The high-pressure branch is still linear (provided mesopores are absent), but when extrapolated to the adsorption axis it gives a positive intercept which is equivalent to the micropore volume. The slope of the linear branch is now proportional to the external surface area of the material.

To estimate the specific surface area, S_α, of a porous material from the slope, b_α, of its α_s-plot, one notes that[40, 41]

$$S_\alpha = \frac{b_\alpha}{b_{\alpha,ref}} S_{ref} \tag{3.11}$$

where S_{ref} and $b_{\alpha,ref}$ are the specific surface area and the slope of the α_s-plot of

the reference material, respectively.

The nitrogen isotherm results in Figure 3-12 have also been examined using the α_s-method[19], employing the 0.25 μm nonporous, crosslinked polystyrene latex particles as the reference material. The α_s-method provides an alternative mean of assessing pore size. Thus, any deviations from the standard monolayer-multilayer isotherm are presented in the form of the α_s-plot, i.e., the plot of the amount adsorbed against the reduced adsorption, α_s, given by a nonporous reference material. These α_s-plots, presented in Figure 3-17, were calculated from the adsorption-desorption isotherm results presented in Figure 3-12. The fact that the α_s-plot is linear for the entire isotherm and passes through the origin as represented in Figure 3-17A, indicates that the porous polymer particles are primarily composed of macropores. When the lower molecular weight linear polymers were used as inert diluent, the plots exhibited some positive deviations from linearity at α_s values greater than unity as shown in Figures 3-17B, C and D. Such behavior is typical of materials exhibiting mesoporosity. The greater the deviation of the α_s-plot from linearity, the higher the content of mesopores. The linear sections of the α_s-plots extrapolated to the origin, furthermore indicates that little or no micropores are present.

Values of the corresponding surface areas S_α from the α_s-plots can be calculated from the slopes b_α of the linear portions of the curves through the use of the relationship

$$S_\alpha = 3.76 b_\alpha \tag{3.12}$$

where the multiplication factor of 3.76 was obtained by calibration against the BET-nitrogen surface area of the reference 0.25 μm nonporous polystyrene latex particles. This method is an alternative approach for obtaining the specific

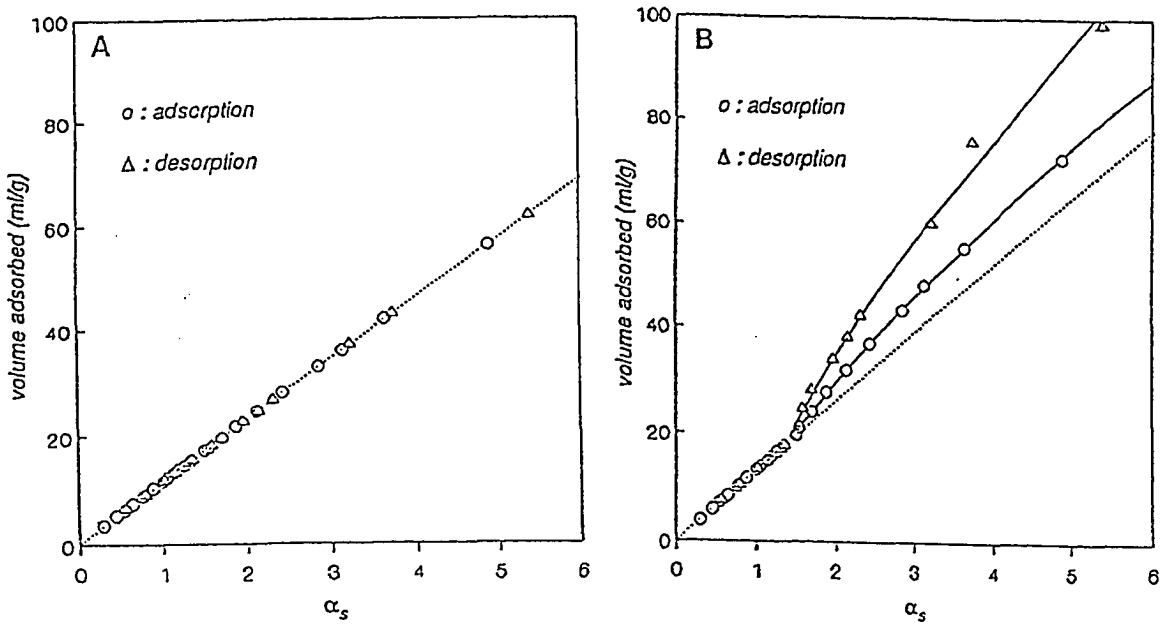

Figure 3-17: *α_s-plots for 11 μm-diameter monodisperse porous polymer particles prepared with linear polystyrene seed of different molecular weight $M_{W,LP}$: (A) LP1-H: $M_{W,LP}$= 14.9 x 10^5; (B) LP2-H: $M_{W,LP}$= 10.8 x 10^5; (C) LP3-H: $M_{W,LP}$= 5.68 x 10^5; and (D) LP4-H: $M_{W,LP}$= 4.46 x 10^5. The dotted lines correspond to the linear portion of the α_s-plots which pass through origin. [diluent: linear polystyrene/n-hexane, 15% DVB]*

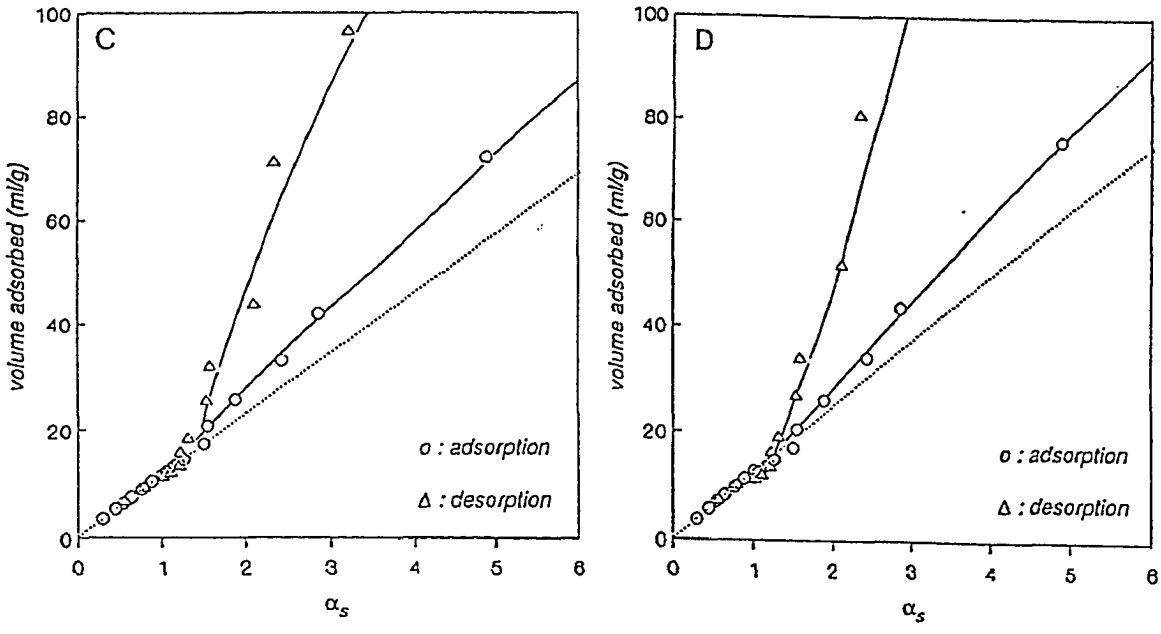

Figure 3-17: continued.

surface area of porous particles. The calculated values, as indicated in Table 3-2, compare very well with the apparent BET-nitrogen surface areas S. The surface areas of all porous polymer particles samples, furthermore, are of the same order of magnitude. Again, the high molecular weight linear polymers demonstrate the same precipitating ability to create porous polymer particles with the same specific surface area.

3.4 SUMMARY AND CONCLUSIONS

Monodisperse porous styrene-divinylbenzene copolymer particles were synthesized using monodisperse polystyrene latex particles with molecular weights on the order of 10^6 as inert diluent. Pore size distributions by mercury porosimetry revealed that the majority of the pores were in the macropore region, which implied that the high molecular weight linear polystyrene was responsible for the creation of these macropores. Using the same linear polymer as inert diluent, the pore size distribution patterns were rather similar. The pore size distributions, however, were very sensitive to the molecular weight of the linear polymer. Nitrogen adsorption-desorption isotherms were also used to assess pore structure and pore size distribution of mesopores and micropores. Qualitative evidence from nitrogen adsorption isotherms and α_s-plot analyses indicated that the monodisperse porous polymer particles were composed primarily of macropores, but contained some mesopores, with little or no microporosity being present. When the molecular weight of the linear polymer decreased, the porous polymer particles exhibited properties over a complex spectrum of macro-mesopore structures, with an increase in the proportion of mesopores.

Scanning electron microscopy showed evidence of the microglobular

nature of the internal structure and the existence of voids between the microspheres and agglomerates. This observation was also confirmed by the nitrogen adsorption-desorption isotherms, which implied that the mesopores, as well as the macropores, of the porous polymer particles were indeed due to the interstices between the crosslinked microspheres and their agglomerates.

3.5 REFERENCES

1. C. M. Cheng, M. S. El-Aasser, and J. W. Vanderhoff, presented at *"64th Colloid and Surface Science Symposium"*, Lehigh University, Bethlehem, PA, June 18-20, 1990.

2. C. M. Cheng, M. S. El-Aasser, and J. W. Vanderhoff, Presented at *"AIChE 1990 Annual Meeting"*, Chicago, November 11-16, 1990.

3. C. M. Cheng, F. J. Micale, J. W. Vanderhoff, and M. S. El-Aasser, *J. Polym. Sci., Polym. Chem. Ed.*, accepted (1991).

4. C. M. Cheng, J. W. Vanderhoff, and M. S. El-Aasser, *J. Polym. Sci., Polym. Chem. Ed.*, accepted (1991).

5. J. Seidl, J. Malinsky, K. Dusek, and W. Heitz, *Adv. Polym. Sci.*, **5**, 113 (1967).

6. J. Haradil, M. Wojaczynska, F. Svec, and B. N. Kolarz, *React. Polym.*, **4**, 277 (1986).

7. J. Ugelstad, L. Soderberg, A. Berge, and J Bergstrom, *Nature*, **303**, 95 (1983).

8. K. S. W. Sing, D. H. Everett, R. A. W. Haul, L. Moscou, R. A. Pierotti, J. Rouquerol, and T. Siemieniewska, *Pure & Appl. Chem.*, **57**, 603 (1985).

9. J. M. Singer, in *"Future Directions in Polymer Colloids"*, M. S. El-Aasser and R. M. Fitch, eds., NATO ASI Series **E138**, 371 (1987).

10. K. S. W. Sing, *Colloids Surfaces*, **38**, 113 (1989).

11. K. A. Kun and R. Kunin, *J. Polym. Sci.*, **A6**, 2689 (1968).

12. W. L. Sederel and G. J. de Jong, *J. Appl. Polym. Sci.*, **17**, 2835 (1973).

13. H. Jacobelli, M. Bartholin, and A. Guyot, *J. Appl. Polym. Sci.*, **23**, 927 (179).

14. H. Jacobelli, M. Bartholin, and A. Guyot, *Angew. Makromol. Chem.*, **80**, 31 (1979).

15. D. Y. D. Chung, M. Bartholin, and A. Guyot, *Angew. Makromol. Chem.*, **103**, 109 (1982).

16. O. Okay, *J. Appl. Polym. Sci.*, **32**, 5533 (1986).

17. K. A. Kun and R. Kunin, *J. Polym. Sci.*, **C16**, 1457 (1967).

18. S. Brunauer, P. H. Emmett, and E. Teller, *J. Amer. Chem. Soc.*, **60**, 309 (1938).

19. S. J. Gregg and K. S. W. Sing, *"Adsorption, Surface Area and Porosity"*,

2nd ed., Academic Press, London (1982).

20. E. W. Washburn, *Proc. Nat. Acad. Sci.*, **7**, 115 (1921).

21. S. Lowell and J. E. Shields, *"Powder Surface Area and Porosity"*, 2nd ed., Chapman & Hall, London (1984).

22. J. R. Benson and D. J. Woo, *J. Chromatogr. Sci.*, **22**, 386 (1984).

23. J. A. Davidson, *Powder Technol.*, **23**, 239 (1979).

24. H. K. Palmer and R. C. Rowe, *Powder Technol.*, **9**, 181 (1974).

25. H. K. Palmer and R. C. Rowe, *Powder Technol.*, **10**, 225 (1974).

26. M. Ciftcioglu, D. M. Smith, and S. B. Ross, *Powder Technol.*, **55**, 193 (1988).

27. D. M. Smith and S. Schentrup, *Powder Technol.*, **49**, 241 (1987).

28. W. D. Machin and P. D. Golding, *Langmuir*, **5**, 608 (1989).

29. S. Lowell and J. E. Shields, *Powder Technol.*, **28**, 201 (1981).

30. S. Lowell and J. E. Shields, *Powder Technol.*, **29**, 225 (1981).

31. S. Brunauer, L. S. Deming, W. S. Deming, and E. Teller, *J. Amer. Chem. Soc.*, **62**, 1723 (1940).

32. J. W. Vanderhoff and H. J. van den Hul, *J. Macromol. Sci.*, **A7**, 677 (1973).

33. M. Day and R. Fletcher, in *"Characterization of Porous Solids"*, K. K. Unger, ed., Elsevier Science, Amsterdam, 491 (1988).

34. D. Dollimore, P. Spooner, and A. Turner, *Surf. Technol.*, 4, 121 (1976).

35. D. Dollimore and G. R. Heal, *Surf. Technol.*, **6**, 231 (1978).

36. C. Pierce, *J. Phys. Chem.*, **57**, 149 (1953).

37. C. Orr and J. Dallavalle, *"Fine Particle Measurement"*, MacMillen, New York (1959).

38. B. C. Lippens, B. G. Linsen, and J. H. de Boer, *J. Catalysis*, **3**, 32 (1964).

39. J. Hearn, P. L. Smelt, and M. C. Wilkinson, *J. Colloid Interface Sci.*, **133**, 284 (1989).

40. F. G. R. Gimblett and M. U. Z. Qazi, *J. Colloid Interface Sci.*, **123**, 148 (1988).

41. F. G. R. Gimblett and M. U. Z. Qazi, *J. Colloid Interface Sci.*, **125**, 534 (1988).

42. B. C. Lippens and J. H. de Boer, *J. Catalysis*, **4**, 319 (1965).

Chapter 4
Monodisperse Porous Polymer Particles: Formation of the Porous Structure

4.1 INTRODUCTION

Monodisperse porous styrene-divinylbenzene copolymer particles in the size range of 10 μm in diameter were prepared via seeded emulsion polymerization. Linear polymer (polystyrene seed) or a mixture of linear polymer and solvent or nonsolvent were used as inert diluents[1, 2, 3]. Porous structure was formed by the removal of diluents via solvent extraction after polymerization. The pore diameters of these porous polymer particles were on the order of 1,000 $\mathring{A}$ with pore volumes up to 0.9 ml/g and specific surface areas up to 200 m^2/g. Porous polymer particles with a macroporous structure (pore size > 500 $\mathring{A}$ in diameter) can be used as precursors for ion exchangers, adsorbents and GPC column materials[4]. It is expected that the improved separation efficiency and optimal packing can be achieved with monodisperse porous polymer particles compared to polydisperse separation media[5].

The synthesis process of monodisperse porous polymer particles is generally divided into three stages: (1) swelling; (2) copolymerization; and (3) removal of diluents (solvent extraction)[3]. This is depicted schematically in Figure 4-1. In the swelling stage, the linear, monodisperse polystyrene seed latex particles are swollen by monomers and solvent-type diluent (solvent or nonsolvent) in which swollen particles behave as individual bulk polymerization sites. For the most part, the swelling step is not considered to play a role in the formation of pore structure. Direct observation of the interior structures of macroporous polymer particles by electron microscopy shows that the pores result from interstices between the microspheres and their agglomerates.

Therefore, the development of pore structure during the copolymerization process may be considered as the production, agglomeration and fixation of the interior microspheres[6, 7, 8]. Phase separation occurs between the copolymer and diluents during copolymerization and as a result the porosity of the polymer particles is observed after removal of the inert diluents. Since the linear polymer (diluent) is removed by a good solvent, the solvent-extraction process should also affect the pore structure formation.

Since this is a new synthesis approach for the preparation of monodisperse porous polymer particles via the seeded emulsion polymerization technique using the linear polymer seed as inert diluent, there is a need to developa proper understanding of the mechanism by which the pores are generated. The purpose of this study is to provide an experimental basis for the mechanism of pore formation of the porous structure during the copolymerization and solvent extraction processes.

4.2 EXPERIMENTAL

4.2.1 Materials

Styrene (Polysciences) and divinylbenzene 55 crosslinking monomer (Dow Chemical) were washed with 10% aqueous sodium hydroxide solution and water, dried over sodium sulfate, and passed through an activated aluminum oxide column to remove the inhibitors. The composition of divinylbenzene 55 is given in Table 4-1. The other materials were used as received: 2,2'-azobis-(2-methylbutyronitrile) initiator (E. I. duPont de Nemours), hydroquinone inhibitor (Fisher Scientific), sodium bicarbonate buffer (Fisher Scientific), Aerosol MA emulsifier (dihexylester of sodium sulfosuccinic acid; American Cyanamid), Polywet KX-3 oligomeric surfactant (n-octyl-S-[acrylonitrile]$_8$-[acrylic acid]$_8$-H, M_w= 1,500; Uniroyal Chemical), poly(N-vinyl pyrrolidone) K-90 surfactant (GAF

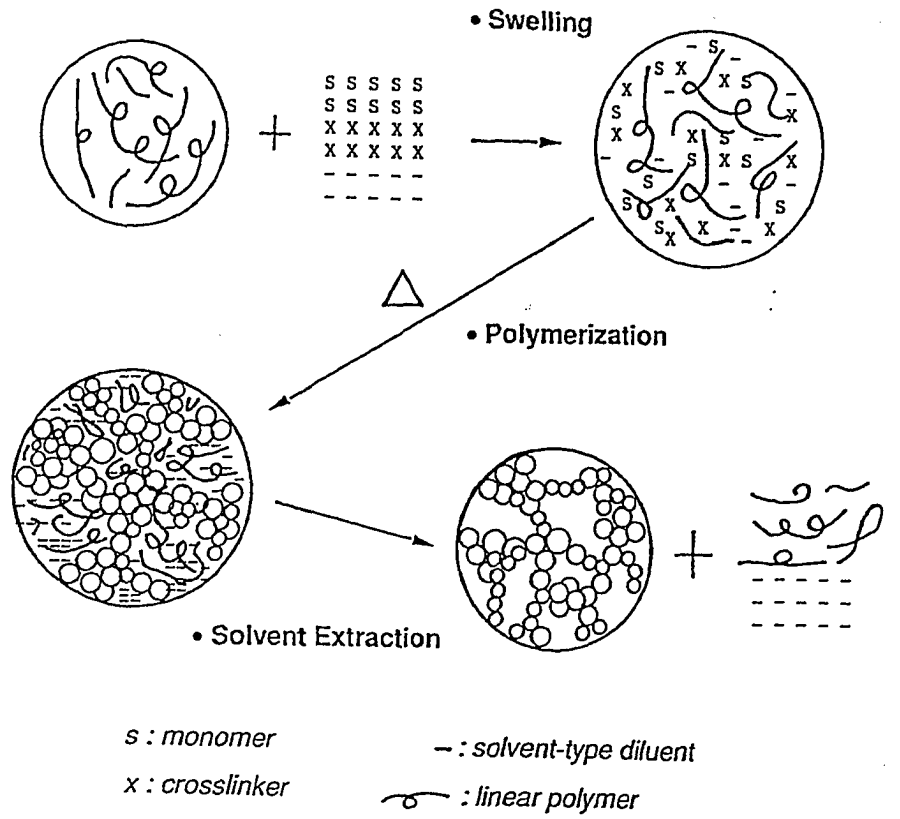

Figure 4-1: *A schematic model for the preparation of the monodisperse porous polymer particles using linear polymer seed and solvent or nonsolvent as inert diluents.*

Corp.), and solvents such as n-hexane, n-heptane, toluene, benzene, ethylbenzene, methylene chloride, methanol and tetrahydrofuran (Fisher Scientific). Distilled deionized water was used in the preparation of aqueous solutions.

Table 4-1: Composition of Divinylbenzene 55

Component	wt%
m-Divinylbenzene *(m-DVB)*	38.2
p-Divinylbenzene *(p-DVB)*	17.7
m-Ethylvinylbenzene *(m-EVB)*	32.0
p-Ethylvinylbenzene *(p-EVB)*	10.9
Diethylbenzene	0.2
Naphthalene	0.5

4.2.2 Seeded Emulsion Polymerization

Monodisperse porous styrene-divinylbenzene copolymer particles in the size range of 10 μm in diameter were prepared by seeded emulsion polymerization using different types of diluent and concentrations of divinylbenzene. The general procedure for the preparation was described previously in Chapter 2. The 8.7 μm-diameter monodisperse polystyrene latexes were used as seed particles. The seeded emulsion polymerizations were carried out at 30% organic phase according to the basic recipe given in Table 4-2. The ingredients used comprised monodisperse polystyrene seed latex, styrene and divinylbenzene (DVB) monomers, diluent, initiator, inhibitor, buffer, and emulsifiers. The molar ratio of solvent-type diluent to monomers was 1 with the swelling ratio (the weight ratio of the mixture of solvent-type diluent with

monomers to polystyrene seed) set to 3. The ingredients were weighed and charged into a capped bottle, which was tumbled end-over-end for 12 hours at room temperature (23 °C) to allow the seed particles to swell. The mixture was divided equally (ca. 20 g) into several 1-oz. glass bottles, capped and sealed. The bottles were then placed in safety baskets supported on a rotor, and were tumbled end-over-end at 16 rpm in a thermostated water bath at 70 °C. During the course of the polymerization, bottles were removed from the tumbling reactor at various time intervals, and the polymerizations stopped by immediately quenching the reaction mixture with hydroquinone in ice water.

4.2.3 Polymer Analysis

Samples picked up at various polymerization times were divided into three parts for different analyses. The conversion was determined by gas chromatography (GC) (Hewlett-Packard Model 5890) to measure the residual monomer concentration. Tetrahydrofuran was added to extract unreacted monomers while toluene was used as an internal calibration standard for the GC analysis. In the cases where toluene was used as an inert diluent for the preparation of the porous polymer particles, ethylbenzene was used as an internal standard for the GC analysis[7].

The conversion to gel was estimated from the fraction of methylene chloride-insoluble materials after methylene chloride extraction since this solvent readily dissolves the sol (nongel) polystyrene species. The product from the methylene chloride extraction was washed with methanol to remove residual methylene chloride and low molecular weight solvent-type diluents (solvent or nonsolvent). The weights of the insoluble material were converted to fractional conversions to gel. Molecular weight measurements of extracted polystyrene were carried out using a Waters Model 440 gel permeation

Table 4-2: Typical Polymerization Recipes for 11 μm-Diameter Monodisperse Porous Polymer Particles

Ingredient	wt%
Polystyrene seed particles (8.7 μm in diameter)	7.5
Aerosol MA	0.005
Polywet KX-3	0.014
Poly(N-vinyl pyrrolidone) K-90	0.800
Water	69.11
Monomers	
styrene	12.8 - variable
divinylbenzene 55	variable[a]
n-Heptane	9.7
2-2'-Azobis-(2-methylbutyronitrile)	0.018
Sodium bicarbonate	0.027
Hydroquinone	0.021

[a] *Different levels: 5, 15, and 25% divinylbenzene content (based on total polymer and monomers).*
• *Total charged amount = 20 grams; polymerization temperature = 70 °C.*

chromatograph (GPC) with tetrahydrofuran as the eluant solvent.

Infrared spectroscopy analysis of the copolymer, washed with methanol to extract unreacted monomers, was carried out in KBr pellets with a Mattson Sirus 100 FTIR spectrometer. This was used to detect residual double bonds of divinylbenzene units, which had not reacted, either by crosslinking or in cyclization reactions[9, 10, 11]. Two peaks due to vinyl groups were analyzed. These are the bands at 1630 cm^{-1} (C=C stretching vibration) and 990 cm^{-1} (out of plane deformation γ_{C-H})[12]. The band at 905 cm^{-1} was used as a reference for polystyrene (monosubstituted phenyl ring)[13].

Samples obtained after solvent extraction were dried in air at room temperature and then vacuum-dried in an oven at 45°C. The surface morphology and particle size of porous polymer particles were characterized using an ETEC Autoscan scanning electron microscope. The surface area *(S)* of the particles was measured by nitrogen adsorption isotherms. Nitrogen adsorption at 77°K was determined volumetrically in a Quantasorb Sorption System as outlined in Chapter 2. The BET equation was used to analyze the low relative pressure region of the isotherm in order to find the surface areas of the particles[14, 15]. Pore volume and pore size distribution were determined by mercury intrusion porosimetry on a Micromeritics AutoPore 9200 porosimeter as discussed in Chapter 2. Cumulative pore volumes (V_p) were estimated from the intruded mercury volumes, and pore radii quoted were those of the equivalent hollow cylinders. The volume *ln* pore radius distribution function $D_v(ln\ r)$ was used to express pore size distribution[16, 17].

The crosslinking density of the copolymer after solvent extraction was determined by equilibrium swelling in toluene. The dried copolymer was pressed by means of a hot press (Pasadena Hydraulics Model IIA-35) at 135°C and 14 tons platen pressure to obtain a transparent specimen, which was placed in a

stoppered flask containing toluene to allow the swelling of the gel polymer.

Swelling of individual particles in the extracting solvent was investigated using an optical microscope (BioVision Microscope). The images were recorded on micrographs from which particle diameters of the swollen particles was then estimated.

4.3 RESULTS AND DISCUSSION

Monodisperse porous polymer particles were prepared via seeded emulsion copolymerization of styrene and divinylbenzene by the use of linear polystyrene (polystyrene seed) or a mixture of linear polystyrene and solvent or nonsolvent as inert diluents, then extracted with methylene chloride/methanol to develop porosity. The polymerizations were carried out with different diluent type and divinylbenzene concentration in a bottle polymerizer at 70 °C.

The overall conversion of monomers, as determined by gas chromatographic analysis, is shown in Figures 4-2 and 4-3 as a function of polymerization time. The polymerizations took a relatively long time to reach high conversion owing to the large particle size; however, the final conversions based on monomers were all above 93% at 24 hours of polymerization time. The increased rate of polymerization as the reaction proceeded is a consequence of autoacceleration, which is due to diffusion-controlled chain termination, occurring in the viscous reaction site. The use of hydroquinone inhibitor did not have any significant effect on the polymerization kinetics in terms of an observed induction period or a retardation effect. At a fixed crosslinker concentration (15% DVB), the polymerization rate depended on diluent type (Figure 4-2). The polymerization rate is always more rapid in the absence of solvent or nonsolvent diluent (Curve A). The initial rates of polymerization were slightly greater with nonsolvent (n-heptane) (Curve B) as diluent than those

with solvent (toluene) (Curve C). The polymerization rates increased with increasing divinylbenzene concentration (Figure 4-3). The increased rate of polymerization at the higher crosslinker contents might also be a consequence of autoacceleration[8].

The polymer particles after the 24-hour polymerization were extracted with methylene chloride to remove the linear polymer portion. This step was followed by washing the particles with methanol. The purpose of the methanol is to remove residual methylene chloride and low molecular weight diluents (solvent and nonsolvent) and preserve the structure edifice of the pore structure after methylene chloride extraction. In these experiments, the aqueous polymer latex particles were added to methylene chloride in capped bottles at a low concentration (aqueous polymer particles/methylene chloride ratio less than 1%). Since methylene chloride is not miscible with water, the bottles were tumbled end-over-end at room temperature to ensure extraction. After 18 hours, the methylene chloride was replaced with fresh solvent, and the extraction was continued for another 18 hours to ensure the removal of linear polymer. These steps were followed by washing the particles with a mixture of methylene chloride and methanol, and then methanol only. This extraction process allowed us to handle many samples at the same time. After extraction, the particles were dried overnight in air at room temperature and then vacuum-dried in an oven at 45 °C. It was found that the development of pore structure obviously depended on the methylene chloride-extraction time. Thirty-six hours of extraction was the time chosen since the pore structure, i.e., specific surface area and pore volume, was found to be well developed at this point (Table 4-3). The inclusion of linear polymer in the network structure was also minimized at this time as shown in the "LP_{in}" column in Table 4-3. There is an inclusion of high molecular weight fraction of the linear polymer in the copolymer network,

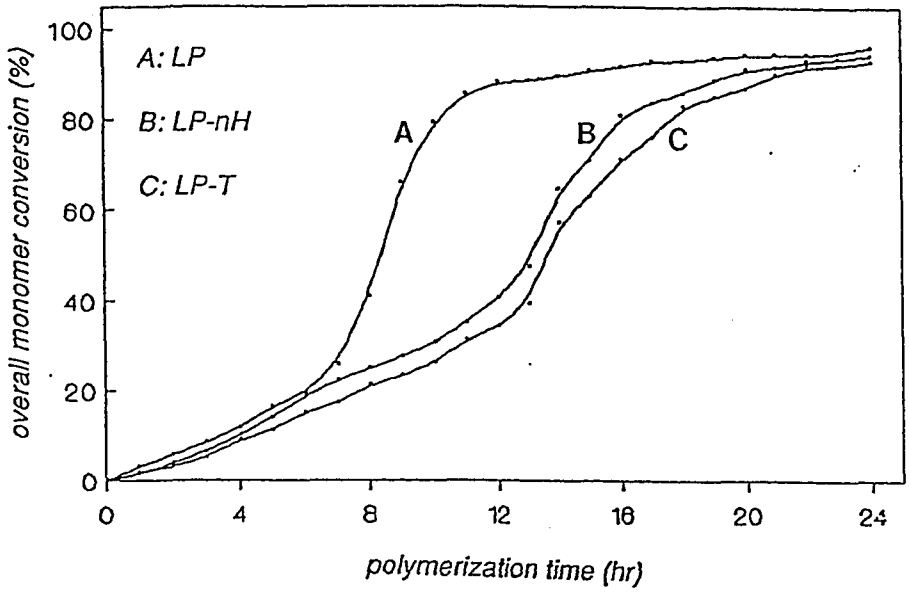

Figure 4-2: *Overall comonomer (styrene-divinylbenzene) conversion for the preparation of monodisperse porous polymer particles with different diluents: (A) LP: linear polystyrene; (B) LP-nH: linear polystyrene/n-heptane; and (C) LP-T: linear polystyrene/toluene. [15% DVB]*

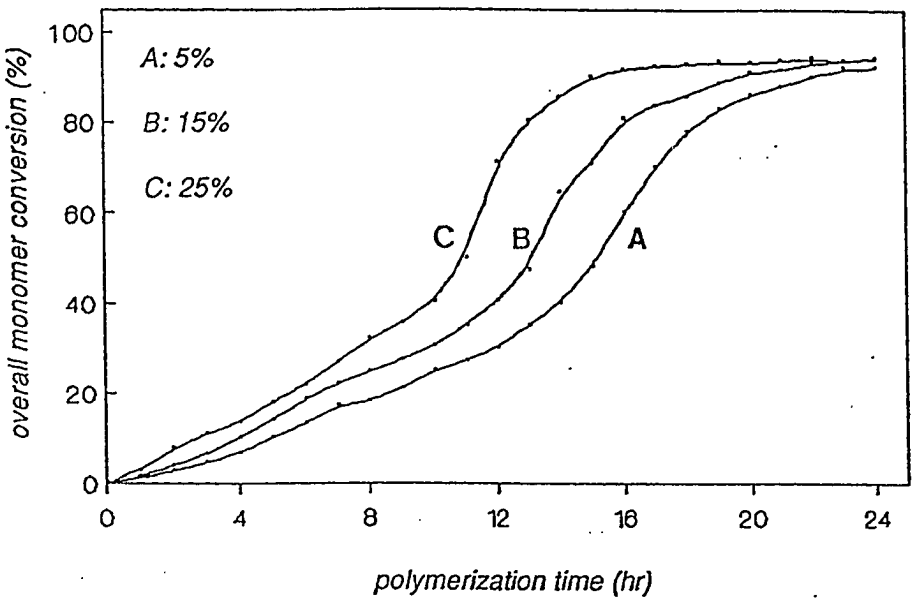

Figure 4-3: *Overall comonomer (styrene-divinylbenzene) conversion for the preparation of monodisperse porous polymer particles with different divinylbenzene contents: (A) 5%; (B) 15%; and (C) 25%. [diluent: linear polystyrene / n-heptane]*

as evidenced by the molecular weight of the extracted polystyrene, which cannot be avoided due to the chemical grafting and physical steric hindrance. The implications of this inclusion will be discussed in more detail later.

Table 4-3: Experimental Results of Methylene Chloride Extraction

[Diluent: linear polystyrene/n-heptane; 15% DVB; $M_{W,LP}$= 1.49 x 10^6][a]

Extraction time hr	S m^2/g	V_p ml/g	LP_{in} %	$M_{W,e}$ x 10^{-5}
0.5	37	0.44	44	9.74
2	44	-	33	10.5
6	45	0.67	29	11.3
12	51	-	20	11.9
24	52	0.73	15	12.2
36	51	0.72	14	12.1

[a] *%DVB: weight percentages of divinylbenzene in the polymer particles and $M_{W,LP}$: weight-average molecular weight of linear polystyrene seed.*
* *S: specific surface area; V_p: pore volume; LP_{in}: fraction of linear polystyrene included within network structure; and $M_{W,e}$: weight-average molecular weight of extracted polystyrene.*

An attempt was made to compare this process with Soxhlet extraction process which was decribed in previous chapters. In Soxhlet extraction, the polymer particles were extracted with methylene chloride in a Soxhlet apparatus for 36 hours (polymer particles/methylene chloride ratio less than 0.5%). Then, the polymer particles were extracted in the Soxhlet apparatus in methanol for 24 hours. After solvent extraction, the particles were dried in air and in a vacuum oven at 45°C. The results, given in Table 4-4, reveal that the physical properties of porous polymer particles obtained from both extraction

processes were almost identical. The differences in specific surface area and pore volume were below 5% which were around the accuracy range of both the measurements. The fraction of inclusion of linear polymer within the network structure and the molecular weights of extracted polystyrene polymers, as determined by GPC, were almost the same and lower than the molecular weight of the linear polymer seed (M_W = 1.49 x 10^6). The solvent extraction processes routinely used gave results equivalent to the Soxhlet extraction process. Regardless of the extraction method used, the inclusion of some fraction of linear polymer in the copolymer structure could not be avoided.

Table 4-4: Experimental Results of Methylene Chloride Extractions

[Diluent: linear polystyrene/n-heptane; $M_{W,LP}$=1.49 x 10^6][a]

DVB %	S m^2/g	V_p ml/g	LP_{in} %	$M_{W,e}$ x 10^{-5}
1. Solvent Extraction				
5	18	0.42	10	12.5
15	51	0.72	14	12.1
25	104	0.88	19	11.0
2. Soxhlet Extraction				
5	18	0.44	11	12.3
15	51	0.73	14	12.1
25	109	0.86	18	11.0

[a] *$M_{W,LP}$: weight-average molecular weight of linear polystyrene seed.*
* *DVB%: weight percentages of divinylbenzene in the polymer particles; S: specific surface area; V_p: pore volume; LP_{in}: fraction of linear polystyrene included within network structure; and $M_{W,e}$: weight-average molecular weight of extracted polystyrene.*

The polymer particles prepared for this investigation were designed to provide a proper understanding of the formation of monodisperse porous

polymer particles. Owing to the number of synthesis parameters involved, a system with 15% divinylbenzene content was chosen for more detailed study. Linear polystyrene seed with weight-average molecular weight ($M_{W,LP}$) of 1.49 x 10^6 and n-heptane were used as inert diluents. The polymerization was carried out in a bottle polymerizer at 70 °C. Samples were taken in order to allow for characterization of the porous structure at various conversions, as well as the polymerization kinetics of all the monomers involved and the consumption of residual double bonds of divinylbenzene over the whole range. The time for methylene chloride-extraction was set to 36 hours in order to develop maximum porosity. The mode of pore structure formation, however, should follow this kinetic scheme of investigation in which the diluent type and crosslinker content are varied.

4.3.1 Copolymerization

The overall conversion of monomers in the copolymerization of styrene-divinylbenzene with a mixture of linear polystyrene and n-heptane as inert diluents and 15% divinylbenzene content, is represented by the curves labelled B in Figures 4-2 and 4-3. A chemical study of the copolymerization of styrene and technical divinylbenzene should involve two main processes: (1) the copolymerization itself, i.e., the incorporation of the various monomers in the copolymer, involving styrene and the various components of technical divinylbenzene (divinylbenzene 55 (Dow Chemical)) (a mixture of four main components: para- and meta-divinylbenzene, p-DVB and m-DVB; para- and meta-ethylvinylbenzene, p-EVB and m-EVB; with some minor impurities such as diethylbenzene and naphthalene) (Table 4-1); and (2) the crosslinking process, i.e., the consumption of the second double bond of p-DVB and m-DVB, which might give intramolecular cyclization instead of intermolecular

crosslinking[18, 19, 20, 21, 22, 23, 24, 25, 26, 27].

Typical individual monomer conversion curves, as determined from GC analysis, are shown in Figure 4-4. The most reactive monomer is p-DVB, followed by m-DVB, both being totally polymerized after 20 hours of reaction time. Conversion curves of all other monomers, styrene and both m-EVB and p-EVB cannot be distinguished; they are not totally consumed. It may be thus concluded that substitution of alkyl groups on the aromatic ring does not change the reactivity of styrene monomer. Those results shown in Figure 4-4 confirm the fact that p-DVB is more reactive than m-DVB itself being more reactive than styrene and the isomers of ethylvinylbenzene[18, 20, 28, 29, 30, 31, 32, 33, 34].

The crosslinking process was rather efficient, since most of the polymer became insoluble quickly. Whereas the conversion of monomer to polymer was determined by GC analysis, conversion to gel was estimated from the fraction of methylene chloride-insoluble material since this solvent dissolved the sol (nongel) polymer species. Typical data for the amount of sol and gel material are given in Figure 4-5. They show that gelation occurs rather readily, i.e., at an early stage in the polymerization. The polymer and gel content rapidly converged, and only 4% sol polymer was detectable beyond ca. 30% conversion. Extrapolation of the gel conversion curve to zero gel content gave a gel time from which the fractional conversion at gelation might be found. The gel point was estimated at around 2 hours with 5% monomer conversion.

Combined GC and Infrared (IR) analyses allow one to obtain data about the reactivity of residual double bonds. Figure 4-6 shows the relative concentrations of the residual DVB double bonds (as compared with the residual double bond intensity at the initial gel point: 2 hours with 5% monomer conversion) in the copolymer versus reaction time, which decrease with

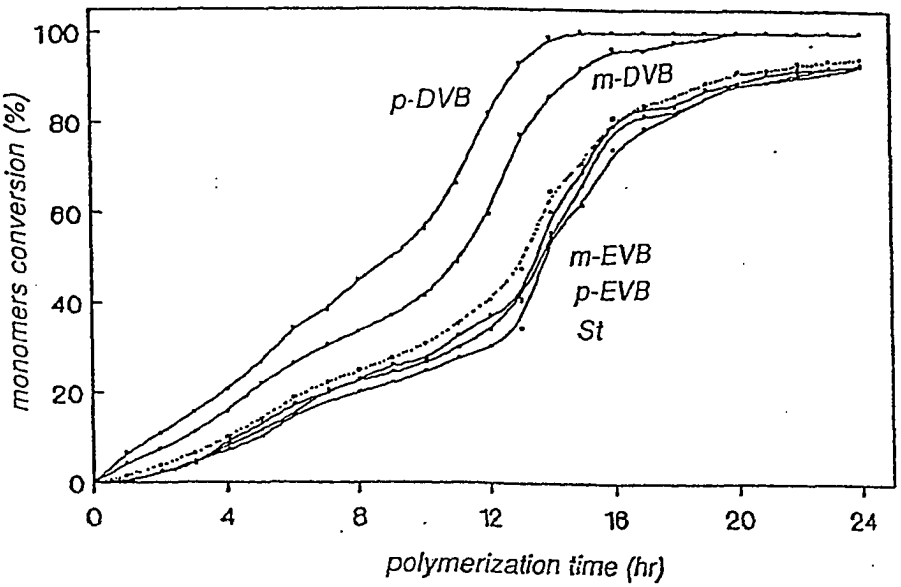

Figure 4-4: *Individual monomer conversions (as determined by GC analysis) of para- and meta-divinylbenzene (p-DVB & m-DVB), para- and meta-ethylvinylbenzene (p-EVB & m-EVB), and styrene (St). The dotted lines represents the overall comonomer conversion. [diluent: linear polystyrene / n-heptane; 15% DVB; $M_{W,LP}$= 1.49 x 10^6]*

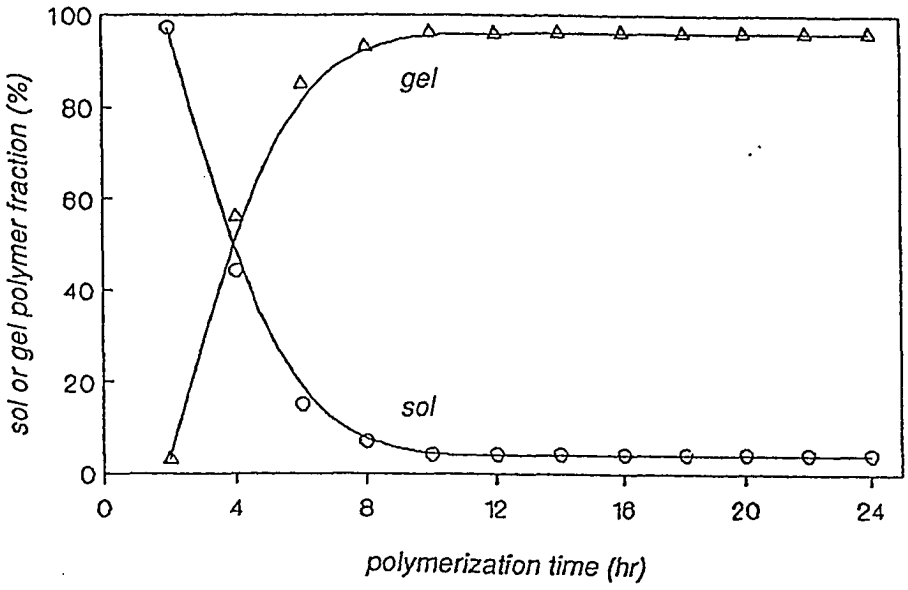

Figure 4-5: *Residual sol fraction (soluble fraction in methylene chloride) and calculated gel fraction versus polymerization time. [diluent: linear polystyrene / n-heptane; 15% DVB; $M_{W,LP}$= 1.49 x 10^6]*

increasing monomer conversion. The consumption of the second double bond was much higher at the beginning of the polymerization, but its rate decreased very much at the end of the process. The earlier precipitation during copolymerization in the presence of nonsolvent could effectively increase reactant concentrations and might enhance the consumption of the second double bond which would favor the formation of crosslinking copolymer. The second double bond was not totally consumed; some unreacted double bonds from crosslinker molecules were trapped in the gel polymer as a consequence of physical restriction of their mobility. The fractional conversion to polymer at any stage exceeded the corresponding consumption of double bonds.

At the beginning of the copolymerization, much more divinylbenzene is incorporated into the copolymer than is expected based on the initial composition of the monomer mixture. Thus, the divinylbenzene constituents, which at first are more tightly embedded into the copolymer structure, induce the formation of regions of narrow-mesh, entangled networks interspaced with less crosslinked members, which are formed in a later stage of the copolymerization when the major part of the divinylbenzene monomers have been used up. This will cause an internal heterogeneity of the copolymer.

Direct observation of polymer morphology after solvent extraction at different stages by scanning electron microscopy (Figure 4-7) gives a physical view of the copolymerization process. At the very early stage of the polymerization (about 5% conversion), the copolymer was almost completely soluble in methylene chloride and miscroscopy showed an amorphous matrix comprised of some embedded spherical particles (Figure 4-7A). After 6 hours (Figure 4-7B) with conversion above 20%, the copolymer particles were broken while being subjected to solvent extraction. Crosslinked microspheres and their agglomerates were visible, but they were clustered and stuck to a big fused

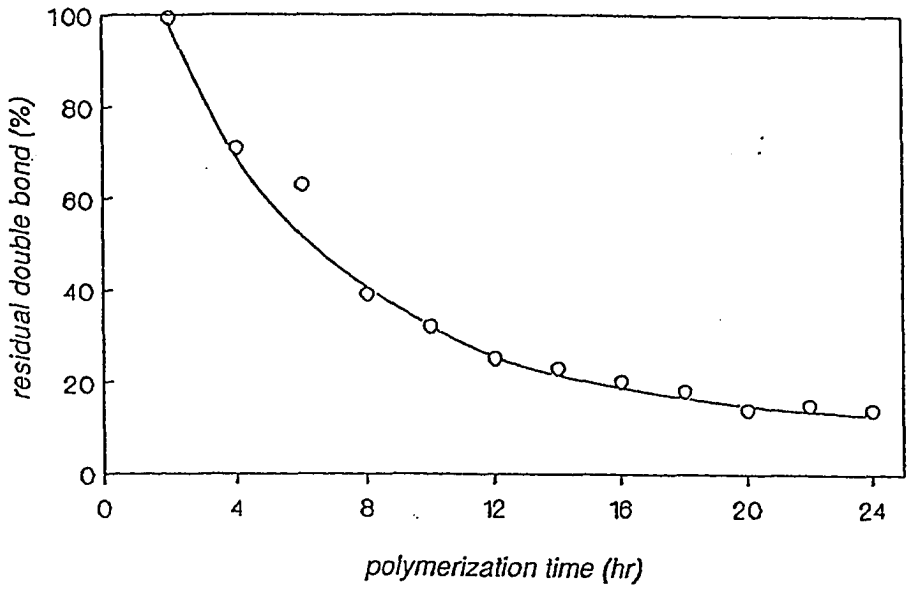

Figure 4-6: *Relative concentration of residual double bonds in the copolymer versus reaction time. [diluent: linear polystyrene/n-heptane; 15% DVB; $M_{W,LP}$= 1.49 x 10^6]*

mass when dried. Later on, at 65% conversion, the porous structure was roughly formed due to the binding together of microspheres and agglomerates (Figure 4-7C). However, the structure was not fully built up. The removal of unreacted monomers and linear polymer caused the polymer particles to collapse. Finally, at the latest stage of reaction, the porous structure was actually formed due to the fixation of the network structure. As shown in Figure 4-7D, spherical particles with macroporous morphology were prepared.

Assuming that the sol fraction approaches a constant at higher conversions, as in the general case of styrene-divinylbenzene copolymerization[4, 35], the inclusion of linear polymer (diluent) in the network structure could be estimated from the fraction of methylene chloride-extracted linear polymer. As the porous structure was built up, linear polystyrene began to be included in the copolymer structure. Two causes of this are possible: either chemical incorporation due to chain transfer to the linear polymer, or actual trapping in the network of the copolymer, due to a strong steric hindrance. Chain transfer to polymer would take place at high monomer conversion or high polymer concentration. Thirty-six hour extraction was quite sufficient and further extraction (for a total of 48 hours) did not increase the yield, although the inclusion by steric hindrance cannot be ruled out with certitude. Once the pore structure is fully formed at about 18 hours, the fraction of linear polymer inclusion reaches a maximum at 14 weight percent (Figure 4-8). Linear polystyrene macromolecules with high molecular weights were included in the network structure of the macroporous copolymers. Evidence of this was also given by the results obtained for the molecular weights of the extracted polystyrene measured by gel permeation chromatography (GPC), as given in Table 4-5. Without the binding of microspheres and agglomerates (estimated to take place after the first 12 hours of polymerization), the extracted

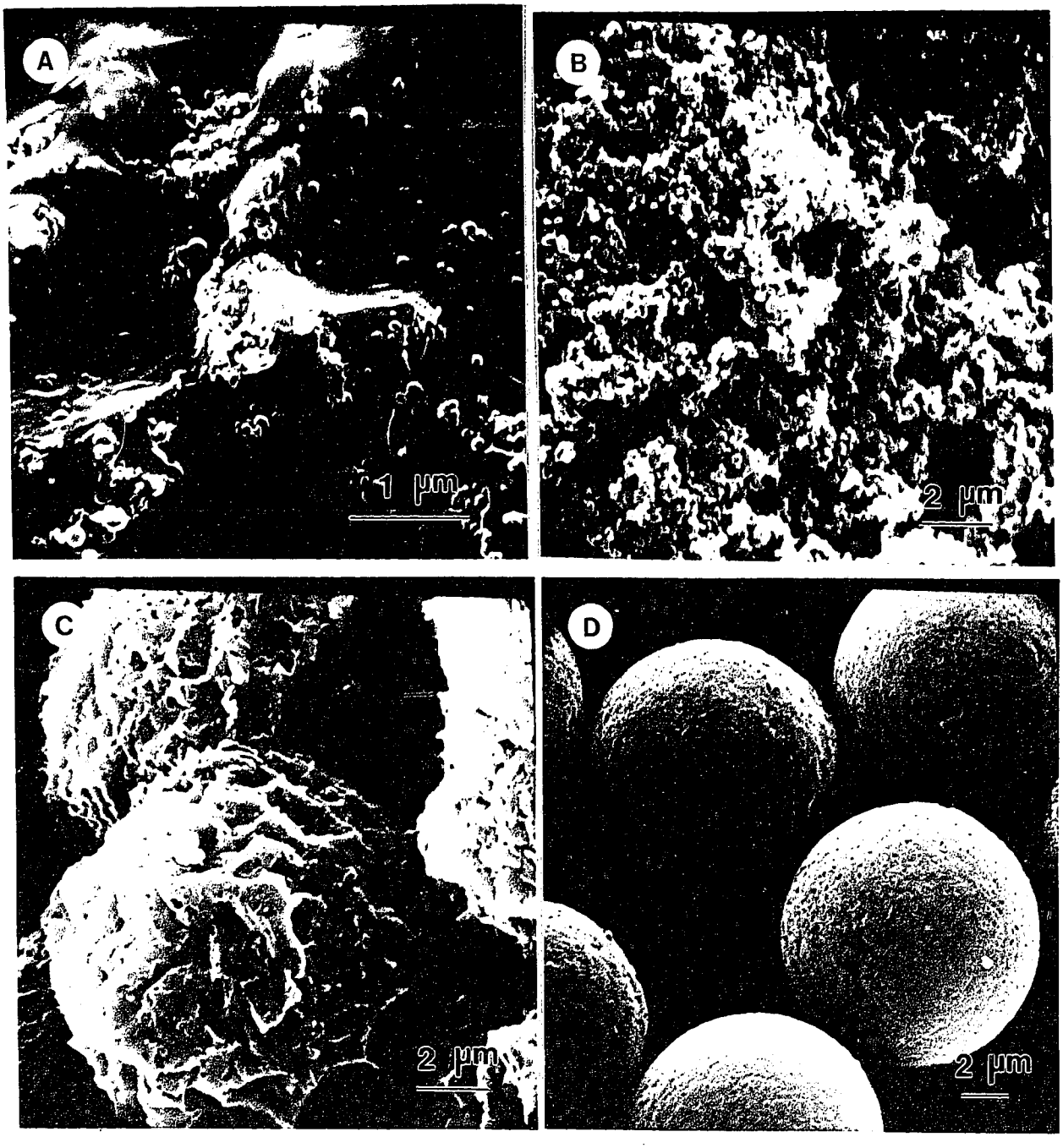

Figure 4-7: *Scanning electron micrographs of methylene chloride-extracted copolymer at different conversions (reaction times): (A) 5% (2 hr); (B) 20% (6 hr); (C) 65% (14 hr); and (D) 93% (22 hr). [diluent: linear polystyrene / n-heptane; 15% DVB; $M_{W,LP}$= 1.49 x 10^6]*

molecular weight of the linear polymer was almost the same as the molecular weight of polystyrene seed. The lower values of $M_{N,e}$ might indicate the generation of smaller molecular weight copolymer during the copolymerization process, which have a molecular weight about 2 x 10^4 as estimated from the GPC chromatogram. Once the binding and fixation proceeded (which takes place during the last 12 hours of the polymerization process), some fraction of high molecular weight linear polymer was included in the network structure, as indicated by the reduction of $M_{W,e}$ of the extracted polymer.

The inclusion of linear polystyrene within the network also depends on the diluent type and crosslinker content, as well as the molecular weight of polystyrene seed particles. Table 4-6 shows the inclusion and extracted molecular weight of polystyrene after 24-hour polymerization. Using only the linear polymer as diluent, the amount of the higher molecular weight portion of the linear polystyrene trapped within the network structure were large, which might reveal the low degree of phase separation between diluent and copolymer during the synthesis process. The higher the molecular weight of the polymer seed particles the greater the fraction being included in the network structure. A relatively higher divinylbenzene content resulted in an increase in the amount of inclusion; during copolymerization in the presence of nonsolvent, the higher polymerization rate together with the earlier precipitation, might favor the entrapment of the linear polymer chains.

Changes in specific surface area and pore volume during the synthesis of the porous polymer particles reflect the structural changes that lead to the macroporous resins. Figure 4-9 graphically represents the relationship between pore structure and polymerization time. Without the full fixation of the microspheres and agglomerates (up to 12 hours polymerization time), the collapse of structure and cohesion of gel polymer chains after solvent extraction

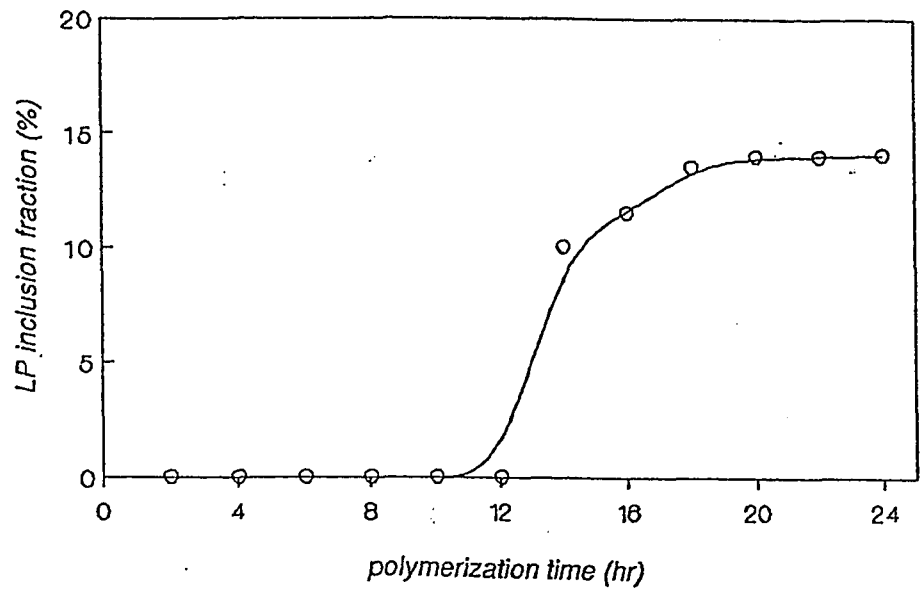

Figure 4-8: *Weight fraction of linear polymer (LP), used as diluent, included in the copolymer network during the copolymerization process. [diluent: linear polystyrene/n-heptane; 15% DVB; $M_{W,LP}$= 1.49 x 10^6]*

Table 4-5: Extracted Molecular Weight of Linear Polystyrene

[Diluent: linear polystyrene/n-heptane; 15% DVB; $M_{W,LP}$= 1.49 x 10^6]

Sample[a]	$M_{N,e}$ x 10^{-5}	$M_{W,e}$ x 10^{-5}	PDI
Seed	2.99	14.9	4.98
PF02	2.16	14.5	6.71
PF04	2.08	14.7	7.06
PF06	2.36	15.0	6.36
PF08	2.48	14.7	5.93
PF10	2.71	15.2	5.61
PF12	2.59	14.6	5.64
PF14	2.40	12.9	5.38
PF16	2.36	12.6	5.34
PF18	2.34	12.4	5.30
PF20	2.31	11.8	5.11
PF22	2.29	12.2	5.33
PF24	2.33	12.1	5.19

[a] *The number in the sample coding denotes the reaction time in hours.*
* *$M_{N,e}$ and $M_{W,e}$: number and weight average molecular weights of extracted polystyrene; and PDI: molecular weight distribution polydispersity index.*

reduced the specific surface area and total pore volume.

The crosslinking density of the copolymer after solvent extraction was determined by equilibrium swelling in toluene. The swelling equilibrium between solvent and swollen gel can be described by the Flory-Rehner equation[36]:

$$-[ln(1-v_2)+v_2+\chi_1 v_2^2] = V_1 n[v_2^{1/3}-\frac{v_2}{2}] \quad (4.1)$$

Table 4-6: Inclusion and Extracted Molecular Weight of Linear Polystyrene

Diluent	$M_{W,LP}$ x 10^{-5}	DVB %	LP_{in} %	$M_{W,e}$ x 10^{-5}
LP	14.9	15	24	9.74
LP/n-Hexane	14.9	15	13	12.3
LP/n-Heptane	14.9	15	14	12.1
LP/Toluene	14.9	15	15	12.0
LP/n-Hexane	10.8	15	10	9.29
LP/n-Hexane	5.68	15	7	5.28
LP/n-Hexane	4.46	15	5	4.23
LP/n-Heptane	14.9	5	10	12.5
LP/n-Heptane	14.9	25	18	11.0

* *LP: linear polystyrene seed; $M_{W,LP}$: weight-average molecular weight of linear polystyrene seed; DVB%: weight percentages of divinylbenzene in the copolymer; LP_{in}: fraction of linear polystyrene included within network structure; and $M_{W,e}$: weight-average molecular weight of extracted polystyrene.*

where v_2 is the volume fraction of copolymer in the swollen mass, V_1 is the molar volume of solvent, χ_1 is the Flory-Huggins polymer-solvent interaction parameter, and n is the crosslinking density. For the styrene-divinylbenzene and toluene pair, $\chi_1 = 0.46$ and $V_1 = 106$ ml/mole were used[37]. n could be estimated by determining v_2 from the swelling equilibrium between copolymer and toluene. The plot of crosslinking density versus polymerization time (Figure 4-10) practically follows the same trend as the consumption of the divinylbenzene second double bond given in Figure 4-6. At high conversions, the overall crosslinking density was slightly lower as a consequence of the linear polymer being included in the polymer network. It is necessary to note that, as a result of unreacted residual vinyl groups and cyclization, the true degree of

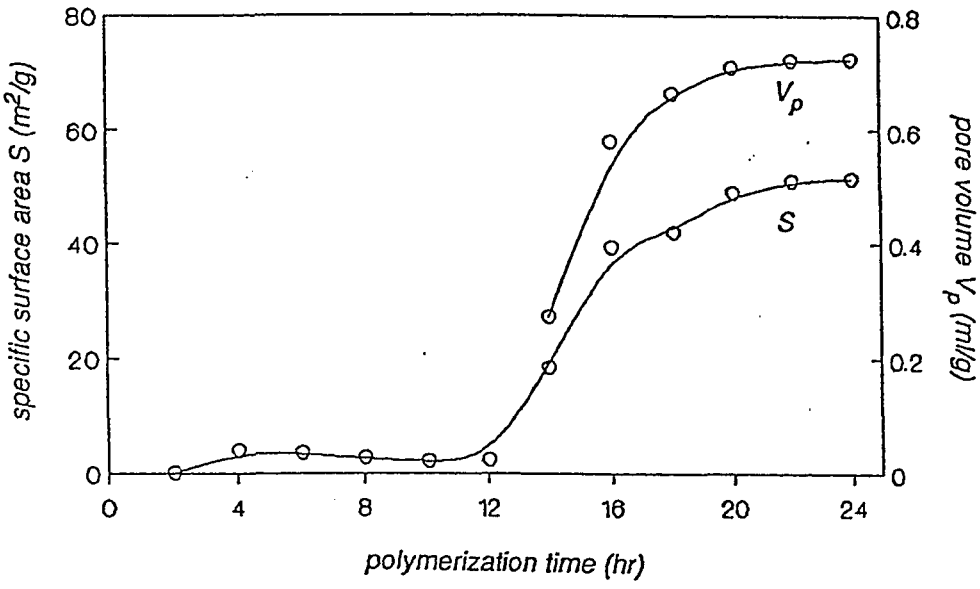

Figure 4-9: *Specific surface area (S) and pore volume (V_p) changes during copolymer synthesis. [diluent: linear polystyrene / n-heptane; 15% DVB; $M_{W,LP}$= 1.49 x 10^6]*

crosslinking is smaller than the quantity of divinylbenzene incorporated into copolymer network. Owing to the phase separation, the network phase was highly concentrated at the beginning of copolymerization and the microspheres formed were highly crosslinked.

4.3.2 Mechanism of Pore Formation in the Copolymerization Process

Based on the observations of particle structure and the kinetic analysis of the copolymerization, a mechanism for pore formation during the copolymerization stage using linear polymer and nonsolvent as inert diluents is proposed as a two-stage process. This is depicted schematically in Figure 4-11. After swelling, each particle is composed of a solution of monomers, initiator and the diluents (linear polymer and nonsolvent); it is suspended in an aqueous solution and stabilized with surfactants. Since the DVB has a high reactivity ratio, during the very early stages of the polymerization DVB-rich copolymer molecules are formed which are composed of straight chains with pendent vinyl groups. Further reaction leads to the increase of intermolecular linkages, with the result of formation of small crosslinked nuclei of polymer molecules. Continued polymerization yields intramolecularly crosslinked microgels and linear molecular chains that are soluble in the monomers. The monomers are transformed into crosslinked copolymer as the reaction proceeds; phase separation occurs between copolymer and linear polystyrene and nonsolvent, which gives a copolymer-rich phase and a diluent-rich phase, the monomers being distributed between the two phases. Linear polymer used as diluent will be in a swollen state because the monomers themselves are good solvents. Since solvated and very lightly crosslinked copolymers can behave, in some respects, like a liquid, the interfacial tension at the polymer-rich phase gives it the low-

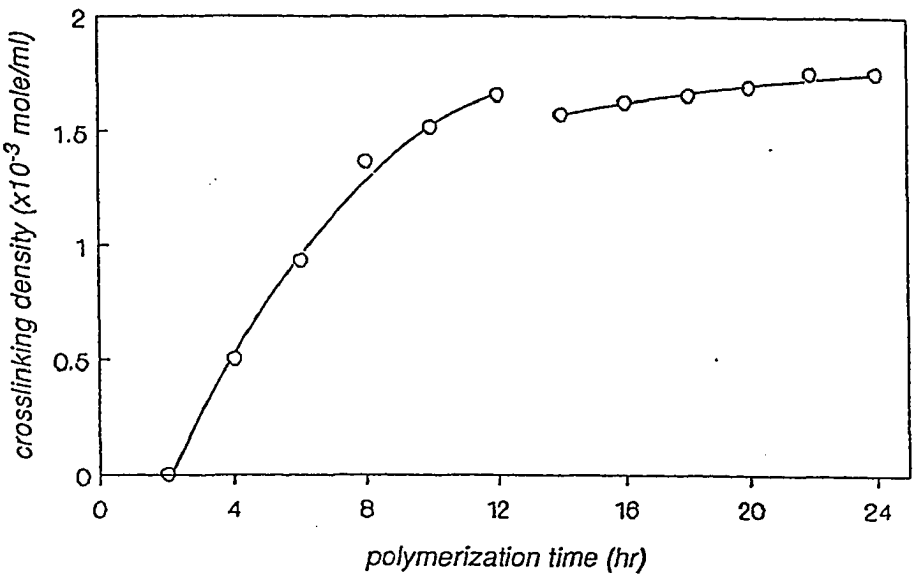

Figure 4-10: *Crosslinking density of copolymer versus polymerization time. [diluent: linear polystyrene/n-heptane; 15% DVB; $M_{W,LP}$= 1.49 x 10^6]*

energy spherical form, and the polymer is separated as a mass of microspheres[6]. At a certain conversion of monomer to polymer macrogelation occurs and gives a gel type of particle composed of an agglomeration of microspheres. The first stage in the formation of a macroporous structure is the production and agglomeration of highly crosslinked microspheres such that they make a polymer particle.

The second stage in pore-structure formation is the binding together and fixation of the microspheres and agglomerates. As the polymerization and formation of microspheres continue, the microspheres are bound together by the polymerization of the monomers, which have a higher percentage of the monovinyl components in composition (as estimated from the individual monomer consumption) and act to solvate the microspherical polymers. Some fraction of the high molecular weight linear polystyrene is trapped within the microspheres and agglomerates while they are binding together; the inclusion of linear polymer is dependent on the nature of linear polymer and the extent of phase separation between the diluent phase and the copolymer phase. It is during this stage that the macroporous structure is actually formed. Voids between microspheres and agglomerates are filled with diluent (linear polymer and nonsolvent). In the diluent phase, entanglement of linear polymer will take place, depending on the molecular weight of the polymer and interaction between nonsolvent and linear polymer, thus explaining the sensitivity of the pore size distribution to the molecular weight of the linear polymer[3]. After the removal of the inert diluents, polymer particles with macroporous structure are obtained.

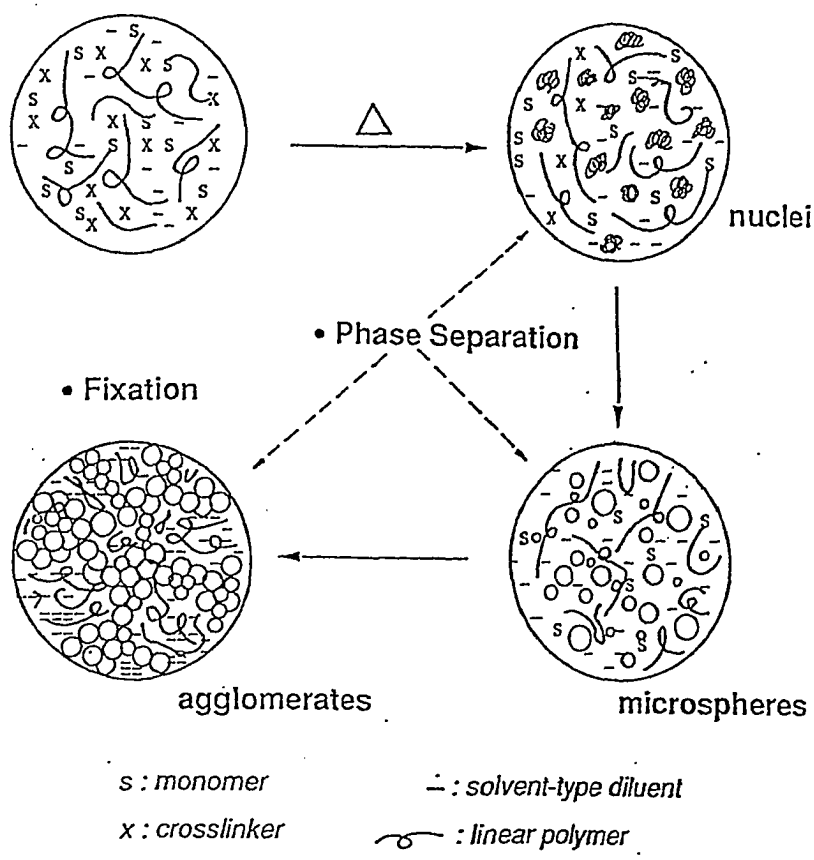

Figure 4-11: *A schematic model for the process of pore formation in the copolymerization stage using linear polymer and nonsolvent as inert diluents.*

4.3.3 Solvent Extraction

In the preparation of monodisperse porous polymer particles, the inert diluent, linear polymer or a mixture of linear polymer and solvent or nonsolvent, has to be removed to create the porous structure after polymerization. Diluents were removed by means of solvent extraction. Figure 4-12 shows the scanning electron micrographs of the polymer particles with or without different solvent extraction processes after polymerization. Polymer particles dried directly after polymerization showed a partially collapsed surface morphology due to the evaporation of n-heptane and unreacted monomers (Figure 4-12A). Nonsolvent such as n-heptane was removed when the polymer particles were extracted by methanol alone; the particle surface is rather smooth, as shown in Figure 4-12B, which indicates the collapse of the structure was prevented by replacing the n-heptane and unreacted monomers by poor solvent (such as methanol). However, no visual pore structure was observed by scanning electron microscopy. The specific surface area (2.0 m^2/g) of these polymer particles was too low to indicate the presence of pores in the particles. When the polymer particles were extracted with a good solvent (e.g., methylene chloride) to remove the linear polymer portion, a porous structure was obtained (Figure 4-12C). Polymer particles swollen with a good solvent tended to fused together while drying; some extracted linear polymer also precipitated on the particle surface when the good solvent evaporated as demonstrated in Figure 4-12C by strands between the particles. Upon removal of the good solvent by drying at room temperature where the polymer is in the rubbery state, this induced the pores to collapse and the fusion of the polymer chains. If this step was followed by washing with a poor solvent (e.g., methanol) prior to drying, the pore structure was preserved, as shown in Figure 4-12D. On the transition from a good solvent to a poor solvent, microsyneresis might appear along with the volume deswelling. The

microsyneresis is a process of a local, spontaneous separation of the poor solvent from a gel due to contraction of the gel[38, 39, 40, 41]. This microsyneresis is then fixed during deswelling when the polymer passes into the glassy state. Here, sorbed poor solvent is contained in the pores, and the polymer matrix is in fact an unswollen copolymer. It has been reported that, in the preparation of porous polymer particles using solvent or nonsolvent as inert diluent, the removal of low molecular diluents by methanol extraction yields more porous structures[42, 43, 44, 45, 46, 47]. Thus the use of methanol to remove residual good solvent and low molecular weight diluents (solvent or nonsolvent) preserves the structural edifice of the pore structure and yields highly porous networks after solvent extraction.

The results in Table 4-3 showed that when a good solvent was used to remove the linear polymer from the matrix pores, the development of pore structure depended on the solvent-extraction time. The use of different solvents should also influence the network porosity, owing to the swelling and deswelling of the polymer network by the solvent. To study the pore structure variation by solvent extraction, polymer particles with different divinylbenzene contents were extracted with different types of good solvents for polystyrene: benzene, toluene and methylene chloride; their solubility parameters (δ) are 9.2, 8.9 and 9.7 cal/cm^3, respectively, compared to the 9.1 cal/cm^3 of polystyrene. The results, given in Table 4-7, reveal that the pore structure is affected by the solvent used to remove the linear polymer. As the polymer particles were swollen by a good solvent during the solvent extraction process, the removal of solvent after isolation of the particles might lead to a structure shrinkage of the pores, i.e., a collapse of expanded network. This collapse phenomenon of the pores is considered as a result of the cohesional forces when the solvated polymer chains are approaching each other by the loss of the solvent.

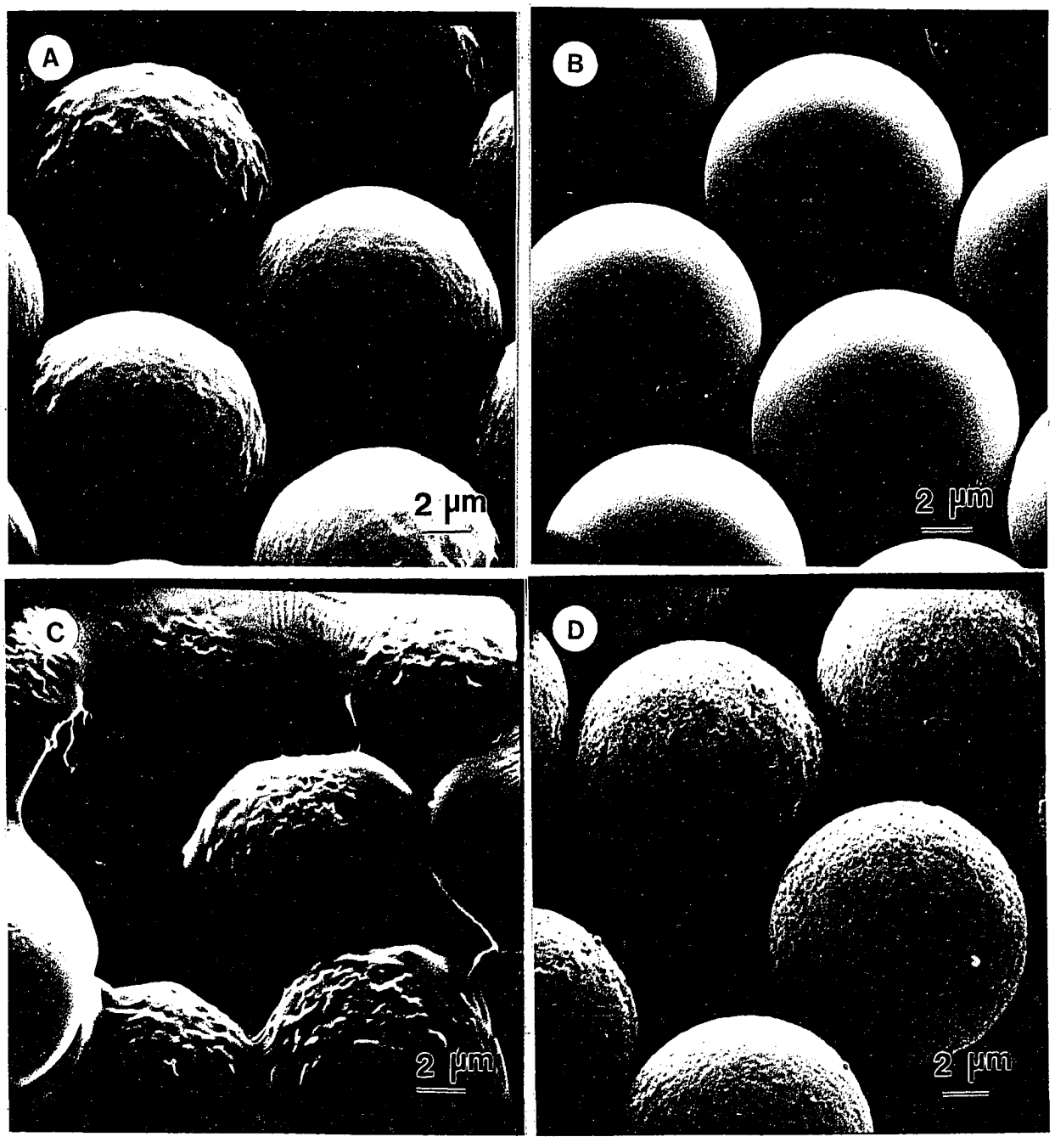

Figure 4-12: *Scanning electron micrographs of copolymer particles: (A) after polymerization; (B) extracted with methanol only; (C) extracted with methylene chloride only; and (D) extracted with methylene chloride, then methanol. [diluent: linear polystyrene/n-heptane; 15% DVB; $M_{W,LP}$= 1.49 x 10^6]*

Methylene chloride, which has the greatest difference in δ value from polystyrene and polydivinylbenzene among the solvents used, retains the greatest fraction of integral pore structure after solvent extraction (as indicated by the surface areas and pore volumes listed in Table 4-7). The preservation of the porosity in the solvent extraction can be attained by decreasing the interactions between polymer chains and the solvent - using solvents with decreasing solvating power.

Table 4-7: Experimental Results of Different Solvent Extraction

[Diluent: linear polystyrene/n-heptane; $M_{W,LP}$= 1.49 x 10^6]

DVB %	S m^2/g	V_p ml/g	LP_{in} %	$M_{W,e}$ x 10^{-5}	d_s μm	d_m μm
1. Benzene						
5	9	0.36	8	12.7	16.4	11.9
15	31	0.64	12	12.0	14.1	11.7
25	109	0.86	18	11.1	12.4	11.6
2. Toluene						
5	13	-	9	12.5	16.0	11.9
15	34	-	13	12.0	14.0	11.7
25	107	-	17	11.4	12.4	11.6
3. Methylene Chloride						
5	18	0.42	10	12.5	15.5	11.9
15	52	0.72	14	12.1	13.5	11.7
25	109	0.88	18	11.0	12.3	11.6

* *DVB%: weight percentages of divinylbenzene in the copolymer; S: specific surface area; V_p: pore volume; LP_{in}: fraction of linear polystyrene included within network structure; $M_{W,e}$: weight-average molecular weight of extracted polystyrene; d_s: swollen particle diameter in extracting solvent; and d_m: particle diameter in methanol.*

The pore stability, the resistance of structure shrinkage, shows a strong

dependence on the divinylbenzene content. As expected, pore shrinkage takes places within the polymer in the rubbery state rather in the glassy state. The stability of the porous structures is determined primarily by the volume fraction of the copolymer in the swollen gel during the solvent extraction. An increase in volume fraction results in an increase in the glass transition temperature of the polymer-solvent system, so that the system may remain in the glassy state during swelling, thus resulting in an increase in the stability of the pores. The degree of swelling, as indicated by the swollen particle diameter (d_s) in Table 4-7, exhibits the expected dependence on the divinylbenzene content and the solvent. The larger the diameter of the swollen particles indicates a higher degree of swelling. With a lower degree of crosslinking, the connection between the microspheres must be weak, thus the pore structure formed must be looser and tended to shrink after removal of good solvent. The relatively higher interaction between polymer chains and the solvent increases the degree of swelling, thus the stability of the pore structure is lower.

Due to the structure shrinkage, the pore size distribution of porous particles varies with the type of solvent used for solvent extraction in which the polymer particles are swollen during the extraction process. Figure 4-13 compares the pore size distributions of porous polymer particles prepared with different divinylbenzene contents and extracted with benzene and methylene chloride. Methylene chloride, as compared to benzene, retains the greater fraction of integral pore structure after solvent extraction. Using benzene as extracting solvent, the pore spectrum shifted slightly to the larger pore portion. The effect of the pore shrinkage phenomenon is stronger in smaller pores than in the larger pores. This can be revealed from the difference in the portion of the Curves A and B below the macroporous region. This can also be confirmed from the difference in specific surface areas, since the small pores contribute

most the surface area of the porous polymer particles. The pore structures of particles prepared with the highest crosslinker content are almost identical regardless of the solvent used for solvent extraction as shown in Figure 4-13C. There is an inhomogeneity in the crosslink distribution in the crosslinked porous styrene-divinylbenzene copolymer particles owing to the different reactivity ratios of monomers[22, 40]. The nuclei are regions of relatively high crosslinking density, while there is a graduation of crosslinking through the microspheres. The lower crosslinking density regions (surface of the microspheres), which have the higher flexibility in polymer chains, can shrink and collapse during the isolation of the solvent. Thus, the micropores and mesopores due to interspaces between microspheres tend to shrink (i.e., collapse) as the polymer chains approach each other after solvent extraction.

Furthermore, the extent of the inclusion of linear polymer within the network structure was almost the same regardless of the extracting solvent used. The inclusion of some fraction of the linear polymer in the copolymer structure cannot be avoided due to chemical grafting or steric hindrance.

4.4 SUMMARY AND CONCLUSIONS

A kinetic investigation of the processes of pore formation of monodisperse porous polymer particles prepared using linear polymer seed and nonsolvent as inert diluents was performed. The process of copolymerization can be described as: (1) the production and agglomeration of highly crosslinked gel microspheres; and (2) the binding together of microspheres/agglomerates and fixation of network structure. The porosity observed is a consequence of phase separation which occurred during copolymerization in the presence of diluents. Following solvent extraction to remove the linear polymer and nonsolvent, monodisperse polymer particles with macroporous structure are formed.

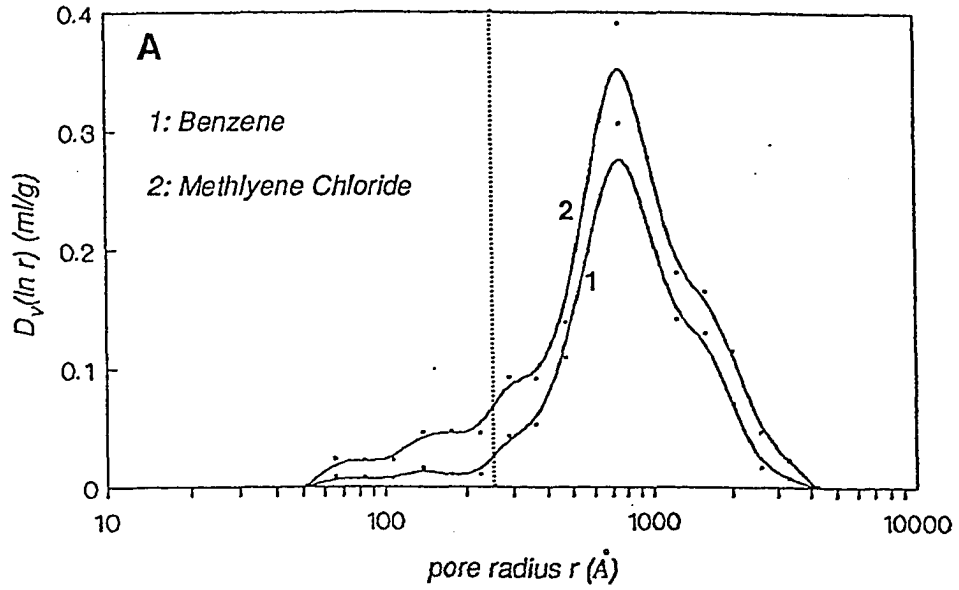

Figure 4-13: *Effect of solvent extraction using benzene and methylene chloride as solvents on pore size distribution of porous polymer particles with different divinylbenzene contents: (A) 5% DVB; (B) 15% DVB; and (C) 25% DVB. The dotted lines indicate the position of 250 Å pore radius. [diluent: linear polystyrene/n-heptane; $M_{W,LP}$= 1.49 x 10^6]*

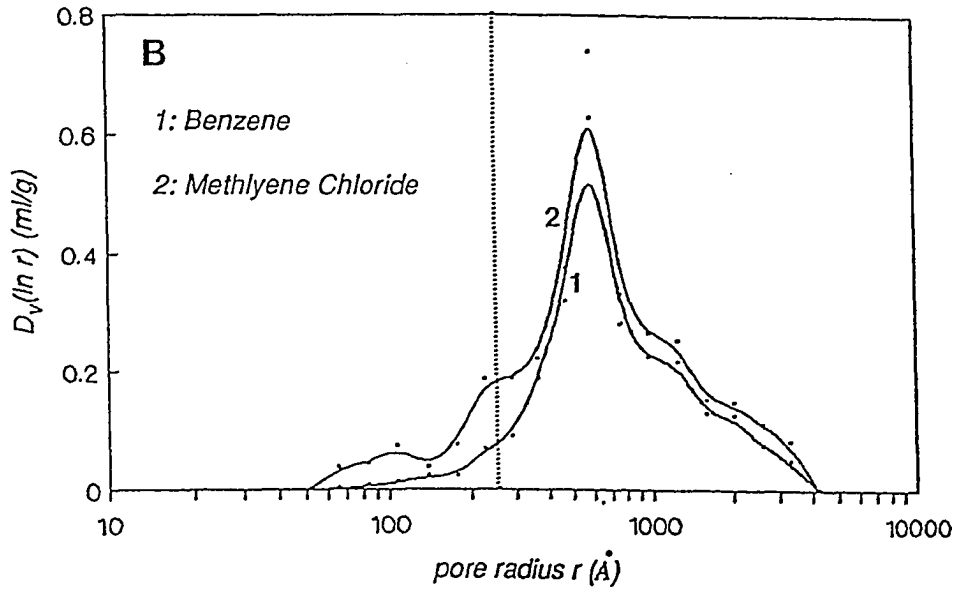

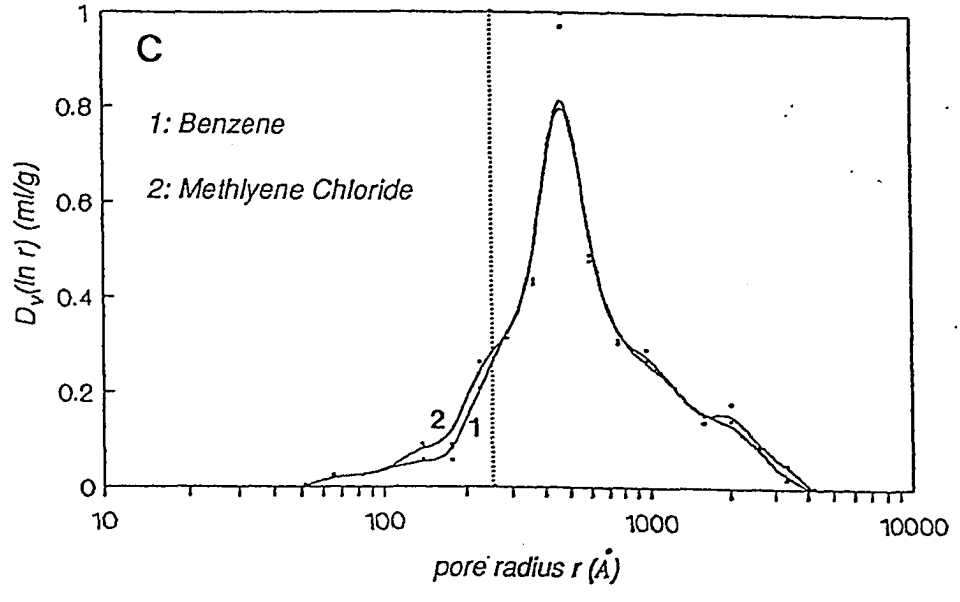

Figure 4-13: continued.

A portion of linear polymer used as inert diluent was included in the copolymer network as the pore structure was built up. A degree of inclusion was a consequence of steric entrapment, or chain transfer to linear polymer at high conversion. This inclusion of linear polymer within the network also depended on the diluent kind and crosslinker content, as well as the molecular weight of linear polymer seed used as inert diluent.

The removal of the linear polymer after the end of the copolymerization process from the matrix pores influenced strongly the pore structure. The preservation of the pore structure during the solvent extraction could be attained by decreasing the interactions between polymer chains and the solvent, i.e., using solvents with decreasing solvating power. The pore stability was dependent on the crosslinker content. The effect of the shrinkage phenomenon increased with decreasing crosslinking, which was more pronounced in smaller pore regions.

REFERENCES

1. C. M. Cheng, M. S. El-Aasser, and J. W. Vanderhoff, presented at *"64th Colloid and Surface Science Symposium"*, Lehigh University, Bethlehem, PA, June 18-20, 1990.
2. C. M. Cheng, M. S. El-Aasser, and J. W. Vanderhoff, Presented at *"AIChE 1990 Annual Meeting"*, Chicago, November 11-16, 1990.
3. C. M. Cheng, F. J. Micale, J. W. Vanderhoff, and M. S. El-Aasser, *J. Polym. Sci., Polym. Chem. Ed.*, accepted (1991).
4. J. Seidl, J. Malinsky, K. Dusek, and W. Heitz, *Adv. Polym. Sci.*, **5**, 113 (1967).
5. J. Ugelstad, L. Soderberg, A. Berge, and J Bergstrom, *Nature*, **303**, 95 (1983).
6. K. A. Kun and R. Kunin, *J. Polym. Sci.*, **A6**, 2689 (1968).
7. D. Y. D. Chung, M. Bartholin, and A. Guyot, *Angew. Makromol. Chem.*, **103**, 109 (1982).
8. G. J. Howard and C. A. Midgley, *J. Appl. Polym. Sci.*, **26**, 3845 (1981).
9. Y. Nitadori and T. Tsuruta, *Makromol. Chem.*, **179**, 2069 (1978).
10. P. W. Kwant, *J. Polym. Sci., Polym. Chem. Ed.*, **17**, 1331 (1979).
11. J. Stokr and B. Schneider, *J. Appl. Polym. Sci.*, **23**, 3553 (1979).
12. M. Bartholin, G. Boissier, and J. Dubois, *Makromol. Chem.*, **182**, 2075 (1981).
13. D. H. Freeman, W. L. Zielinski, and W. F. Rittner, *Proceedings of the International Conference on Ion Exchange in the Process Industries*, Society of Chemical Industry, London, 27 (1970).
14. S. Brunauer, P. H. Emmett, and E. Teller, *J. Amer. Chem. Soc.*, **60**, 309 (1938).
15. S. J. Gregg and K. S. W. Sing, *"Adsorption, Surface Area and Porosity"*, 2nd ed., Academic Press, London (1982).
16. E. W. Washburn, *Proc. Nat. Acad. Sci.*, **7**, 115 (1921).
17. S. Lowell and J. E. Shields, *"Powder Surface Area and Porosity"*, 2nd ed., Chapman & Hall, London (1984).
18. B. Walczynski, B. N. Kolarz, and H. Galina, *Polym. Commun.*, **26**, 276 (1985).
19. B. T. Storey, *J. Polym. Sci.*, **A3**, 265 (1965).

20. G. Schwachula, *J. Polym. Sci., Symp. Ser.*, **53**, 113 (1975).

21. G. Schwachula and G. Popov, *Pure & Appl. Chem.*, **54**, 2103 (1982).

22. G. Schwachula and G. Popov, *Polym. Bull.*, **21**, 189 (1989).

23. G. Hild and P. Rempp, *Pure Appl. Chem.*, **53**, 1541 (1981).

24. G. Hild and R. Okasha, *Makromol. Chem.*, **186**, 93 (1985).

25. G. Hild, R. Okasha, and P. Rempp, *Makromol. Chem.*, **186**, 407 (1985).

26. G. Hild, R. Okasha, M. Macret, and Y. Gnanou, *Makromol. Chem.*, **187**, 2271 (1986).

27. R. H. Wiley, S. P. Rao, J. I. Jin, and K. S. Kim, *J. Macromol. Sci. Chem.*, **A-4**, **7**, 1453 (1970).

28. R. Okasha, G. Hild, and P. Rempp, *Eur. Polym. J.*, **15**, 975 (1979).

29. R. H. Wiley and E. E. Sale, *J. Polym. Sci.*, **17**, 491 (1960).

30. R. H. Wiley and B. Davis, *J. Polym. Sci.*, **B1**, 463 (1963).

31. R. H. Wiley, W. K. Mathews, and K. F. O'Driscoll, *J. Macromol. Sci. Chem.*, **A-1**, **3**, 503 (1967).

32. R. H. Wiley and T. Ahn, *J. Polym. Sci.*, **A1**, 6 (1968).

33. R. H. Wiley and J. I. Jin, *J. Macromol. Sci. Chem.*, **A-2**, **6**, 1097 (1968).

34. J. Malinsky, J. Klaban, and K. Dusek, *J. Macromol. Sci. Chem.*, **A5**, 1071 (1971).

35. J. Exner and M. Bohdanecky, *Coll. Czech. Chem. Commun.*, **31**, 3985 (1966).

36. P. J. Flory and J. Rehner, *J. Chem. Phys.*, **31**, 521 (1943).

37. H. Beranova and K. Dusek, *Coll. Czech. Chem. Commun.*, **34**, 2932 (1969).

38. H. Galina and B. N. Kolarz, *Polym. Bull.*, **2**, 235 (1980).

39. J. Baldrian, B. N. Kolarz, and H. Galina, *Coll. Czech. Chem. COmmum.*, **46**, 1675 (1981).

40. H. Galina, B. N. Kolarz, P. P. Wieczorek, and M. Wojcynska, *British Polym J.*, **17**, 215 (1985).

41. A. Wlochowicz, R. Sanetra, and B. N. Kolarz, *Angew. Makromol. Chem.*, **161**, 23 (1988).

42. O. Okay, *Angew. Makromol. Chem.*, **143**, 209 (1986).

43. O. Okay and T. I. Balkas, *J. Appl. Polym. Sci.*, **31**, 1785 (1986).

44. O. Okay, *J. Appl. Polym. Sci.*, **32**, 5533 (1986).

45. O. Okay, *Angew. Makromol. Chem.*, **153**, 125 (1987).

46. O. Okay, *Angew. Makromol. Chem.*, **157**, 1 (1988).

47. I. C. Poinescu, C. Vald, A. Carpov, and A. Ioanid, *Angew. Makromol. Chem.*, **156**, 105 (1988).

Chapter 5
Monodisperse Porous Polymer Particles: Influence of Synthesis Parameters on Pore Structure

5.1 INTRODUCTION

Monodisperse macroporous styrene-divinylbenzene copolymer particles in the size range of 10 μm in diameter were prepared via seeded emulsion polymerization techniques. Linear polymer (polystyrene seed) or a mixture of linear polymer and solvent or nonsolvent were used as inert diluents[1, 2, 3, 4, 5]. By the incorporation of solvent together with a mixture of styrene (St) and divinylbenzene (DVB) into swellable, monodisperse polystyrene seed latex particles, a porous structure was obtained by removal of the diluents following polymerization. The monodispersity was maintained during the synthesis process. Type II nitrogen adsorption-desorption isotherms and low C (BET constant) values indicate that most of pores are in the macroporous region (pore size larger than 500 Å). Direct observation of interior structures shows that the macroporous polymer particles are composed of many interior microspheres and their agglomerates. The pores are indeed due to the interstices formed between the crosslinked microspheres and agglomerates. The working surface area of the porous polymer particles is actually the surface area of those interior microspheres. The pore shape is irregular as compared to silica packing materials[6]. The porous polymer particles exhibit a flat surface shell consisting of more compactly arranged globules. The morphology of the monodisperse macroporous polymer particles based on these observations is depicted in Figure 5-1. Macroporous polymer particles may be considered to have two degrees of inhomogeneity. The inhomogeneity of the copolymer network always arises in

vinyl-divinyl copolymerization resulting in more or less crosslinked regions (gel regions). The phase separation occurs during the copolymerization. Another inhomogeneity, i.e. porosity, of the polymer particles is also observed.

Synthesis parameters which would affect the physical properties (e.g., specific surface area, pore volume, and pore size distribution) of the monodisperse porous polymer particles were investigated in order to prepare porous polymer particles with desired properties. The synthesis parameters studied were:

(1) the diluent type;

(2) the overall crosslink density;

(3) the molecular weight of the seed particles;

(4) the type of solvent or nonsolvent;

(5) the amount of diluent;

(6) the initiator concentration; and

(7) the polymerization temperature.

The effects of the type of diluent, the crosslink density, as well as the molecular weight of the polystyrene seed particles were investigated and the results were reported in Chapter 2. Emphasis in this chapter will be put on the effect of the kind of solvent and nonsolvent, the amount of diluent, the initiator concentration, and the reaction temperature on the physical features of the monodisperse porous polymer particles. Selected samples were subjected to the pore volume and pore size distribution measurements using the mercury porosimeter.

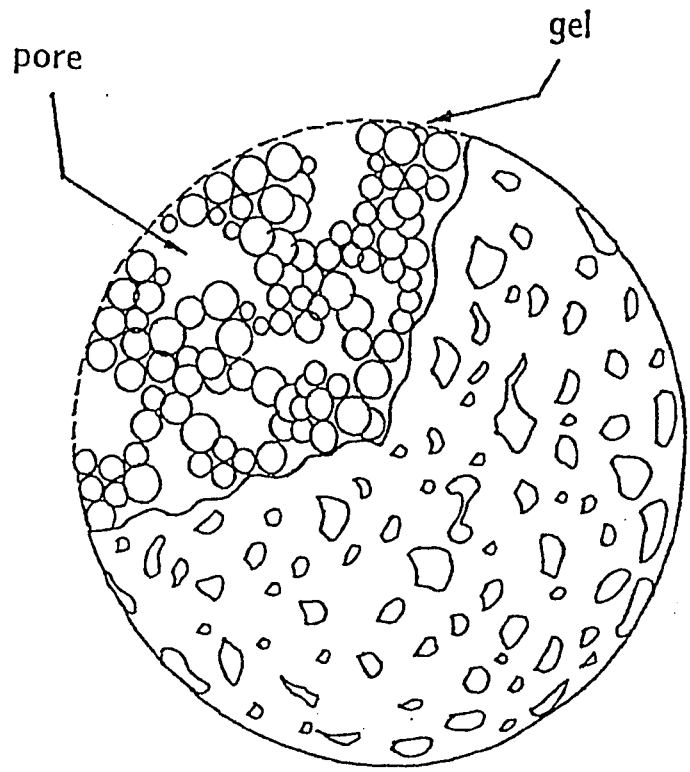

Figure 5-1: *Schematic representation of the morphology of monodisperse porous polymer particles.*

5.2 EXPERIMENTAL

5.2.1 Materials

Styrene (Polysciences) and divinylbenzene 55 crosslinking monomer [55.9% divinylbenzene (DVB) and 42.9% ethylvinylbenzene (EVB), by GC; Dow Chemical] were washed with 10% aqueous sodium hydroxide solution and water, dried over sodium sulfate, and passed through an activated aluminum oxide column to remove the inhibitors. The other materials were used as received: 2,2'-azobis-(2-methylbutyronitrile) initiator (E. I. duPont de Nemours), hydroquinone inhibitor (Fisher Scientific), sodium bicarbonate buffer (Fisher Scientific), Aerosol MA emulsifier (dihexylester of sodium sulfosuccinic acid; American Cyanamid), Polywet KX-3 oligomeric surfactant (n-octyl-S-[acrylonitrile]$_8$-[acrylic acid]$_8$-H, M_w= 1,500; Uniroyal Chemical), poly(N-vinyl pyrrolidone) K-90 surfactant (GAF Corp.), and solvents such as n-hexane, n-heptane, 1-hexanol, toluene, methylene chloride and methanol (Fisher Scientific). Distilled deionized water was used in the preparation of aqueous solutions.

5.2.2 Preparation of Monodisperse Porous Styrene-Divinylbenzene Copolymer Particles

A series of 11 μm diameter monodisperse porous styrene-divinylbenzene copolymer particles were prepared by seeded emulsion polymerization using different types of diluent and concentrations of divinylbenzene. 8.7 μm-diameter monodisperse polystyrene latexes were used as seed particles. The polymerization recipes and general procedure for the preparation were previously described in Chapter 2. The seeded emulsion polymerizations were carried out at 30% organic phase and comprised monodisperse polystyrene seed latex, styrene and divinylbenzene (DVB) monomers, diluent, initiator, inhibitor,

buffer, and emulsifiers. The molar ratio of solvent-type diluent (if used) to monomers was 1 with the swelling ratio (the weight ratio of the mixture of solvent-type diluent with monomers to polystyrene seed) set to 3. The use of a low swelling ratio prevented coagulation of the soft monomer-swollen latex particles. The use of higher swelling ratios caused the monomer-swollen particles which were soft and sticky to cream in the early stages of polymerization and coalesce into a big mass. The use of low swelling ratio also eliminated the free monomer phase after swelling the seed particles, so that the chances of nucleating a new crop of particles were reduced. A typical polymerization recipe can be found in Table 2-5. The ingredients were added to capped bottles, which were tumbled end-over-end for 12 hours at room temperature (23 °C) to allow the seed particles to swell with the n-hexane-monomer mixture. The polymerizations were carried out by tumbling the bottles end-over-end at 16 rpm in a thermostated water bath at 70 °C for 24 hours. The concentration of emulsifiers was selected to prevent formation of coagulum or small secondary particles during the polymerization. The use of polymeric surfactant poly(N-vinyl pyrrolidone) K-90 with molecular weight of 3.6×10^5 to stabilize the latex particles by a steric stabilization mechanism also increased the viscosity of the medium, which reduced the tendency of the swollen particles to cream and coalesce. After polymerization, the polymer particles were extracted with methylene chloride (a good solvent for polystyrene) in a Soxhlet apparatus for 36 hours to remove the linear polymer, followed by washing with methanol to remove residual methylene chloride and low molecular weight solvent-type diluents (solvent or nonsolvent). After solvent extraction, the polymer particles were dried in air at room temperature and then vacuum-dried in an oven at 45 °C. More experimental details were given in the previous chapters.

5.2.3 Characterization

The surface morphology and particle size of the porous polymer particles were characterized using an ETEC Autoscan scanning electron microscope. Particle-size histograms were constructed from measurements of 250 - 300 individual particles from the electron micrographs. A Zeiss MOP-3 digital image analyzer was used to measure of the particle diameters.

The surface area *(S)* of particles was measured by nitrogen adsorption isotherms. Nitrogen adsorption at 77 °K was determined volumetrically in a Quantasorb Sorption System as described in Chapter 2. The BET equation was used to analyze the low relative pressure region of the isotherm in order to find the surface areas of the particles[7, 8].

Pore volumes and pore size distributions were determined by mercury intrusion porosimetry on a Micromeritics AutoPore 9200 porosimeter as described in Chapter 2. The pore radii (*r*) quoted were those of equivalent hollow cylinders obtained from the intruded pressure (*P*), using the Washburn equation[8, 9]. The volume *ln* pore radius distribution function $D_v(ln\ r)$ was used to express pore size distribution to reduce the wide range of values which the volume pore-size distribution function $D_v(r)$ could exhibit[10].

5.3 RESULTS AND DISCUSSION

Monodisperse porous styrene-divinylbenzene copolymer particles in the size range of 10 μm in diameter were prepared via seeded emulsion polymerization. Linear polymer (polystyrene seed) with molecular weight on the order of 10^6, or a mixture of linear polymer and solvent or nonsolvent were used as inert diluents. The role of linear polymer was to create macroporous structure; the presence of the low molecular weight solvent-type diluent (solvent or nonsolvent) enhanced the phase separation and structure heterogeneity.

Porous structure was formed by the removal of diluents by solvent extraction after polymerization.

The pore size distribution was very sensitive to the molecular weight of the polystyrene seed particles. Using linear polystyrene with molecular weight on the order of 10^6 as inert diluents, the monodisperse porous polymer particles prepared were macroporous (average pore size larger than 500 $\mathring{A}$) in nature.

Particles prepared using a mixture of linear polystyrene and nonsolvent (i.e., n-hexane) as inert diluent resulted in the largest pore volumes and specific surface areas. Particles prepared using linear polystyrene alone yielded the smallest pore volumes and surface areas owing to the relatively large amount and higher molecular portion of linear polystyrene trapped within the network structure. Regarding the pore size, particles prepared using linear polystyrene alone or a mixture of linear polystyrene and solvent (i.e., toluene) resulted in larger pore radii compared to the linear polystyrene-nonsolvent system.

The pore volume increased as the divinylbenzene content was increased, while the average pore size decreased with the divinylbenzene content. The higher the divinylbenzene content, the higher the crosslinking density, and the more dense and smaller the interior microspheres. This can be observed from the profile of crosslinking density as a function of divinylbenzene content (Figure 5-2) and from the interior structure of the particles (Table 5-1). The crosslinking density of the porous polymer particles was determined by equilibrium swelling in toluene; the particle size of the interior microspheres was estimated by scanning electron microscopy. It has been asserted that porous polymer particles may have different levels of particle substructure with the particle consisting of randomly packed microspheres and the microspheres in turn packed with crosslinked nuclei. In between the nuclei, there is a family of small pores (in the microporous or lower mesoporous regions) which are

chiefly responsible for the high surface area of the porous polymer particles. When the amount of divinylbenzene is increased, the nuclei are less fused and the surface area is increased. For a given divinylbenzene concentration, the surface areas of porous polymer particles prepared using a mixture of linear polymer and nonsolvent (i.e., n-hexane and n-heptane) as inert diluents are larger than those prepared using linear polymer or a mixture of linear polymer and solvent (i.e., toluene). This can be also observed form the interior structure of the porous polymer particles prepared with different types of diluent (Table 5-1). The presence of nonsolvent will enhance the phase separation and structure inhomogeneity, which lead to the smaller interior microspheres and higher surface area of the porous polymer particles.

Using a mixture of linear polymer and n-hexane as inert diluent with 33% divinylbenzene content, monodisperse macroporous polymer particles having a pore volume of 0.9 ml/g (porosity of 50%, apparent density of 0.55 g/ml) and a surface around 200 m^2/g were prepared.

Monodisperse porous polymer particles with sizes down to 3 μm and up to 30 μm in diameter were prepared by the use of linear polystyrene of various particle diameters and n-hexane as inert diluents according to the polymerization recipes listed in Table 5-2. Monodisperse polystyrene latex particles with different particle sizes used as inert diluents were prepared via successive seeded emulsion polymerization according to the recipes given in Tables 2-2, 2-3 and 2-4. Figure 5-3 shows scanning electron micrographs of the 3 and 30 μm monodisperse porous styrene-divinylbenzene copolymer particles. These porous polymer particles also possess pores with diameter on the order of 1,000 $\mathring{A}$, which are evenly distributed at the particle surface. As shown in Table 5-2, although the particle size is different, the nearly constant specific surface area (40 m^2/g) reveals that the surface area is strongly governed by the

Table 5-1: Particle Size Distribution of Interior Microspheres within the Monodisperse Porous Polymer Particles

$[M_{W,LP}= 1.49 \times 10^6]$

Diluent	DVB %	d_{im} μm	SD_n %
LP/n-Hexane	8	0.21	28.7
LP/n-Hexane	15	0.16	35.9
LP/n-Hexane	25	0.14	26.1
LP/n-Heptane	5	0.24	27.1
LP/n-Heptane	8	0.20	29.8
LP/n-Heptane	15	0.15	30.6
LP/n-Heptane	25	0.13	28.9
LP/n-Heptane	33	0.12	26.5
LP/Toluene	8	0.22	29.9
LP/Toluene	15	0.17	30.6
LP/Toluene	25	0.15	28.1
LP	10	0.22	23.0
LP	15	0.21	24.6
LP	25	0.18	23.2

* *LP: linear polystyrene seed; DVB%: weight percentage of divinylbenzene in the polymer particles; d_{im}: number-average diameter of the interior microspheres estimated from scanning electron microscopy; and SD_n: coefficient of variation based on the measurement of 250 particles of the interior microspheres.*

divinylbenzene content. Monodisperse porous styrene-divinylbenzene copolymer particles in the size range of 3 to 30 μm in diameter were also prepared by the use of linear polystyrene alone as inert diluent (as shown in Table 5-3). However, the specific surface areas were much lower compared to the linear polystyrene/n-hexane system.

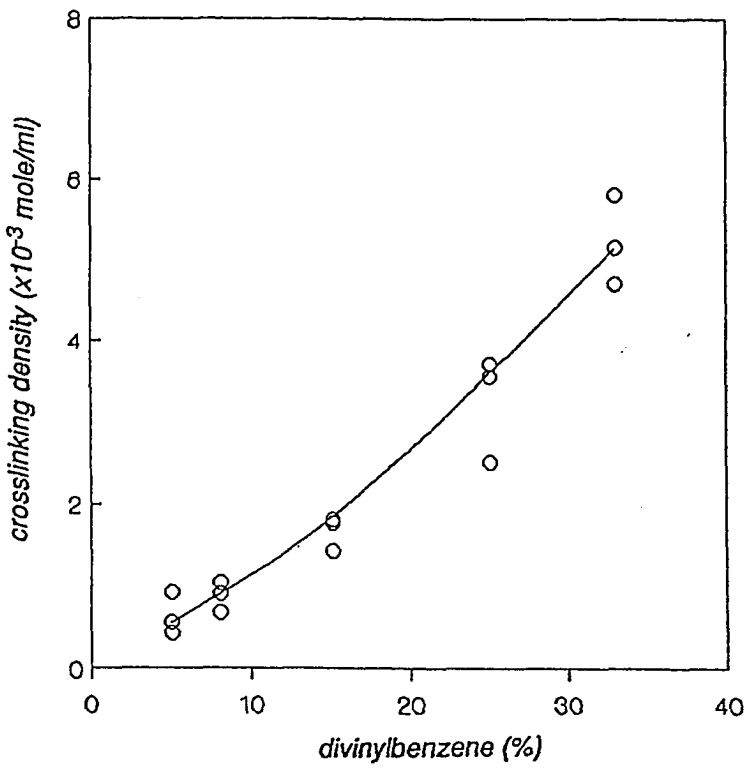

Figure 5-2: *Crosslinking density of the monodisperse porous styrene-divinylbenzene copolymer particles as a function of divinylbenzene content. [diluent: linear polystyrene / n-heptane,* $M_{W,LP}$ *= 1.49 x* 10^6*]*

Table 5-2: Polymerization Recipes and Specific Surface Areas of Monodisperse Porous Polymer Particles

[Diluent: linear polystyrene/n-hexane; DVB= 15%]

d_{seed} (μm)	1.9	3.0	5.5	8.7	16	23
PS seed[a]	7.5	7.5	7.5	7.5	7.5	7.5
Styrene	6.9	6.9	6.9	6.9	6.9	6.9
DVB 55	5.6	5.6	5.6	5.6	5.6	5.6
n-Hexane	9.5	9.5	9.5	9.5	9.5	9.5
AMBN	0.018	0.018	0.018	0.018	0.018	0.018
AMA	0.005	0.005	0.005	0.005	0.005	0.005
KX-3	0.01	0.01	0.014	0.014	0.014	0.014
PVP K-30	1.2	1.2	-	-	-	-
PVP K-90	-	-	0.8	0.8	1.6	1.6
HQ	0.021	0.021	0.021	0.021	0.021	0.021
$NaHCO_3$	0.027	0.027	0.027	0.027	0.027	0.027
Water	68.72	68.72	69.11	69.11	68.31	68.31
d (μm)	2.8	3.9	7.2	11.6	21	31
S (m^2/g)	36	38	42	44	44	48

[a] *Linear, monodisperse polystyrene latex particles prepared accroding to the recipes given in Tables 2-2, 2-3, and 2-4 except the use of divinylbenzene monomer.*

* d_{seed}*: diameter of monodisperse polystyrene seed latex; d: diameter of porous polymer particles; and S: specific surface area.*

• *Total charged amount of 20 grams in 1 oz. bottles; polymerization temperature = 70 °C.*

Table 5-3: Polymerization Recipes and Specific Surface Areas of Monodisperse Porous Polymer Particles

[Diluent: linear polystyrene seed; DVB= 15%]

d_{seed} (μm)	1.9	3.0	5.5	8.7	16	23
PS seed[a]	7.5	7.5	7.5	7.5	7.5	7.5
Styrene	14.3	14.3	14.3	14.3	14.3	14.3
DVB 55	8.2	8.2	8.2	8.2	8.2	8.2
AMBN	0.034	0.034	0.034	0.034	0.034	0.034
AMA	0.01	0.01	0.01	0.01	0.01	0.01
KX-3	0.02	0.02	0.028	0.028	0.028	0.028
PVP K-30	1.2	1.2	-	-	-	-
PVP K-90	-	-	0.8	0.8	1.6	1.6
HQ	0.042	0.042	0.042	0.042	0.042	0.042
$NaHCO_3$	0.027	0.027	0.027	0.027	0.027	0.027
Water	68.66	68.66	69.05	69.05	68.25	68.25
d (μm)	3.1	4.3	7.7	13.2	23	34
S (m^2/g)	14	15	16	16	17	15

[a] *Linear, monodisperse polystyrene latex particles prepared accroding to the recipes given in Tables 2-2, 2-3, and 2-4 except the use of divinylbenzene monomer.*

* d_{seed}*: diameter of monodisperse polystyrene seed latex; d: diameter of porous polymer particles; and S: specific surface area.*

• *Total charged amount of 20 grams in 1 oz. bottles; polymerization temperature = 70 °C.*

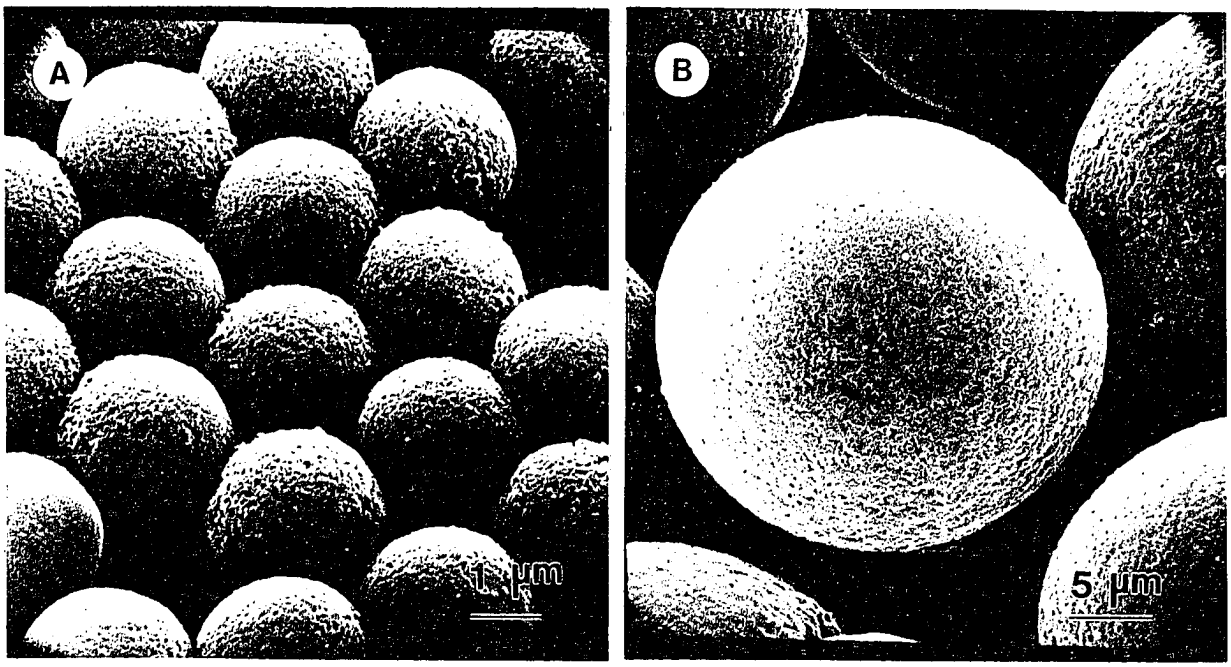

Figure 5-3: *Scanning electron micrographs of the monodisperse porous styrene-divinylbenzene copolymer particles: (A) 3 µm; and (B) 30 µm. [Diluent: linear polystyrene/n-hexane; 15% DVB,* $M_{W,LP}$*= 1.49 x* 10^6*]*

5.3.1 Effect of Type of Solvent or Nonsolvent

Based on their penetrating properties, organic liquids can be classified as solvents or nonsolvents for polystyrene[11, 12, 13]. Solvents for polystyrene are organic compounds with intermolecular attractive and repulsive forces similar to those of polystyrene, as quantified by the solubility parameter δ, which is defined as the square root of the cohesive energy density. Most aromatic hydrocarbons and aliphatic halogenated hydrocarbons exhibit at most a weak tendency to form hydrogen bonds, and are classified as solvents for polystyrene. Most aliphatic hydrocarbons and alcohols are typical nonsolvents for polystyrene. Such organic substances are miscible with the monomers but precipitate polystyrene chains. Table 5-4 shows the δ-parameter values and characteristics of the diluents used in the experiments. Figures 5-4 to 5-6 show scanning electron micrographs of the monodisperse porous styrene-divinylbenzene copolymer particles prepared according to the recipe given in Table 5-5 by the use of a combination of linear polystyrene and different solvent-type diluents (solvent or nonsolvent) as inert diluents. The porous polymer particles possess pores with an average diameter in the macroporous region. Mixtures of nonsolvents, such as kerosene (a mixture of C_{10} to C_{16} alkanes), can be also used with linear polystyrene to prepare porous polymer particles.

Good solvents for polystyrene other than toluene can also be used together with linear polystyrene seed as inert diluents for the preparation of monodisperse macroporous polymer particles (Table 5-6). Once again, monodisperse polystyrene latex particles of 8.7 μm diameter was used as seed in the recipe given in Table 5-5 with the type of solvent as the only variable. The removal of the good solvent after the isolation of the polymer particles caused the small pores to collapse as a consequence of cohesion when the agglomeration of the crosslinked microspheres caused the polymer chains to approach each

Table 5-4: Characteristics of the Diluents[14]

Diluent	Formula	δ $(cal/cm^3)^{1/2}$	ρ g/cm^3	b.p. °C
Polystyrene	$(CH_2CH\phi)_n$	9.1	1.050	-
Benzene	C_6H_6	9.2	0.877	80
Toluene	$C_6H_5CH_3$	8.9	0.870	111
Ethylbenzene	$C_6H_5C_2H_5$	8.8	0.867	136
Xylene	$C_6H_4(CH_3)_2$	8.8	0.864	140
Methylene Chloride	CH_2Cl_2	9.7	1.317	40
Ethylene Chloride	$C_2H_4Cl_2$	9.8	1.257	83
Pentane	C_5H_{12}	7.0	0.626	36
n-Hexane	C_6H_{14}	7.2	0.660	69
n-Heptane	C_7H_{16}	7.4	0.684	98
i-Octane	C_8H_{18}	7.5	0.703	125
Nonane	C_9H_{20}	7.6	0.718	151
Decane	$C_{10}H_{22}$	7.7	0.730	174
Dodecane	$C_{12}H_{26}$	7.9	0.749	216
Hexadecane	$C_{16}H_{34}$	8.0	0.773	287
2-Propanol	C_3H_7OH	11.9	0.781	82
1-Butanol	C_4H_9OH	11.4	0.810	118
1-Pentanol	$C_5H_{11}OH$	10.9	0.813	138
1-Hexanol	$C_6H_{13}OH$	10.7	0.814	157
1-Heptanol	$C_7H_{15}OH$	10.6	0.822	176
1-Octanol	$C_8H_{17}OH$	10.3	0.827	194
1-Decanol	$C_{10}H_{21}OH$	10.0	0.829	231
1-Dodecanol	$C_{12}H_{23}OH$	9.8	0.831	261

* δ: *solubility parameter;* ρ: *density; and b.p.: boiling point.*

Table 5-5: Typical Polymerization Recipes for 11 μm-Diameter Monodisperse Porous Polymer Particles

Diluent	LP*/Alkane	LP*/Alcohol	LP*/Solvent
Ingredient		wt%	
PS seed[a]	7.5	7.5	7.5
Monomers			
styrene	13 - variable	13 - variable	12 - variable
DVB 55	variable[c]	variable[c]	variable[c]
Diluent[b]	9.5	9.5	10.5
AMBN	0.018	0.018	0.017
AMA	0.005	0.005	0.010
KX-3	0.014	0.014	0.028
PVP K-90	0.8	1.0	0.6
HQ	0.021	0.021	0.021
$NaHCO_3$	0.027	0.027	0.027
Water	69.14	68.94	69.34

* *LP: linear polystyrene seed.*
[a] *Linear, monodisperse polystyrene latex particles (8.7 μm in diameter).*
[b] *Solvent-type diluent (solvent or nonsolvent).*
[c] *Different levels: 5, 15, and 25% divinylbenzene content (based on total polymer and monomers).*
• *Total charged amount = 20 grams; polymerization temperature = 70 °C.*

other. In general, the specific surface area is lower than that of particles prepared using a mixture of linear polystyrene and nonsolvent as diluents. The specific surface areas were almost identical regardless of the solubility parameter of the good solvent used.

Mixtures of diluents composed of a linear polymer and nonsolvents, yielded polymer particles with large pore volumes and specific surface areas. A

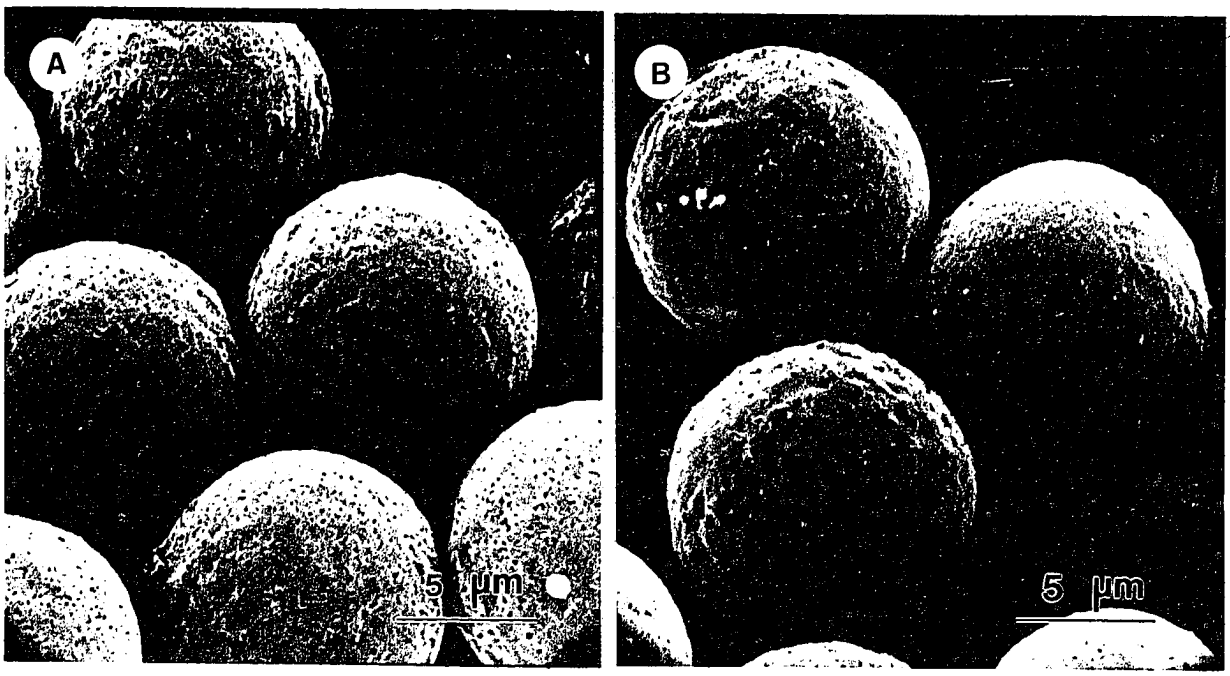

Figure 5-4: *Scanning electron micrographs of the monodisperse porous styrene-divinylbenzene copolymer particles prepared using a mixture of linear polystyrene with different solvents as inert diluents: (A) xylene; and (B) methylene chloride. [15% DVB, $M_{W,LP}$= 1.49 x 10^6]*

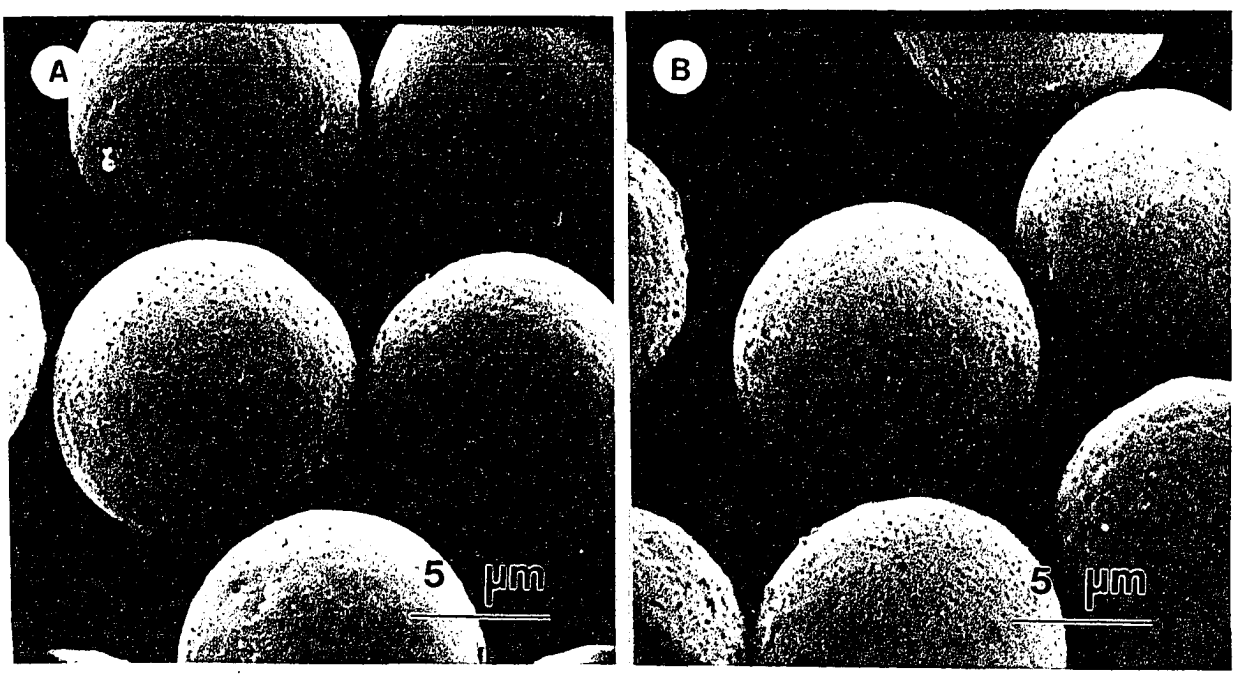

Figure 5-5: *Scanning electron micrographs of the monodisperse porous styrene-divinylbenzene copolymer particles prepared using a mixture of linear polystyrene with different aliphatic hydrocarbons (alkanes) as inert diluents: (A) 1-octane; and (B) nonane. [15% DVB,* $M_{W,LP}$*= 1.49 x* 10^6*]*

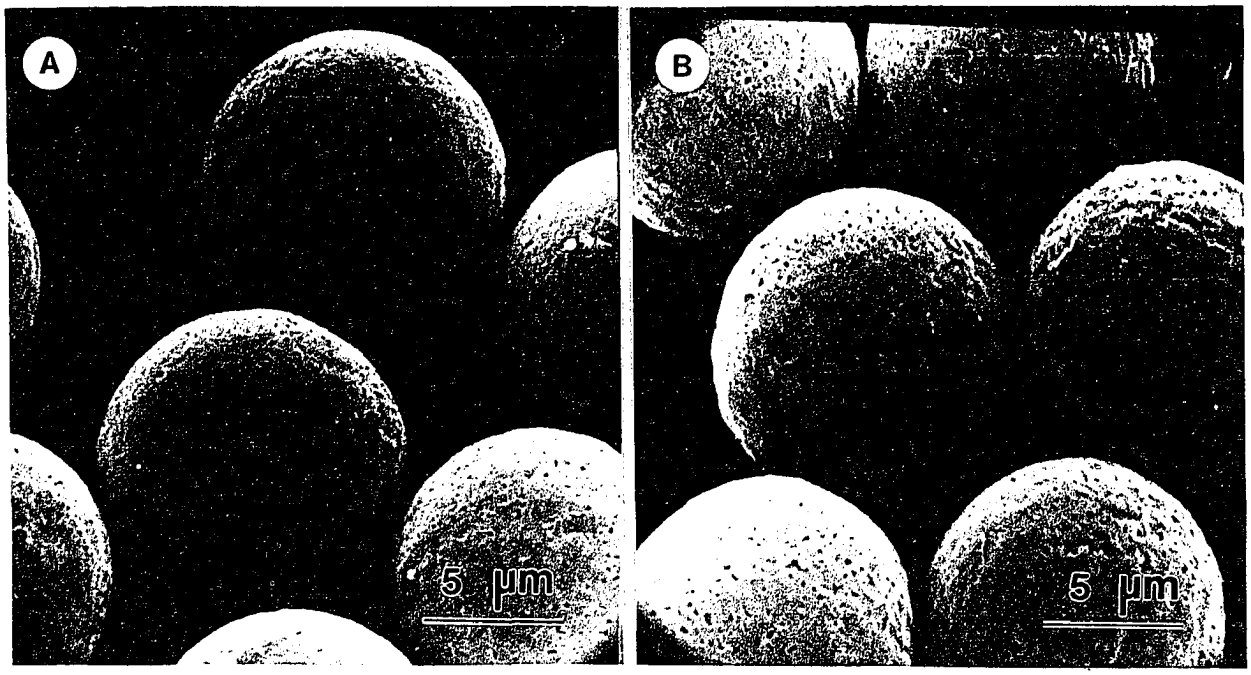

Figure 5-6: *Scanning electron micrographs of the monodisperse porous styrene-divinylbenzene copolymer particles prepared using a mixture of linear polystyrene with different alcohols as inert diluents: (A) 1-heptanol; (B) 1-octanol. [15% DVB, $M_{W,LP}$= 1.49 x 10^6]*

Table 5-6: Solvents used with Linear Polystyrene as Diluents for Preparing Monodisperse Porous Polymer Particles

[DVB=15%; $M_{W,LP}$=1.49 x 10^6]

Solvent	δ $(cal/cm^3)^{1/2}$	d μm	S m^2/g
Benzene	9.2	12	30
Toluene	8.9	12	32
Xylene	8.8	12	34
Ethylbenzene	8.8	12	35
Methylene chloride	9.7	11	31
Ethylene chloride	9.8	11	32

* δ: *solubility parameter; d: diameter of porous polymer particles; and S: specific surface area.*

relationship was found in the homologous series of aliphatic hydrocarbons and alcohols (Figure 5-7) between specific surface areas and the number of CH_2 groups. An increase in the number of CH_2 groups in the nonsolvent molecules lead first to an increase in the specific surface area of the porous polymer particles followed by a decrease. The surface area is high when the lower molecular weight alkanes are used as inert diluents, but drops drastically when the higher molecular weight nonsolvents, such as dodecane, are used as inert diluents. This phenomena is also observed when alcohols are used as inert diluents, although the effect of alcohols on surface area is not as obvious as alkanes. The value of the solubility parameter of the solvent approaches the 9.1 $(cal/cm^3)^{1/2}$ of styrene-divinylbenzene copolymer as the number of CH_2 groups in the molecule increases (Table 5-4). Indeed, the precipitating ability of the

nonsolvent used is dependent on the molecular size as well as the solubility parameter[11, 15, 16, 17, 18].

5.3.2 Effect of Diluent Amount

Figure 5-8 shows that specific surface area of porous polymer particles increases with increasing amount of linear polymer used as inert diluent. If the amount of linear polymer used as inert diluent is too low, the distance between the nuclei or microspheres will be very small and there will not be enough available volume for the polymerization to proceed to completion without complete coalescence or overlap of the microspheres. As a result, a gel-like copolymer particles with no measurable surface area or pore volume will be produced. When the amount of linear polymer passes a critical threshold value and the distance between the microspheres becomes greater, because of a dilution effect, some empty space will remain between the microspheres at the completion of the polymerization, resulting in the production of porous polymer particles with a high surface area[19, 20]. However, the porous polymer particles tend to break after solvent extraction when too much (ca. > 40%) linear polymer was used as inert diluent.

Figures 5-9 and 5-10 show how the physical characteristics (pore volume and specific surface area, respectively) of the porous polymer particles can be varied by changing the amount of solvent or nonsolvent used in the polymerization mixture. The results presented in Figure 5-9 are expected because the pore volume can generally be related to the amount of nonsolvent used in the polymerization mixture; the pore volume of porous polymer particles increases with the amount of nonsolvent used as inert diluent. The variation in the surface area is less easily predicted. As illustrated in Figure 5-10, specific surface area increased with the increase of the amount of solvent; however, an

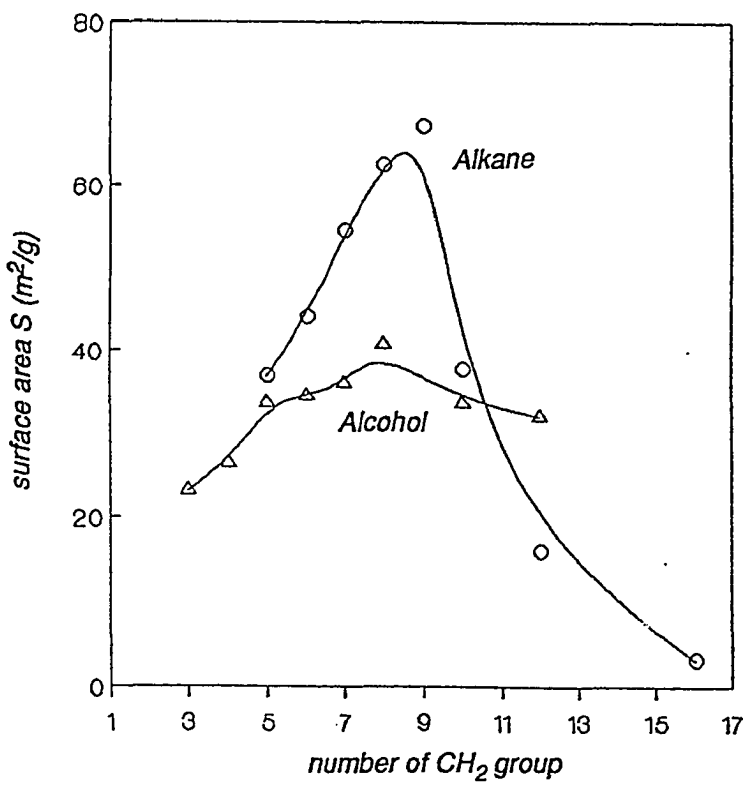

Figure 5-7: *Specific surface area as a function of the molecular size of aliphatic hydrocarbons (alkanes) and alcohols used with linear polystyrene as inert diluents in the preparation of monodisperse macroporous polymer particles. [Diluent: linear polystryrene seed (8.7 μm) / alkane or alcohol; 15% DVB; $M_{W,LP}$= 1.49 x 10^6]*

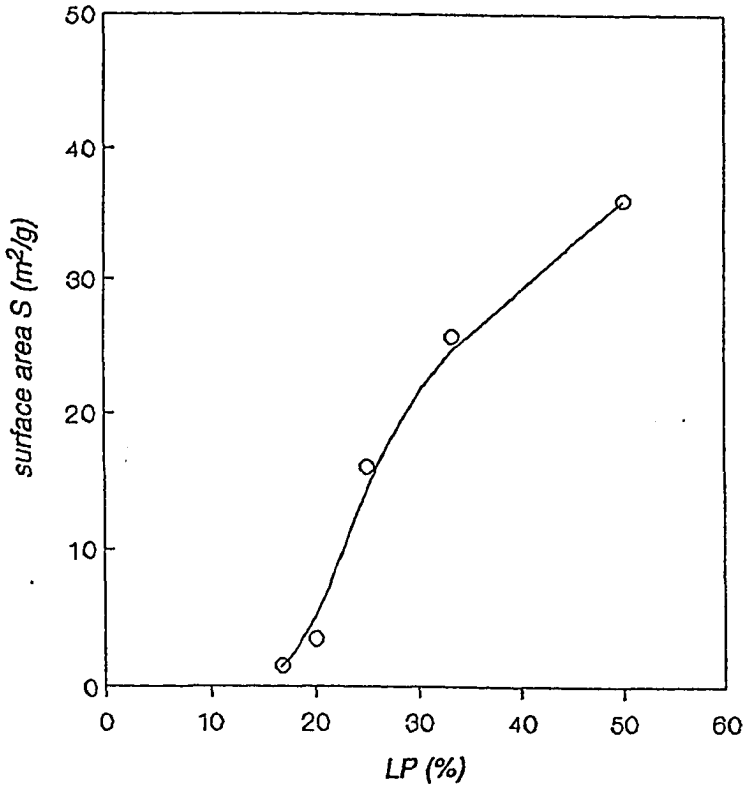

Figure 5-8: *Specific surface area as a function of the amount of linear polymer in the preparation of monodisperse porous polymer particles with diluent. [diluent: linear polystyrene seed; 15% DVB; $M_{W,LP}$= 1.49 x 10^6]*

excess of nonsolvent causes the surface area to decrease. This is due to the overlap of the interior microspheres when the concentration of nonsolvent is higher than the optimum value for phase separation, i.e., creating maximum specific surface area[21, 22]. Basically, the critical concentration of nonsolvent is dependent on the type of nonsolvent used as inert diluent. This effect is also reflected by the shapes of the pore size distribution curves for porous polymer particles prepared with different amounts of n-heptane. Figure 5-11 shows the differential mercury porosimetry curves for porous polymer particles prepared using different amounts of n-heptane as inert diluent. For the smallest n-heptane concentration the distribution was the narrowest one. As the amount of n-heptane is increased, the average pore size was found to increase and the pore size distribution became wider. However, the area under Curve C left of the dotted line for 250 $\mathring{A}$-pore radius is less than Curves A and B. This corresponds to a reduction in the specific surface area for sample C prepared with 2 molar ratio of n-heptane to monomers in Figure 5-10.

In the analysis of pore structure of porous polymer particles, a porous domain was defined, where the structure can be described as an agglomeration of quasi-spherical particles with different levels of agglomerations[19, 20, 23]: the smaller particles, nuclei, are nonporous particles of about 100 $\mathring{A}$ diameter. Nuclei are agglomerated in microspheres of about 1,000 $\mathring{A}$ diameter and microspheres are agglomerated again in larger irregular moieties inside the polymer bead. It is noted that the styrene-divinylbenzene copolymers are inhomogeneous because the divinyl components of this mixture (p- and m-divinylbenzene) are incorporated into the copolymer much faster than the monovinyl components (styrene, p- and m-ethylvinylbenzene). This gives rise to regions of high crosslink density, the nuclei or microspheres, which are connected by the less highly crosslinked molecules formed at a later stage of the

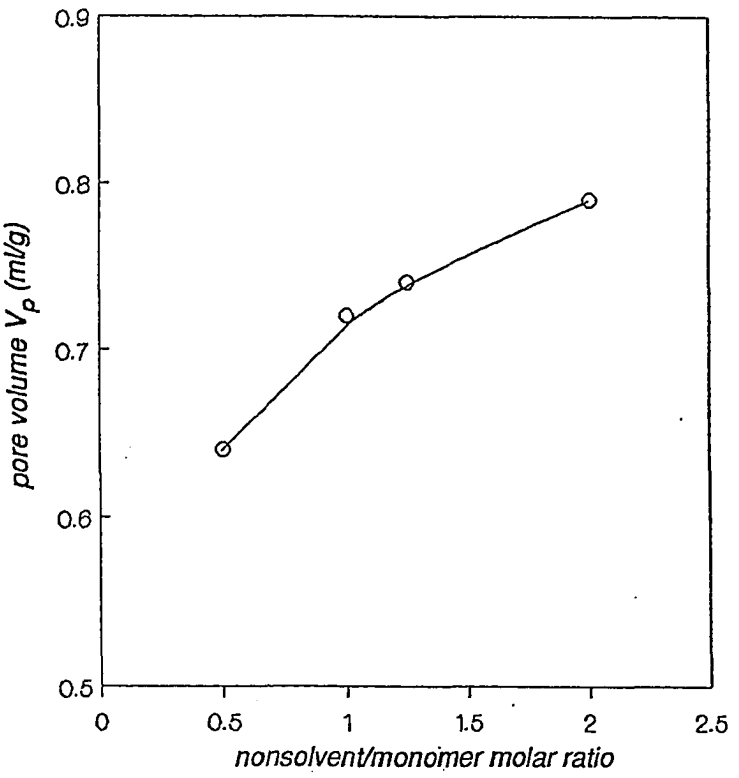

Figure 5-9: *Pore volume as a function of nonsolvent to monomer molar ratio for the preparation of monodisperse porous polymer particles. [diluent: linear polystyrene / n-heptane; 15% DVB; $M_{W,LP}$=1.49 x 10^6]*

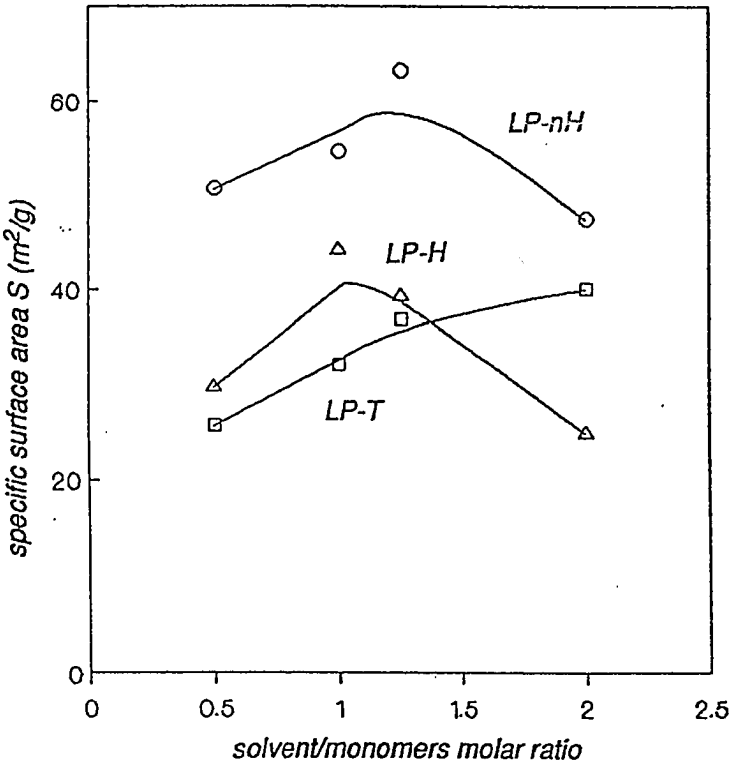

Figure 5-10: *Specific surface area as a function of solvent or nonsolvent to monomer molar ratio for monodisperse macroporous polymer particles prepared with diluent: (A) LP-T: linear polystyrene/toluene; (B) LP-H: linear polystyrene/n-hexane; and (C) LP-nH: linear polystyrene/n-heptane. [15% DVB; $M_{W,LP}$=1.49 x 10^6]*

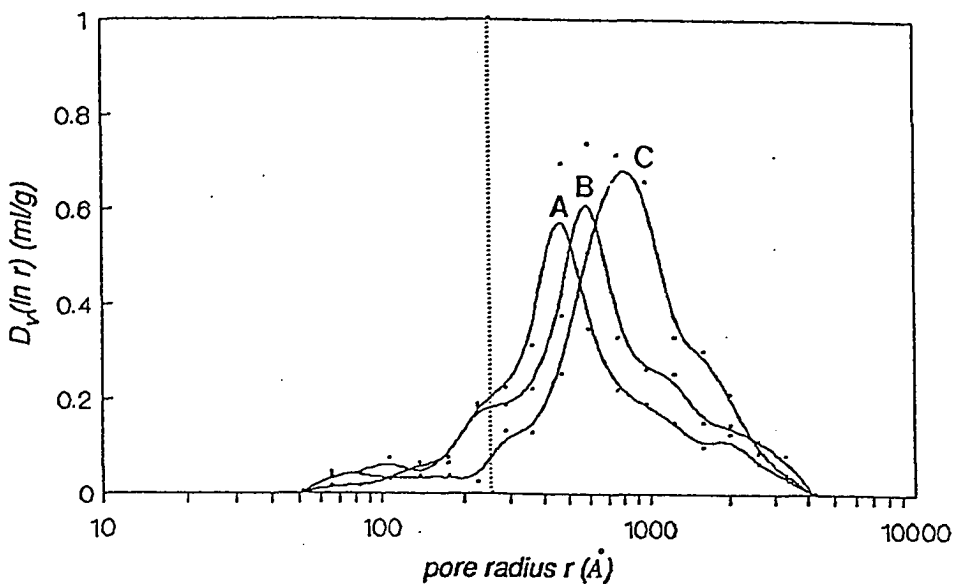

Figure 5-11: *Pore size distributions of monodisperse porous polymer particles prepared with different molar ratio of nonsolvent to monomers: (A) 0.5; (B) 1.0; and (C) 2.0. The dotted line indicates the position of 250 Å pore radius. [diluent: linear polystyrene/n-heptane; 15% DVB; $M_{W,LP}$= 1.49 x 10^6]*

polymerization[24, 25, 26]. When a solvent such as toluene is used as inert diluent, the situation is simple. As the amount of solvent is increased, the distance between the microspheres becomes greater due to the dilution effect, and there will be sufficient volume for the polymerization to proceed to completion without complete coalescence of the microspheres. As a result, porous polymer particles with higher specific surface areas are prepared. When nonsolvent such as n-heptane or n-hexane is used as inert diluent, the situation is more complex. In the early stages of polymerization, the liquid mixture consists of the nonsolvent and unreacted monomers. As the polymerization proceeds, the monomers are incorporated into the copolymer and the composition of the nonsolvent-monomer mixture shifts towards a higher percentage of the nonsolvent. When the percentage of nonsolvent in the diluent mixture becomes large enough, phase separation occurs, in which most of the diluent is exuded from the regions between the copolymer molecules. Two bulk phases are created, one containing a high concentration of copolymer molecules, and the other containing mostly diluent (linear polymer plus nonsolvent). The volume occupied by the exuded diluent corresponds to the large pores seen in the pore size distributions. As a larger amount of nonsolvent is used, phase separation occurs at a relatively early stage in the polymerization. The microspheres do not shrink very much when the diluent is extruded from this initial region because it contains highly crosslinked copolymer molecules. However, within the polymer particle, the volume occupied by the swollen network molecules is reduced when the amount of nonsolvent is too high, and molecular overlap or coalescence will occur between the crosslinked microdomains (nuclei and microspheres)[15, 25, 27, 28]. Porous polymer particles with lower surface area will result. The pore size distribution will shift to larger pores owing to the overlap of the nuclei and

microspheres.

5.3.3 Effect of Initiator Concentration

Increasing the initiator concentration over the range of 0.0375 to 3.75 wt% based on monomers in the polymerization recipe given in Table 2-5 was found to decrease the surface area of the resulting porous polymer particles (Table 5-7). The mass and higher molecular weight portion of linear polystyrene trapped within the network structure were larger during the copolymerization process as the initiator content increased. As expected, chain transfer to linear polystyrene was increased with increasing amount of initiator used in the seeded emulsion polymerization, the amount of chemical grafting was increased[29, 30, 31]. This increased inclusion of linear polymer lowered the specific surface area of the porous polymer particles, the total pore volume was also expected to be reduced. With the highest initiator concentration, the specific surface area of the polymer particles prepared by using linear polymer alone as inert diluent was too low (3 m^2/g) to be considered as porous polymer particles.

5.3.4 Effect of Polymerization Temperature

To determine the effect of polymerization temperature, monodisperse porous polymer particles were prepared according the recipe given in Table 4-2 using linear polystyrene and n-heptane as inert diluents and polymerized for 120 hours at 50 °C, 72 hours at 60 °C, and 24 hours at 70, 80 and 90 °C. Figure 5-12 shows the specific surface area as a function of polymerization temperature. The increase in polymerization temperature not only altered the thermodynamic equilibria (i.e., increases the solvency of the nonsolvent), but also changed the polymerization kinetics, i.e., increased the generation rate of radicals and the polymerization rate especially of the divinylbenzene. Also, the

Table 5-7: Effect of Initiator Concentration on the Physical Features of Monodisperse Porous Copolymer Particles

[15% DVB; $M_{W,LP}$= 1.49 x 10^6]

[I]/[M] %	d μm	S m^2/g	LP_{in} %	$M_{W,e}$ x 10^{-5}
1.Diluent: linear polystyrene				
0.0375	13	18	21	10.3
0.15	13	16	24	9.74
0.60	13	11	27	8.43
3.75	13	3	32	6.88
2. Diluent: linear polystyrene/n-hexane				
0.0375	11	60	11	13.0
0.15	11	44	13	12.3
0.60	11	36	16	11.5
3.75	11	36	17	11.4

* *[I]/[M]: weight ratio of initiator based on monomers; d: diameter of porous polymer particles; S: specific surface area; LP_{in}: fraction of linear polystyrene included within network structure; and $M_{W,e}$: weight-average molecular weight of extracted polystyrene.*

higher polymerization temperature resulted in a higher degree of phase separation in the particles, which was attributed to the effect of temperature on the elastic-retractive force[32, 33]. As a result, smaller interior microspheres were obtained, and the specific surface area became higher.

Figure 5-13 indicates that the pore volume increases as the polymerization temperature increases. The higher polymerization temperature would have resulted in a greater increase in the elastic-retractive force upon heating, which would have led to a large phase separation. As a result, higher pore volumes were obtained.

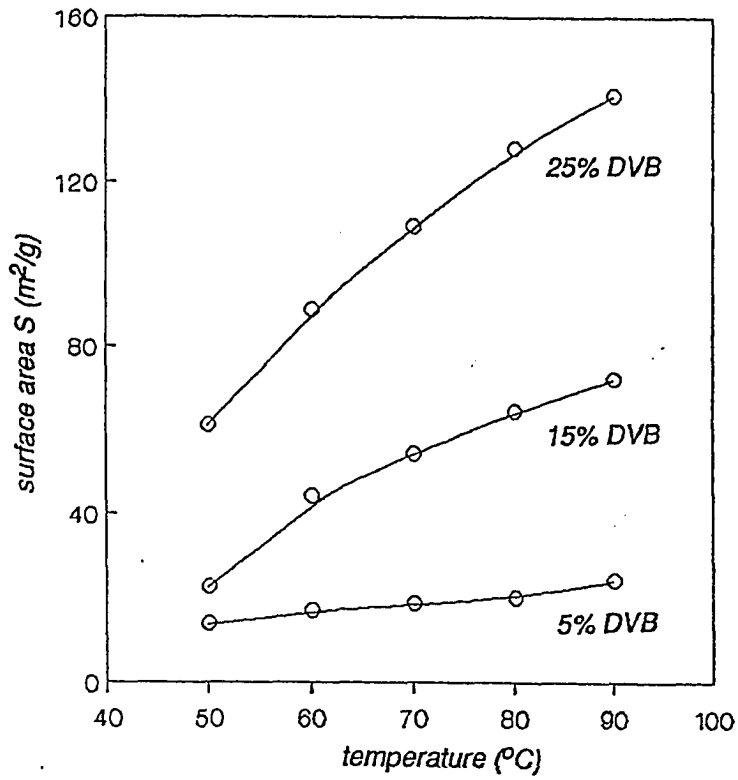

Figure 5-12: *Specific surface area of porous polymer particles prepared with different divinylbenzene content as a function of polymerization temperatures. [diluent: linear polystyrene/n-heptane,* $M_{W,LP}$ *= 1.49 x* 10^6*]*

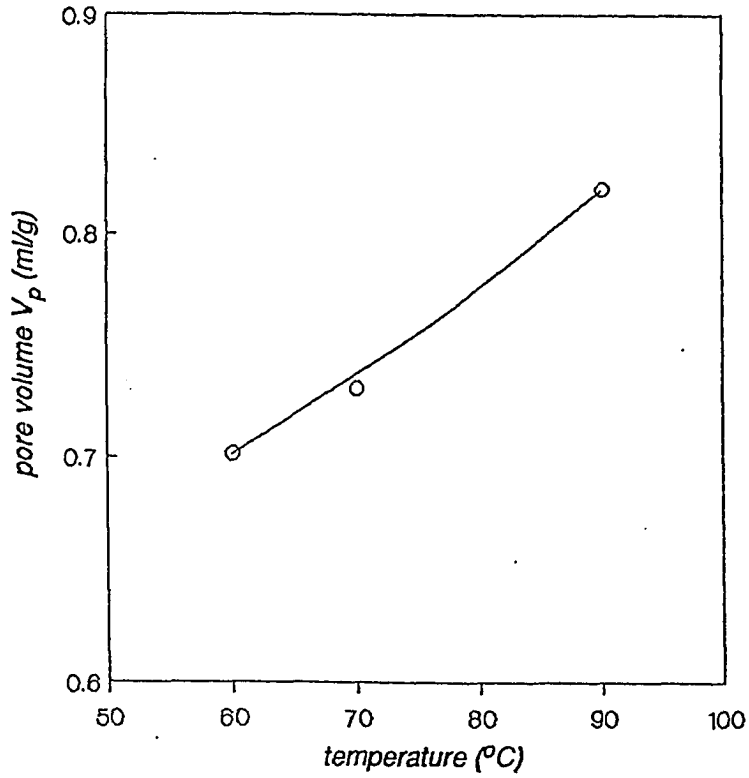

Figure 5-13: *Effect of polymerization temperature on pore volume of monodisperse porous polymer particles. [diluent: linear polystyrene / n-heptane, $M_{W,LP}$= 1.49 x 10^6, DVB= 15%]*

Figure 5-14 compares the pore size distribution of the porous polymer particles prepared at different polymerization temperatures. At higher polymerization temperature, the pore size distribution shifted to larger pores, as the linear polymer used as inert diluent was in a more expanded state during the onset of polymerization. However, the proportion of smaller pores was reduced due to annealing of microspheres at higher polymerization temperatures.

5.4 SUMMARY AND CONCLUSIONS

Monodisperse porous styrene-divinylbenzene copolymer particles in the size range of 3 to 30 μm in diameter were prepared via seeded emulsion polymerization techniques by using linear polystyrene seed particles or a combination of linear polystyrene seed and solvent or nonsolvent as inert diluents. The physical characteristics of the monodisperse porous polymer particles were governed by various synthesis parameters, such as the: (1) diluent type; (2) overall crosslink density; (3) molecular wight of the polystyrene seed particles; (4) type of nonsolvent; (5) amount of diluent; (6) initiator concentration; and (7) polymerization temperature. By the variation of these parameters, porous polymer particles with different physical features could be prepared.

The specific surface area increased with the overall divinylbenzene content of the polymer particles owing to the higher crosslinking density which led to the more dense and smaller interior microspheres. The precipitating ability of nonsolvent was dependent on its molecular size and solubility parameter. Pore volume and average pore size increased with the amount of diluent; however, a critical concentration of nonsolvent was observed at the point of the molecular overlap of the the network copolymer during the phase

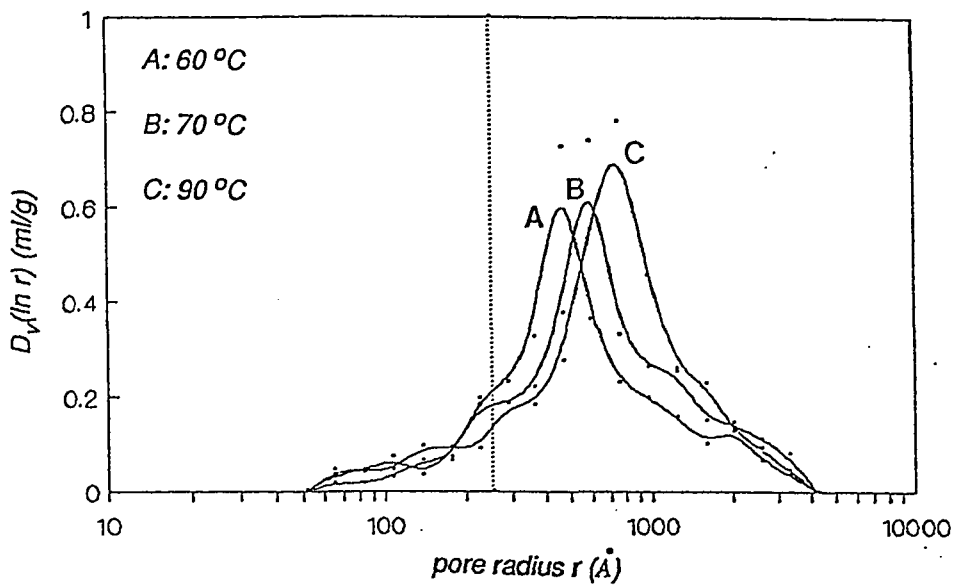

Figure 5-14: *Pore size distributions of monodisperse porous polymer particles prepared at different temperatures: (A) 60 °C; (B) 70 °C; and (C) 90 °C. The dotted line indicates the position of 250 Å pore radius. [diluent: linear polystyrene/n-hexane; 15% DVB; $M_{W,LP}$=1.49 x 10^6]*

separation process.

The fraction of the linear polymer included within the network structure increased with the increase of the initiator concentration used in the seeded emulsion polymerization, while the specific surface area, pore volume, and average pore size increased with increasing polymerization temperature.

5.5 REFERENCES

1. C. M. Cheng, M. S. El-Aasser, and J. W. Vanderhoff, presented at *"64th Colloid and Surface Science Symposium"*, Lehigh University, Bethlehem, PA, June 18-20, 1990.

2. C. M. Cheng, M. S. El-Aasser, and J. W. Vanderhoff, Presented at *"AIChE 1990 Annual Meeting"*, Chicago, November 11-16, 1990.

3. C. M. Cheng, F. J. Micale, J. W. Vanderhoff, and M. S. El-Aasser, *J. Polym. Sci., Polym. Chem. Ed.*, accepted (1991).

4. C. M. Cheng, J. W. Vanderhoff, and M. S. El-Aasser, *J. Polym. Sci., Polym. Chem. Ed.*, accepted (1991).

5. C. M. Cheng, F. J. Micale, J. W. Vanderhoff, and M. S. El-Aasser, submitted to *J. Colloid Interface Sci.*

6. J. R. Benson and D. J. Woo, *J. Chromatogr. Sci.*, **22**, 386 (1984).

7. S. Brunauer, P. H. Emmett, and E. Teller, *J. Amer. Chem. Soc.*, **60**, 309 (1938).

8. S. J. Gregg and K. S. W. Sing, *"Adsorption, Surface Area and Porosity"*, 2nd ed., Academic Press, London (1982).

9. E. W. Washburn, *Proc. Nat. Acad. Sci.*, **7**, 115 (1921).

10. S. Lowell and J. E. Shields, *"Powder Surface Area and Porosity"*, 2nd ed., Chapman & Hall, London (1984).

11. A. A. Tager, M. V. Tsilipotkina, E. B. Makovskaya, Y. I. Lyustgarten, A. B. Pashkov, and M. A. Lagunova, *Vysokomol. Soyed.*, **A13**, 2370 (1971).

12. P. Cornel and H. Sontheimer, *Chem. Eng. Sci.*, **41**, 1791 (1986).

13. D. K. Swatling, J. A. Manson, D. A. Thomas, and L. H. Sperling, *J. Appl. Polym. Sci.*, **26**, 591 (1981).

14. J. Brandrup and H. Immergent, eds., *"Polymer Handbook"*, 2nd. Ed., Wiley Interscience, New York, 1975.

15. H. Jacobelli, M. Bartholin, and A. Guyot, *Angew. Makromol. Chem.*, **80**, 31 (1979).

16. M. Eder, A. Wlochowicz, and B. N. Kolarz, *Angew. Makromol. Chem.*, **126**, 81 (1984).

17. H. Galina, B. N. Kolarz, P. P. Wieczorek, and M. Wojcynska, *British Polym J.*, **17**, 215 (1985).

18. A. B. Wojcik, *J. Appl. Polym. Sci.*, **30**, 781 (1985).

19. W. L. Sederel and G. J. de Jong, *J. Appl. Polym. Sci.*, **17**, 2835 (1973).

20. J. Seidl, J. Malinsky, K. Dusek, and W. Heitz, *Adv. Polym. Sci.*, **5**, 113 (1967).

21. M. Wojaczynska, V. Marousek, and B. N. Kolarz, *React. Polym.*, **11**, 141 (1989).

22. A. B. Wojcik, *J. Appl. Polym. Sci.*, **39**, 179 (1990).

23. K. A. Kun and R. Kunin, *J. Polym. Sci.*, **A6**, 2689 (1968).

24. W. Rolls, F. Svec, and J. M. Frechet, *Polymer*, **31**, 165 (1990).

25. D. Y. D. Chung, M. Bartholin, and A. Guyot, *Angew. Makromol. Chem.*, **103**, 109 (1982).

26. A. Guyot and M. Bartholin, *Prog. Polym. Sci.*, **8**, 277 (1982).

27. H. Jacobelli, M. Bartholin, and A. Guyot, *J. Appl. Polym. Sci.*, **23**, 927 (179).

28. P. G. De Gennes and C. Taupin, *J. Phys. Chem.*, **86**, 2294 (1982).

29. G. Odian, *"Principles of Polymerization"*, 2nd ed., Wiley-Interscience, New York (1981).

30. M. P. Merkel, V. L. Dimonie, M. S. El-Aasser, and J. W. Vanderhoff, *J. Polym. Sci. Polym. Chem. Ed.*, **25**, 1755 (1987).

31. M. P. Merkel, *Ph.D. Dissertation*, Lehigh University (1986).

32. H. R. Sheu, M. S. El-Aasser, and J. W. Vanderhoff, *J. Polym. Sci. Polym. Chem. Ed.*, **28**, 629 (1990).

33. H. R. Sheu, M. S. El-Aasser, and J. W. Vanderhoff, *J. Polym. Sci. Polym. Chem. Ed.*, **28**, 653 (1990).

Chapter 6
Conclusions and Recommendations

6.1 CONCLUSIONS

From the present investigation, a number of conclusions were drawn and summarized as follows:

1. A new synthesis approach was presented for the preparation of monodisperse porous polymer particles in the size range of 3 to 30 μm in diameter. The approach involves seeded emulsion polymerization, using linear polystyrene seed or a mixture of linear polystyrene seed and solvent or nonsolvent as inert diluents. The role of the linear polymer was to create the macroporous structure; the presence of low molecular weight solvent-type diluent enhanced the phase separation and structure heterogeneity. Porous structures were formed by the removal of diluents by solvent extraction after polymerization. The monodispersity of the particles was maintained during this synthesis process. The pore diameters of the resulting macroporous polymer particles were on the order of 1,000 $\mathring{A}$ with pore volumes up to 0.9 ml/g and specific surface areas up to 200 m^2/g. Polymer seed with a low degree of crosslinking could also be used to prepare porous polymer particles with smaller pores and pore volumes.

2. In the synthesis of monodisperse porous styrene-divinylbenzene copolymer particles, monodisperse polystyrene latex particles with molecular weights on the order of 10^6 were used as inert diluent. Pore size distributions by mercury porosimetry revealed that the majority of the pores were in the macropore region, which implied that the high molecular weight linear polystyrene was responsible for creating these macropores. Using the same linear polymer as inert diluent, the pore size distribution patterns were rather

similar. However, the pore size distributions were very sensitive to the molecular weight of the linear polymer.

3. Nitrogen adsorption-desorption isotherms were used complementary to assess pore structure and pore size distribution of mesopores and micropores. Qualitative evidence from nitrogen adsorption isotherms and α_s analyses indicated that the monodisperse porous polymer particles were predominantly macroporous but contained some mesopores, with little or no microporosity being present. As the molecular weight of the linear polymer decreased, the porous polymer particles were exhibited properties over a complex spectrum of macro-mesopore structures, with an increase in the proportion of mesopores.

4. Scanning electron microscope evidenced the microglobular nature of the internal structure and the existence of voids between microspheres and agglomerates. This was also confirmed by the nitrogen adsorption-desorption isotherms, which implied that the mesopores, as well as the macropores, of the porous polymer particles were indeed due to the interstices between the crosslinked microspheres and their agglomerates.

5. A kinetic investigation of the processes of pore formation of monodisperse porous polymer particles prepared using linear polymer seed and nonsolvent as inert diluents was performed. The process of copolymerization can be described as: (1) the production and agglomeration of highly crosslinked gel microspheres; and (2) the binding together of microspheres/agglomerates and fixation of network structure. The porosity observed is a consequence of phase separation which occurred during copolymerization in the presence of diluents. Following solvent extraction to remove the linear polymer and nonsolvent, monodisperse polymer particles with macroporous structure are formed.

6. A portion of linear polymer used as inert diluent was included in the

copolymer network as the pore structure was built up. A degree of inclusion was a consequence of steric entrapment, or chain transfer to linear polymer at high conversion. This inclusion of linear polymer within the network also depended on the diluent kind and crosslinker content, as well as the molecular weight of linear polymer seed used as inert diluent.

7. The removal of the linear polymer after the end of the copolymerization process from the matrix pores influenced strongly the pore structure. The preservation of the pore structure during the solvent extraction could be attained by decreasing the interactions between polymer chains and the solvent, i.e., using solvents with decreasing solvating power. The pore stability was dependent on the crosslinker content. The effect of the shrinkage phenomenon increased with decreasing crosslinking, which was more pronounced in smaller pore regions.

8. The physical characteristics of the monodisperse porous polymer particles were governed by various synthesis parameters, such as the: (1) diluent type; (2) overall crosslink density; (3) molecular weight of the polystyrene seed particles; (4) type of nonsolvent; (5) amount of diluent; (6) initiator concentration; and (7) polymerization temperature. By the variation of these parameters, porous polymer particles with different physical features could be prepared.

9. Particles prepared using a mixture of linear polymer and nonsolvent as inert diluent resulted in the largest pore volumes and specific surface areas, while particles prepared using linear polymer alone or a mixture of linear polymer and solvent resulted in larger pore sizes compared to the linear polymer-nonsolvent system. Particles prepared using linear polymer alone yielded the smallest pore volume and surface area.

10. Pore volume increased as the crosslink content increased, while

average pore size decreased with crosslink content. The specific surface area increased with the overall divinylbenzene content of the polymer particles owing to the higher crosslinking density which led to the more dense and smaller interior microspheres.

11. The precipitating ability of nonsolvent was dependent on its molecular size and solubility parameter. Pore volume and average pore size increased with the amount of diluent; however, a critical concentration of nonsolvent was observed as the molecular overlap of the the network copolymer during the phase separation process.

12. The fraction of the linear polymer included within the network structure increased with the increase of the initiator concentration used in seeded emulsion polymerization, while the specific surface area, pore volume, and average pore size increased with increasing polymerization temperature.

6.2 RECOMMENDATIONS

As a consequence of this research, several research areas requiring further study are recommended:

1. In the preparation of porous polymer particles, if the monomers were converted to solid polymer upon polymerization and the volume occupied by diluents becomes the void volume, a limiting pore volume, $V_{p,lim}$, may be defined as equal to $V_d/V_m\rho_m$, where the V_d is the volume fraction of diluents, V_m is that of monomer, and ρ_m is the monomer density[1]. The measured pore volume of porous polymer particles prepared using a mixture of linear polystyrene and nonsolvent (such as n-heptane) as inert diluents was always smaller than the designed limiting pore volume, but larger than the lower bound $V_{p,lim,l}$, where only the linear polymer was considered as inert diluent. The difference between the measured pore volume and the designed limiting

pore volume may indicate the volume shrinkage of the particles, owing to the extrusion of nonsolvent and the cohesion of polymer chains during the polymerization and solvent extraction processes. The formation of inhomogeneous pore structure during polymerization with nonsolvating diluent was described by Dusek et al[2, 3, 4, 5, 6, 7] as χ-induced syneresis. Phase separation is induced mostly when the interaction parameter χ between copolymer and diluents (linear polymer and nonsolvent) becomes larger than 0.5 (according to the Flory-Huggins theory[8, 9]). The consumption of monomers reduces the degree of mixing between the copolymer and the monomer or diluents and leads to phase separation. It is suggested to measure the interfacial tension between the diluents and the copolymer at different monomer conversions to follow the phase separation behavior during the polymerization process. Different concentrations of crosslinker (divinylbenzene) and nonsolvent can be used to prepare the polymer particles. Thus, a thermodynamic treatment involving the mixing, elastic and interfacial free-energy changes[10, 11, 12] may be developed to described the mechanism of phase separation during the formation of pore structure. The shrinkage of the particle volume during the polymerization and solvent extraction processes can be monitored *in situ* using an optical microscope since the particles prepared are monodisperse. Therefore, these kinetic studies of phase separation may provide the information of the pore-structure changes during the particle synthesis.

2. Study of the kinetics of seeded emulsion copolymerization of polystyrene seed with styrene and commercial divinylbenzene should provide more information to elucidate the phase separation and the gel-effect in the pore structure formation. The parameters which affect the crosslinking copolymerization kinetics to be examined should be the: (1) concentration of divinylbenzene; (2) molecular weight of the polystyrene seed particles; (3) type

of solvent and nonsolvent; (4) amount of diluent; (5) initiator concentration; and (6) polymerization temperature.

3. The concentrations of surfactants used in the polymerization recipes were determined in an empirical and comparative fashion. The number of smaller offsize particles has been shown to increase with increasing particle size of the seed latex. Determination of the adsorption isotherms and loci of all three surfactants as a function of the particle size by using serum replacement is recommended to eliminate the formation of new crops of small particles.

4. Post-copolymerization of functional monomers with residual double bonds of macroporous styrene-divinylbenzene copolymer particles can be used for grating functional groups, provided the grafted monomer is copolymerized with styrene-like units. These double bonds should be at least partly reacted, undergo cationic polymerization during chloromethylation by chlomethylether in the presence of Friedel-Crafts catalysts[13]. Monodisperse macroporous polymer particles with different functionality may be prepared.

5. Monodisperse magnetic polymer particles may be prepared by the magnetization of monodisperse porous polymer particles by in-situ precipitation of iron oxide in the particle pores. Such porous magnetic particles, up to 3 μm, have been made by seeded emulsion polymerization[14, 15, 16, 17]. The high density of these particles can be offset, at least partially, by sealing the unused pores by seeded polymerization, thus incorporating air voids in the particles.

6. Monodisperse microcarrier for cell culture functions may be prepared in order to develop the specialty particles for studying the hydrodynamic effects on cell cultures for bioreactor system design and to determine the mechanisms and parameters involved in protein interaction with particle surfaces and cell attachment/detachment[18]. Successive seeded emulsion polymerization can be used to prepare monodisperse polystyrene latexes in the size range of 100 - 250

μm. The incorporation of surface functional groups into the monodisperse polystyrene latexes for binding of proteins, carbohydrates or haptens can be achieved by the choice of initiator, a copolymerization using functional monomer or a post-polymerization reaction.

6.3 REFERENCES

1. G. J. Howard and C. A. Midgley, *J. Appl. Polym. Sci.*, **26**, 3845 (1981).
2. K. Dusek, *Coll. Czech. Chem. Commun.*, **32**, 1182 (1966).
3. K. Dusek, J. Seidl, and J. Malinsky, *Coll. Czech. Chem. Commun.*, **32**, 2766 (1967).
4. H. Beranova and K. Dusek, *Coll. Czech. Chem. Commun.*, **34**, 2932 (1969).
5. K. Dusek, in *"Polymer Networks, Structure and Mechanical Properties"*, A. J. Chompff and S. Newman, eds., Plenum Press, New York, 245 (1971).
6. K. Dusek, in *"Developments in Polymerization - 3"*, R. N. Haward ed., Applied Science, London, 143 (1982).
7. K. Dusek, *Macromolecules*, **17**, 716 (1984).
8. P. J. Flory, *J. Chem. Phys.*, **10**, 51 (1942).
9. M. L. Huggins, *J. Chem. Phys.*, **46**, 151 (1942).
10. H. R. Sheu, *Ph.D. Dissertation*, Lehigh University (1988).
11. H. R. Sheu, M. S. El-Aasser, and J. W. Vanderhoff, *J. Polym. Sci. Polym. Chem. Ed.*, **28**, 629 (1990).
12. Y. C. Chen, V. L. Dimonie, and M. S. El-Aasser, *J. Appl. Polym. Sci.*, **42**, 1049 (1990).
13. T. Brunelet, M. Bartholin, and A. Guyot, *Angew. Makromol. Chem.*, **106**, 79 (1982).
14. J. Ugelstad, T. Ellingsen, A. Berge, and B. Helgee, *PCT Int. Appl.* WO 83 03,920 (1983).
15. J. Ugelstad, A. Berge, T. Ellingsen, J. Bjorgum, R. Schmid, P. Stenstad, O. Aune, T. N. Nilsen, S. Funderud, and K. Nustad, in *"Future Directions in Polymer Colloids"*, M. S. El-Aasser and R. M. Fitch, eds., NATO ASI Series, **E138**, 355 (1987).
16. C. D. Platsoucas, F. H. Chae, N. Collins, N. Kernan, J. Laver, T. Ellingsen, P. Stenstad, J. Bjorgum, A. Rembaum, R. A. Good, R. O'Reilly, and J. Ugelstad, in *"Microspheres: Medical and Biological Applications"*, A. Rembaum and Z. A. Tokes, eds., CRC Press, Boca Raton, Florida, 89 (1988).
17. J. Ugelstad and T. Ellingsen, presented at *"64th Colloid and Surface Science Symposium"*, Lehigh University, Bethlehem, PA, June 18-20,

1990.

18. C. M. Cheng, M. S. El-Aasser, J. A. Phillips, and J. W. Vanderhoff, *Graduate Research Progress Reports*, Emulsion Polymers Institute, Lehigh University, **30**, 7 (1988).

Appendix A
Development and Evaluation of a 2L Rotating-Cylinder Reactor for Use in Preparing Large-Particle-Size Latexes

A.1 Introduction

The goal of this research is to apply ground-based emulsion polymerization reactor technology developed under NASA sponsorship to improve the production of monodisperse latex particles and commercial latexes. Previously, two polymerization reactor concepts were evaluated to assess their potential for commercial development. The Monodisperse Latex Reactor (MLR) program was designed to produce large-particle-size monodisperse latexes in space, based on the rationale that the coagulum formed during polymerization on earth would be eliminated under microgravity conditions[1, 2, 3, 4, 5, 6, 7]; this was demonstrated on the Shuttle flights STS-3, STS-4, STS-6, STS-7, and STS-11, which produced the 10 μm (STS-6) and two 30 μm (STS-11) latexes, which were accepted by the National Bureau of Standards (now the National Institute for Standards and Technology) as Standard Reference Materials, making them the first products made in space for sale on earth. The ground-based production of these large-particle-size monodisperse latexes would be of interest for preparing quantities sufficient for uses less demanding than calibration, e.g., in chromatographic separation columns; however, the formation of coagulum remains a serious problem. In the early stages of polymerization, the soft and sticky monomer-swollen particles tend to cream, and increasing the agitation rate to offset this creaming causes more violent particle-particle collisions, resulting in flocculation and coalescence of the

particles. A more gentle but thorough method of agitation must be developed to produce these large-particle-size latexes on earth.

A new reactor design, which promised to alleviate the formation of coagulum, was the horizontal rotating-cylinder reactor, which was proposed to simulate polymerizations in microgravity. This reactor design gives less mechanical shear during polymerization than the stirred-tank reactor. NASA's Marshall Space Flight Center (MSFC) developed a 235-ml prototype reactor, which was subsquently tested at Lehigh for the preparation of polystyrene latexes with diameters as large as 62 μm[8]. Commercial latexes could also be produced in such a rotating-cylinder reactor with minimal mechanical shear and hence less coagulum. The space- and ground-based polymerizations in the MLR 100-ml piston-cylinder reactors showed that the formation of coagulum in monodisperse latexes could be alleviated by the slow stirring rate and uniform mixing of the H-blade stirrer. Thus this reactor design could serve as the basis for scaleup of ground-based emulsion polymerizations for both large-particle-size monodisperse latexes and commercial latexes.

Therefore, the present research was initiated to design and construct three two-liter polymerization reactors based on the rotating-cylinder and piston-cylinder reactor designs, and to demonstrate the applicability of these reactors in the preparation of large-particle-size monodisperse latexes and commercial latexes.

A.2 Rotating-Cylinder and Piston-Cylinder (RC/PC) Reactor

The RC/PC reactor system has been designed and constructed where the entire polymerization reaction chamber is rotated horizontally about its long axis and is fully computer controlled. The reactor is designed to maintain maximum uniformity in particle concentration and temperature with a minimal amount of stirring. The particles would be kept in suspension strictly through the rotation of the reactor, which is variable over a rpm range (5 to 32 rpm).

The RC/PC reactor is basically a piston/cylinder dilatometer. It can be filled completely with a swollen latex eliminating any air-liquid interface. The variation of the latex volume as a function of degree of polymerization and temperature can be monitored continuously from the movement of the piston. Piston movement is measured by a linear voltage differential transformer (LVDT). Three temperatures are measured in the reactor: (1) the fluid temperature (T_f); (2) the reactor wall temperature (T_w) (also the control); and (3) the base temperature (T_b). These reading are converted by a HP data acquisition device to digital format and recorded on computer.

A cut-away drawing of the RC/PC reactor is shown in Figure A-1. The mechanical aspects of the reactor were designed to provide temperature control, fluid containment, and data measurement. The apparatus consists of a stainless steel (SS) cylinder in which rides a SS piston, sealed by a Viton O-ring. The reactor is a two liter chamber. In the operational position it stands 24.5 inches in length and 11.75 inches in diameter. The LVDT sensor is attached to the piston and fixed relative to the cylinder.

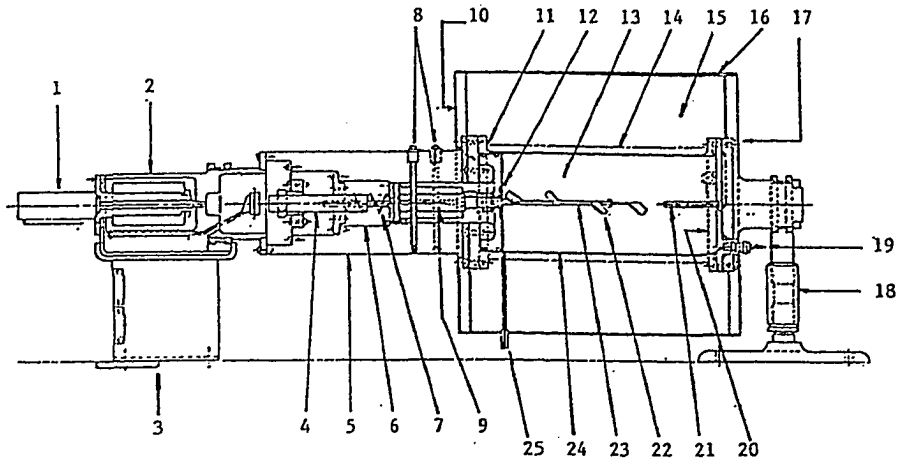

1. gear moter
2. rotating assembly
3. base plate
4. LVDT
5. LVDT housing
6. piston assembly
7. spring
8. pins
9. stirrer motor
10. insulator shield
11. Viton O-ring
12. O-ring
13. chamber assembly
14. heater wire leads
15. fiberglass insulation
16. cylinder assembly
17. end cap
18. end cap stand
19. quick disconnect
20. base temp. sensor
21. fluid temp. sensor
22. H-blade stirrer
23. stirrer drive shaft
24. wall temp. sensor
25. vent tube

Figure A-1: *Schematic diagram of the RC/PC reactor.*

A.3 Reactor Evaluation

Currently, all three reactors have been fabricated, assembled, and subjected to leak-tests in the static mode (SM mode, i.e., the upright piston-cylinder mode without rotating). Reactor 1 has been tested by conducting seeded polymerizations in both the SM and RM (horizontal rotating-cylinder) modes. Based on recipe developments in the MLR program to produce monodisperse latexes in microgravity, seeded emulsion polymerizations were run in the RC/PC reactor in both SM and RM modes in an attempt to investigate the feasibility of preparing large-particle-size latexes of narrow size distribution. The seed used in the experiments was a monodisperse 0.33 μm polystyrene latex (LS-1103A, Dow Chemical). The polymerization recipe included seed particles, styrene monomer, potassium persulfate initiator ($K_2S_2O_8$), sodium bicarbonate buffer ($NaHCO_3$), anionic emulsifier (Aerosol MA), and distilled-deionized water, as listed in Table A-1. The monomer to polymer weight ratio was 1 to 1, and the designed final solids content was 9.2%.

2,300 grams of monomer-swollen latex was prepared by end-over-end rotation (20 rpm) of a bottle containing the ingredients for 12 hours at room temperature. The swollen latex was de-gassed via aspirator for 45 minutes until bubble formation had ceased. This degassed latex was then poured into the reactor. 40 grams of the degassed latex mixture was added to a 2 oz. capped bottle, and this reference bottle polymerization was carried out by tumbling the bottle end-over-end at 32 rpm for 5 hours in a thermostated water bath at 70 °C.

Once loaded, the temperature of the reactor was increased from room temperature to 70 °C. The stirrer was oscillated at 40 rpm for both the SM and RM modes, and the rotational speed used for the RM mode was 20 rpm. The piston movement was monitored by the LVDT reading to record the volume change of the latex and any possible leakage. The polymerization was monitored

Table A-1: Recipe for Seeded Emulsion Polymerization

Ingredient	wt%
LS-1103A latex	4.6
Styrene	4.6
Aerosol MA	0.04
$K_2S_2O_8$	0.03
$NaHCO_3$	0.03
Water	90.7

• *Solids content: 9.2%; total charge: 2,300 grams; polymerization temperature: 70 °C.*
* *LS-1103A: 330 nm-diameter monodisperse polystyrene latex (Dow Chemical); and Aerosol MA (sodium dihexyl sulfosuccinate; American Cyanamid).*

until completion (about 3 hours) as indicated by the cessation of piston movement. The final conversion was determined by the gravimetric method. Transmission electron microscopy was used to determine the particle size and uniformity.

Two seeded emulsion polymerization experiments were conducted in both the SM and RM modes. The conversions and particle size distributions of these runs together with those of the corresponding bottle polymerizations are listed in Table A-2. These results indicate that the size distributions of those products are as narrow as the original seed latex. The polydispersity and uniformity were about the same for all the runs. Also, there was no obvious coagulum in the latex or on the wall of the reactor chamber after polymerization. The lower conversions of SM runs may indicate a lower average fluid temperature as the extent of mixing in the static mode is lower than that of the rotating mode. However, the uniformity, expressed as the coefficient of variation S_n, of the

particles prepared via the RC/PC reactor was better than those prepared via bottle polymerization.

Table A-2: Conversions and Particle Size Distribution

Sample	Conversion %	D_n nm	D_w nm	PDI	SD_n %
Seed	-	332	336	1.010	5.70
SM-1	96.1	426	429	1.007	4.77
SM-2	95.1	429	435	1.014	6.11
BP/SM-1	99.9	432	436	1.009	5.48
BP/SM-2	98.4	421	426	1.012	6.34
RM-1	98.5	400	402	1.006	4.55
RM-2	99.5	399	401	1.005	4.03
BP/RM-1	98.6	388	392	1.009	5.53
BP/RM-2	98.5	402	404	1.006	4.50

** SM: static mode; RM: rotating mode; and BP: corresponding bottle polymerization of the run.*
*** D_n: number average diameter; D_w: weight average diameter; PDI: polydispersity index; and SD_n: coefficient of variation.*

Figures A-2 and A-3 show the LVDT and fluid temperature (T_f) vs. time profiles in SM and RM modes, respectively. As shown in Figure A-2, during the initial temperature rise, the LVDT reading increases, indicating a rise of the piston or an increase in volume, followed by an isothermal polymerization in which the LVDT reading decreases corresponding to a decrease in the volume due to polymerization. As the polymerization was completed, the LVDT reading reached a constant value indicating the cessation of piston movement. The difference in the LVDT profiles of the two curves produced in the SM mode may have been caused by the inclusion of an air void during the loading. This

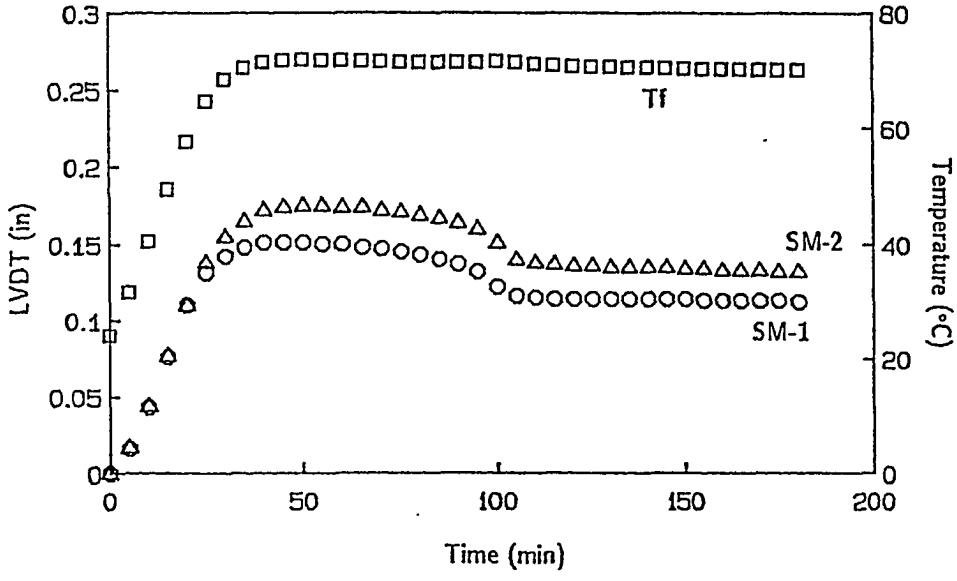

Figure A-2: *LVDT and fluid temperature (T_f) histories for seeded emulsion polymerizations in the static mode (SM).*

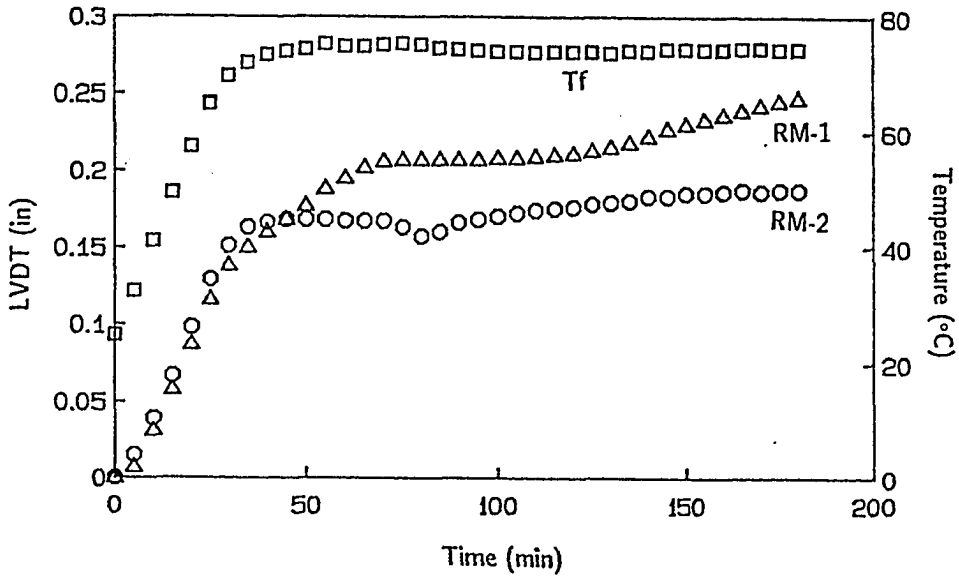

Figure A-3: *LVDT and fluid temperature (T_f) histories for seeded emulsion polymerizations in the rotating mode (RM).*

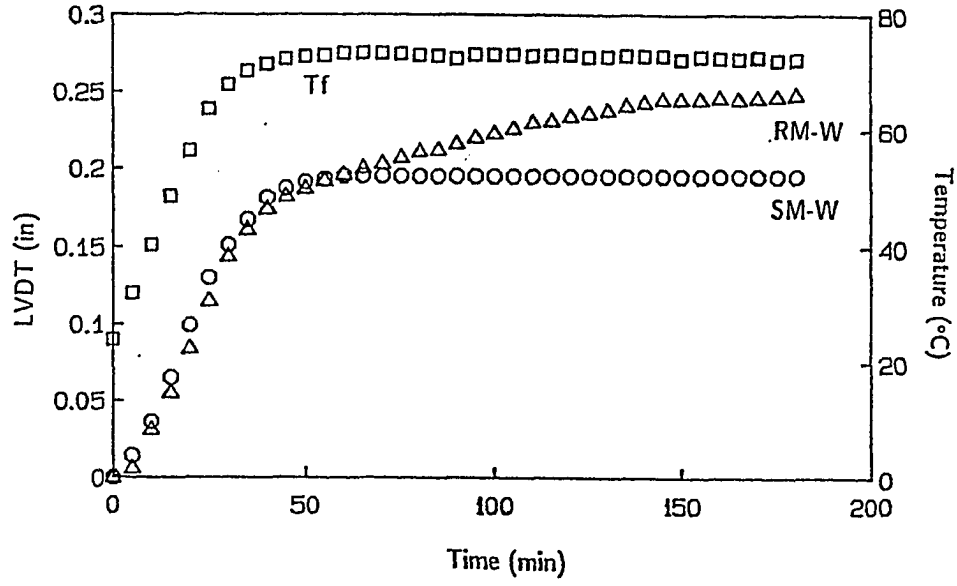

Figure A-4: *LVDT and fluid temperature (T_f) vs. time profiles for water test: in both static (SM) and rotating (RM) modes.*

procedure needs to be improved to ensure that no air is trapped inside the reactor chamber.

In the rotating cylinder experiments the reactor worked well in terms of producing uniform latexes; however, the LVDT-time curves produced did not reflect the polymerization kinetics as given in the static mode or in the RM mode (Figure A-3). The LVDT reading kept increasing and showed no sign of leveling off even when the system was kept at a constant temperature. This behavior was also found in a water test conducted in the RM mode (see Figure A-4). The LVDT reading correlated well with an external micrometer reading; the increase in the LVDT reading indicates an expansion of volume. The reason for this is unknown and thus efforts will be made to understand this behavior[9].

A.4 Summary

The 2 liter RC/PC reactors have been designed and manufactured, and preliminary results show that these can be used in seeded emulsion polymerizations to prepare monodisperse latex particles. Further refinements in the mechanical and data acquisition systems are needed in order to use the RC/PC reactor for the preparation of large-particle-size monodisperse latex particles.

A.5 References

1. J. W. Vanderhoff, F. J. Micale, M. S. El-Aasser, and D. M. Kornfeld, *U. S. Patent, 4,247,434* (1981).

2. J. W. Vanderhoff, M. S. El-Aasser, F. J. Micale, E. D. Sudol, C. M. Tseng, A. Silwanowwicz, D. M. Kornfeld, and F. A. Vicente, *J. Disp. Sci. Tech.*, 5, 231 (1984).

3. J. W. Vanderhoff, M. S. El-Aasser, F. J. Micale, E. D. Sudol, C. M. Tseng, A. Silwanowicz, and D. M. Kornfeld, *Proceedings of the Second Symposium on Space Industrialization*, NASA CP-2313, C. M. Jernigan,

ed., Huntsville, Alabama (1984).

4. J. W. Vanderhoff, M. S. El-Aasser, F. J. Micale, E. D. Sudol, C. M. Tseng, A. Silwanowicz, and D. M. Kornfeld, presented at *"AIChE 1984 Summer National Meeting"*, Philadelphia, August 19-22, 1984.

5. E. D. Sudol, *Ph.D. Dissertation*, Lehigh University (1983).

6. C. M. Tseng, *Ph.D. Dissertation*, Lehigh University (1983).

7. E. D. Sudol, M. S. El-Aasser, F. J. Micale, and J. W. Vanderhoff, *Rev. Sci. Instrum.*, **57**, 2332 (1986).

8. J. H. Kim, E. D. Sudol, M. S. El-Aasser, J. W. Vanderhoff, and D. M. Kornfeld, *Chem. Eng. Sci.*, **43**(8), 2025 (1988).

9. V. Mishra, E. D. Sudol, J. W. Vanderhoff, and M. S. El-Aasser, *Graduate Research Progress Reports*, Emulsion Polymers Institute, Lehigh University, **35**, 215 (1991).

Appendix B
Determination of Styrene, Divinylbenzene, and Ethylvinylbenzene Concentration by Gas Chromatography

B.1 Gas Chromatogram

A Hewlett-Packard Model 5890 gas chromatograph (GC) equipped with a HP-17 column, 10 meters long and 530 μm in diameter was used to determine the concentration of styrene (St), meta- and para-divinylbenzene (m-DVB and p-DVB), and meta- and para-ethylbenzene (m-EVB and p-EVB) in the emulsion. Toluene (T) (or ethylbenzene) was used as an external standard[1,2,3]. The injecting samples were prepared by adding a known amount of toluene to 1 ml emulsion and then diluting with 10 ml of tetrahydrofuran. Initially, the oven temperature of GC was at 50 °C. After injecting 0.2 μl sample into the GC, the temperature was increased at a rate of 5 °C/min to the final temperature of 120 °C.

A representative result from GC is shown in Figure B-1. Peak 1 is that of n-heptane used as inert diluent, peak 2 of tetrahydrofuran, peak 3 of toluene, peak 4 of styrene, peaks 5 and 6 of meta- and para-ethylvinylbenzene, and peaks of 7 and 8 of meta- and para-divinylbenzene, respectively.

B.2 Calibration Curves

Calibration curves shown in Figures B-2 and B-3 were established by injecting samples of known m-DVB & p-DVB/T, m-EVB & p-EVB/T, and St/T weight ratios into the GC to obtain the area ratios of m-DVB/T, p-DVB/T, m-EVB/T, p-EVB/T, and St/T. After obtaining the area ratios for the samples, the calibration curves were used to determine the weight ratios. Since the amount

of toluene added in the samples is known, the concentration of m-DVB, p-DVB, m-EVB, p-EVB, and St can be determined from the weight ratios.

B.3 References

1. D. Y. D. Chung, M. Bartholin, and A. Guyot, *Angew. Makromol. Chem.*, **103**, 109 (1982).
2. R. H. Wiley and E. E. Sale, *J. Polym. Sci.*, **17**, 491 (1960).
3. R. H. Wiley, G. DeVenuto, and T. K. Venkatachalam, *J. Gas Chromatogr.*, **5**, 590 (1967).

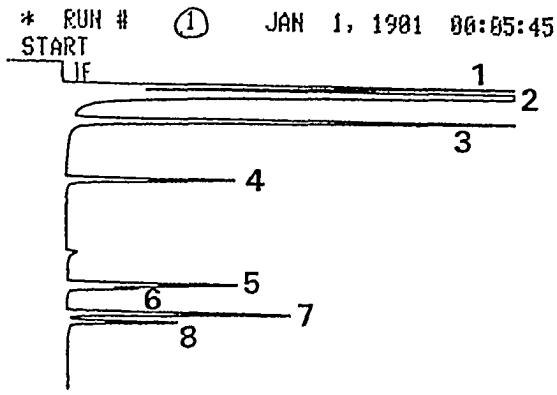

RUN# 1 JAN 1, 1901 00:05:45

METHOD NAME: A:CHENG.MET

AREA%

RT	AREA	TYPE	WIDTH	AREA%
1.210	17885024	PV	.144	6.44641
1.488	209699840	VB	.148	75.58342
2.932	22791392	PB	.162	8.21484
5.874	6497213	PB	.152	2.34183
9.415	772480	PV	.268	.27843
10.300	90074	VP	.196	.03247
10.919	6270640	PV	.145	2.26017
11.087	2175730	VB	.120	.78421
12.313	7681720	PV	.135	2.76877
12.703	3491464	VB	.125	1.25845
15.485	86125	I VP	.180	.03104

TOTAL AREA=2.7744E+08
MUL FACTOR=1.0000E+00

Figure B-1: *Representative gas chromatograph result for seeded emulsion samples using toluene as an external standard and tetrahydrofuran as diluent. 1: n-heptane; 2: tetrahydrofuran; 3: toluene; 4: styrene; 5: meta-ethylvinylbenzene; 6: para-ethylvinylbenzene; 7: meta-divinylbenzene; and 8: para-divinylbenzene.*

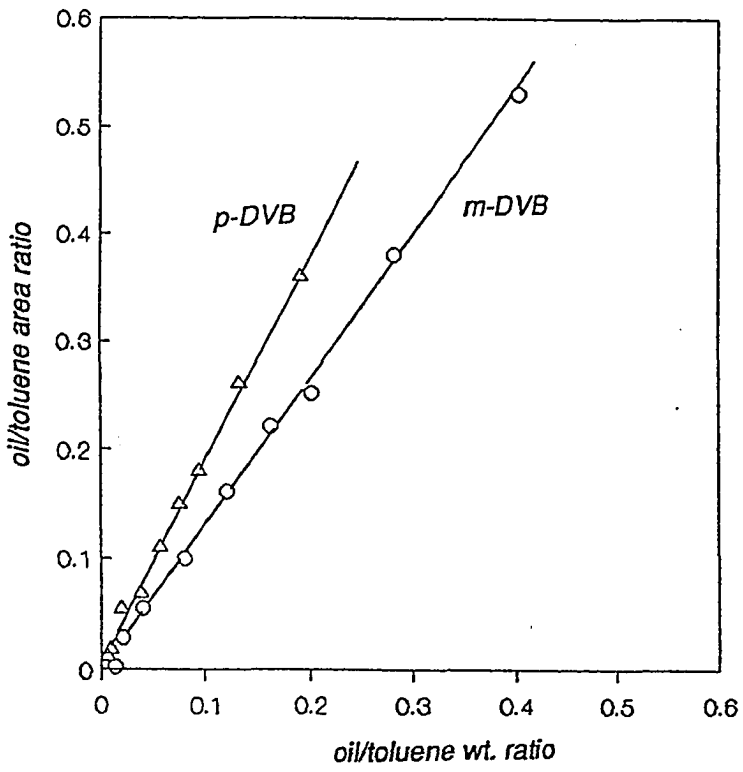

Figure B-2: *Gas chromatography calibration curves for meta-divinylbenzene and para-divinylbenzene using toluene as an external standard.*

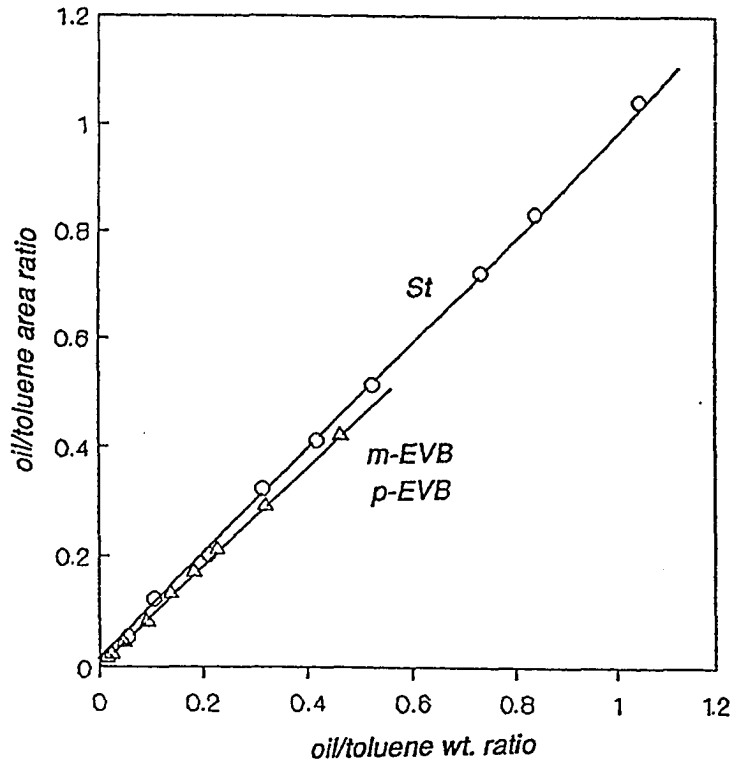

Figure B-3: *Gas chromatography calibration curves for meta-ethylvinylbenzene, para-ethylvinylbenzene and styrene using toluene as an external standard.*

Vita

Chieh-Min Cheng was born on August 2, 1959 in Penghu Archipelago, Taiwan, Republic of China, the second son of Hui-Hsiung Cheng and Chin-Feng Chen Cheng. He received a B.S. degree in Chemical Engineering from National Taiwan University, Taipei, Taiwan in June 1982. After two-year military service in Army Communication Corps, he worked as a research assistant at National Taiwan University for one year.

Mr. Cheng was awarded a NPIRI Fellowship from National Printing Ink Research Institute in August 1985, and became a research assistant at the Center for Surface and Coatings Research at Lehigh University. He studied the rheology and surface energetics of printing inks applied to ink transfer and printability, and received his M.S. degree in Chemical Engineering in May 1987. He then continued his research pursuing a Ph.D. degree in Polymer Science and Engineering at the Emulsion Polymers Institute, and was financially supported by the Emulsion Polymers Industrial Liaison Program and the National Aeronautics and Space Administration. In 1988 and 1990, he received University Scholarships to pursue graduate research in Chemical Engineering at Lehigh University.

Mr. Cheng has published a report describing the viscoelastic properties of printing inks, and three papers from his doctoral work. Parts of his research have been presented at the June 1990 64th Colloid and Surface Science Symposium in Bethlehem, Pennsylvania, and the 1990 AIChE Annual Meeting in Chicago. He is a member of the American Chemical Society.

Mr. Cheng was married to Nienwen Chow in the summer of 1986.